Evaluation of characteristics of alginate/hyaluronic acid and alginate/hydroxyapatite hydrogels during differentiation of Wharton's Jelly mesenchymal stem cells

Hao Yu

Ecole Doctorale BioSE (Biologie-Santé-Environnement)

Thèse

Présentée et soutenue publiquement pour l'obtention du titre de

DOCTEUR DE L'UNIVERSITE DE LORRAINE

Mention : Science de la Vie et de la Santé

Evaluation des caractéristiques des hydrogels d'alginate supplémentés en acide hyaluronique ou en hydroxyapatite lors de la différenciation des cellules souches mésenchymateuses issues de la gelée de Wharton.

Hao YU

Soutenue le 18/07/2017

Membres de jury:

Rapporteurs :	
Mme Magali Cucchiarini	Professeur, Université de Saarland, Allemagne
M. Daniel George	MCF-HDR, ICUBE, Biomécanique, Strasbourg
Examinateurs :	
Mme Céline Huselstein	MCF-HDR, UMR 7365, Directeur de thèse
M. Rachid Rahouadj	Professeur, UMR 7563, Co-Directeur de thèse
M. Gregory Pourié	MCF-HDR, INSERM U954, Nancy
Mme Sophie Gangloff	Professeur, BioS, Université de Reims
Membres invités	
M. Yun Chen	Professeur, Université de Wuhan, Chine
Mme Yinping Li	Docteur, Université de Wuhan, Chine

UMR 7365 CNRS-Université de Lorraine, Ingénierie Moléculaire et Physiopathologie Articulaire (IMoPA)

Acknowledgments

First of all, I would like to thank the director of IMoPA laboratory (**Pr. Jean-Yves Jouzeau**) and the responsibles of team 5, **Pr. Patrick Menu, and Pr. Pierre Gillet** for welcoming me in the laboratory and team 5, respectively.

I would like to thank **Pr. Jean-Francois Stoltz** and **Dr. Jacques Magdalou** who thanks to the "without wall laboratory" between Nancy-Wuhan have allowed me to come in France to study for my thesis.

Especially, I would like to express the deepest appreciation to my principal supervisor, **Dr. Céline Huselstein**, for her agreement to guide my thesis, for her patience to listen and practical suggestions, for her encouragement and confidence on my study and life, for her humor with me when I am depressed.

Concurrently, I want to thank my co-director and mentor **Pr. Rachid Rahouadj**. He has tried his best to spend the maximum time to work with me. From the language to the experiments, he is always patient to listen to me. He never made complaints about me. He is filled with humor, which is often applied by him to encourage me during my life and work. I think we are very good friends now. All in all, greatest thanks for you in four years.

I would like to thank the judges:

Dr. Magali Cucchiarini for having been member of my thesis committee during these 4 years and for accepting to judge my work;

Dr. Daniel George, for taking his precious time to judge my report;

Dr. Sophie Gangloff, for spending her precious time to judge my manuscript;

Dr. Gregory Pourie, for accepting to be examiner for my Ph.D defence and for evaluating my report;

Acknowledgments

I want to thank the jury members from Wuhan University particularly: **Dr. Yinping Li** and my supervisor in china **Pr. Yun Chen** for offering me the chance to study in France. My deepest thank for your help.

Thanks for the entire cooperative members: **Pr. Jean-luc Six, Dr. Nicolas Louvet, Dr. Jean-Francois Schmitt**.

To all those who have participated in this work,
I would like to thank all the staff and students of the laboratory (**Ghislaine, Nadia, Jean-Marc, Christophe, Loïc, Léonore, Anne-Sophie, Mathieu, Irfan and others ...**). Thanks for your work, your availability and your sympathy.

I also want to thank all the Chinese students in Nancy. Without you, I don't know how to spend the four years in France: **Zhen Li, Yueying Li, Yu Xiong, Song Xu, Junsong Ye, Yun Luo, Yingying Wang, Huili Cai, Xianglei Wu, Xu Yang, Zhe Xie, Lin Zhang, Pan Dan, MengMeng Niu, Xiaomeng Pang, Shiheng Liang, Xing Liu, Chao hua Deng, Yun Zhang, Ganggang Zhang, Chongsheng Qian, Yu Xie, Chaojie Wei.**

Thanks to the ***Chinese Scholarship Committee*** for financing my 4 years of Ph.D thesis.

Finally, I want to thank **my family (parents, wife and sister) and friends**.
Thanks for your support and encouragement.
Without you, nothing would have been possible!

Table of contents

Table of contents

List of publications and presentations

Publications:

- Loïc Reppel, Jessica Schiavi, Naceur Charif, Léonore Leger, **Hao Yu,** Astrid Pinzano, Christel Henrionnet, François Stoltz, Danièle Bensoussan, Céline Huselstein. Chondrogenic induction of mesenchymal stromal/stem cells from Wharton's jelly embedded in alginate hydrogel and without added growth factor: an alternative stem cell source for cartilage tissue engineering. *Stem Cell Res Ther.* 2015; 6: 260-273.
- **Hao Yu**, Ghislaine Cauchois, Nicolas Louvet, Yun Chen, Rachid Rahouadj, Céline Huselstein. Comparison of MSC properties in two different hydrogels: Impact of mechanical properties. *Biomed Mater Eng*. 2017; 28(s1):S193-S200.
- **Hao Yu,** Ghislaine Cauchois, Jean-François Schmitt, Jean-Luc Six, Nicolas Louvet, Yun Chen, Rachid Rahouadj, Céline Huselstein. Is there a cause-and-effect relationship between physicochemical properties and cell behavior of alginate-based hydrogel obtained after sterilization? *J Mech Behav Biomed Mater*. 2017 Jan 25; 68: 134-143.
- **Hao Yu**, Ghislaine Cauchois, Franck Demeurie, Pascal Thomann, Jean-François Schmitt, Nicolas Louvet, Dominique Dumas, Yun Chen, Rachid Rahouadj, Céline Huselstein. Effect of microenvironment induced by 3D scaffolds on cell behavior: from differentiation to immune properties. Relationship among of mechanical and biological properties. *Biomacromolecules*, 2017, Submitted.

Presentations:

(Poster Presentation)

- **Hao Yu**, Ghislaine Cauchois, Jean-François Schmitt, Jean-Luc Six, Nicolas Louvet, Yun Chen, Rachid Rahouadj, Céline Huselstein. *Evaluation of physicochemical and biological properties of aginate-based hydrogel after UV sterilization.* 18èmes Journées Françaises de Biologie des Tissus Minéralisés (JFBTM), 1-3 Juin 2016.

- **Hao Yu**, Ghislaine Cauchois, Nicolas Louvet, Yun Chen, Rachid Rahouadj, Céline Huselstein**.** *Comparison of MSC properties in two different hydrogels: Impact of mechanical properties.* The 6th Europe - China Symposium on Stem cells and regenerative medicine. First Meeting of the Research Network CNRS GDRI (0851) on Mesenchymal Stem Cells and Regenerative Medicine, 11-13Juillet 2016.

(Oral Presentation)

- **Hao Yu**, Ghislaine Cauchois, Jean-François Schmitt, Jean-Luc Six, Nicolas Louvet, Yun Chen, Rachid Rahouadj, Céline Huselstein. *Evaluation of physicochemical and biological properties of aginate-based hydrogel after UV sterilization.* Colloque BIOMAT 2015, Association Française affiliée à la Société Européenne des Biomatériaux, 12-14 Octobre 2015.
- **Hao Yu**, Yinping LI, Xiaohu He, Chen Li, Yuan He, Céline Huselstein, Jean-François Stoltz, Yun Chen. *Membranes composites de zéine/chitosan: fabrication, caractérisation et évaluation de la différenciation des cellules souches mésenchymateuses en ostéoblastes.* Journée de la FR CNRS-UL 3209 BMCT, Bioingénierie Moléculaire Cellulaire & Thérapeutique, 11 septembre 2014.

List of abbreviations

Alg:	Alginate
ACECM:	Articular cartilage extracellular matrix
CFU-F:	Fibroblasts Colony-Forming Unit
CTE:	Cartilage Tissue Engineering
CD:	Differentiation Cluster
CTL:	Cytotoxic T Cell
CH-PCLs:	Chitosan-polycaprolactone
DMF:	Dimethylformamide
ESCs:	Embryonic Stem Cells
ECM:	Extracellular Matrix
FGF:	Fibroblast Growth Factor
HGF:	Hepatocyte Growth Factor
hMSCs:	human Mesenchymal Stem Cells
HA:	Hyaluronic Acid
Hap:	Hydroxyapatite
HLA-DR:	Human Leukocyte Antigen - antigen D Related
HES:	Hematoxylin Eosin Safran
iPSCs:	induced Pluripotent Stem Cells
ISCT:	International Society for Cellular Therapy
IDO:	Indoleamine-2, 3-Dioxygenase
IL-10:	Interleukine-10
iDC:	immature Dendritic Cell
GAG:	Glycosaminoglycan
MFI:	Mean Fluorescence Intensity
MHC:	Major Histocompability complex
mDC:	Mature Dendritic Cell
NO:	Nitric Oxide

List of abbreviations

NK:	Natural killer cells
NPCs:	Neural Progenitor Cells
NMR:	Nuclear Magnetic Resonance
OPN:	Osteopontin
OCN:	Osteocalcin
PGE_2:	Prostaglandines E2
PMN:	Polymorphonuclear leukocyte
PLA:	Polylactic acid
PEG:	Poly(ethylene glycol)
PLGA:	Poly (lactic/glycolic acid)
PGA:	Polyglycolic acid
PVA:	Poly(vinyl alcohol)
PD-L1:	Programmed Death Ligand 1
PD-1:	Programmed Cell Death Protein 1
RT-PCR:	Reverse Transcription Polymerase Chain Reaction
RGD:	Arg–Gly–Asp
Runx2:	Runt-related transcription factor 2
SSEA:	Stage-specific embryonic antigen
SEM:	Scanning electron microscopy
TGF-β:	Transforming Growth Factor-β
Treg:	T regulatory
Th:	T helper
UV:	Ultraviolet light
UC:	Umbilical Cords
VEGF:	Vascular Endothelial Growth Factor
WJ-MSCs:	Wharton's jelly mesenchymal stem cells

List of figures

List of figures

List of tables

Summary in French

Contexte scientifique

Le cartilage articulaire et l'arthrose:

Le cartilage articulaire est un tissu conjonctif avasculaire et non innervé. Situé entre deux surfaces osseuses et baignant dans le liquide synovial, il se caractérise par ses propriétés mécaniques en permettant le glissement des pièces osseuses grâce à un coefficient de friction très faible et en amortissant les contraintes liées aux mouvements et au poids du corps qui s'appliquent à sa surface. Le cartilage se compose d'un seul type cellulaire : le chondrocyte, et d'une matrice extracellulaire spécifique contenant : des collagènes (de type II, IX, X ou encore XI), des protéoglycannes (agrécannes, décorine…), de petites protéines telles que la COMP (Cartilage Oligo Matrix Protein), des ions et de l'eau. Ces éléments matriciels organisés de façon zonal depuis la superficie jusqu'en profondeur confèrent au tissu sa résistance à la contrainte mécanique pouvant atteindre 20 MPa au cours d'une activité physique intense (*Grodzinsky AJ et al, 2000*). Lorsque le cartilage articulaire est exposé à des sollicitations répétitives ou excessives, il se fragilise et laisse apparaître des fissures puis des lésions. En raison de son avascularisation et du faible métabolisme cellulaire, la capacité d'auto-renouvellement du cartilage est limité et le tissu cicatriciel, qui dans un premier temps comble la lésion chondrale, reste un tissu fibro-cartilagineux, dont les propriétés mécaniques sont faibles par rapport à celles du tissu natif. Un cartilage lésé évoluera à plus ou moins long terme vers un cartilage arthrosique. L'évolution de la pathologie, se caractérise par une dégradation progressive et irréversible de la matrice cartilagineuse et peut se résumer en trois stades (*Gomoll AH et al, 2010*).

- stade 1 : Le tissu cartilagineux perd son aspect lisse et des microfissures apparaissent.

- stade 2 : Les microfissures s'approfondissent perpendiculairement à la direction des forces de cisaillement et le long des fibres de collagènes mais ne s'étendent pas jusqu'à la plaque sous-chondrale.
- stade 3 : La lésion est dite ostéochondrale car les microfissures s'étendent sur toute la profondeur du cartilage jusqu'à l'os sous-chondral. A ce stade, une inflammation synoviale peut alors être observée.

Ces stades sont associés à (i) une modification du phénotype chondrocytaire, avec l'expression de marqueurs hypertrophiques, (ii) un processus inflammatoire médié par différents tissus articulaires tels que l'os sous chondral qui présente une densité minérale anormale. Par conséquent, l'arthrose induit non seulement des modifications au niveau des cellules cartilagineuses (chondrocytes) mais aussi au niveau des ostéoblastes. Il existerait une synergie entre ces 2 types cellulaires dans ce processus pathologique.

La prévalence de l'arthrose peut dépasser 90% chez les personnes de plus de 70 ans, altère leur qualité de vie, et constitue une des principales causes de consultation médicale, de consommation médicamenteuse et de handicap. Les données médico-économiques françaises les plus récentes sur l'arthrose datent de 2010 et situent le coût annuel de la maladie autour de 5 milliards d'euros avec plus de 90 000 patients hospitalisés dans des établissements médico-chirurgicaux pour une coxarthrose et plus de 80 000 pour une gonarthrose (*Bertin P et al, 2014*).

Les principaux traitements actuels sont les traitements pharmacologiques antidouleurs et anti-inflammatoires ou des approches chirurgicales (autogreffes de cartilage ou de chondrocytes, greffes de tissus synthétiques, stimulation de la réparation spontanée par microfractures). Cependant, aucune thérapie ne permet la régénération d'un véritable tissu fonctionnel (*Orth P et al, 2014*). Depuis quelques années, le développement de travaux de médecine régénérative constitue une ouverture prometteuse notamment avec l'ingénierie tissulaire. Ce concept permettrait de traiter les lésions cartilagineuses en développant des biomatériaux contenant des cellules encapsulées dans des matrices support d'origine naturelle ou

synthétique. L'ingénierie tissulaire permettrait ainsi de produire *in vitro* des biotissus ayant les mêmes propriétés physiques et physiologiques que le tissu natif.

Les cellules souches mésenchymateuses:

Les études publiées sur l'ingénierie du cartilage, au cours des dix dernières années, utilisent le plus souvent des cellules stromales mésenchymateuses (CSM) adultes.

Ces CSM sont des cellules souches d'origine mésodermique qui donnent naissance aux différentes composantes du tissu conjonctif et génèrent également la composante stromale de la niche hématopoïétique. Dans un souci d'harmonisation, le comité de l'ISCT (International Society for Cellular Therapy) a proposé des standards de caractérisation des CSM (*Dominici M et al, 2006*), établissant des critères minimums de définition : (i) l'adhérence cellulaire au plastique dans des conditions de culture in vitro, (ii) l'expression de certains marqueurs de surface tels que CD73, CD90, CD105 et l'absence d'expression des marqueurs CD34, CD45, CD14 ou CD11b, CD79a ou CD19, (iii) la capacité de différenciation en ostéoblastes, adipocytes et chondrocytes (cellules d'origine mésodermique).

De plus, des effets immunomodulateurs des CSM ont été démontrés aussi bien *in vitro* qu'*in vivo*. Les CSM possèdent, en effet, des propriétés immunosuppressives très vastes liées à la production de facteurs solubles inductibles qui inhibent l'activation des principaux effecteurs de l'immunité. Les CSM ont la capacité de protéger les lymphocytes T de l'apoptose tout en inhibant leur activation et leur prolifération en réponse à de nombreux stimuli (*Benvenuto F et al, 2007*). *In vivo*, les propriétés immunosuppressives des CSM ont également été prouvées. Chez l'animal, l'administration de CSM induit la tolérance d'organes lors d'allogreffes et chez l'homme, un rôle bénéfique comme traitement préventif ou curatif de la maladie du greffon contre l'hôte (GvHD) a été observé (*Tisato V et al, 2007*). Les CSM sont également utilisées dans près de 720 essais cliniques et dans des indications très variées telles que les lésions osseuses et cartilagineuses, l'infarctus du

myocarde, des maladies auto-immunes ou encore dans des pathologies neurodégénératives. (www.clinical trialgov, consulté le 22/05/17)

Actuellement, les critères de choix du tissu d'origine des CSM pour les essais cliniques reposent essentiellement sur la richesse des prélèvements et leur facilité d'accès. L'isolement des CSM à partir de prélèvements de tissus adultes (moelle osseuse ou tissu adipeux) reste la méthode la plus employée. Cependant, il est nécessaire d'avoir recours à un geste invasif potentiellement douloureux (anesthésie) et associé à un risque plus élevé de contamination virale des prélèvements. De plus, les CSM issues de tissus adultes à partir de donneurs âgés présenteraient une nette diminution de leur prolifération (*Katsara O et al, 2011; Choudhery MS et al, 2014*). Le potentiel de prolifération limité *in vitro* est le résultat de la sénescence associée à l'arrêt de la croissance, un phénomène connu comme sénescence réplicative. Cette forme de sénescence est causée par plusieurs facteurs, notamment le raccourcissement progressif des télomères au cours de la culture continue *in vitro* attribuable à l'absence d'activité télomérase. Il a également été décrit que la capacité de différenciation *in vitro* et de régénération tissulaire *in vivo* des CSM issues de tissus adultes diminuent avec l'âge.

C'est pourquoi, les chercheurs se sont tournés vers d'autres sources de CSM, notamment la gelée de Wharton (GW) du cordon ombilical. Leur obtention est relativement simple et non invasive. Bien qu'ayant des caractéristiques comparables aux CSM issues de tissus adultes (moelle osseuse ou tissu adipeux), les CSM provenant du cordon semblent plus immatures sur le plan immunologique, ont un potentiel de prolifération plus élevé et peuvent se différencier en un nombre de tissus plus important (elles peuvent se différencier en adipocytes, ostéocytes ou en chondrocytes et même dans certaines conditions en cellules cardiaques ou hépatiques) (*Zheng L et al, 2010*).

Tous ces avantages font que les CSM-GW représentent une source potentiellement inépuisable de CSM, leur conférant ainsi une place de choix en ingénierie tissulaire. Cependant, leur utilisation ne peut se faire qu'en situation

allogénique et nécessite, de ce fait, une connaissance précise de leurs propriétés immunomodulatrices.

Les propriétés immunomodulatrices des CSM reposent sur trois principaux mécanismes : l'arrêt du cycle cellulaire en phase G1 chez les cellules immunitaires, un contact cellule-cellule entre CSM et cellules immunitaires et un effet paracrine des CSM. Les principaux facteurs exprimés par les CSM en réponse à une stimulation des cellules immunitaires sont : les microARN (en particulier miR-155), PD-L1, HLA-G, la prostaglandine E2 (PGE2), des cytokines (TGFß, IL6, IL10, HGF, VEGF...) et une enzyme (Indoleamine 2,3 -dioxygenase : IDO). Ces propriétés immunomodulatrices sont largement décrites, dans la littérature, pour les CSM issues de tissus adultes et commencent à l'être pour les CSM-GW. Cependant, le maintien de ces propriétés au cours de la différenciation chondrogénique reste peu connu en particulier lorsque les CSM sont maintenus en culture dans un biomatériau. De plus, certains des facteurs impliqués dans les propriétés immunomodulatrices sont connus pour jouer, également, un rôle dans la chondrogenèse. Ainsi, le TGF-β est impliqué dans l'une des étapes les plus importantes de la chondrogenèse : l'étape de prolifération et de condensation, et le VEGF intervient pendant la phase d'ossification (*Barry F et al, 2001; Dai J et al, 2007*).

Les matrices support :

La composition des matrices-support permet non seulement d'orienter la différenciation des cellules, mais aussi de leur donner un environnement tridimensionnel (3D) afin de guider la différenciation chondrogénique. Etant donné la finalité de l'ingénierie tissulaire du cartilage, le cahier des charges de ces matrices-support doit être précis et respectes les "bonnes pratiques de fabrication". Ces biomatériaux doivent avoir :

- des propriétés physico-chimiques :
- structure 3D : les biomatériaux doivent combler la lésion cartilagineuse par un échafaudage tridimensionnel et donner aux cellules un environnement similaire à celui du cartilage natif ;

- stérilisation: les biomatériaux doivent posséder une excellente résistance à la stérilisation ;
- porosité : les biomatériaux doivent posséder une haute porosité et présenter une importante interconnexion entre les pores afin de permettre les échanges de nutriments, de déchets et d'oxygène dans toute la structure.

❖ des propriétés fonctionnelles :

- biofonctionnelle: les biomatériaux doivent remplir leur fonction afin de s'intégrer au tissu et d'avoir les mêmes propriétés structurelles que le tissu natif ;
- biocompatible: les biomatériaux doivent être tolérés par l'organisme, au niveau local et général (non immunogène, non carcinogène). Cette biocompatibilité du biomatériau est nécessaire dès le départ de l'étude pour pouvoir y cultiver les cellules ensemencées ;
- biodégradable pour être détruit ou dissous une fois que son rôle de soutien n'est plus nécessaire ; lorsque les cellules auront produit leur propre matrice extracellulaire;
- résistance mécanique pour pouvoir subir des contraintes mécaniques similaires à celles subies par le cartilage articulaire in vivo et ne pas être dégradés.

Les biomatériaux utilisés pour l'ingénierie tissulaire du cartilage se présentent sous plusieurs formes : hydrogels, éponges ou réseaux de maillage et peuvent être d'origine synthétique ou naturelle. Des gels polymères naturels, tels que l'acide hyaluronique, le collagène et l'alginate (*Atala A et al, 1994*), ont été employés avec succès (*Risbud M et al, 2001*). Un essai clinique utilisant un hydrogel d'acide hyaluronique vient de s'achever, en janvier 2017, aux Etats Unis, pour soigner l'arthrose du genou (www.clinical trialgov, consulté le 22/05/17).

L'alginate (Alg), d'origine végétale, est un copolymère polyanionique, formé par des chaines de polysaccharides constituées de groupes acide guluronique et mannuronique. Il est soluble dans les solutions aqueuses et forme un gel stable. Ce polymère constitue un modèle de référence pour des études de morphologie cellulaire, de synthèse des protéoglycannes et de collagènes mais aussi, de

mécanobiologie des chondrocytes articulaires. Bien que l'alginate de sodium ne soit pas un composant naturel de la matrice extracellulaire, il présente une structure similaire à celle des glycosaminoglycannes du cartilage (*Wang X et al, 2009*). Les hydrogels d'alginate peuvent se présenter sous forme de biomatériau injectable, sous forme de billes ou de moules après polymérisation dans un bain de $CaCl_2$. Dernièrement, une équipe a développé un process de fabrication des hydrogels d'alginate basé sur la pulvérisation (*Jessica Tritz et al, 2010*). L'hydrogel contenant les cellules est ainsi pulvérisé sur un support, afin d'obtenir une colonisation homogène des cellules au sein du biomatériau.

L'acide hyaluronique (HA) est un des composants de la MEC du cartilage natif. Pour l'ingénierie tissulaire, il permet d'améliorer la prolifération des cellules et leur attachement au biomatériau grâce à des récepteurs membranaires. Il possède non seulement des propriétés rhéologiques remarquables en solution notamment en termes de viscoélasticité, mais il a aussi une action bénéfique sur l'activité de prolifération et de synthèse des chondrocytes (*Gigant-Huselstein C et al, 2004*). Ce biomatériau, extrait de tissu animal, peut être utilisé seul (*Jakobsen RB et al, 2010*) ou combiné avec d'autres biomatériaux comme l'alginate. Ainsi, dans des hydrogels d'alginate supplémentés en HA (Alg/HA), Reppel et al ont montré qu'après 4 semaines de culture, des CSM-GW étaient capables de s'adapter à leur environnement et d'exprimer les gènes et protéines spécifiques du tissu cartilagineux et notamment le collagène de type 2 (*Reppel L et al, 2015*).

Ces polymères se présentent souvent sous la forme d'hydrogels. Cette forme de biomatériaux a été identifiée comme un choix attractif de matrices support et se trouve d'ailleurs utilisée dans des applications médicales dès les années 1960. Ils répondent effectivement à de nombreux critères physico-chimiques et fonctionnels imposés par le cahier des charges des biomatériaux. Le premier étant la structure 3D puisque des cellules peuvent y être encapsulées. Ils possèdent également une teneur élevée en eau, présentent une faible toxicité et une bonne biocompatibilité. Ces propriétés en font par conséquent de bons candidats pour la régénération tissulaire,

en particulier dans le domaine du tissu cartilagineux. Enfin, comme tous biomatériaux, ils doivent être stérilisables et stérilisés avant que les cellules ne soient introduites à l'intérieur. Pour cela, plusieurs procédés sont utilisés tels que l'autoclave, la filtration si l'hydrogel n'est pas trop visqueux, l'irradiation germicide aux UV ou aux rayons gamma, en exposant l'hydrogel à l'oxyde d'éthylène (*Leo WJ et al, 1990; Lee DW et al, 2003; Mao S et al, 2012*). Bien que toutes ces approches soient efficaces, il faut faire attention à choisir une technique qui ne se dégrade pas, ne dénature ou ne change pas les propriétés physiques de l'hydrogel. Par exemple, un traitement UV prolongé peut dénaturer le collagène et favoriser la dégradation des peptides dans les hydrogels fonctionnalisés, tandis que l'irradiation gamma peut dégrader l'alginate (*Lee DW et al, 2003*).

Utilisés seuls, ces biomatériaux dits « monophasiques » ne permettent pas de mimer la structure zonale du cartilage. Ils peuvent seulement combler les lésions superficielles. La réparation des lésions cartilagineuses profondes appelées ostéochondrales nécessite alors d'utiliser un biomatériau multiphasique capables de mimer les propriétés physiologiques et la structure de deux tissus différents : le cartilage et l'os sous-chondral. Deux approches concernant une construction zonale sont décrites dans la littérature (*Klein TJ et al, 2009*).

- La première consiste à ensemencer des cellules différentes dans des couches de biomatériau de composition identique. Dans cette approche, les cellules, de phénotypes différents, vont synthétiser une MEC spécifique. En 2003, Kim T.K. a utilisé des sous-populations chondrocytaires issues des différentes couches cartilagineuses (superficielle, moyenne, profonde) dans un polymère synthétique (*Kim TK et al, 2003*).
- La seconde consiste à ensemencer des cellules identiques (chondrocytes ou CSM) dans des couches de biomatériaux de composition différente. La spécificité du biomatériau doit guider la différenciation des cellules vers un phénotype spécifique. Ainsi, Schiavi et al. ont mis au point un biomatériau biphasique composé d'alginate supplementé en acide hyaluronique pour

mimer le cartilage et en hydroxyapatite, principale composante de la matrice osseuse, pour mimer l'os sous chondral. Cette technique de conception basée sur la pulvérisation d'une suspension biomatériau/cellules, couche par couche a permis de reproduire une organisation zonale du cartilage mais dans laquelle les propriétés physico-chimiques du biomatériau sur les cellules doivent encore être étudiées (*Schiavi J et al, 2017*).

Objectifs scientifiques

L'enjeu de ce travail de thèse est donc, tout d'abord, de caractériser les CSM issues de la gelée de Wharton selon les critères de l'ISCT. Ce travail se situant dans le cadre de l'ingénierie ostéo-articulaire, notre finalité est de poursuivre le travail initié par Jessica Tritz-Schiavi en étudiant le comportement des CSM-GW dans un biomatériau multiphasique Alg/HA-Alg/Hap en étudiant les relations existant entre les propriétés physico-chimiques des hydrogels et le comportement cellulaire pour en améliorer la différenciation. Pour cela, nous évaluerons, tout d'abord, l'impact du procédé de stérilisation sur les propriétés physico-chimiques des hydrogels d'Alg/HA et d'Alg/Hap avant d'étudier l'évolution du comportement mécanique des hydrogels au cours de la différenciation chondrocytaire ainsi que leur impact sur le comportement des CSM (propriétés de différenciation et d'immunomodulation).

Caractérisation des CSM issues de la gelée de Wharton

L'ensemble des travaux ayant été réalisés sur 3 cordons ombilicaux différents, les CSM obtenues par la méthode des explants puis amplifiées jusqu'au 3ème passage en conditions hypoxiques ont été caractérisées sur le plan phénotypique, leur capacité à former des CFU-F (Fibroblast Colony Forming-Units) et leur viabilité. Les cellules obtenues et charactérisées présentaient un phénotype mésenchymateux par l'expression des marqueurs CD44, CD90, CD73, CD105 et CD166 et l'absence d'expression des marqueurs hématopoïétiques (CD34 et CD45) ainsi que du Complexe Majeur d'Histocompatibilité de classe II (HLA-DR). Les trois souches

maintenaient leur capacité clonogénique et moins de 6% des CSM étaient sénescentes. Ces résultats ont fourni la caractérisation des CSM avant leur ensemencement dans les hydrogels d'alginate.

Impact de l'ajout d'éléments matriciels dans des hydrogels d'alginate sur le comportement des CSM-GW

S'il est bien connu que l'incorporation de nanoparticules ou de polymères dans des hydrogels peut moduler les propriétés mécaniques des biomatériaux, nous ne possédons aucune étude du comportement des CSM issues de la gelée de Wharton dans un hydrogel d'alginate supplémenté en HA ou Hap (*Tautzenberger A et al, 2012*).

Cette étude vise alors à comparer l'impact des hydrogels d'alginate (Alg)/acide hyaluronique (HA), qui imiteront le cartilage, et des hydrogels d'alginate (Alg)/ hydroxyapatite (Hap), qui imiteront l'os sous chondral sur les CSM-GW. Ces hydrogels 3D-Alg/HA et Alg/Hap ont été obtenus par la méthode de pulvérisation d'origine décrite par Tritz et al (*Jessica Tritz et al, 2010*). Les propriétés mécaniques des hydrogels ainsi que la cytocompatibilité et les propriétés de différenciation ont été les élements de comparaison retenus dans cette étude.

Il apparaît ainsi que le biomatériau et plus spécifiquement l'apport d'éléments matriciels à l'intérieur de l'alginate impacte la viabilité ainsi que la prolifération des CSM-GW. En effet, le pourcentage de cellules vivantes dans les hydrogels d'alginate enrichis en Hap est significativement plus élevé que dans les hydrogels enrichis en HA. Ces résultats sont vraisemblablement associés aux propriétés rhéologiques et mécaniques des hydrogels puisque les hydrogels Alg/Hap présentent une résistance à la contrainte plus importante que les hydrogels Alg/HA (**Figure 1**)**.** En revanche, les CSM-GW cultivées pendant 30 jours dans ces différents hydrogels ont montré une capacité à synthétiser une matrice extracellulaire contenant du collagène et des protéoglycannes.

Cette étude a également souligné l'impact de l'autoclave sur les propriétés physico-chimiques des hydrogels étudiés. Nous pouvons alors nous interroger de l'impact réel des élements matriciels sur les cellules lorsque le procédé de stérilisation réalisé en amont semble aussi délétère sur la viscosité et la résistance à la contrainte de la matrice support.

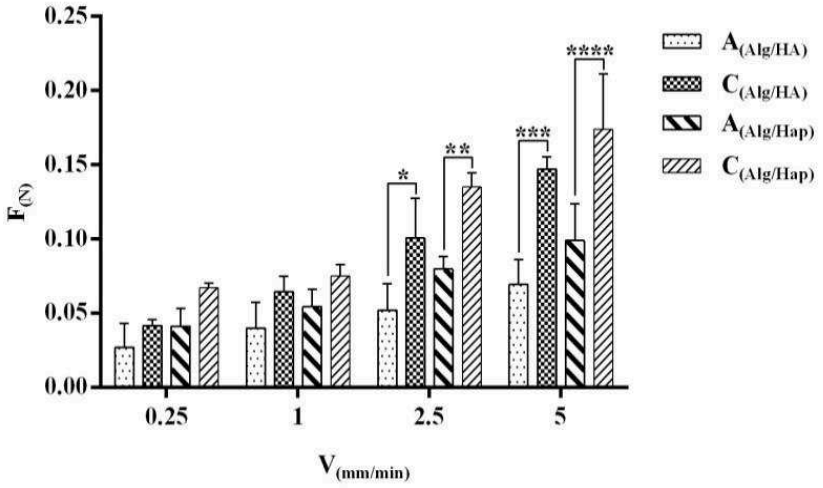

Figure 1: Résistance des échafaudages hydrogel 3D-Alg/HA et Alg/Hap correspondant à une indentation de 0.35mm effectuée à différentes vitesses. Les résultats correspondent à des valeurs en moyennes ± SD, avec n ≥3 et ont été analysés par l'analyse de la variance (ANOVA) (*p < 0.05, **p < 0.01, ***p < 0.001 and ****p < 0.0001; autoclave (A), control (C)). On consaste d'abord que les hydrogels présentent un comportement de type viscoélastique ou/et viscoplastique. Par ailleurs, la sensibilité à la vitesse est plus marquée pour les échantillons de contrôle que pour ceux qui ont été traités à l'autoclave.

Influence du procédé de stérilisation sur les propriétés physico-chimiques des hydrogels Alg/HA

De nombreuses études rapportent que l'alginate reste un polymère difficile à stériliser et à manipuler (*Puppi D et al, 2010*). Quelle que soit la procédure utilisée (autoclave, oxyde d'éthylène, irradiation gamma,…), elle conduit le plus souvent à la dépolymérisation des chaînes d'alginate. De plus, il n'existe aucune analyse statistique qui étudie l'interrelation entre les caractéristiques physico-chimiques de l'hydrogel d'alginate après la stérilisation et le comportement des cellules en particulier les CSM.

Dans cette partie du travail, nous avons évalué l'impact de deux procédés de stérilisation (autoclave et rayonnement UV pendant 25 et 50 minutes, respectivement nommés UV1 et UV2) sur les propriétés physico-chimiques d'un hydrogel Alg/HA ainsi que sur les fonctionnalités des CSM. L'objectif étant également d'estimer s'il existe une relation significative entre l'évolution des propriétés physico-chimiques des hydrogels induit par la stérilisation et le comportement des cellules. Pour cela, la poudre Alg/HA ainsi que l'hydrogel à l'état polymérisé ont été analysés à l'aide d'ATR-FTIR, de HPLC-SEC, de tests rhéologiques, d'indentation et de tests de stérilité. Les comportements cellulaires des hydrogels ont été évalués par la viabilité et la prolifération des cellules, et la différenciation chondrogénique. Les effets des paramètres de traitement et leur corrélation avec les autres caractéristiques ont été déterminés statistiquement par l'analyse des composants principaux (PCA). Dans cette étude, nous avons montré que le comportement cellulaire dans les hydrogels à base d'alginate n'était pas seulement régulé par la masse molaire ou la de l'hydrogel, mais également au procédé de stérilisation, en particulier au temps de stérilisation. Le procédé de stérilisation par UV, pendant 50 minutes semble être un bon compromis pour préserver les propriétés physico-chimiques de l'Alginate et du HA tout en favorisant la prolifération des CSM ainsi que leur différenciation chondrogénique (**Figure 2**).

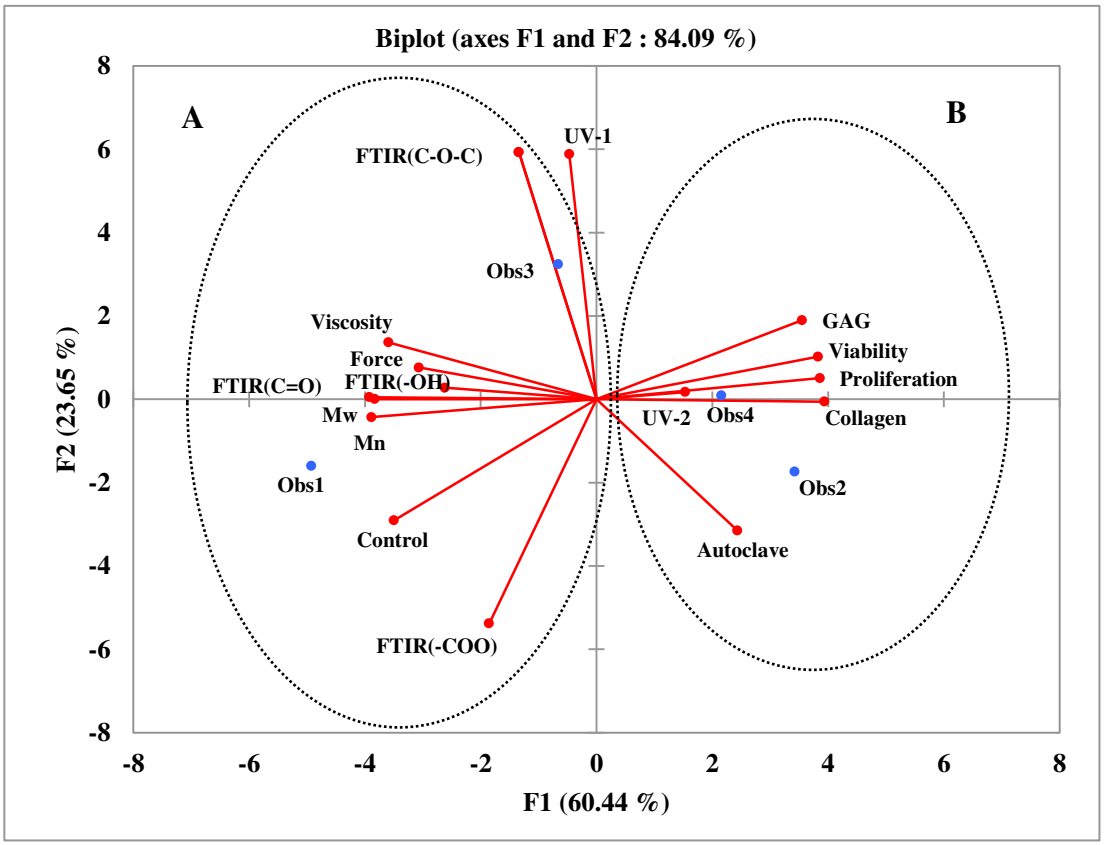

Figure 2: Illustration du plan principal (F1, F2) de l'ensemble des données concernant le gel d'Alg/HA, en fonction des divers traitements de stérilisation. Ces données répresentent les caractéristiques physiques et mécaniques (masses Mw and Mn, viscosité, strength), les caractéristiques relatives au comportement cellulaire (viabilité, prolifération, production de collagène, GAG), les différents traitements (UV-1, -2, Autoclave, Contrôle). On constate que le traitement UV-2 représente le meilleur traitement, notamment pour ce qui concerne le comportement des cellules.

Evolution du comportement mécanique des hydrogels au cours de la différenciation chondrocytaire et impact sur le comportement des CSM-GW

Dans cette dernière partie de notre travail, nous avons voulu savoir comment évoluaient les propriétés mécaniques des hydrogels Alg/HA et Alg/Hap et quel était le lien entre cette évolution et le potentiel de différenciation des CSM mais également sur leurs propriétés immunomodulateurs. A notre connaissance, aucune étude ne s'est encore intéressée au lien potentiel entre l'environnement mécanique des CSM et leur propriété paracrine. Sur la base des résultats obtenus et de l'analyse des composantes principales (**Figure 3**), nous avons constaté qu'il existait une

inter-relation entre les propriétés mécaniques, biologiques mais aussi immunologiques. Ainsi, nous avons montré qu'il existait une corrélation positive entre la résistance à la contrainte de l'hydrogel et la sécrétion de la Prostaglandine de type 2 (**Figure 3**).

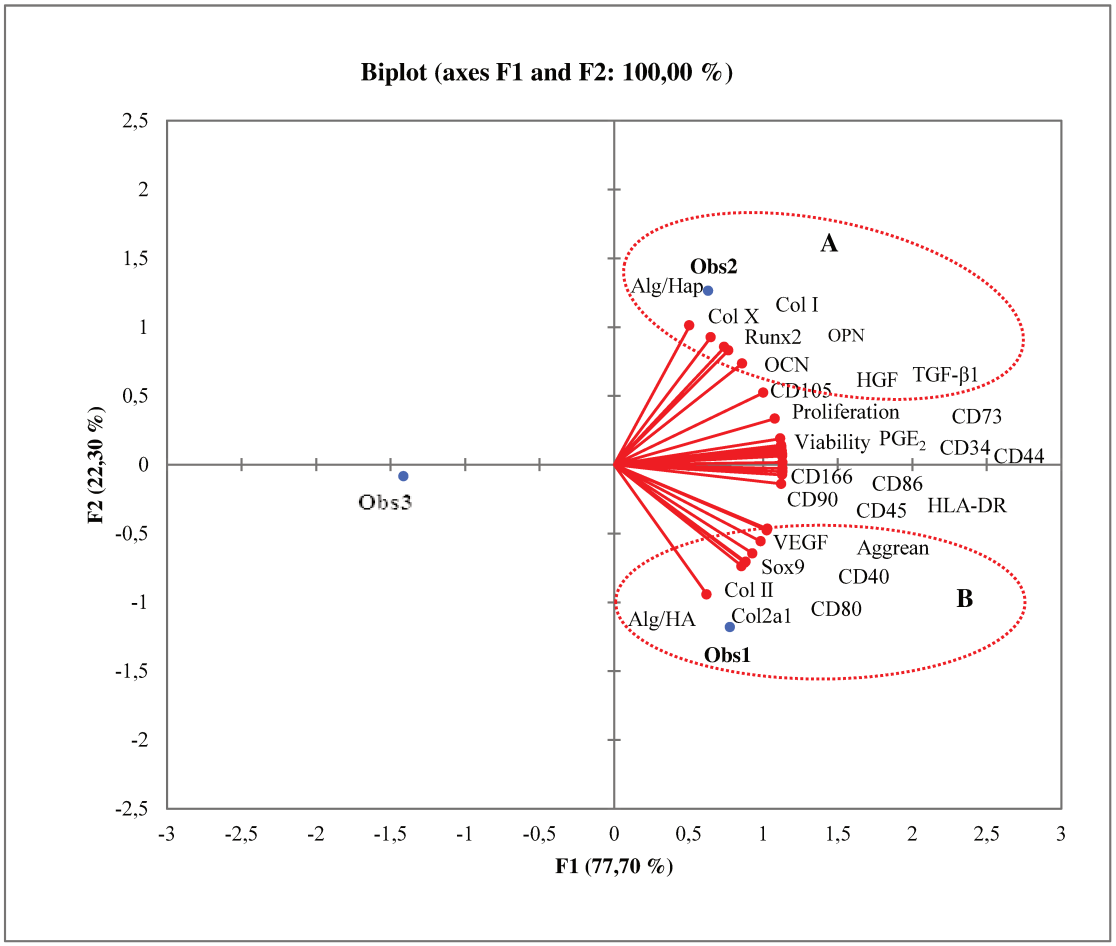

Figure 3: Représentation à l'aide de l'analyse en composantes principales des différentes caractéristiques des cellules contenues dans les hydrogels Alg/HA et Alg/Hap. Les comportements sont très différents dans les deux cas.

State of the art

1. Articular cartilage

Articular cartilage (also called hyaline cartilage) is the most abundant type of cartilage in human body because it appears on the ends of bones and facing the synovial fluid where they form mobile joint (**Figure 4**). Their main function is to allow the gliding of the latter thanks to an extremely low coefficient of friction. This highly specialized connective tissue is also characterized by its mechanical properties, resulting from cyclic tension, shear and compression forces induced by weight and body movement.

It is a non-innervated and non-vascularized tissue, composed of a single cell type (the chondrocyte), and abundant extracellular matrix rich in type II collagen and proteoglycans, which contribute to its elasticity.

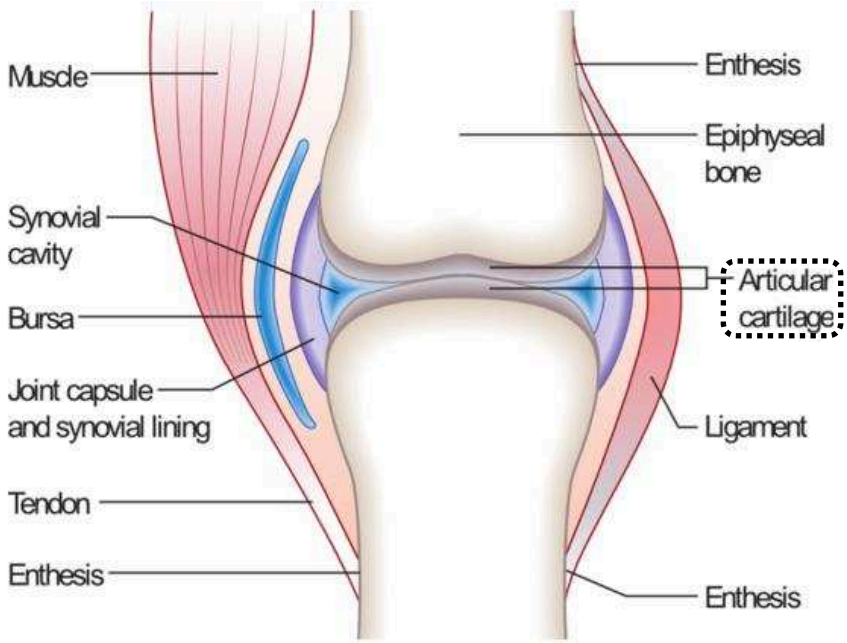

Figure 4: Representation of the synovial joint at the level of a knee. It is comprised of bone, cartilage, synovial fluid/membrane, tendons and ligaments. ("Structure of Synovial Joints" Boundless Anatomy and Physiology, 11 oct 2016)

1.1. Organization of articular cartilage

Cartilage is composed of water (60-85% of the tissue weight), collagen (50-75%), chondrocyte and an extracellular matrix (ECM) (proteoglycan =15-30%). Giving the articular cartilage remarkable mechanical and load-bearing properties are type II collagen for tensile strength and glycosaminoglycan (GAGs) for resilience (*Schulz RM et al, 2007*). For the articular cartilage, it can be distinguished into 4 layers (**Figure 5**) (*Madry H et al, 2010; Wang F et al, 2009; Lyons TJ et al, 2006*).

1.1.1. Superficial layer

It makes up 10-20% of cartilage volume. The extracellular matrix is rich in type II collagen fibers which are tangent to the surface of articular and parallel to mechanical stress. Flattened chondrocytes and collagen fibers are arranged tangentially to the articular surface as well as the highest content of collagen and the lowest concentration of proteoglycans; it has greatest ability to resist to shear stresses and serves as a guiding surface for joint.

1.1.2. Transitional layer

It makes up 40-60% of cartilage. Collagen fibers and chondrocytes are directed perpendicularly to the subchondral plate. Its role is not only to distribute loads to the tissue but also to resist to compression stresses.

1.1.3. Deep layer

It makes up 30% of cartilage volume and is composed of type X collagen, but without proteoglycan (PG). It separates hyaline cartilage from subchondral bone. Moreover, it also contains the tidemark layer which straddles the boundary between calcified and un-calcified cartilage.

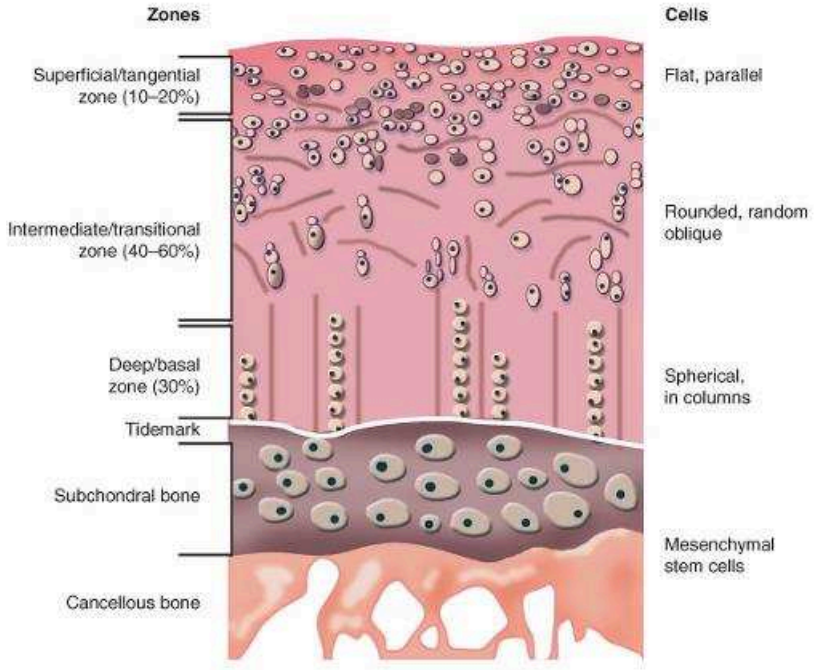

Figure 5: Organization of articular cartilage. Different cell morphology, collagen orientation and proteoglycan (PG) content is found in the stratified organization of cartilage: the superficial zone has flattened cells with the highest content of collagen and the lowest concentration of proteoglycans. Intermediate zone has rounded cells with randomly oriented collagen fibers and higher PG content. Deep zone has spherical cells in columns distribution, without PG and the collagen fibers are perpendicular to tidemark. (https://musculoskeletalkey.com)

1.2. Composition

1.2.1. Chondrocyte

The chondrocyte is the only cell type found in articular cartilage (*Lin Z et al, 2006*). They produce and maintain the cartilaginous matrix, which consists mainly of collagen and proteoglycans; but they are also able to degrade this matrix. Comparing with other tissues, chondrocyte represents a relative low percentage of the cartilage matrix volume (1–5 %). Due to the lacking of cell-cell contact in adult tissue, the regulation of tissue homeostasis has to occur *via* the extracellular matrix (ECM). Between the ECM and the underlying bone is synovial fluid which is provided nutrients and oxygen for chondrocytes. The passage of water and nutrients between cartilage and synovial fluid is possible thanks to cyclical forces. In addition, due to the avascular structure, chondrocytes have metabolism close to anaerobic one (*Das RH et al, 2010; Sengers BG et al, 2005*).

1.2.2. Extracellular matrix

1.2.2.1. Collagen

The collagen molecule consists of three polypeptide chains, called a chain, with the characteristic triplet repeat sequence Gly-X-Y and each chain is generally more than 1000 residue long (*Bhattacharjee A and Bansal M, 2005*). As shown in **Figure 6**, three a chains that assemble into triple helices of procollagen, at the ends of procollagen are cut to form tropocollagen which assembles into fibrils.

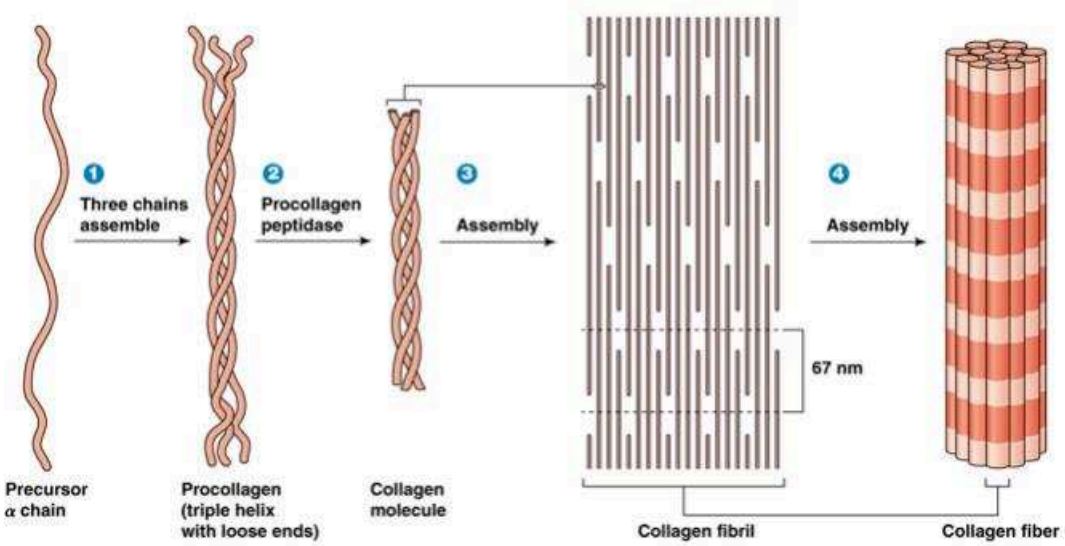

Figure 6: Assembly of the α-chains of collagen into fibrils. The collagen is formed from three α chains that assemble in triple procollagen helixes, then, the ends of the procollagen are cut to form a tropocollagen which will assemble into fibril. (BIOL2060: Principles of Cell Biology)

a) *Type II collagen*

This kind of collagen represents 90 % of total collagens found in articular cartilage. Type II collagen in mature cartilage is composed of three identical polypeptide chains which contain a lot of hydroxylysine and glucosyl galactosyl residues and allowing interactions with PG, α 1 (II), and belong to the fibril forming class of collagens (class 1). Alternative splicing occurs in the type II collagen gene. In the procollagen gene exon 2 encodes for a cysteine-rich domain in the amino-terminal propeptide which results in a type II A procollagen. This type IIA is expressed by immature chondrocytes but is not expressed in mature cartilage. Type IIB collagen is present in mature cartilage and its exon 2 is spliced out. Type II

collagen is synthesized and secreted as a procollagen precursor whose non-helical extensions are removed by enzymes. During this process the large (35 kDa) chondrocalcin is released (The N-terminal propeptide). Hereafter the trimmed collagen is incorporated into the ECM where it is crosslinked. Within the deep layer of cartilage arcades of thick fibrils are formed whereas in the surface fine fibrils are arranged horizontally (*McAlinden A et al, 2002; Ryan MC et al 1990; Aydelotte MB et al, 1988*).

b) *Type VI collagen*

It is only found in the pericellular matrix surrounding the chondrocyte (*Poole CA et al 1992; Chang J et al, 1997; Hambach L et al, 1998*). The cell surrounded by hyaluronan and the layer of type VI collagen is called a "chondron". Chondrons harbor and protect the chondrocytes from mechanical forces (*Youn I et al, 2006; Knight MM, 2011*).

c) *Type IX collagen*

It belongs to the class 3 short-helix molecules which may function as a connector between type II collagen fibers. A molecule chondroitin sulfate can be linked covalently to a globular domain of the protein and the favored interaction with other collagen fibers. Type XI collagen is a class1 (fibril forming) collagen and is co-assembled in the heterotypic fibrils of articular cartilage (**Figure 7**).

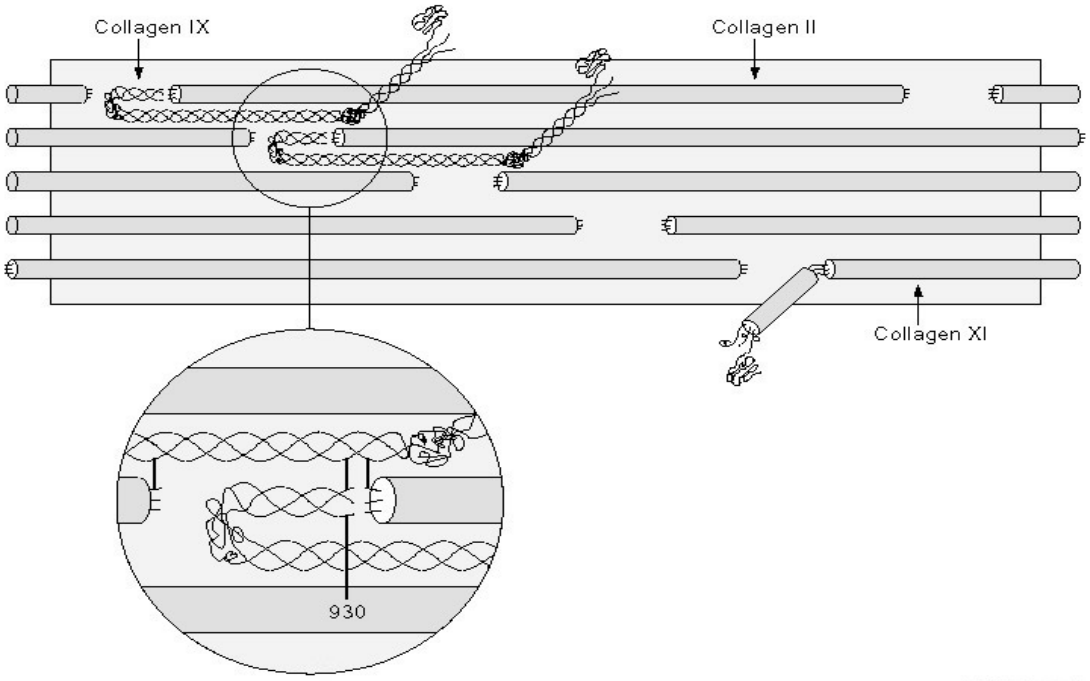

Figure 7: Assemblage of collagen fibers of type II, IX and XI. In cartilage, the types II, IX and XI collagen are assembled to form heterotypic fibrils, in particular by means of bonds between the globular domains of type IX collagen and type II collagen. (Seibel et al. 2006)

1.2.2.2. Proteoglycan and glycosaminoglycans

The proteoglycan aggregate is the major structural component of the extracellular matrix of the cartilage, composed of aggrecan, hyaluronan (HA) and link protein (LP) (**Figure 8**) *(Watanabe H et al, 2004).* Aggrecan is the major proteoglycan in the articular cartilage which consists of a central protein with multiple sulfated glycosaminoglycans (GAG's), especially Ketatan Sulfate and Chondroitine Sulfate, covalently attached to it. Its abundance and unique molecular features provide the disc with its osmotic properties and ability to withstand compressive loads *(Sivan SS et al 2014).* Aggrecan is a multi-modular molecule expressed by chondrocytes. Its core protein is composed of three globular domains (G1, G2, and G3) and a large extended region (CS) between G2 and G3 for glycosaminoglycan chain attachment. G1 comprises the amino terminus of the core protein. This domain has the same structural motif as link protein. Functionally, the G1 domain interacts with hyaluronan acid and link protein, forming stable ternary complexes in the extracellular matrix. G2 is homologous to the tandem repeats of G1

and of link protein and is involved in product processing. G3 makes up the carboxyl terminus of the core protein *(Aspberg A et al 2012).* Aggrecan plays an important role in mediating chondrocyte-chondrocyte and chondrocyte-matrix interactions through its ability to bind hyaluronan *(Kiani C et al 2002. Maroudas A et al, 1998).* Keratan sulfate (KS) is acting as a constitutive molecule of the extracellular matrices, this GAG also plays a role as a hydrating and signaling agent in cornea and cartilage tissues *(Pomin VH.et al 2014).* Hyaluronic acid (HA) is a polysaccharide chain composed of repeating disaccharide units. HA is found in high concentrations in various tissues in the body including cartilage and other connective tissues as well as synovial fluid. It is known to support the normal joint biology as an effective lubricator and shock absorber *(Watterson JR et al, 2000)*. As shown in **Figure 8**, Aggrecan binds hyaluronan through its N-terminal G1 domain in ternary complex with link proteins. The G1 domain and link proteins are homologous, with an immunoglobulin-like repeat (A) followed by two proteoglycan tandem repeats (B and B'). In aggrecan, the G1 is followed by a second globular domain (G2), separated from the G1 by an extended interglobular domain. The G2 domain consists of two proteoglycan tandem repeats (B and B'). The central, and largest, part of aggrecan is the glycosaminoglycan attachment region, an extended protein stretch carrying keratan sulfate and chondroitin sulfate chains. This is followed by the C-terminal G3 domain, which consists of an epidermal growth factor (EGF) repeat (E1), a calcium-binding EGF repeat (E2), a C-type lectin domain (L), and a complement regulatory protein repeat (C). Hyaluronan (HA) is shown in red, aggrecan in blue (core protein) with red glycosaminoglycan chains, link protein in green. The structural repeat composition of each globular domain of link protein and aggrecan is shown above and below the two proteins, respectively, as indicated by dashed lines.

A glycoprotein, LP (40-48 kDa) stabilizes the aggregate by binding to both hyaluronic acid and aggrecan. In the absence of LP, aggregates are smaller and less stable than they are in the presence of LP. The amino acid sequences of LP can be

divided into three domains; an N-terminal domain that falls into the immunoglobulin super-family and two C-terminal domains that are similar to each other.

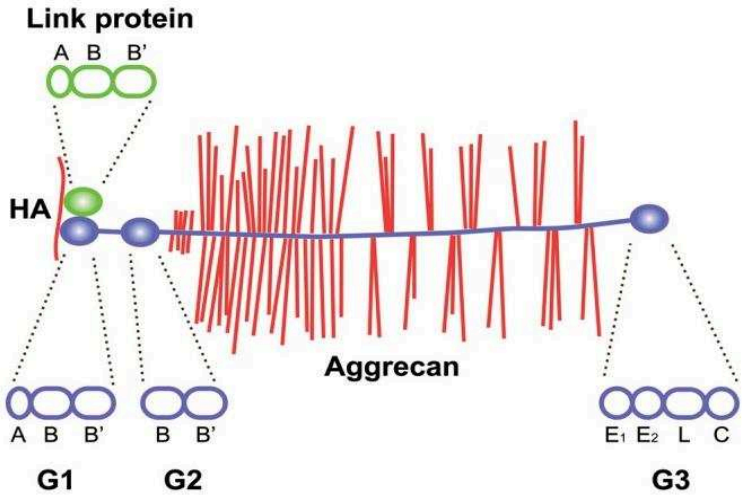

Figure 8: Composition of aggrecan. It is composed of a core protein that consists of 3 globular domains (G1, G2 and G3) between which chondroitin sulphate and keratan sulphate are attached; this molecule is very hydrophilic and large in size. The cores proteins can bind to an HA chain and form an assembly whose volume may be that of a bacterium. (Watanabe H et al, 2004)

1.3. Articular cartilage disease and repair

Under normal condition, articular cartilage can be effective against the harsh mechanical circumstance of the joint. However, it has difficult ability to self-repair due to poor blood supply and low metabolic activity. Once cartilage is damaged from trauma or degenerative pathology, it will degrade and ultimately turn into osteoarthritis (OA) (*Jiang Y et al, 2015; Lories RJ et al, 2011; Panseri S et al, 2012; Beyzadeoglu T et al, 2012*). OA is a chronic disease which along with severe pain, joint deformities, and motion losses. Resulting in the destruction of cartilage structure and worse affects its mechanical function (*Madry H et al, 2011*). Hence the treatment of partial- and full-thickness cartilage lesions is becoming more and more important. Several treatments have been developed for cartilage repair including microfracture, periosteal arthroplasty, mosaicplasty and autologous chondrocyte transplantation (ACT) as seen in **Figure 9**. Although these treatments are effective, disadvantages exist, as microfracture (delay cartilage degeneration only in the short-term) (*Solomon DJ et al, 2007; Goyal D et al, 2013; Xing L et al 2013*),

periosteal arthroplasty (donor site morbidity, limited available tissues) (*Getgood AM et al, 2012; Siclari A et al, 2012*), mosaicplasty (a new defect at the donor site) (*Kircher J et al, 2009*), autologous chondrocyte implantation (limited supply of healthy chondrocytes) (*Brittberg M, 1999*), and osteochondral allograft transplantation (immunogenic reaction, less weight-bearing) (*Friedlaender GE et al, 1999; Bugbee W et al, 2012; Kim YS et al 2012*).

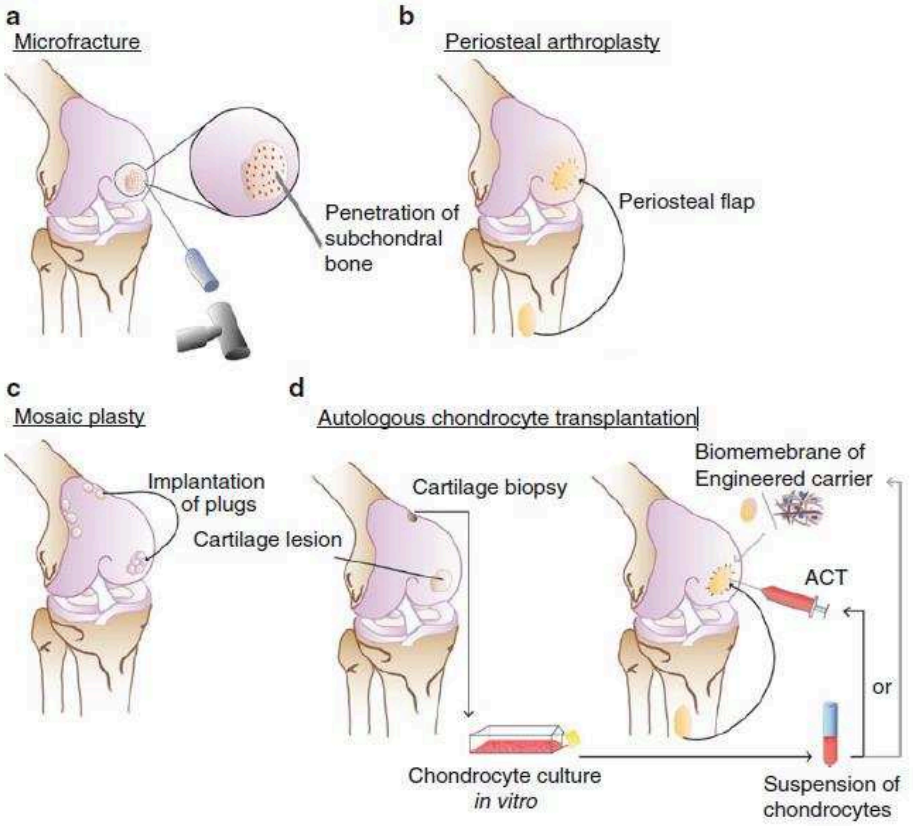

Figure 9: Current treatments for cartilage repair. (a) Schematic diagram of the process of microfracture. (b) Schematic diagram of the process of periosteal arthroplasty. (c) Schematic diagram of the process of mosaicplasty. (d) Schematic diagram of autologous chondrocyte transplantation (ACT) or biomemebrane of engineered carrier. (Pieter J Emans and Lars Peterson, Book, part I, 2014).

2. Cartilage tissue engineering (CTE)

Cartilage tissue engineering is an emerging discipline that combines the principles of engineering and biological sciences that can form functional biological substitutes notably restore the functions of altered articular cartilage. The standard cartilage tissue engineering strategy relies on several essential components including: cells,

biomaterial scaffolds, biological or environmental factors with mechanical stimuli and bioactive factors, as shown in **Figure 10** (Doulabi AH et al, 2014).

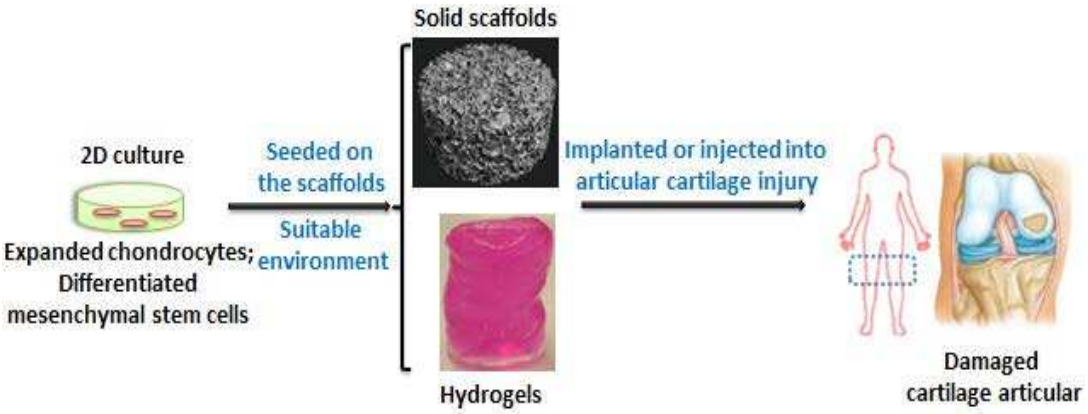

Figure 10: Strategy of articular cartilage tissue engineering and combination of chondrogenic cells (expanded chondrocytes or differentiated msenchymal stem cells) with biomaterials and bio-factors is crucial for the development of cartilage tissue-engineering strategies. (Doulabi AH et al, 2014)

2.1. Stem cells

Stem cells are undifferentiated biological cells that can differentiate into specialized cells in the body during early life and growth. Stem cells are distinguished from other cell types by two important characteristics. First, they are unspecialized cells capable of renewing themselves through cell division, sometimes after long periods of inactivity. Secondly, under certain physiologic or experimental conditions, they can be induced to become tissue- or organ-specific cells with special functions. In mammals, there are two broad types of stem cells: embryonic stem cells, which are isolated from the inner cell mass of blastocysts, and non-embryonic "somatic" or "adult" stem cells, which are found in various tissues.

2.1.1. Mesenchymal stem cells (MSC)

2.1.1.1. Characterization

In order to gain a clear insight of MSC capacities, the International Society for Cell Therapy (ISCT) proposed criteria that comprise (1) adherence to plastic in standard culture conditions; (2) expression of the surface molecules CD73, CD90, and CD105 (**Table 1**) and the absence of CD34, CD45, HLA-DR, CD14, CD11b, CD79a, or CD19 surface molecules; and (3) *in vitro* differentiation potential towards

mesodermal lineage (osteoblasts, adipocytes, chondroblasts, myocytes and keratinocytes) (**Figure 11**).

Table 1: Functions of the main markers expressed on the surface of MSC

Markers expressed on the surface of MSCs	Features
CD73	Ecto-5'-nucleotidase / Hydrolysis of AMP
CD90 (Thy-1)	Glycoprotein / Adherence and migration
CD105 (Endoglin)	Glycoprotein / TGF-β III Receptor

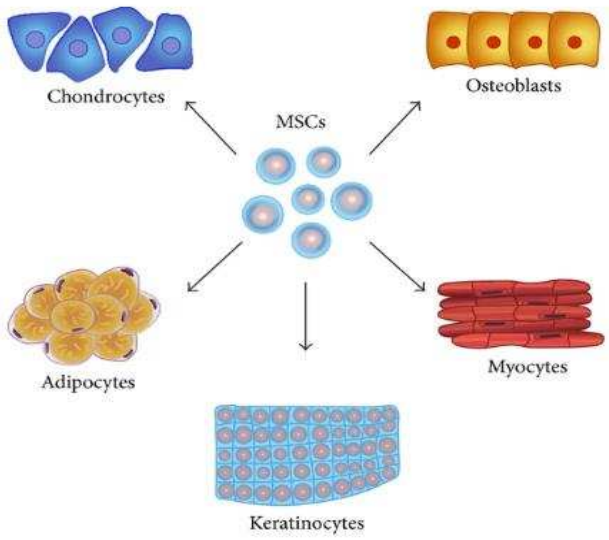

Figure 11: Differentiation potential of mesenchymal stem cells. Human mesenchymal stem cells (hMSCs) are adult stem cells, which have the capacity for multi-lineage differentiation, giving rise to a variety of mesenchymal phenotypes such as osteoblasts (bone), adipocytes (fat), chondrocytes (cartilage), myocytes(muscle tissue) and keratinocytes (skin). (Isakson M et al, 2015)

MSC isolated from these peripheral tissues are frequently thought of as equivalent to those derived from bone marrow due to significantly overlapping properties; however, there is accumulating evidence to suggest that there are differences between these populations, including their expression profiles and diferentiation potential. For example, concerning chondrogenic potential, both synovium- and BM-MSC seem to have a greater ability to generate chondrocytes than ADSC (*Sakaguchi et al, 2005*). These differences seem to be link to a tissue-of-origin « memory ». Additionally, colony-forming unit–fibroblast (CFU-F) and proliferation potential determined by the population doubling time are also criteria

which are used to evaluate the capacity of MSC. These criteria were established to standardize human MSC isolation but may not apply uniformly to other species (*Dominici M et al, 2006*).

2.1.1.2. Chondrogenesis

Chondrogenesis is a key event in developing limb buds beginning in the center of condensed mesenchyme *(Urist MR et al, 1976).* Chondrogenesis begins with mesenchymal cell recruitment and migration, proliferation *(Grassel S et al, 2007)*, then to form the chondroprogenitor mesenchymal cells. This first step called mesenchymal condensation is a pre-requisite of chondrogenesis and depended on the signals initiated by cell-cell and cell-matrix interaction (*Vinatier C et al, 2009*) (**Figure 12**). It is also associated with increased cell adhesion and formation of gap junctions and changes in the cytoskeletal architecture. At this stage, the matrix of cellular synthesize type I collagen, type IIA collagen, fibronectin, and proteoglycans (*Sandell LJ et al, 1994*). After, MSC turn to chondroblasts and chondrocytes. The Sox9 transcription factor plays an important role in the developing of this tissue. It begins to be expressed at the chondroprogenitor stage, and stimulates the expression of type II, IX and XI collagen and aggrecan of the hyaline cartilage (*Lefebvre V et al, 2005*).

Hypertrophic maturation of chondrocytes requires the Runx domain family transcription factors Runx2 and Runx3 as well as a decrease in the expression and/or activity of the Sox proteins (*Yoshida CA et al, 2005*). The Runx2 transcription factor have benefited for the mineralization of the tissue with the deposition of calcium crystals (*Cook D et al, 2013*), such as hydroxyapatite and chitosan. Chondrocytes stop at this stage of maturity in the process of endochondral ossification. However, during chondrogenesis, Wnt/β-catenin acts at two stages, at low levels to promote chondroprogenitor differentiation and later at high levels to promote hypertrophic chondrocyte differentiation and subsequent endochondral ossification. (*Tamamura Y et al, 2005*). Thus, a complex transcriptional network governs the process of chondrogenesis from mesenchymal stem cell commitment to

terminal differentiation. The proliferation and differentiation of MSC is elaborately controlled by the interplay of positive and negative factors (*Michigami T et al, 2014*).

Lastly, several studies point toward a functional role for microRNAs (miRs) in controlling chondrocyte differentiation (**Figure 13**). In their review, Wu C. *et al.* indicated that more than 25 miRs are implicated in chondrogenesis (*Wu C et al, 2014*). These miRs mainly participate in the regulation of cell differentiation by targeting the transcription factors and growth cytokines. Thus, over-expression of miR-145 and miR101 decreased not only expression of Sox9 at protein levels but also mRNA levels for chondrogenic marker genes, like type II collagen, aggrecan, COMP, type IX collagen and type XI collagen.

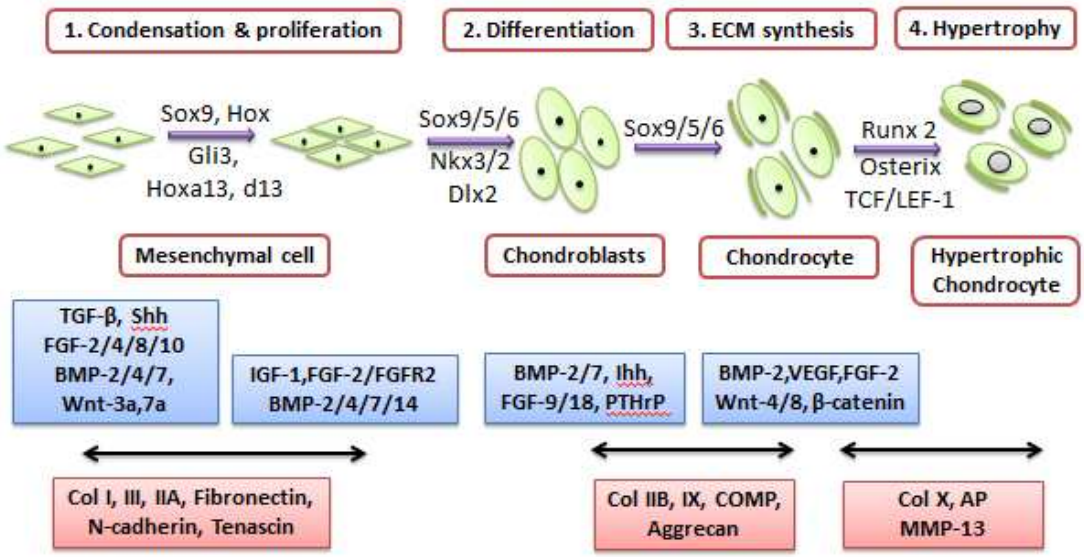

Figure 12: The different stages of chondrogenesis, showing the temporal patterns of growth and differentiation factors. (1) MSCs condense to from a dense cell mass. (2) MSCs proliferate and differentiate into chondroblasts. (3) The cells start to secret the ECM of cartilage and become mature chondrocytes. (4) Eventually, chondrocytes start to become hypertrophic. (Vinatier C et al, 2009)

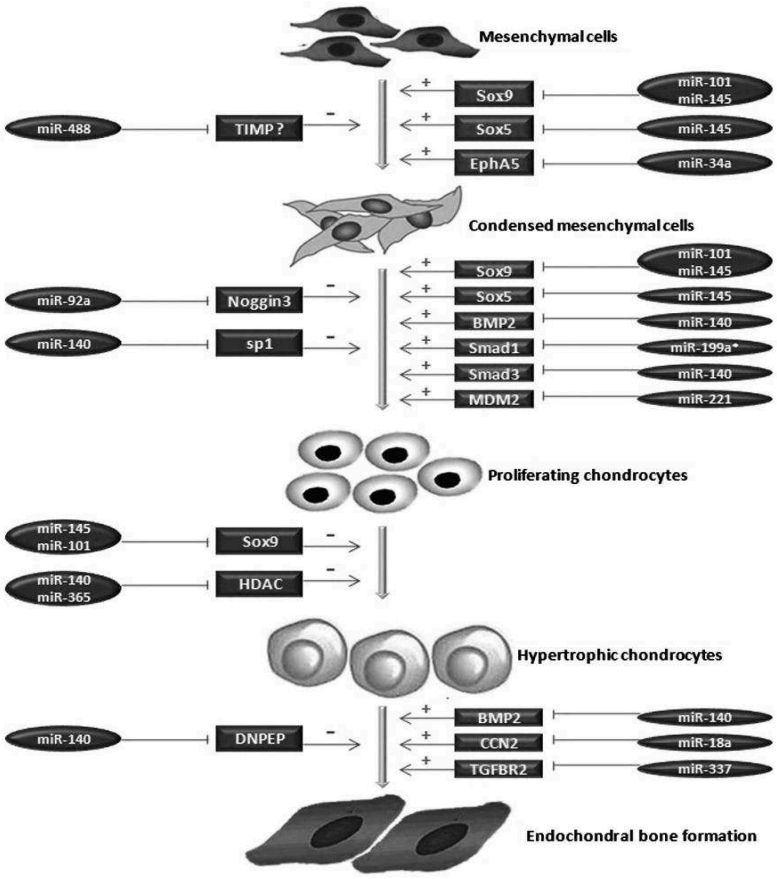

Figure 13: MicroRNAs (miRNAs) and their target factors in the process of chondrogenic differentiation. The roles of inhabitation are indicated by the '–' symbol and the roles of promotion are indicated by the '+' symbol. (Wu C et al, 2014)

2.1.1.3. Immunoregulatory of MSC

The cellular microenvironment and inflammatory context play key roles in determining MSC phenotype and their effects on the immune system. MSC demonstrate marked plasticity, exerting both pro- and anti-inflammatory phenotypes dependent on these environmental stimuli (*Waterman RS et al, 2010*). Through balancing this activating or suppressive phenotype MSC may be central to regulating immune control and tissue repair and regeneration. So, in function of the microenvironment, MSC are able to modulate the response of immune cells of the innate and adaptive immune system (**Figure 14**). Immune properties of MSC rely on three main mechanisms: the arrest of the cell cycle of immune cells at the G1 phase, a direct interaction of MSC with immune cells and a paracrine effect of MSC.

❖ Arrest of the cell cycle of immune cells at the G1 phase:

MSC are capable involving “cell to cell” contact and soluble molecules, to keep T cells quiescent in the G0 phase of the cell cycle while supporting their survival. Work by various groups supports the notion that MSC induce cell cycle arrest at the G0/G1 phase by down-regulating cyclin D2 expression and decreasing the transcription and translation levels of IL-2 and soluble IL-2 receptors in T cells (*Glennie S et al, 2005*). MSC are also able to act on arrest division of other immunocompetent cells including B cells (*Corcione A et al, 2006*), dendritic cells (*Ramasamy R et al, 2007*) and NK cells (*Li Y et al, 2015*). Recently, Vellasamy S et al. suggested that transcriptomic changes in activated T cells are at the origin of this mechanism. In fact, they reported that pro-inflammatory cytokines and chemokines such as IFN, CXCL9, IL2 and CCND3, were greatly downregulated. These changes in gene expression profoundly affect the canonical pathway of T-helper differentiation (*Vellasamy S et al, 2016*).

❖ Direct interaction of MSC with immune cells:

Many studies have demonstrated that MSC can regulate the activation and function of adaptive immune through direct interaction (*Uccelli A et al, 2006; Deng W et al, 2005*). For example, MSC can suppress T cells at several key steps of T cell-mediated immune responses, including survival, activation and differentiation of T cell subsets. To understand how these regulations could occur, studies investigated the effect of MSC on T cell in co-cultures. They showed not only that MSC were able to suppress T-cell proliferation and induce apoptosis of activated T cells but also that this phenomenon requires a dynamic cross talk between MSC and T-lymphocytes (*Djouad F et al, 2003; Plumas J et al, 2005*).

❖ Paracrine effect:

MSC produced large amounts of soluble mediators as cytokines, growth factors, or differentiation factors involved in the regulation of inflammation, immune responses but also in angiogenesis, chimioattraction and cell differentiation (*Nauta AJ et al, 2007; Cao HJ et al, 2017*). The main factors expressed by MSC in response to

immune cell interactions are: microRNAs, PD-L1, HLA-G, Prostaglandin E2 (PGE_2), cytokines (transforming growth factor-β, TGF-β), IL6, IL10, HGF, VEGF…), and one enzyme (Indoleamine 2, 3–dioxygenase: IDO). Immune properties of adult MSC have been widely described.

In an allogenic context, MSC exhibit significant immunomodulatory properties, they are able to escape the immune system recognition mechanisms and modulate the defense mechanisms of the host through secretion of soluble factors (Jarvinen L et al, 2008; Ge W et al, 2010; Najib El Haddad, 2011). The MSC are able to inhibit the proliferation of T helper (Th) and cytotoxic T cells. The maturation of immature dendritic cells (iDCs) is inhibited by IL-6, while reduction in the expression of co-stimulatory molecules CD40, CD80, and CD86 could cause an inhibition of T cell activation. Through the actions of MSC, monocytes are directed to differentiate into alternative anti-inflammatory M2 phenotype.

The soluble factor HLA-G which is expressed by MSC fulfils an important function in allogenic context. In fact, HLA-G molecules could reverse MSC ability to (i) generate in vitro the expansion of CD4+CD25+ FoxP3+ regulatory T cells, (ii) inhibit the alloproliferative T cell response, and (iii) suppress the cytotoxic function of NK cells. These results show that HLA-G molecules actively contribute to the immunosuppressive properties exerted by MSC (*Selmani et al, 2008; Selmani et al, 2009*). Among the previously mentioned factors involved in their immunosuppressive properties, HLA-G plays a critical role. Interestingly, all these factors are interconnected and were shown to induce HLA-G, thereby constituting amplification loops maintaining and favoring tolerogenic environment surrounding MSC. This has major clinical implications, such as the development of future anti-rejection therapeutic strategies using MSC (*Naji et al, 2013*).

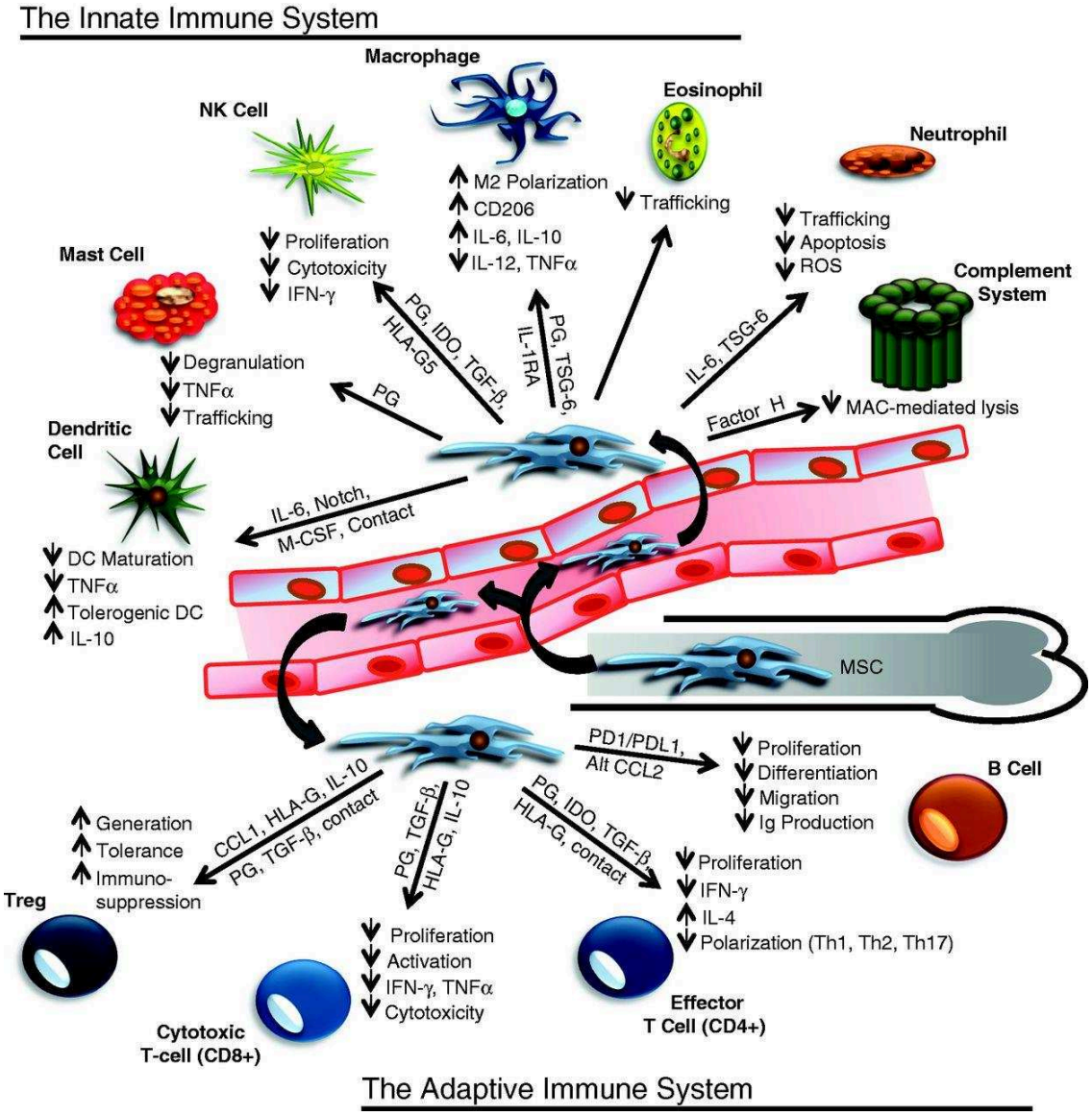

Figure 14 : Immunosuppressive properties of MSCs on both the innate and adaptive arms of the immune system. (Brennen WN et al, 2013)

2.1.1.4. Sources

MSC were first isolated in bone marrow (BM), in 1974 by Friedenstein et al. (*Friedenstein AJ et al, 1974*). Then, these cells have been isolated from a multiplicity of adult sources such as lung tissue, adipose tissue, tendon, synovial membrane but also foetal ones as placenta or umbilical cord (**Figure 15**). For Kock L *et al.*, (*2012*) the ideal cell source for cartilage tissue engineering is one that can easily be isolated and expanded, and which synthesizes abundant cartilage-specific extra-cellular matrix components, e.g., aggrecan and type II collagen. There is

evidence that MSC from bone marrow have higher chondrogenic potential than the MSC from other origins such as lung or placenta (*Bernardo ME et al, 2007*). That's why they were firstly used in the cartilage tissue engineering.

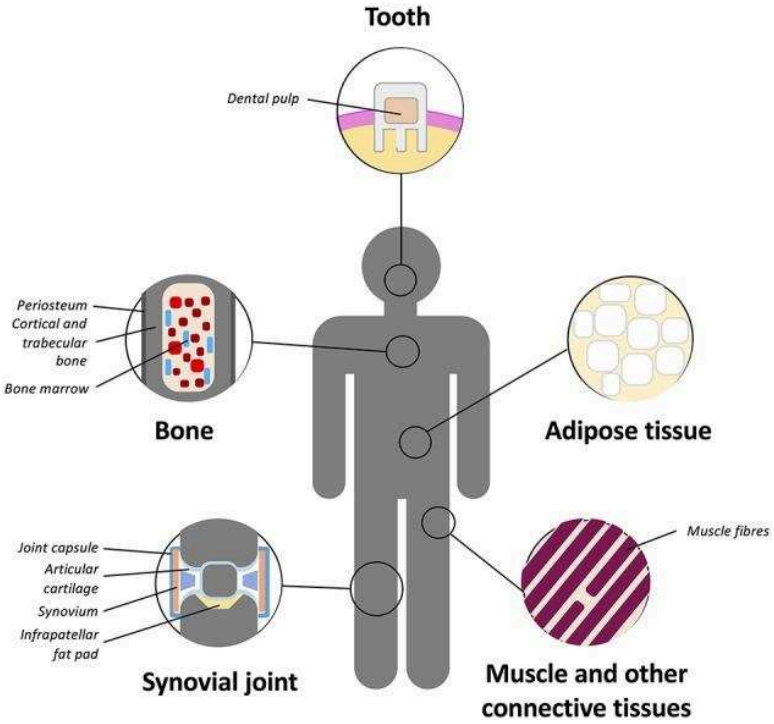

Figure 15: Main adult sources of MSC. In adult tissue, MSC have been found in the bone marrow, adipose tissue, synovial tissue, skeletal muscle, dental pulp, circulatory system, heart, brain, and other connective tissues. (Christopher R et al, 2016)

But, like for other applications, it has shortcomings with ethical constraint and problems associated with painful harvesting and donor site morbidity, and lower differentiation potential *in vitro* (*Roobrouck VD et al, 2008*). Moreover, as BM-MSC come from adult sources, it is now well-known that aging influences cell behavior. Adult MSC decline in numbers, lifespan, and proliferation and differentiation ability with increasing age (*Gao P et al, 2017*). Recently, Fabian C *et al.* demonstrated, *in vivo*, that MSC biodistribution post transplantation was detrimentally affected by aging. Aging of both the recipient and the donor MSC used attenuates transplantation efficiency (*Fabian C et al, 2017*). To overcome this age-related problem, during the last years, MSC obtained from foetal sources as Wharton's Jelly (WJ) of umbilical cords (UC) have gained much attention. This source can be

easily isolated, without any ethical concerns since they come from a tissue which is discarded after birth.

2.1.2. Wharton's jelly mesenchymal stem cell (WJ-MSC)

Wharton's jelly was first described in 1656 by Thomas Wharton. During pregnancy, the umbilical cord represents the bond between the mother and the fetus. The human umbilical cord contains distinct anatomical regions comprising two arteries and a vein, surrounded by a gelatinous matrix: a connective tissue called Wharton's jelly, and covered with an amniotic epithelium (**Figure 16**) (*Yang SM et al, 2012*).

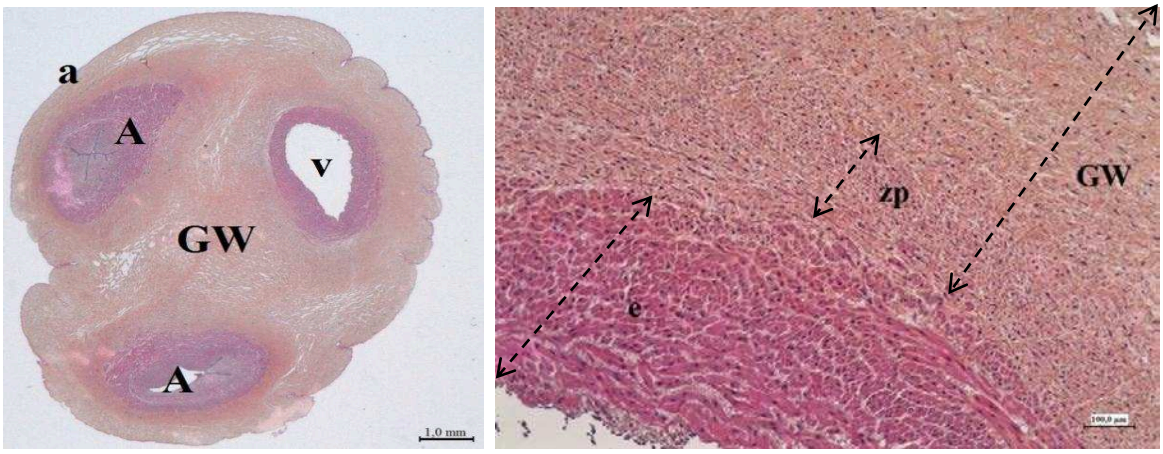

Figure 16: Transverse histological cross section of a human umbilical cord. Left: Macroscopy image, objective x1, staining with Hematoxylin Eosin Safran (HES). Right: Image with optical microscope, objective x10, staining at the HES. (A: arteries, v: vein, GW: Wharton jelly, a: amniotic epithelium, zp: perivascular zone, e: paroi veineuse). (Yang SM et al, 2012)

The main role of Wharton jelly is to prevent compression and twisting of the umbilical vessels that provide blood flow between the mother and the fetus (*Can A and Karahuseyinoglu S, 2007*). It is an avascular and highly hydrated structure, which contains significant amounts of hyaluronic acid and some sulfated GAG immobilized in an insoluble collagen fibril (*Valiyaveettil M et al, 2004*). The ECM components of WJ are also known to be associated with a large number of growth factors like the insulin growth factor (IGF), the fibroblast growth factor (FGF), and the transforming growth factor-β (TGF-β), which control cellular proliferation, differentiation, synthesis, and remodeling of the ECM (*Jadalannagari S et al, 2015*). Meanwhile,

researchers detected the Sox-9 and type II collagen, and found they are positive in WJ-MSC. Due to the similar extracellular matrix and positive expression of cartilage-specific genes in WJ-MSC, it is supposed that these cells may be superior to other stem cells, such as bone marrow stem cells or adipose stem cells *(Liu S et al, 2014)*. Thus, in this work, we have used the Wharton's jelly mesenchymal stem cells to be as raw stem cell, which was seeded into hydrogel scaffolds.

2.1.2.1. WJ-MSC Phenotype

WJ-MSC can express the surface markers of MSC. It has also been confirmed by the expression of specific lineage cytoskeletal markers, such as Vimentin or αSMA (Smooth Muscle Actin) (*La Rocca et al, 2009*). In general, WJ-MSC showed lower CD106 and HLA-ABC expression (*El Omar R et al, 2014*) as compared to bone marrow MSC, whereas expression of CD117, CD146 (*Baksh D et al, 2007*), FLK-1 (Vascular Endothelial Growth Factor (VEGF) receptor) or CD44 (hyaluronic acid receptor) is increased (*Weiss ML et al, 2006*). Some embryonic pluripotency markers such as Oct4, Sox2, Nanog, Rex-1, SSEA-1, SSEA-4, Tra-1-60 and Tra-1-80 have been found at low levels of expression within WJ-MSC (*Carlin R et al, 2006; Fong CY et al, 2007*), suggesting a more immature profile of these cells as compared with adult MSC and hence higher potential for differentiation. In addition, Conconi et al had reported that CD105(+)/CD31(−)/KDR(−) cells from WJ are able not only to differentiate *in vivo* towards the myogenic lineage, but also to contribute to the muscle regenerative process (*Conconi M T et al, 2006*). *In vitro* culture, after several passages, WJ-MSC are able to maintain the length of their telomeres (*La Rocca G et al, 2009*), evoking an active telomerase. However, the telomere length is significantly reduced compared to that observed at the beginning of the culture (*Wang Y et al, 2013*) after 30 passages. The paracrine activity of WJ-MSC may also result in secretion of cytokines such as IL-10, TGF-β, VEGF, angiopoietin-1, or chemokines (CXCL1, CXCL2, CXCL5, Etc.) that promote angiogenesis and intervene in tissue repair mechanisms (*Shohara R et al, 2012*).

2.1.2.2. Immune properties of WJ-MSC

The immune properties of WJ-MSC have been described for the first time by Weiss et al. in 2008 (*Weiss ML et al, 2008*). WJ-MSC was reported that it could inhibit the proliferation of activated T lymphocytes, increase the production of regulatory T lymphocytes, and appear to inhibit the terminal differentiation of B lymphocytes into mature antibody-producing cells (*McGuirk J P et al, 2011*). However, WJ-MSC do not demonstrate immunogenicity; even though it performed a low MHC-I level and absence of MHC-II expression protect them from NK-mediated lysis (*Kalaszczynska et al, 2015; Wang M et al, 2009; Zhou C et al, 2011*). The mechanisms of immuno-privilege are still investigated. Notably, WJ-MSC do not express class II HLA antigens (such as HLA-DR), nor co-stimulatory molecules such as CD40, CD80, and CD86. High levels of inhibitors of immune response: indoleamine-2, 3-dioxygenase (IDO) and prostaglandin E2 (PGE_2) are expressed by these cells. The upregulation of PGE_2 has been shown to inhibit T-cell proliferation after co-culture of MSC with peripheral blood mononuclear cells. IDO is able to inhibit the growth and function of immune cells by catalyzing the conversion of tryptophan to kynurenine. Secretion of IDO by MSC has been shown to inhibit allogeneic T-cell responses and induce kidney allograft tolerance (*Jarvinen L et al, 2008; Ge W et al, 2010; Najib El Haddad, 2011*). On the other hand, WJ-MSC express HLA-G (class I HLA antigen), IL-6 and VEGF: molecules involved in the immunomodulation properties of MSC (*Weiss et al, 2008, La Rocca G et al, 2009*). Besides mechanisms described above, immune-privilege of WJ-MSC depends on immunosuppressive functions mediated by the wealth of paracrine factors as well as cell-cell contact (*Jyothi Prasanna S et al, 2011; Ma S et al, 2014*). The question remains if immuno-privilege of allogeneic WJ-MSC upon differentiation is maintained. La Rocca et al has demonstrated that immunomodulatory molecules such as HLA-G or TGF-β expressed by undifferentiated WJ-MSC, which are also found at the level of these same cells after mesodermal differentiation in vitro. Thus, following the acquisition of a mature phenotype, cells derived from WJ-MSC retain their immunological properties (*La*

Rocca G et al, 2013). Moreover, results published demonstrated that costimulatory factors (CD40, CD80, and CD86) were not expressed and could not activate T lymphocytes during the chondrogenic differentiation of human WJ-MSC. Differentiated WJ-MSC detected high levels of potent inhibitors of immune response (IDO, HLA-G, and PGE2) (*Liu S et al, 2012*). So far, it seems that state of immune-privilege is stable in WJ-MSC upon multidirectional differentiation.

2.2. Scaffolds/Matrices

To choose an appropriate scaffold is an important step in cartilage tissue engineering. In terms of delivering stem cells for articular cartilage regeneration, biomaterials should be biocompatible and biodegradable, and allow for cell adherence and migration (*Raghunath J et al, 2007*). In addition, biomaterials should provide the essential signals for the cells to active anabolic activities (*Bryant SJ et al, 2003; Awad HA et al, 2004*). Numerous materials, both natural and synthetic biopolymers have been investigated for cartilage application (**Figure 17**).

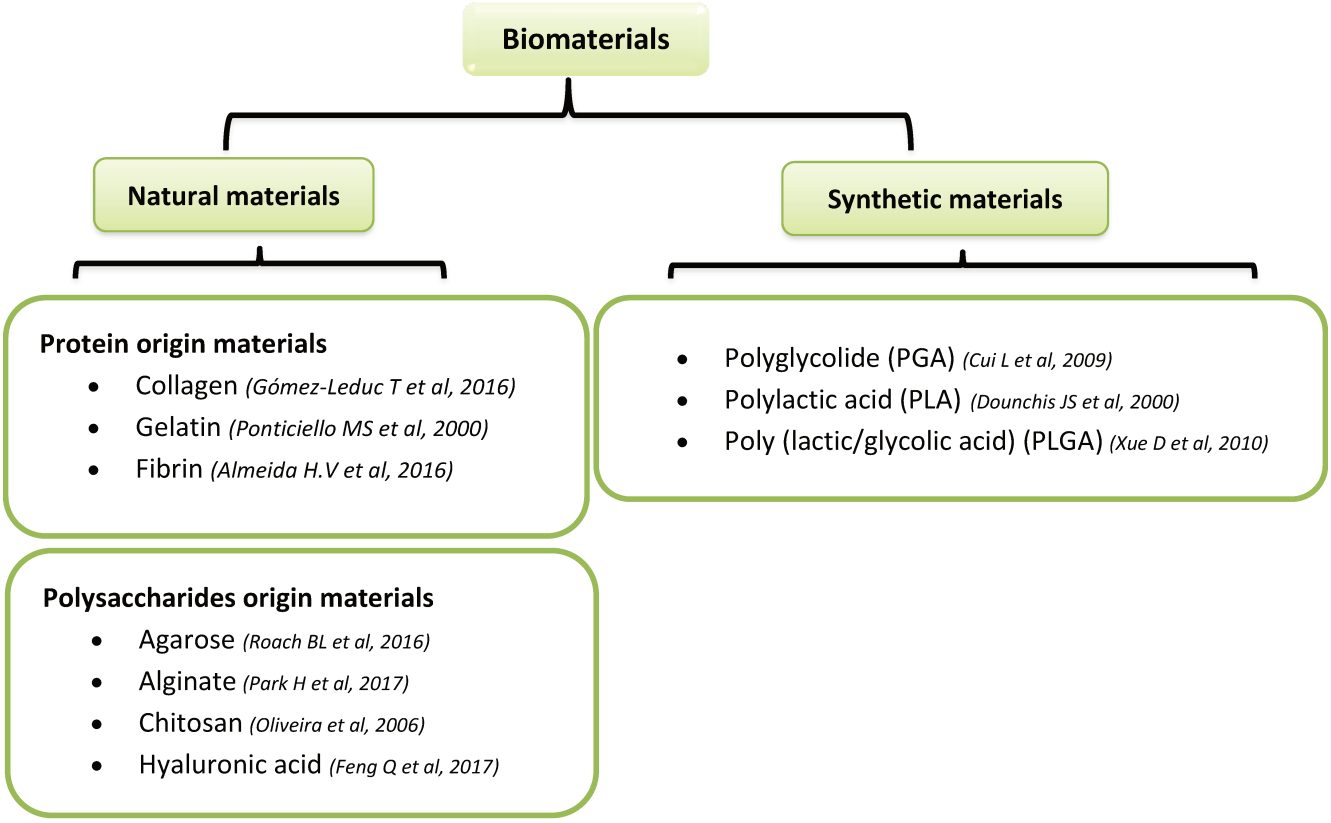

Figure 17: Types of biomaterials used in cartilage tissue engineering.

2.2.1. Synthetic biopolymers

Synthetic biopolymers including polylactic acid (PLA) (*Dounchis JS et al, 2000*), poly (lactic/glycolic acid) (PLGA) (*Xue D et al, 2010; Uematsu K et al, 2005*) and polyglycolic acid (PGA) (*Cui L et al, 2009*) have also been commonly used. All of them have been widely used in bone and cartilage tissue engineering due to their preferable mechanical properties and amendable degradation rate (*Hutmacher DW et al, 2000*). Even though PGA, PLA and PLGA, as the few synthetic materials that have been investigated for cartilage tissue engineering *in vitro* and regeneration of full-thickness cartilage defects *in vivo* (*Freed et al, 1993; Liu Y et al, 2002; Zhou G et al, 2006*), they may require modifications to enhance biocompatibility and bioactivity (*Toh WS et al, 2011; Nooeaid P et al, 2012*). For example, Arg–Gly–Asp (RGD) sequence was used to modify the synthetic biopolymers, which support cell adhesion and regulate cellular function. But also, their degradation products may cause inflammation that possibly results in failure of the implant in vivo (*Ceonzo K et al, 2006; Lu L et al, 2001*). The physical and chemical properties of synthetic scaffold can be modified to affect cellular behavior. For example, cell adhesion molecules, enzymatic degradation sites or growth factor-binding regions can be incorporated into the synthetic scaffold to mediate cell-specific bioactivities (*Rajaram A et al, 2012; Zhu J et al, 2011*).

2.2.2. Natural polymers

Natural materials have been used to produce scaffolds (solids) and hydrogels for cartilage tissue engineering. Some of the materials, such as alginate (*Park H et al, 2017*), hyaluronic acid (*Park H et al, 2017; Feng Q et al, 2017*), chitosan (*Oliveira et al, 2006*), chondroitin sulfate (*RAA Muzzarelli et al, 2012*), fibrin (*Almeida H.V et al, 2016*), type I/III collagen and type II collagen (Gómez-Leduc T *et al, 2016*), have been prepared as porous scaffolds or 3D-hydrogels. Among the natural materials, hyaluronic acid has emerged in the last decade as a promising candidate for cartilage tissue engineering since it is one of the components of ECM of native

cartilage, which has a beneficial effect on the proliferation and synthesis activity of chondrocytes (*Yoo HS et al, 2005; Burdick JA et al, 2011; Highley CB et al, 2016*). Thus, many researchers have used hyaluronic acid as scaffold or in combination with other biopolymers in fabrication of scaffold for cell delivery to treat osteochondral defects or osteoarthritis (*Nehrer S et al, 2009; Collins MN et al, 2013*). Recently, many groups have focused on hydrogels for repairing of articular cartilage damaged such as alginate, hyaluronic acid, agarose and fibrin.

2.2.3. Hydrogels

Hydrogels are three-dimensional (3D) networks consisting of hydrophilic polymer chains. There are some remarkable characteristics for it, including tunable physical, chemical, and biological properties, high biocompatibility, versatility in fabrication, and similarity to native extracellular matrix (ECM), which can support growth, multiplication, and differentiation of cells to produce regenerated organ transplants. So, hydrogels (highly hydrated polymer networks) are typical scaffold materials and have been widely investigated for cartilage tissue engineering. For examples, they are capable of retaining large amounts of water which contributes to their excellent biocompatibility (*Van Vlierberghe S et al, 2011*); they are easily prepared and embedded with chondrocytes, which retain their phenotype and morphology through impregnation (*Sechriest V F et al, 2000*). They also exhibit characteristics similar to soft tissues and therefore provide a supportive matrix for chondrocyte activity and cartilage ECM secretion both in vitro and in vivo (*Perka C et al, 2000; Mouw JK et al, 2005*). High efficiency of cell encapsulation and uniform cell distribution within the hydrogel are advantages that influence the quality of formed tissue. Hydrogels can be made of a wide variety of biomaterials, including: natural materials, which may be carbohydrate-based (e.g., alginate, agarose, chitosan, hyaluronic acid (HA)), protein-based (e.g., fibrin glue, collagen type I and II, silk) (*Chang CH et al, 2005; Athanasiou KA et al, 2009*) or some combination of two synthetic materials, such as poly (hydroxyethyl methacrylate), polyethylene glycol

and its derivatives, or poly(vinyl alcohol) (PVA) (*Gibas I et al, 2009*). **Table 2** summarizes the advantages and disadvantages of these main polymers (*Puppi D et al, 2010*). As we mentioned some advantages of 3D-hydrogels before, it can been as more realistic models used in the application of cell culture. However, how to guide the hydrogels to apply for cell culture, so, the sterilization, fabrication, and characterizations of hydrogel should be considered by us firstly.

Table 2: Advantages and disadvantages of biopolymers used in cartilage tissue engineering (Puppi D et al, 2010)

Biopolymers	Advantages	Disadvantages
Natural	Low toxicity; Low cost; Recyclable; Cell adhesion(+++); Biodegradability	Low mechanical stability, thermal and chemical. Infectious risk; Possible loss of biological properties during formulation
Type I collagen	Low immune ogenicity; Cell adhesion(+++); Mechanical properties; Biocompatibility	Rapid biodegradation, cell division
Alginate	Biocompatibility; Biodegradability; Cellular integration; Injectable	Mechanical stability (--); Difficulty sterilizing; Impurities
Hyaluronic acid	Non-immunogenic; Interactions with cells / matrix (++); Large-scale production (Ferm.bact.)	Mechanical resistance (-); Tissue formation (--)
Hydroxyapatite	Biocompatibility; Osteoconductivity; Osteoinductivity	Solubility(--); Formation of crystals
Synthetic	Wide varieties, physical, chemical and mechanical properties (+++); Little immunogenic; Infectious risk	High cost; Potentially toxic; Little data on biological responses

2.2.3.1. Hydrogel sterilization

Hydrogel has to undergo the progress of sterilization before implantation, which could be used in tissue engineering or drug delivery. For example, Stoppel W L et al showed the ethanol wash to be an effective sterilization to sterilize the alginate /Pluronic F68 hydrogel, which results in minimal influence on mechanical properties,

water content, and eliminates bacterial persistence (*Stoppel W L et al, 2013*). Tohfafarosh M et al reported that gamma ray and e-beam could sterilize a novel hydrogel (Cyborgel), the results exhibited that no significant difference between them as swelling ratio, mechanical and tribological properties (*Tohfafarosh M et al, 2016*). Many authors used gamma ray, ethylene oxide, 70% ethanol, e-beam and UV to sterilize the already formed hydrogels (*Karajanagi SS et al, 2011*; *Kanjickal D et al, 2008*). However, the precursor solutions must be sterilized before the formation of hydrogel for cell encapsulation. Considering if the changing of hydrogel native properties or not (*Huebsch N et al, 2005*), the filtering (relatively lower viscous) or UV irradiation methods can be used to sterilize the solution or dry polymer (*Caliari SR et al, 2016*). In addition, Commercial hydrogel kit (eg: Alginate NOVAMATRIX) can provide the sterilized of hydrogel production.

2.2.3.2. Fabricating hydrogels

Crosslinking in hydrogels occurs physical by noncovalent or chemical by covalent, by a phase translation of the liquid precursor solutions into solid materials (**Table 3**). Various hydrogels have been fabricated for different applications in the field of biomedical, which depends on the chemical structure and crosslinking methods. For physical hydrogels, the process of crosslinking is physical. This is achieved through physical processes such as association, aggregation, entanglements, electrostatics (hydrogen bonding), and crystallite formation. For example, divalent cations induce gelation of anionic alginate polymers. On the contrary, chemical covalent crosslinking of polymers can also be used for a chemical hydrogel formation. For instance, in order to rapidly form hydrogels, various stimuli (photo-initiation or redox initiation) can induce the covalent reaction of reactive groups (such as acrylates, methacrylate or acrylamide) (*Omidian H et al, 2012; Ahmed EM et al, 2015*).

Table 3: Physical and chemical crosslinking of hydrogels

Physical crosslinking	Chemical crosslinking
Hydrophobic association: isopropyl groups in poly(N-isopropyl acrylamide); methyl groups in methyl cellulose; propylene oxide blocks in (ethylene oxide)–(propylene oxide)–(ethylene oxide) terpolymers ***Ion/polymer-polymer complexation:*** acrylic-based hydrogels treated with calcium, aluminum, iron; sodium alginate treated with calcium and aluminum; poly(vinyl alcohol) treated with borax ***Chain aggregation:*** heat treatment of hydrocolloids in water ***Hydrogen bonding:*** poly(vinyl alcohol)/poly (vinyl alcohol) chains; poly(acrylic acid)/ polyacrylamide chains	***Covalent crosslinking***: olefinic crosslinkers containing unsaturated bonds or reactive functional groups ***Simultaneous polymerization and crosslinking:*** Acrylic acid or acrylamide, crosslinked with methylene bisacrylamide, ethylene glycol diacrylate, ethylene glycol dimethacrylate, poly(ethylene glycol dimethacrylate) ***Post-polymerization chemical crosslinking:*** Acrylic-based hydrogel, crosslinked with glycerin; gelatin cross-linked with glutaraldehyde; poly(vinyl alcohol) crosslinked with an aldehyde

2.2.3.3. Characterization of hydrogel properties

Many people have reported results on the properties of hydrogels including viscosity, swelling, mechanics, mesh size, and degradation. All of them may influence the utility of hydrogels for cell culture applications. So it is important to understand how these characteristics are described and evaluated.

a) Viscosity of gel

It is well known that rheology is the science of the flow and deformation of liquid or soft solid under the effect of applied force and strain rate. The viscosity (kinematic or dynamic) which characterizes the viscoelastic or viscoplastic behaviors is defined as a material's resistance to deformation for fixed strain rate amplitude. Thus, the viscosity is a function of strain rate and is temperature, which provides some information about internal degrees of freedom,

microstructure and the molecular structure of a polymer (*De Kee D et al, 1994*). Notably, viscosity is related to the internal friction, for example, water and honey have a low and high viscosity respectively. As shown in **Figure 18A**, fluid's viscosity can be defined from the shear stress of the medium between two parallel plates with a distance, noted y, between these two plates and separated by the homogeneous medium. The lower plate is fixed, the upper plate is moving horizontally at constant speed V_0 as a force F be applied to the upper plate. In practice, this experiment is developped using a rotational rheometer with cone-plate systems. The cone shape produces a smaller gap height closer to inside (the shear on the sample is constant) (**Figure 18B**). This instrument is able to measure viscosity as a function of shear rate (corresponding to constant rotational velocity), which would be used to infer the molecular weight distribution of a linear polymer and some information about the level of long-chain branching. It is described by Mark–Houwink equation: $[\eta] = KM^a$. The values of the Mark–Houwink parameters, K and a, depend on the particular polymer-solvent system (*Paul Hiemenz C et al, 2007*).

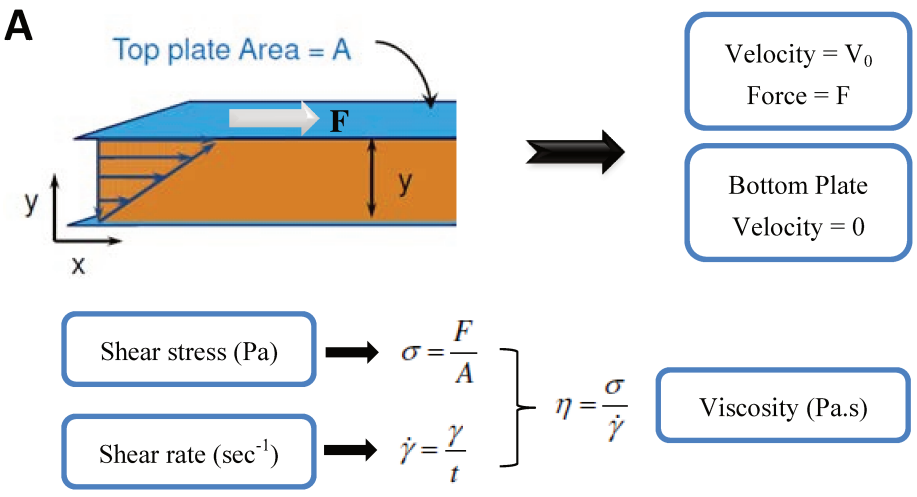

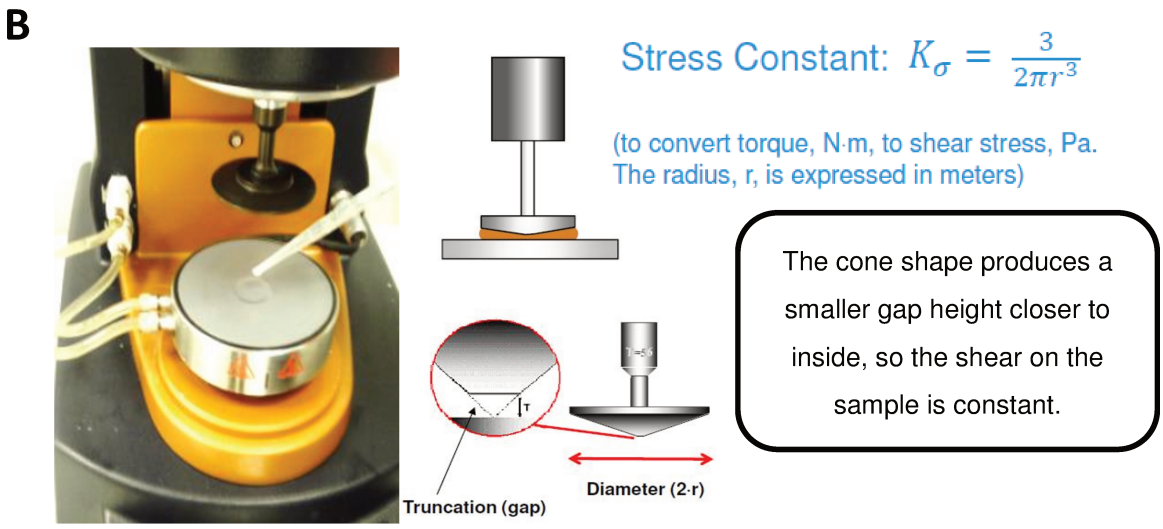

Figure 18: (A) Shear flow of fluid between two plates, friction between the fluid and the moving plates causes the fluid to shear. The force required for this action is a measure of the fluid's viscosity. (B) Theory of TA Instruments Rheometers. (Rheology theory and applications, TAINSTRUMENTS.COM)

b) Swelling behavior

Another important hydrogel property is swelling, determined as the amount of space inside the hydrogels network available to accommodate water. The swelling property of hydrogel is associated with many factors such as network parameters, porosity, and drying techniques, which directly reflect the hydrophilicity and crosslinking density of hydrogels, as well as stiffer networks typically exhibiting lower swelling (*Ganji F et al, 2010; Lee K Y et al, 2000*). A very high swelling hydrogels can offer greater swelling but may have inferior mechanical properties. So, the swelling properties not only can be used as an indicator of bath to batch variations, but also help understand if the hydrogel mechanics are changing over time (*Caliari SR et al, 2016*). In addition, a hydrogel is made up of a polymer and water. The final swelling properties of the hydrogels are also determined by the composition ratio of polymer to water as seen in **Figure 19**. To measure the swelling ratio of hydrogels, allowing the hydrogels to reach equilibrium swelling. Wiped with filter paper to remove excess solvent and weighed to obtain the wet weight (M_w). The hydrogel is then dried and to weight (M_d) again. The volumetric swelling ratio (Q_m) is typically

calculated using the following equation (*Li X M, et al, 2016*): $Q_M = (W_w - W_d)/W_d \times 100$ %.

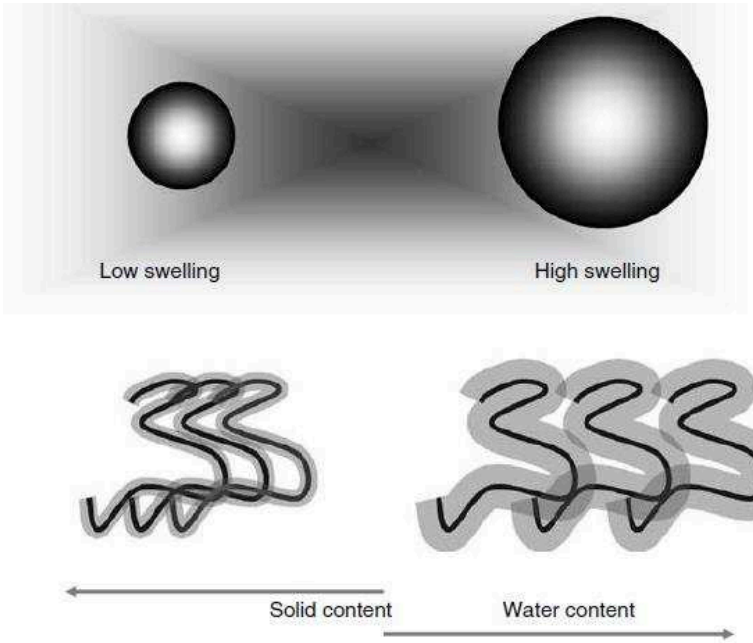

Figure 19: Swelling properties of hydrogels. A low- or a high-swelling hydrogels is characterized by a high or low-polymer/water ratio, respectively. (Raphael M. Ottenbrite, Biomedical Application of Hydrogel Handbooks, 2010, DOI 10.1007/978-1-4419-5919-5)

c) Mechanical properties

The mechanical property of hydrogels has been recognized as fundamentally important for biomedical application especially because they have significant effects on cell behavior. Many studies have dealt with mechanotransduction for several decades now. The conversion of mechanical signaling from the microenvironment into biochemical signaling in terms of alerting cells behavior such as spreading, migration, and stem cell differentiation has been recently identified (*Ingber DE et al, 2006; Brandl F et al, 2007; Kloxin AM et al, 2010*). The measurements of hydrogel mechanical properties are typically extracted from tensile (a), compressive (b), confined compression (c), indentation (d), shear rheometry (e) and dynamic mechanical testing (f) as showed on **Figure 20** (*Oyen ML et al, 2014*). Generally, tensile testing consists in applying a tensile strain rate to strips of material held between two grips which is particularly difficult to use for hydrogels. Compression test is another method that has previously been used for

this kind of biomaterials, but there are also some specific limitations as difficulty in applying pressure uniformly and bulging of the hydrogel under compression. Even though a number of studies have used compression or tensile testing to evaluate the mechanical properties of hydrogels, these methods could not allow non-destructive monitoring of the hydrogel under cells culture conditions. In other words, few methods can be used to measure the mechanical properties of cell-seed hydrogels. In recent years, indentation method (at the nano, micro or macro levels) has been widely used to characterize the mechanical properties of 3D-hydrogels (*Marc Farine, 2013*). It is well suited for examining minimal sample as well as is suitable for examining cell-seeded hydrogels under the cell culture condition. For examples, at the large (mm) or small (nm to um) length scales of hydrogels were characterized by indentation tests. This has several advantages as it is quite simple and straight-forward; the shear modulus and diffusivity of hydrogel can be extracted directly; the tests measures solvent transport through the lateral dimensions of the thin hydrogel as opposed to the through-thickness dimensions (*Ahearne M et al, 2008*).

For indentation testing, an indenter is brought into contact with the hydrogel surface, pressed into it with a predetermined displacement depth, the force being recorded (**Figure 21a**). During the testing, the hydrogel will undergo a stress-relaxation process (**Figure 21b**). Actually, this relaxation processes includes viscoelastic and poroelastic relaxation. The former is associated with conformational changes of the polymer chain due to the applied deformation. The latter is related with the transport of water molecules out of the region of hydrogel under deformation as defined by the contact area πa^2 (**Figure 21a**) (*Chan EP et al, 2011*). In terms of this indentation, a corresponding load develops that is defined by the hydrogel tangent stiffness. Therefore, it has ability to assay the mechanical properties of hydrogel at multiple length scales.

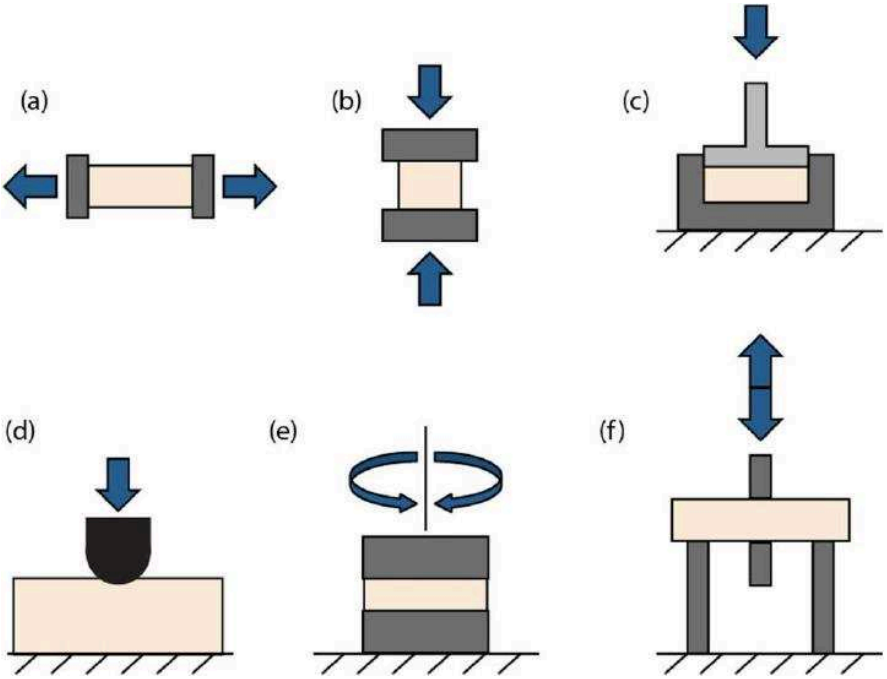

Figure 20: Different types of mechanical testing used for measuring hydrogel mechanical properties. (a) tension; (b) compression; (c) confined compression; (d) indentation; (e) shear rheometry; (f) dynamic mechanical analysis (DMA), illustrated here for three-point bending (Oyen ML et al, 2014)

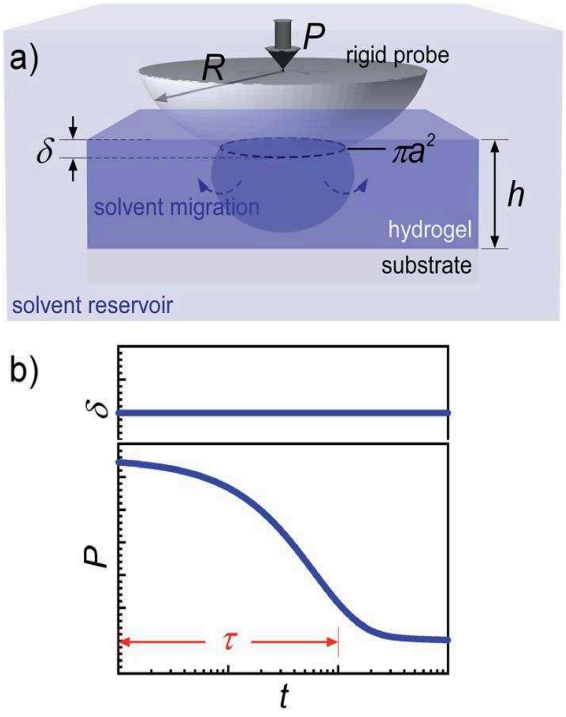

Figure 21: (a) An indenter is brought into contact with the hydrogel surface in a water environment; (b) At the fixed displacement (δ) results in a relaxation in load (P) as a function of a relaxation time (τ). (Chan EP et al, 2011)

d) Mesh size

The porosity of hydrogels is typically on the nanometer scale and can influence nutrient flux throughout the matrix. The distribution of pore size is correlated to the swelling behavior and mechanical properties of hydrogels, since lower swelling and higher modulus indicate a smaller mesh size (*Collins MN et al, 2008; Rennerfeldt DA et al, 2013; Marmorat C et al, 2016*). Scanning electron microscopy (SEM), mercury porositometry, liquid intrusion, and image analysis are commonly used to assess to the porous hydrogel microstructure. However, these techniques are innate shortcomings for this application since the sample must be dried before analysis, which alters the native structure of hydrogel. For example, Kirchhof et al reported that the mesh size of the prepared hydrogels was determined by swelling studies, rheology, and low field NMR spectroscopy (*Kirchhof S et al, 2015*). The mesh size of step-growth hydrogels can also be estimated using theoretical approaches.

e) Degradation

The degradability of hydrogels being the essential factors, when implanted / rejected into the body might exhibit long-term physiological and psychological damage. Moreover, hydrogel degradation can result in the change of the mechanical properties and swelling over time, which furtherly affect cells behavior such as motility and spreading (*Khetan S et al, 2013*). For examples, Ashton RS used the neural progenitor cells (NPCs) to seed into alginate-based hydrogel in order to observe the proliferation property. The results shown that the modified alginate hydrogel with degradable property have significantly stimulated NPCs proliferation compared to alginate standard (*Ashton R S et al, 2007*). Different types of hydrogels possess the degradation ability depends on the goal of the study. There are two kinds of typical mechanisms for hydrogel to degrade being hydrolytic or enzymatic. To be precise, hydrolysis occurs throughout the entire hydrogel and enzymatic degradation is local to the presented enzyme. One study synthesized the PEG-based photodegradable hydrogel with a good spreading for hMSCs that degrade

in response to cells-secreted matrix metalloproteinase (*Kloxin A M et al, 2010*). In general, controling the rate of hydrolysis can be done through altering the polymer concentration or the crosslinking density during hydrogel fabrication. More advanced hydrogels used ultraviolet (UV) light as external triggers to control degradation (*Kloxin A M, 2009*).

2.2.4. Selecting an alginate-based hydrogel for CTE

Alginate (Alg) is unbranched polysaccharide derived from brown seaweed or bacteria, It is composed of a repeating disaccharide of (1-4)-linked b-D-mannuronic acid (M) and its C-5 epimer a-L-guluronic acid (G) (**Figure 22a**). Typically, the blocks are composed of three different forms of polymer segments: consecutive G residues, consecutive M residues and alternating MG residues (*Sun J et al, 2013; Pawar SN et al, 2012*). According to their gelation mechanisms, alginate hydrogels can be classified into physical and covalent gels, obtained by methods including ionic interaction, phase transition, cell-crosslinking and free radical polymerization to prepare the alginate hydrogels (*Tan H et al, 2010*). In general, to chelate with divalent cations (Mg^{2+}, Ca^{2+}) is the easiest way to prepare alginate hydrogels from an aqueous solution under gentle conditions (**Figure 22b**) (*Reis CP et al, 2006*).

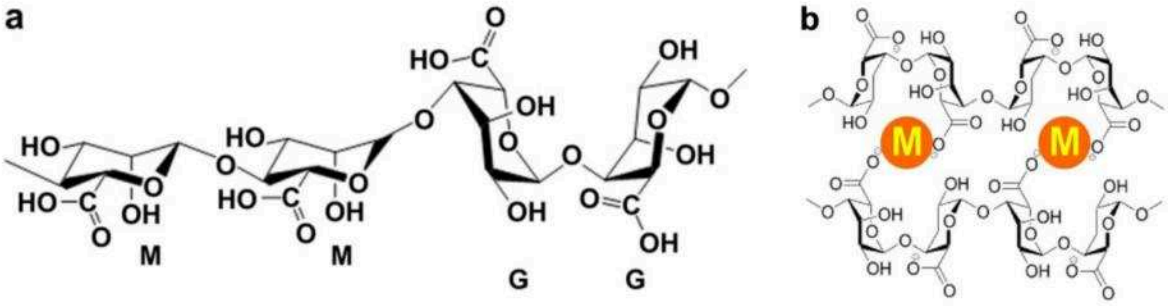

Figure 22: (a) Chemical structure of alginate; (b) Mechanism of ionic interaction between alginate and divalent cations. (Reis CP et al, 2006)

This polymer can be used a reference model to study cell morphology, synthesis of proteoglycans and collagens, but also mechanobiology of articular chondrocytes. Although sodium alginate is not a natural component of the extracellular matrix, it has a structure similar to that of cartilage glycosaminoglycan (*Wang X et al, 2009*).

Several studies have already shown that alginate hydrogels constitute three-dimensional culture models relevant for inducing chondrogenesis of MSCs (*Ma HL et al, 2003, Tritz-Schiavi J et al, 2010*). Immobilizing cells with chondrogenic potential in an alginate hydrogel has shown that neocartilage can be formed by mesenchymal stem cells (*Olderøy M Ø, 2014*). Wang et al. prepared an organized 3D alginate microsphere scaffold using a microfluidic device, which was effective for chondrocyte culture in vitro (*Wang CC et al, 2011*). Interestingly, alginate pre-culture has been used to form scaffold-free in vitro constructs using zonal chondrocytes that maintained stratification and zonal function (*Klein TJ et al, 2003*). However, alginate disadvantages are a low mechanical rigidity (mean viscoelastic properties) and a low degradation rate.

Hyaluronic acid (HA) is one of the major ECM components of articular cartilage and is composed of β-1, 4-D-glucuronic acid-β-1, 3-N-acetyl-D-glucosamine residues. It is found throughout the body including articular hyaline cartilage and other connective tissues as well as synovial fluid (*Clegg TE et al 2013*) (**Figure 23**), in which it plays an important role in the resistance to compression of the cartilage for fixing PG.

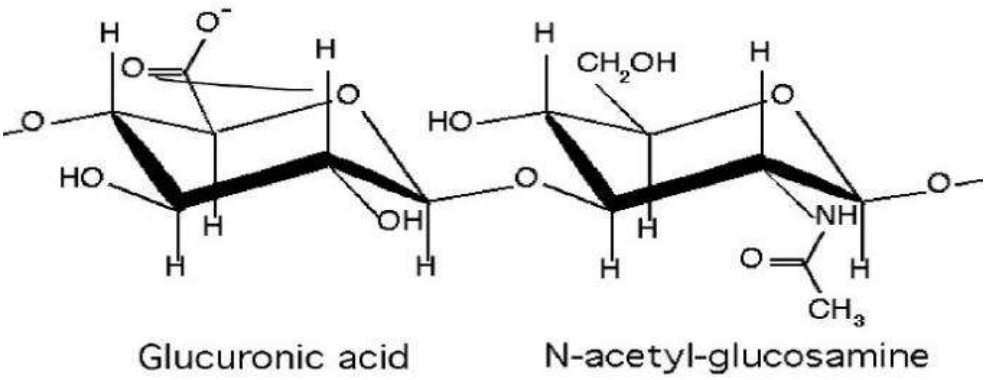

Figure 23: Chemical structure of hyaluronic acid. (Clegg TE et al 2013)

HA offers many advantages as a tissue scaffold which include: (a) Biodegradability and biocompatibility; (b) HA is a major intracellular component of connective tissues where it plays an important role in lubrication, cell differentiation and cell growth.

These functions can be transferred to the scaffold; (c) HA contains functional groups (carboxylic acids and alcohols) along its backbone that can be used to introduce functional domains or to form a hydrogel by crosslinking (eg: alginate); (d) Due to its ability to maintain a hydrated environment conducive for cell infiltration, HA-based hydrogels are ideal as wound grafts to treat chronic wounds or wounds in patients with impaired healing such as diabetic patients; (e) HA can be part of a new kind of tissue engineering scaffold that is bioactive both in its full length and in the degraded form. More recently, Hyaluronic acid has been broadly and consistently used for cartilage regeneration (*Kim IL et al, 2011*) due to its intrinsic viscoelasticity and CD44-specific interactions with chondrocytes (*Volpi N et al, 2009; Knudson CB et al, 2004*).

Hydroxyapatite (Hap) is the major components of bone matrix- a very complex tissue with general formula $Ca_{10}(OH)_2(PO_4)_6$. Hap as a bone substitute and/or replacement in biomedical applications due to its biocompatibility, slow biodegradability in situ, and good osteoconductive and osteoinductive capabilities (*Zhou H et al, 2011*). For example, Poinern GE et al. showed that Hap exhibits excellent biocompatibility with soft tissues such as skin, muscle and gums (*Poinern GE et al, 2009*). Thorpe a et al reported that hydroxyapatite nanoparticle injectable hydrogel scaffold support osteogenic differentiation of human mesenchymal stem cells (*Thorpe AA et al, et al 2016*). Here, we are concern with the buildup of Alg/HA-Alg/Hap hydrogel scaffolds for reconstructing biological tissue with three dimensional cells construction for mimicking cartilage architecture. This study aims to compare the characteristics of Alg/HA hydrogels which will mimic cartilage and Alg/Hap hydrogels which will mimic subchondral bone.

3. Influence of the mechanical properties of hydrogel on cell behavior

There are complex relationships between hydrogels and stem cells. The understanding of the effects and how certain factors can impact the hydrogels ability to regulate the stem cell fact turns to be necessary. The mechanical interactions between cells and extracellular matrix can be considered as symbiotic. In other words, the hydrogel stiffness has also affected the ability of cells to remodel their surrounding matrix, to regulate intracellular processes through the mechanical, structural and chemical properties of these surrounding's matrix. Generally, hydrogel matrix stiffness can be controlled by the polymer concentration and crosslink density, which can be increased by increasing the concentrations of the crosslinker (*Lin S et al, 2011*). In addition, the incorporation of hydrophobic domains, nanoclays sacrificial chains, ionic crosslinkers (*Haraguchi K et al, 2002; Gong J P et al, 2003; Sun J Y et al, 2012*) into hydrogel can also improve the mechanical properties of matrix. *In vitro* studies, hydrogel matrix stiffness plays an important role in the regulation stem cell fate such as adhesion, cytoskeleton, migration, differentiation and mobility (*Lo CM et al, 2000; Pelham RJ et al, 1997; Peyton SR et al, 2005; Engler AJ et al, 2006*). The effect of matrix stiffness on phenotype behavior of cells is noticeable (*Wozniak MA et al, 2009*). In 2D culture, for example, mesenchymal stem cells have demonstrated an increase in proliferation and cell spreading when cultured on stiff hydrogels is compared with softer hydrogels (*Marklein RA et al, 2010*). HMSCs were cultured on hydrogels with an elastic modulus (E) ranging from 0.1–1 kPa underwent neurogenesis, while those cultured on stiffer hydrogels of modulus ranging from 8–17 kPa and 25–40 kPa underwent myogenesis and osteogenesis, respectively (*Engler AJ et al, 2006*) (**Figure 24**). These findings show that the stiffness of the hydrogels has influenced specifically the different cell types. In 3D culture, for example, one study demonstrated that stress-stiffening-mediated control of hMSCs differentiation in polyisocyanopeptide-based hydrogel (*Das RK et al, 2016*). This could be widely used to study the tractive stresses generated by encapsulated hMSCs, as high/low tractive

stresses of cells supported their osteogenic and adipogenic differentiation, respectively. Cells respond to hydrogel matrix stiffness through exerting traction forces, which are associated with the cytoskeleton. Changing of cytoskeleton tension resulted in trigger various signaling cascades such as RhoA signaling (*McBeath R et al, 2004*), which can influence the differentiation characters of MSCs through the adjustment of RhoA signaling expression. In addition, to adjust the elasticity of matrix was also widely reported by researchers. For instance, Stowers et al. fabricated that a 3D alginate hydrogels embedded with light-sensitive liposomes, which used light-triggered and spatially-controlled stiffness of hydrogel. Guvendiran et al. have created the methacrylated hyaluronic acid hydrogels with dynamic subtract stiffening by using of photo-polymerization. The encapsulated hMSCs increased in response to an increase of hydrogel's stiffness within 4h. Additionally, hMSCs differentiated into different cell types depending on the time where they were cultured in either soft or stiff hydrogels (*González-Díaz EC et al, 2016*).

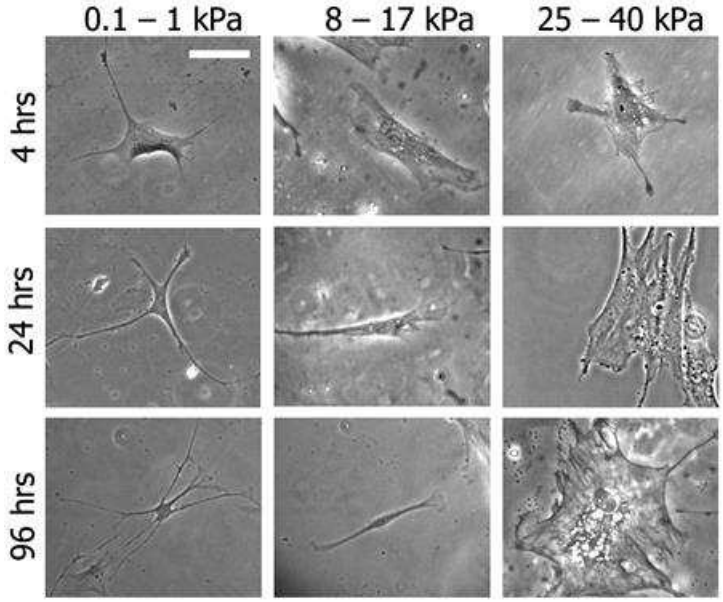

Figure 24: Adhesion of MSCs in various stiffness of hydrogel substrate. (Engler AJ et al, 2006). Scale bar = 20 m

Objectives of the thesis

This work is in line with the theme of cartilage engineering and continues the work initiated by Jessica Tritz-Schiavi (2008-2011) and Loic Reppel (2011-2014).

The purpose of Jessica Tritz-Schavi's work was to build up layer-by-layer a stratified hydrogel by alternating gels and multilayers polyelectrolytes film spraying, in order to obtain a neotissu *in vitro* to fill osteochondral defects. These stratified hydrogels were composed by an upper layer with an Alg/HA hydrogel to mimic cartilage tissue and a deeper layer composed of Alg/Hap hydrogel to mimic osteochondral tissue.

Loic Reppel's work consisted in characterizing WJ-MSC and optimizing their culture conditions for their subsequent clinical use. The second phase of his project was to induce cell differentiation into chondrocytes by seeding them in Alginate/Hyaluronic Acid hydrogel scaffold and to compare the chondrogenic differentiation with bone marrow MSC.

Our objective is to investigate the behavior of WJ-MSC seeded into scaffolds used in multiphase biomaterial (Alg/HA and Alg/Hap) and to study the relationships between the physico-chemical properties of hydrogels and cell behavior to improve their differentiation.

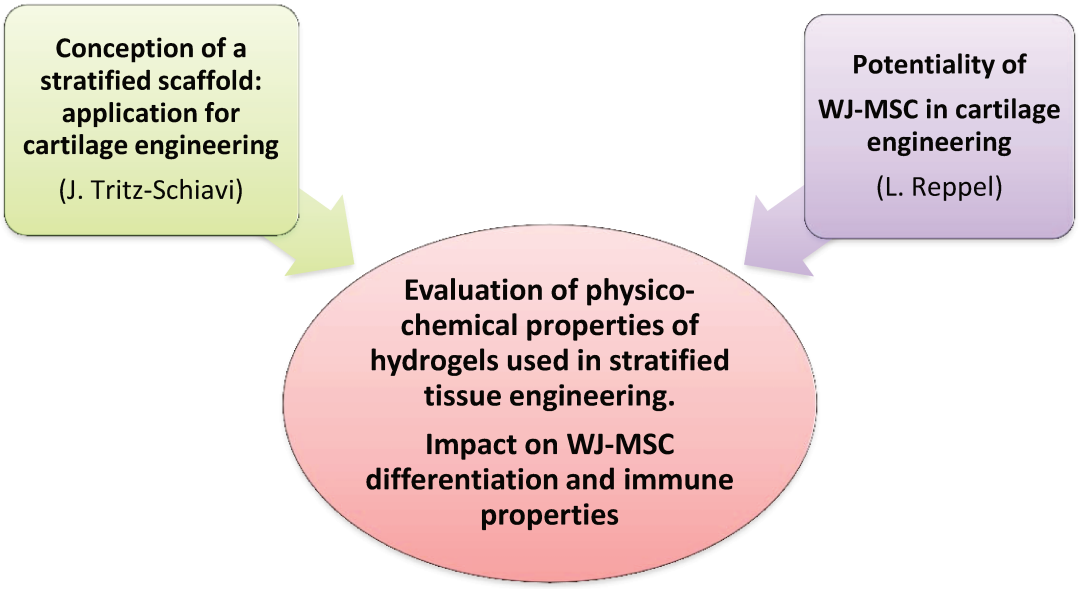

For that, after characterizing WJ-MSC used in this work:

- First, we will evaluate the general behavior of WJ-MSC in Alg/HA and Alg/HAP hydrogel;
- In a second part, we will investigate the impact of different sterilization treatments (autoclaving, UV) on the physicochemical properties of Alg/HA and Alg/HAP hydrogels as well as their impact on the behavior of MSC (viability and differentiation). We could retain a sterilization process which preserves the physico-chemical properties of hydrogels to continue our work;
- Lastly, we will study the evolution of the mechanical behavior of hydrogels during chondrocyte differentiation as well as their impact on the behavior of MSC (differentiation and immunomodulation properties). We will also be interested in the inter-correlation between mechanical properties, biological properties and immunological properties.

Results

I. Characteristics of monolayer cells (WJMSC-A, B C)

This work was carried out during my first year of university thesis. The aim was to study the harvested characteristics of Wharton's jelly derived from human umbilical cord by using explant method.

Methods:

Umbilical cords (UC) were collected by the Regional Maternity of Nancy (CHRU, Brabois) after the mothers' informed consent and complied with national legislation regarding human samples collection, manipulation and personal data protection between 2013 and 2014. The transfer of the UC to the laboratory is governed by an agreement signed between the Faculty of Medicine, Maternity and the CHRU of Nancy. At the same time, they are still considered operational waste.

Here, we had used the Wharton's jelly mesenchymal stem cell from three kinds of human umbilical cords, and they have been named as MSC-A, MSC-B and MSC-C, respectively. Cells were extracted by explant method previously described by Reppel et al (*Reppel et al, 2014*). MSC were incubated at 37°C under a humidified atmosphere with 5% CO_2, 5% O_2 and cultivated up to the third passage before characterization. To perform phenotypic analysis of extracted WJ-MSC (A, B, C) from UC, cells were incubated with fluorescein isothiocyanate (FITC) or phycoerythrin (PE) conjugated mouse anti-human antibodies CD34-PE, CD45-FITC, HLA-DR-FITC, CD73-PE, CD44-FITC, CD105-PE and CD166-PE (Beckman Coulter, Brea, CA) for 30 min. at room temperature before analyses by Gallios flow cytometer (Beckman Coulter, Brea, CA). Cell viability but also formations of colony-forming-unit fibroblast (CFU-F) and senescene were investigated respectively by flow cytometry using AnnexinV and Propidium Iodure (PI), Cristal Violet and "Senescence β-Galactosidase staining kit "(CELL SIGNALING). To detect CFU, the cells were, first, seeded into a six-well plate (10cells/cm^2). After 10 days, they were washed with PBS, stained with

Cristal Violet solution and rinsed with water several times. Data expressed as total colony number per 100 cells.

Results and conclusions:

Owing to the plastic adhesion properties of cells are not sufficient to characterize the mesenchymal stem cells. As no MSC-specific markers have been identified, their characterization is performed by the detection or the absence of detection of certain receptors. Our results have shown that, at the end of passage 3 (P3), the cultivated cell possess a $CD90^+$, $CD44^+$, $CD73^+$, $CD105^+$, $CD166^+$, $CD34^-$, $CD45^-$ and $HLR\text{-}DR^-$ phenotype (**Figure 25A and B**). It appears that the specific receptors of the hematopoietic cells (CD34 and CD45) are absent from the surface of the cultured cells. And an absence of expression of HLA-DR was also observed. In contrast, cells express the CD90, CD44, CD73, CD105 and CD166 receptors. In addition, the average percentage of viable, apoptotic and necrotic of WJ-MSC are 98.4 ± 0.4, 1.2 ± 0.5 and 0.1 ± 0.1, respectively (**C)**. It means that cell extraction from plastic surface by enzymatic digestion does not interfere on viability. Then, when cells were encapsulated into hydrogel, they were considered alive. The proliferation potential of WJ-MSC was evaluated from clonogenic capacity through CFU-F number (**Figure 26A and B).** Lastly, SA-β-gal was used to examine the presence of senescence in WJ-MSC A, B and C. Whatever the source of MSC, the percentage of senescent cells is less than six percent and there is no significant difference between the percentages of senescent cells in each group of MSC ($p > 0.05$) (**Figure 27**). These results have provided a basic reference of the extracted WJ-MSC which can be used in alginate hydrogel in the other parts of our work.

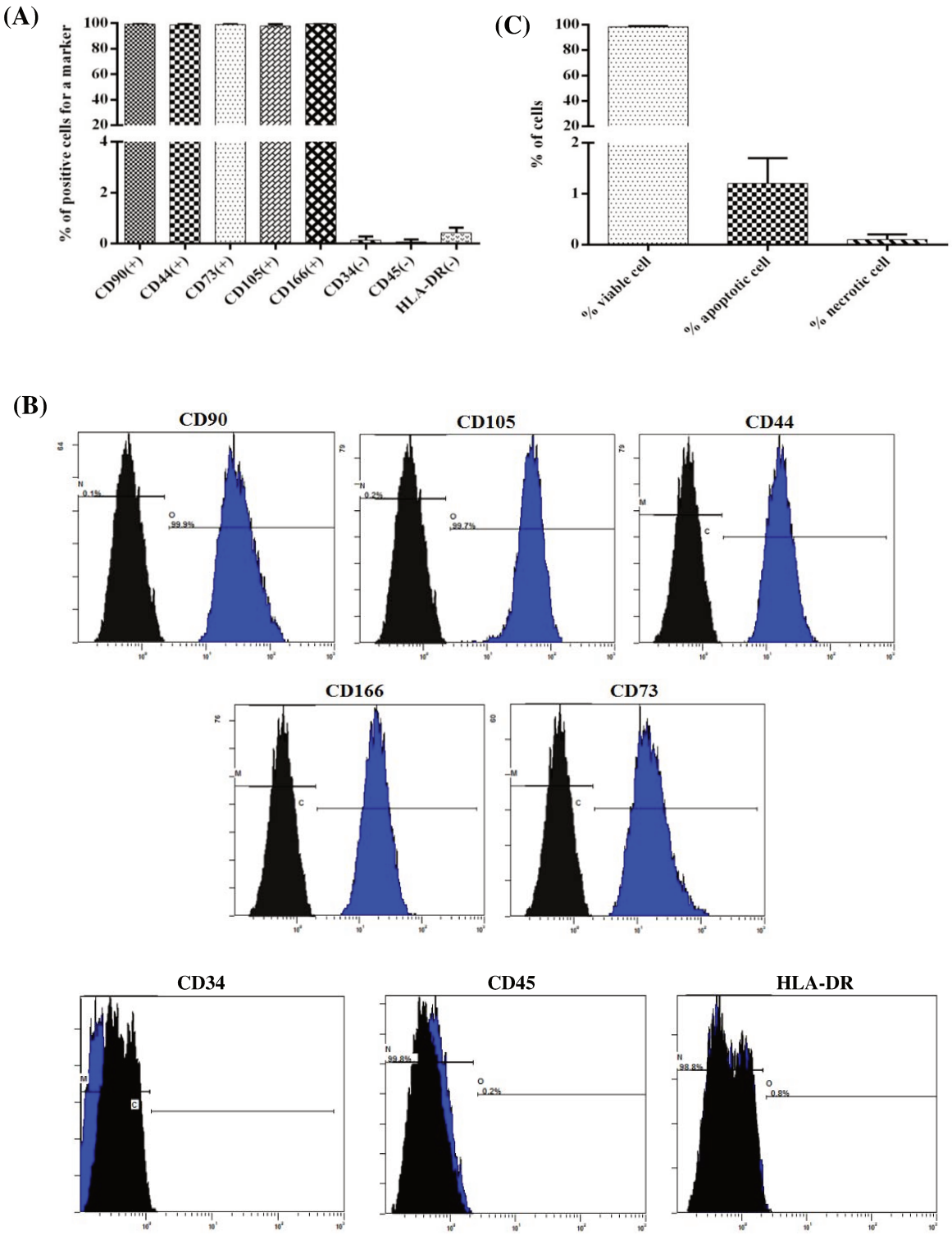

Figure 25: Immunophenotypic analysis of WJ-MSC (A, B and C) by flow cytometry during monolayer expansion. (A): Percentage of mesenchymal markers for WJ-MSC; (B): Expression of the CD90, CD44, CD73, CD105 and CD166 markers on the surface of WJ-MSCs; CD34, CD45 and HLA-DR markers are negative; (C): Viability analysis of WJ-MSC (A, B and C) by flow cytometry during monolayer expansion.

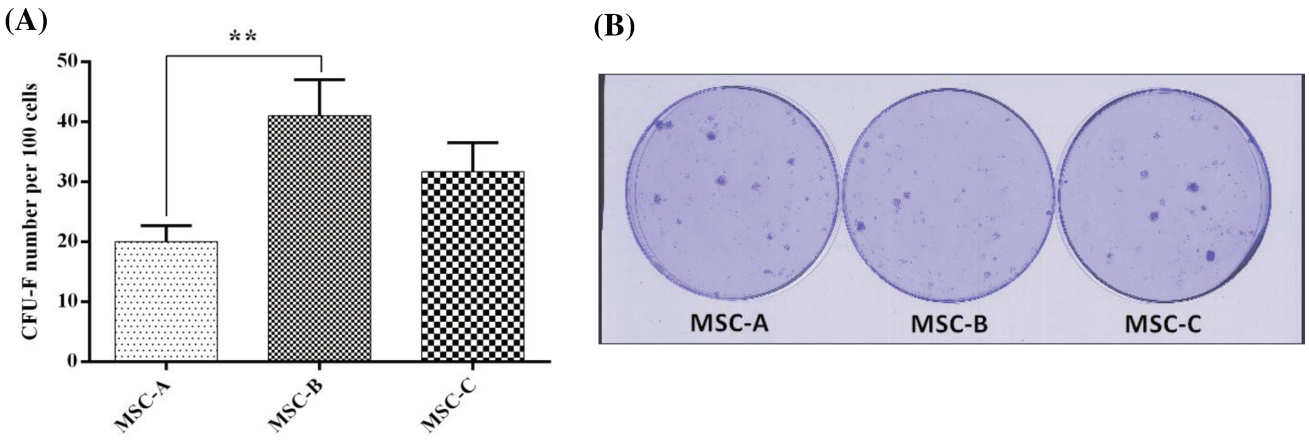

Figure 26: (A) Clonogenic capacity evaluated by CFU-F numbers ($^{**}p < 0.01$, MSC-A vs MSC-B); Representative images of CFU-F (B).

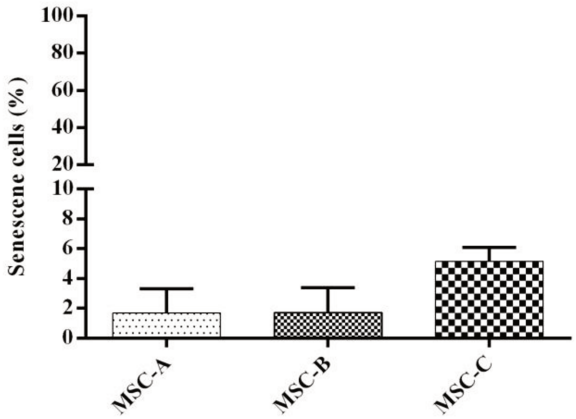

Figure 27: The senescence test was performed at passage 3 for each group of MSCs: the percentage of senescence cell (MSC-A, B and C).

II. Comparison of MSC properties in two different hydrogels

ARTICLE 1:

Comparison of MSC properties in two different hydrogels. Impact of mechanical properties

Hao Yu, Ghislaine Cauchois, Nicolas Louvet, Yun Chen, Rachid Rahouadj, Céline Huselstein.

Bio-Medical Materials and Engineering, 2017, 28(S1): S193-S200.

Once articular cartilage is damaged, it has poor ability to heal. At present, alginate-based hydrogels have 3D-dimensional physical structures with great potential for applications in cartilage tissue engineering. For osteochondral defect, it will be necessary to use stratified scaffold to mimic zonal organization of cartilage. This study aims to compare the characteristics of alginate (Alg)/hyaluronic acid (HA) hydrogels which will mimic cartilage with alginate (Alg)/hydroxyapatite (Hap) hydrogels which will mimic subchondral bone.

Methods:

The methods of viscosity, mechanical behavior, cell viability/proliferation and histochemical staining were used to character the Alg/HA and Alg/Hap hydrogel.

Results and conclusions:

Through the analysis of cell viability and proliferation, the percentage of living cells in Alg/Hap hydrogel is significant higher than in Alg/HA one, which is also associated with the results of shear viscosity. Moreover, under the processing of autoclaving, it has a negative influence on the viscosity behavior and mechanical properties of Alg/HA and Alg/Hap hydrogels. In addition, when WJ-MSCs-laden hydrogels were cultured in a chondrogenic differentiation medium after 30 days, both hydrogels exhibited an extracellular matrix containing collagen and proteoglycans. In conclusion, Alg/Hap hydrogels presented good mechanical properties and cytocompatibility as compared with Alg/HA hydrogels.

Bio-Medical Materials and Engineering 28 (2017) S193–S200
DOI 10.3233/BME-171641
IOS Press

Comparison of MSC properties in two different hydrogels. Impact of mechanical properties

Hao Yu [a,d], Ghislaine Cauchois [a,d], Nicolas Louvet [b], Yun Chen [c], Rachid Rahouadj [b] and Céline Huselstein [a,d,*]

[a] *UMR 7365 CNRS, Ingénierie Moléculaire et Physiopathologie Articulaire (IMoPA), Biopôle, Université de Lorraine, 54500, Vandoeuvre-lès-Nancy, France*
[b] *CNRS UMR 7563, Group of Biomechanics and Bioengineering, Université de Lorraine, 54500 Vandoeuvre-lès-Nancy, France*
[c] *Department of Biomedical Engineering, School of Basic Medical Science, Wuhan University, Wuhan 430071, China*
[d] *Fédération de Recherche 3209, Bioingénierie Moléculaire Cellulaire et Thérapeutique, 54500 Vandoeuvre-lès-Nancy, France*

Abstract. Once articular cartilage is damaged, it has poor ability to heal. At present, alginate-based hydrogels have 3D-dimensional physical structures with great potential for applications in carilage tissue engineering. For osteochondral defect, it will be necessary to use stratified scaffold to mimic zonal organization of cartilage. This study aims to compare the characteristics of alginate (Alg)/hyaluronic acid (HA) hydrogels which will mimic cartilage with alginate (Alg)/hydroxyapatite (Hap) hydrogels which will mimic subchondral bone. In this work, we fabricated the 3D-Alg/HA and Alg/Hap hydrogel scaffolds by the original spraying method. From the physical-mechanical properties, we compared mechanical behaviour of Alg/HA and Alg/Hap hydrogel scaffolds, which were examined using indentation testing and viscosity behaviour. This results showed that the Alg/Hap hydrogels exhibited a relative high mechanical strength, as well as the viscosity of Alg/Hap hydrogels is slight slower than Alg/HA hydrogels. However, autoclaving has more deleterious effect on the mechanical and viscosity properties of Alg/HA and Alg/Hap hydrogels. Cytotoxicity was evaluated through the culture of hydrogel beads-laden Wharton's jelly mesenchymal stem cells (WJ-MSC). In addition, the chondrogenic differentiation of WJ-MSC encapsulated into Alg/HA and Alg/Hap hydrogels were performed by histological analyzing during 30 days of culture. From these results, the percentage of living cells for Alg/Hap is significantly higher than Alg/HA, which also is associated with the results of shear viscosity. Both of hydrogels exhibited differentiate into chondrocyte matrix as collagen and proteoglycans. In conclusion, Alg/Hap hydrogels presented better mechanical property, cytocompatibility and differentiation characteristics than Alg/HA hydrogels.

Keywords: Alginate, hyaluronic acid, hydroxyapatite, Wharton's jelly mesenchymal stem cells, mechanical properties

1. Introduction

Alginate (Alg) is derived from brown seaweed and bacteria, and it is a family of linear co-polysaccharides composed of α-L-guluronic acid (G) and β-D-mannuronic acid (M) units [1]. Alginate

*Corresponding author. E-mail: celine.huselstein@univ-lorraine.fr.

hydrogel can be widely used as scaffolds for tissue engineering, cell delivery, drug, protein immobilization, protein/enzyme and bone/cartilage tissue engineering, due to its have biocompatibility, biodegradability and non-antigenicity [2,3]. For bone or cartilage tissue engineering, alginate is generally combined with others polymers as calcium phosphate [4], Poly(γ-glutamic Acid) [5], chitosan [6], collagen [7], gelatin [4,8], hydroxyapatite (Hap) [7] and hyaluronic acid (HA) [9], to form composite hydrogels. All of them are used as matrix not only to support cell encapsulation and culture, but also to support the cell phenotype and synthesis of matrix-specific macromolecules (cartilage: collagen and proteoglycans; bone: alkaline phosphatase and osteocalcin). Hyaluronic acid, a type of glycosaminoglycuronan, is a linear, high molecular weight polysaccharide consisting of β-D-glucuronic acid and 2-acetamido-2-deoxy-β-D-glucose units, which is a natural component of native cartilage and it can also supports and promotes the chondrogenic differentiation of MSC [9,10]. Hydroxyapatite (Hap, $Ca_{10}(PO_4)_6(OH)_2$), the major inorganic component of bone and tooth, is native to the human body. It is well known that the incorporation of Hap nanoparticles into hydrogels can modulate the mechanical properties of the hydrogel scaffolds [11]. However, we do not possess any element of comparison of mechanical properties of Alg/HA and Alg/Hap hydrogels. In our work, we fabricated the Alg/HA and Alg/Hap hydrogel scaffolds, then compared Alg/HA hydrogel with Alg/Hap hydrogel through analysis the cytocompatibility, mechanical properties and differentiation characteristic.

2. Material and methods

2.1. Preparation of gelling

Two kinds of mixture powder (1.5% (m/v) alginate (medium viscosity, Sigma-Aldrich, France) and hyaluronic acid (Acros organics, USA) at the ratio of 4:1; 1.5% (m/v) alginate and hydroxyapatite (Science Applications Industries, Lyon, France) at the ratio of (19:1)) were sterilized by autoclaving. Then, both of them were homogeneously dissolved in 0.9% sodium chloride (Merck, Germany) to form gel solution (Alg/HA and Alg/Hap) with or without cells by constant stirring in a sterile glass tube. (Without any treatments for the powder, as to be control.)

2.2. Preparation of Alg/HA, Alg/Hap hydrogel scaffolds for mechanical testing

Scaffolds were fabricated by the spraying method which was previously described with cells [12,13]. The spraying system is composed of an airbrush working with a compressor [14]. The spraying bottle containing the gel solution was connected to the airbrush, and then solution was sprayed on a sterile glass plate with the spraying pressure is equal to 0.9 bar, which was quickly and horizontally putted into a bath of 102 mM $CaCl_2$ for 10 minutes, forming the 3D-Alg/HA or 3D-Alg/Hap hydrogel scaffold. And then scaffolds were washed two times with a 0.9% NaCl solution. These scaffold without cells were kept in 1 mM of $CaCl_2$ at room temperature before mechanical testing.

2.3. Expansion in monolayer and differentiation into scaffold of MSC

Wharton's jelly mesenchymal stem cells (WJ-MSC) were isolated by the explant methods from the umbilical cord as previously described [15]. Briefly, human umbilical cords were collected after patents' informed consent which was regarded as surgical waste, as well as on the basis of the guidelines for the care and use of an ethic committee of Nancy Hospital. Umbilical cords were washed with 70% ethanol

hydrogel can be widely used as scaffolds for tissue engineering, cell delivery, drug, protein immobilization, protein/enzyme and bone/cartilage tissue engineering, due to its have biocompatibility, biodegradability and non-antigenicity [2,3]. For bone or cartilage tissue engineering, alginate is generally combined with others polymers as calcium phosphate [4], Poly(γ-glutamic Acid) [5], chitosan [6], collagen [7], gelatin [4,8], hydroxyapatite (Hap) [7] and hyaluronic acid (HA) [9], to form composite hydrogels. All of them are used as matrix not only to support cell encapsulation and culture, but also to support the cell phenotype and synthesis of matrix-specific macromolecules (cartilage: collagen and proteoglycans; bone: alkaline phosphatase and osteocalcin). Hyaluronic acid, a type of glycosaminoglycuronan, is a linear, high molecular weight polysaccharide consisting of β-D-glucuronic acid and 2-acetamido-2-deoxy-β-D-glucose units, which is a natural component of native cartilage and it can also supports and promotes the chondrogenic differentiation of MSC [9,10]. Hydroxyapatite (Hap, $Ca_{10}(PO_4)_6(OH)_2$), the major inorganic component of bone and tooth, is native to the human body. It is well known that the incorporation of Hap nanoparticles into hydrogels can modulate the mechanical properties of the hydrogel scaffolds [11]. However, we do not possess any element of comparison of mechanical properties of Alg/HA and Alg/Hap hydrogels. In our work, we fabricated the Alg/HA and Alg/Hap hydrogel scaffolds, then compared Alg/HA hydrogel with Alg/Hap hydrogel through analysis the cytocompatibility, mechanical properties and differentiation characteristic.

2. Material and methods

2.1. Preparation of gelling

Two kinds of mixture powder (1.5% (m/v) alginate (medium viscosity, Sigma-Aldrich, France) and hyaluronic acid (Acros organics, USA) at the ratio of 4:1; 1.5% (m/v) alginate and hydroxyapatite (Science Applications Industries, Lyon, France) at the ratio of (19:1)) were sterilized by autoclaving. Then, both of them were homogeneously dissolved in 0.9% sodium chloride (Merck, Germany) to form gel solution (Alg/HA and Alg/Hap) with or without cells by constant stirring in a sterile glass tube. (Without any treatments for the powder, as to be control.)

2.2. Preparation of Alg/HA, Alg/Hap hydrogel scaffolds for mechanical testing

Scaffolds were fabricated by the spraying method which was previously described with cells [12,13]. The spraying system is composed of an airbrush working with a compressor [14]. The spraying bottle containing the gel solution was connected to the airbrush, and then solution was sprayed on a sterile glass plate with the spraying pressure is equal to 0.9 bar, which was quickly and horizontally putted into a bath of 102 mM $CaCl_2$ for 10 minutes, forming the 3D-Alg/HA or 3D-Alg/Hap hydrogel scaffold. And then scaffolds were washed two times with a 0.9% NaCl solution. These scaffold without cells were kept in 1 mM of $CaCl_2$ at room temperature before mechanical testing.

2.3. Expansion in monolayer and differentiation into scaffold of MSC

Wharton's jelly mesenchymal stem cells (WJ-MSC) were isolated by the explant methods from the umbilical cord as previously described [15]. Briefly, human umbilical cords were collected after patents' informed consent which was regarded as surgical waste, as well as on the basis of the guidelines for the care and use of an ethic committee of Nancy Hospital. Umbilical cords were washed with 70% ethanol

and Hanks' balanced salt solution (HBSS). The umbilical cord vessels were removed and Wharton's jelly aseptically cut into very small pieces which were cultured in a six-well plate with complete medium (Alpha Modified Eagle Medium, α-MEM, Lonza, belgium) with 10% Fetal bovine serum (Sigma-Aldrich, France), 100 IU/mL penicillin (Gibco, France), 100 μg/mL streptomycin (Gibco, France), 2 mM L-glucose (Sigma-Aldrich, France), and 2.5 μg/mL amphotericin B (Gibco, France). They were incubated at 37°C in 5% CO_2, 5% O_2 incubator. After 7 days, Wharton's jelly pieces were taken out, the culture medium was changed and the culture was maintained until cell subconfluence reached 80%. After 2 weeks, WJ-MSC were harvested with 0.25% Trypsin-EDTA (Sigma-Aldrich, France). Media were changed three times weekly and grown up to the third passage. For viability, proliferation and histological analysis, WJ-MSC were encapsulated into Alg/HA and/or Alg/Hap hydrogel beads, manufactured as previously described [16]. These beads were cultivated in 6-well plates with induced chondrogenic culture medium which contained DMEM-high glucose (Gibco, Grand Island, NY) supplemented with 10% fetal bovine serum, 2 mM L-glutamine, 100 U/mL penicillin, 100 μg/mL streptomycin, 2.5 μg/mL amphotericin B, 1 mM $CaCl_2$, 0.1 μM dexamethasone (Sigma-Aldrich, France), 50 μg/mL ascorbate-2-phosphate (Sigma-Aldrich, France), 100 μg/mL sodium pyruvate (Sigma-Aldrich, France), and 40 μg/mL L-proline (Sigma-Aldrich, France). Scaffolds were incubated at 37°C in a humidified incubator with 5% CO_2, 5% O_2 for 30 days. The differentiation medium was changed three times weekly.

2.4. Viscosity characterization

The preparation of Alg/HA and Alg/Hap gel was manufactured as previously described, shear viscosity of the gels have been measured after autoclaving by using a rheometer DHR-3 (TA Instrument) with a parallel plate. Sample was sheared in between a cone and a plate geometry (diameter = 40 mm, angle = 2°) mounted on a controlled stress rheometer DHR-3 at a temperature of 20°C. In order to measure the steady-state shear viscosity we performed the following protocol: shear rate $\dot{\varepsilon}$ (s^{-1}) was increased step by step from 0.1 to 100 s^{-1} with a maximum time of 180 s at each shearing point and the shear stress τ (Pa) has been recorded. This protocol ensures that transients have disappeared. The shear viscosity (Pa. s^{-1}) is defined by the ratio between the shear stress and shear rate: $\eta = \tau/\dot{\varepsilon}$ [17].

2.5. Spherical indentation testing

The mechanical behavior of 3D-Alg/HA and Alg/Hap hydrogel scaffolds were characterized by using the spherical indentation method. The tests were performed on a Zwick/Roll machine, with 5.5 mm diameter steel sphere. The indenter was pressed into the surface of the hydrogel scaffold at different velocities varying from 0.25, 1, 2.5 and 5 mm/min; three force-displacement curves were obtained for all velocities and scaffolds. The characteristics of hydrogel scaffolds had been evidenced using the force response corresponding to an indenter displacement of 0.35 mm for all specimens whose thickness were between 2 and 3 mm at the same time, it has been clearly shown that the gel exhibits a well-known viscoelastic mechanical behavior.

2.6. Cell proliferation by Alamar Blue® test

The proliferation of encapsulated cells in the Alg/HA and Alg/Hap hydrogel beads were evaluated by using the Alamar Blue™ assay Kit (Thermo scientific, France) for 3, 5, 10, 20 and 30 days. The samples were washed twice with PBS in culture plate, and incubated with Alamar Blue solution (10% v/v of DMEM without phenol red) for 4 hours at 37°C in a humidified incubator with 5% CO_2, 5% O_2.

The fluorescence of reduced Alamar Blue in the solution was determined using a spectrophotometer at wavelengths of 570 nm excitation and 600 nm emission. To calculate the percentage reduction of Alamar Blue™ as following equation:

$$\%\ \text{reduction} = \frac{(\text{OD570}_{(\text{control})} \times 155{,}677) - (\text{OD600}_{(\text{control})} \times 14{,}652)}{(\text{OD570}_{(\text{sample})} \times 117{,}216) - (\text{OD600}_{(\text{sample})} \times 80{,}586)} \times 100$$

2.7. Cell viability assessment

The viability of encapsulated cells were analyzed by flow cytometry using the Annexin-V/propidium iodide (PI) kit (Life technologies, France). Cells were extracted from Alg/HA and Alg/Hap hydrogel beads using 55 mM sodium citrate (Sigma-Aldrich, France) and 50 mM EDTA solution (Merck, Darmstadt, Germany) after 3, 5, 10, 20 and 30 days of culture. After centrifugation (320 g, 5 min), cells were suspended in 100 μL of 1× Annexin-liant buffer with 2.5 μL Annexin V-Alexa 488 and 1 μL PI (100 μg/mL) for 15 minutes at the room temperature. After incubation, 200 μL 1× Annexin V buffer were added to each sample. Then, cells were analyzed by measuring fluorescence emission at 530 nm and 575 nm, respectively, for Alexa 488 (apoptotic cells) and PI (necrotic cells) with a Gallios flow cytometer (Beckman Coulter, Brea, CA, USA).

2.8. Histochemical staining

Matrix synthesis was evaluated by histology. After 30 days of chondrogenic differentiation, Alg/HA and Alg/Hap hydrogel beads were fixed in 4% paraformaldehyde (Sigma), 100 mM sodium cacodylate (Sigma) and 10 mM CaCl2 (Sigma) solution (pH 7.4) for 4 hours and then washed overnight in 100 mM sodium cacodylate and 50 mM BaCl2 (Sigma) buffer (pH 7.4). The hydrogel beads were dehydrated, embedded in paraffin blocks, cut into 5 μm thick sections and mounted onto glass slides. For histological analysis, total collagen and proteoglycans were stained by Sirius red and Alcian Blue, respectively, and observed by light microscopy (DMD 108, Leica, Wetzlar, Germany).

2.9. Statistical analysis

Data are reported and presented as the mean ± standard deviation ($N \geqslant 3$) and were statistically analyzed by two-way ANOVA using Graphpad prism 6 software (GraphPad, San Diego, CA, USA). A value of p less than 0.05 were considered to be significant.

3. Results and discussion

3.1. Rheological characterization

Figure 1 shows the viscosity of Alg/HA and Alg/Hap hydrogel. It presents all the samples behave as shear thinning fluids, i.e. the shear viscosity decreases with the increasing shear rate. After autoclaving, we found that the viscosity of Alg/HA hydrogel is slighter higher than the Alg/Hap hydrogel. It has an effect on the cell behaviour of hydrogels, which it will be discussed later. In addition, for both Alg/HA hydrogel and Alg/Hap hydrogel, it was showed that the viscosity of them by autoclaving is further lower than the control samples, which is due to the depolymerization reaction of alginate under a higher temperature. So, the autoclaving has more deleterious effect on the viscosity of Alg/HA and Alg/Hap hydrogels as compared with controls.

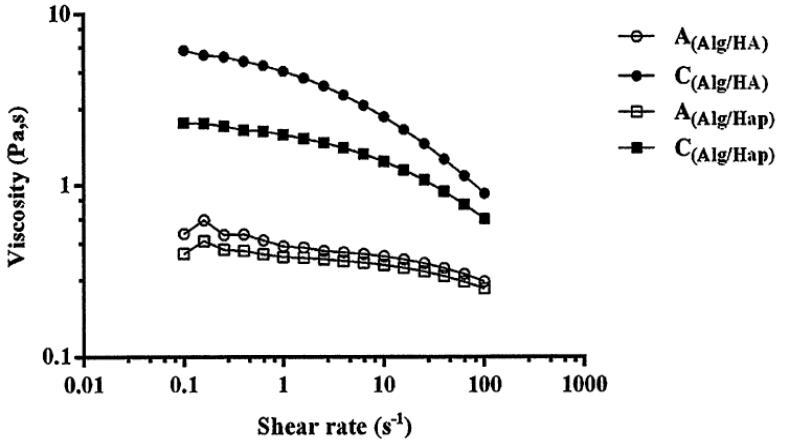

Fig. 1. Shear viscosity of Alg/HA and Alg/Hap hydrogel (autoclave (A), control (C)).

3.2. *Indentation character of hydrogel scaffolds*

Figure 2 illustrates the force-velocity curves of the compression force of 3D-hydrogel scaffolds (Alg/HA and Alg/Hap). As mentioned above, the force measured at 0.35 mm indenter displacement. We found that the mechanical strength of Alg/Hap hydrogel scaffolds is higher than the Alg/HA hydrogel scaffolds under the each velocity, this is because of the incorporation of hap into alginate hydrogel can improve the mechanical properties of hydrogel scaffolds. It also has effect on the cell proliferation of hydrogel, which it will be discussed later. Moreover, whatever the kinds of hydrogel scaffolds, it can be seen that the autoclaving leads to the strength of hydrogel scaffolds decreased. As the velocity equal to 2.5, 5 mm/min, there is obvious significantly difference between autoclaving and control for Alg/HA or Alg/Hap hydrogel scaffolds, which is also believed to be caused by the alginate chain scission and hemolysis (de-polymerization) by the autoclaving. This result demostrated that the Alg/Hap hydorgel scaffolds have a good mechanical properties as compared with Alg/HA hydrogel scaffolds, as well as autoclaving has negatively influenced on the mechanical characteristic of 3D-Alg/HA and Alg/Hap hydrogel scaffolds.

3.3. *Cell viability and proliferation analysis*

Figure 3(A) shows viability of cells encapsulated into Alg/HA and Alg/Hap hydrogel beads. For Alg/HA hydrogel, the cell viability slowly increased from 65 ± 5 to 72 ± 12% with the days of culture. The cell viability of Alg/HA hydrogel is obvious significantly higher than Alg/Hap hydrogel during 5 days of culture ($^{\#}p < 0.0001$). However, from 10 days, the cell viability of Alg/Hap hydrogel rapidly increased, as well as became greater than 90% until 30 days. Which exceed the cell viability of Alg/HA hydrogel ($^{**}p < 0.01$). It could be associated with shear viscosity and tensile strength of hydrogel. In other words, the higher viscosity of hydrogel may decrease cell viability due to the high shear forces required to mix cells, but also stiffer substrate could disrupts cell morphology, and promote the proliferation of cells as had been reported earlier [18,19]. Figure 3(B) presents Alamar Blue reduction of encapsulated cells culture in Alg/HA and Alg/Hap hydrogel beads. It was found that the Alamar Blue reduction of cells in the Alg/HA and Alg/Hap hydrogel beads increased from 3 days to 30 days. At the beginning of cell culture, the Alamar Blue reduction in Alg/HA hydrogel is significantly higher than the

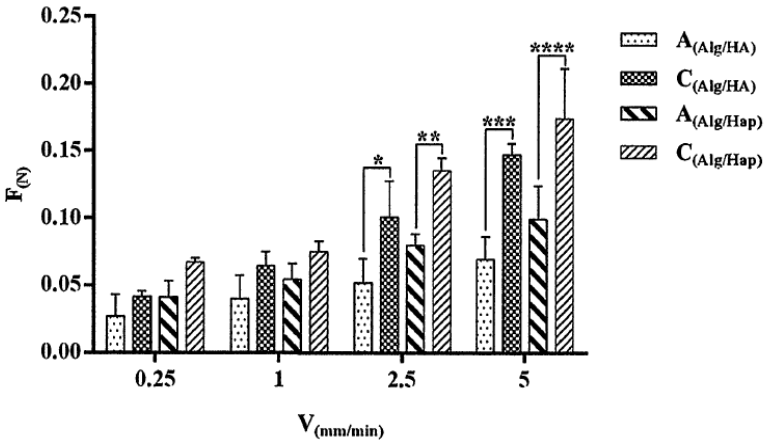

Fig. 2. Typical force-velocity profile of 3D-Alg/HA and Alg/Hap hydrogel scaffolds by the indentation testing, Date are presented as average ± SD with $n \geqslant 3$, analysis of variance (ANOVA). ($^{*}p < 0.05$, $^{**}p < 0.01$, $^{***}p < 0.001$ and $^{****}p < 0.0001$; autoclave (A), control (C).)

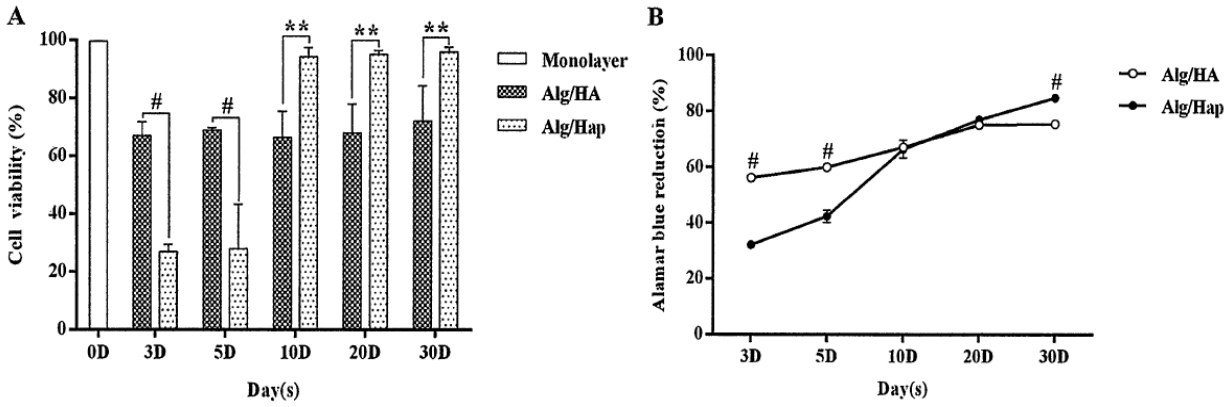

Fig. 3. (A) The viability of encapsulated cells in Alg/HA and Alg/Hap hydrogel scaffolds was measured by flow cytometry after 3, 5, 10, 20, and 30 days of culture and (B) the Alamar Blue reduction of encapsulated WJ-MSCs culture in Alg/HA and Alg/Hap hydrogel scaffold by alamar blue assay after 3, 5, 10, 20 and 30 days. * or # represent a significant difference in each group (Two-way ANOVA, $^{**}p < 0.01$, $^{\#}P < 0.0001$), bars represent the standard deviation, $N = 3$ (viability), $N = 4$ (Alamar blue).

reduction obtained in Alg/Hap hydrogel ($^{\#}p < 0.0001$). Then an important metabolism of cell embedded in Alg/Hap hydrogel was observed after 10 days. This metabolism became significantly higher than that observed in Alg/HA hydrogel at 30 days ($^{\#}p < 0.0001$). This is corresponding to the behavior of cell viability for both of Alg/HA and Alg/Hap hydrogel beads. The results indicated that the cell viability and proliferation in Alg/Hap hydrogel beads was better than in cells embedded in Alg/HA hydrogel beads after the 10 day of culture.

3.4. Histochemical staining

To study chondrogenic differentiation, GAG and collagen synthesis was detected after 30 days of induction. Proteoglycans and total collagen were stained by Alcian blue and Sirius red (Fig. 4), respectively. We found that WJ-MSCs is able to synthesize proteoglycans and collagen in both of Alg/HA and

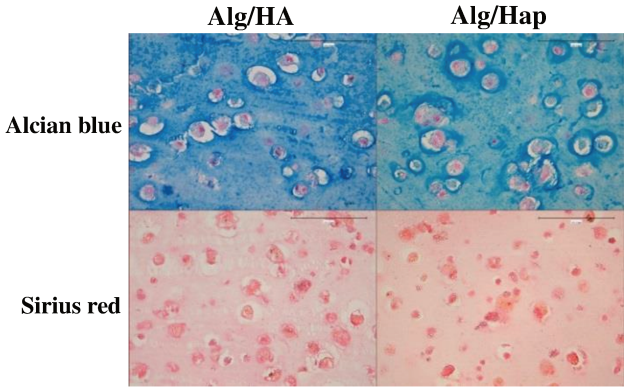

Fig. 4. Histological images of matrix molecules expression by WJ-MSCs encapsulated in Alg/HA and Alg/Hap hydrogel scaffolds after 30 days of chondrogenic induction. Proteoglycans and total collagen were stained by Alcian blue and Sirius red, Scale bar is 100 μm. *WJ-MSC* Wharton's jelly-derived mesenchymal stromal/stem cells.

Alg/Hap hydrogel scaffolds. As well as there is no significant difference in GAG and collagen synthesis were observed between Alg/HA and Alg/Hap hydrogels.

4. Conclusions

Through the analysis of cell viability and proliferation, the percentage of living cells in Alg/Hap hydrogel is significant higher than in Alg/HA one, which also is associated with the results of shear viscosity. Moreover,under the processing of autoclaving, it has negatively influenced on the viscosity behavior and mechanical properties of Alg/HA and Alg/Hap hydrogels. In addition, when WJ-MSCs-laden hydrogels were cultured in a chondrogenic differentiation medium after 30 days, both of hydrogels exhibited an extracellular matrix containing collagen and proteoglycans. In conclusion, Alg/Hap hydrogels presented a good mechanical property and cytocompatibility as compared with Alg/HA hydrogels.

Acknowledgements

This work was supported by the UMR7365 CNRS-Université de lorraine, Ingénierie Moléculaire et physiopathologie Articulaire (IMoPA), Biopôle, and "Program Cai Yuanpei 2013-2015" (CSC No. 201304490192 and 201304490191) from China Scholarship Council.

Conflict of interest

The authors have no conflict of interest to report.

References

[1] J.C. Sun and H.P. Tan, Alginate-based biomaterials for regenerative medicine applications, *Materials* **6**(4) (2013), 1285–1309. doi:10.3390/ma6041285.

[2] J.A. Killion, L.M. Geever, D.M. Devine et al., Fabrication and in vitro biological evaluation of photopolymerisable hydroxyapatite hydrogel composites for bone regeneration, *J Biomater Appl.* **28**(8) (2014), 1274–1283. doi:10.1177/0885328213506951.
[3] N.A. Peppas and B.D. Barr-Howell, *Hydrogels in Medicine and Pharmacy*, N.A. Peppas, ed., CRC Press, Boca Raton, 1986, Chap. 2.
[4] N.T. Linh, K. Paul, B. Kim and B.T. Lee, Augmenting in vitro osteogenesis of a glycine-arginine-glycine-aspartic-conjugated oxidized alginate-gelatin-biphasic calcium phosphate hydrogel composite and in vivo bone biogenesis through stem cell delivery, *J Biomater Appl.* (2016).
[5] W.P. Chan, F.C. Kung, Y.L. Kuo et al., Alginate/Poly(γ-glutamic Acid) base biocompatible gel for bone tissue engineering, *Biomed Res Int.* (2015), 185841.
[6] A.Z. Korzycka, A. Śmieszek, A. Jarmoluk, U. Nowak and K. Marycz, Potential biomedical application of enzymatically treated alginate/chitosan hydrosols in sponges – biocompatible scaffolds inducing chondrogenic differentiation of human adipose derived multipotent stromal cells, *Polymers* **8** (2016), 320.
[7] S.T. Bendtsen and M. Wei, Synthesis and characterization of a novel injectable alginate-collagen-hydroxyapatite hydrogel for bone tissue regeneration, *J Mater Chem B.* **3** (2015), 3081–3090. doi:10.1039/C5TB00072F.
[8] L. Yuan, Y. Wu, J. Fang et al., Modified alginate and gelatin cross-linked hydrogels for soft tissue adhesive, *Artif Cells Nanomed Biotechnol* **8** (2016), 1–8.
[9] L. Reppel, J. Schiavi, N. Charif et al., Chondrogenic induction of mesenchymal stromal/stem cells from Wharton's jelly embedded in alginate hydrogel and without added growth factor: An alternative stem cell source for cartilage tissue
[10] K.Y. Lee and D.J. Mooney, Alginate: Properties and biomedical applications, *Prog Polym Sci.* **37**(1) (2012), 106–126. doi:10.1016/j.progpolymsci.2011.06.003.
[11] Tautzenberger, A. Kovtun and A. Ignatius, Nanoparticles and their potential for application in bone, *Int J Nanomedicine.* **7** (2012), 4545–4557. doi:10.2147/IJN.S34127.
[12] J. Tritz-Schiavi, N. Charif, C. Henrionnet et al., Original approach for cartilage tissue engineering with mesenchymal stem cells, *Biomed Mater Eng.* **20**(3) (2010), 167–174.
[13] J. Tritz, R. Rahouadj, N. de Isla et al., Designing a three-dimensional alginate hydrogel by spraying method for cartilage tissue engineering, *Soft Matter.* **6** (2010), 5165–5174. doi:10.1039/c000790k.
[14] H. Mjahed, C. Porcel, B. Senger et al., Micro-stratified architectures based on successive stacking of alginate gel layers and poly(L-lysine)-hyaluronic acid multilayer films aimed at tissue engineering, *Soft Matter.* **4** (2008), 1422–1429. doi:10.1039/b801428k.
[15] L. Reppel, T. Margossian, L. Yaghi et al., Hypoxic culture conditions for mesenchymal stromal/stem cells from Wharton's jelly: A critical parameter to consider in a therapeutic context, *Curr Stem Cell Res Ther.* **9**(4) (2014), 306–318. doi:10.2174/1574888X09666140213204850.
[16] Y. Wang, N. de Isla, C. Huselstein et al., Effect of alginate culture and mechanical stimulation on cartilaginous matrix synthesis of rat dedifferentiated chondrocytes, *Biomed Mater Eng.* **18**(1) (2008), S47–54.
[17] D. De Kee and C.F. Chan Man Fong, Rheological properties of structured fluids, *Polym Eng Sci.* **34**(5) (1994), 438–445. doi:10.1002/pen.760340510.
[18] E. Schuh, J. Kramer, J. Rohwedel et al., Effect of matrix elasticity on the maintenance of the chondrogenic phenotype, *Tissue Eng Part A* **16**(4) (2010), 1281–1290.
[19] T.A. Ulrich, E.M. de Juan Pardo and S. Kumar, The mechanical rigidity of the extracellular matrix regulates the structure, motility, and proliferation of glioma cells, *Cancer Res.* **69**(10) (2009), 4167–4174. doi:10.1158/0008-5472.CAN-08-4859.

III. Influence of different sterilization methods on the properties of alginate-based hydrogels during the chondrocyte differentiation

ARTICLE 2:

Is there a cause-and-effect relationship between physicochemical properties and cell behavior of alginate-based hydrogel obtained after sterilization?

Hao Yu, Ghislaine Cauchois, Jean-François Schmitt, Nicolas Louvet, Jean-luc Six, Yun Chen, Rachid Rahouadj, Céline Huselstein

Journal of the Mechanical Behavior of Biomedical Materials, 2017, 68:134-143.

As everyone knows, almost all of the biologic scaffold materials are fabricated by the originally polymer in a powder state. To find an effective sterilization method is becoming important for the polymer prior to clinical use. However, in our knowledge, there is no system statistics analysis to evaluate the interrelationship of the characteristics of alginate-based polymer after sterilization.

Alginate-based hydrogel scaffolds are widely used in the field of cartilage regeneration and repair. If the effect of autoclaving on the alginate powder is well known, it is not the same for the possible effects of the sterilization UV treatment on the properties of the hydrogel after polymerization. To select an effective sterilization treatment of alginate-based materials, one must find what are inter-relationship between the characteristics (chemical, physical and mechanical) of alginate-based hydrogel during sterilization, and what consequences have affected on cell behavior.

Methods:

In this study, we investigated the influence of UV sterilization treatments (UV-1 and UV-2: 25 and 50 min, respectively) and autoclaving to obtain alginate (Alg)/hyaluronic acid (HA) hydrogel, as well as further evaluated the relationship between physicochemical properties and cell behavior of Alg/HA hydrogel after UVs and autoclaving. The physicochemical properties of this mixture at the powder or polymerized states were analyzed using ATR-FTIR, HPLC-SEC, rheological, indentation

testing and sterility testing. The cell behavior is evaluated by cell viability and proliferation, and chondrogenic differentiation. The effects of treatment parameters and their correlation with the others characteristics were determined statistically by Principal Component Analysis (PCA).

Results and conclusions:

1): The cell behavior of alginate-based hydrogels were not only regulated by physicochemical properties (as molar mass or/and viscosity), but also associated with the controlling of sterilization time;

2): UV-2 treatment could to be an effective method as compared with others, which minimal impact on the mechanical integrity or physical-chemical properties and maintain its cytocompatibility and its ability to induce chondrogenesis from mesenchymal stem cells.

From these results, it will provide a basis for choosing an effective method of sterilization, but also importantly exhibit the relationship between physicochemical properties and cell behavior of alginate-based hydrogel after sterilization.

Journal of the mechanical behavior of biomedical materials 68 (2017) 134–143

Contents lists available at ScienceDirect

Journal of the Mechanical Behavior of Biomedical Materials

journal homepage: www.elsevier.com/locate/jmbbm

Is there a cause-and-effect relationship between physicochemical properties and cell behavior of alginate-based hydrogel obtained after sterilization?

Hao Yu[a,e], Ghislaine Cauchois[a,e], Jean-François Schmitt[b], Nicolas Louvet[b], Jean-luc Six[c], Yun Chen[d], Rachid Rahouadj[b], Céline Huselstein[a,e,*]

[a] UMR 7365 CNRS, Ingénierie Moléculaire et Physiopathologie Articulaire (IMoPA), Biopôle, Université de Lorraine, 54500 Vandoeuvre-lès-Nancy, France
[b] UMR 7563 CNRS, Group of Biomechanics and Bioengineering, Université de Lorraine, 54500 Vandoeuvre-lès-Nancy, France
[c] UMR 7375, Laboratoire de Chime-Physique Macromoléculaire, ENSIC, Université de Lorraine, 54001 Nancy Cedex, France
[d] Department of Biomedical Engineering, School of Basic Medical Science, Wuhan University, Wuhan 430071, China
[e] Fédération de Recherche 3209, Bioingénierie Moléculaire Cellulaire et Thérapeutique, 54500 Vandoeuvre-lès-Nancy, France

ARTICLE INFO

Keywords:
Sterilization
Alginate
Hydrogel
Autoclave
UV

ABSTRACT

Alginate-based hydrogel scaffolds are widely used in the field of cartilage regeneration and repair. If the effect of autoclaving on the alginate powder is well known, it is not the same for the possible effects of the sterilization UV treatment on the properties of the hydrogel after polymerization. To select an effective sterilization treatment of alginate-based materials, one must find what are inter-relationship between the characteristics (chemical, physical and mechanical) of alginate-based hydrogel during sterilization, and what consequences have affected on cell behavior. In this study, we investigated the influence of UV sterilization treatments (UV-1 and UV-2: 25 and 50 min, respectively) and autoclaving to obtain alginate (Alg)/hyaluronic acid (HA) hydrogel, as well as further evaluated the relationship between physicochemical properties and cell behavior of Alg/HA hydrogel after UVs and autoclaving. The physicochemical properties of this mixture at the powder or polymerized states were analyzed using ATR-FTIR, HPLC-SEC, rheological, indentation testing and sterility testing. The cell behaviors of hydrogels were evaluated by cell viability and proliferation, and chondrogenic differentiation. The effects of treatment parameters and their correlation with the others characteristics were determined statistically by Principal Component Analysis (PCA). In this study, we have shown that the cell behavior in alginate-based hydrogels was not only regulated by physicochemical properties (as molar mass or/and viscosity), but also associated with the controlling of sterilization time. It can provide a basis for choosing an effective method of sterilization, which can keep the mechanical or physical-chemical properties of Alg-based hydrogel scaffold and maintain its cytocompatibility and its ability to induce chondrogenesis from mesenchymal stem cells.

1. Introduction

Articular cartilage has poor ability to self-repair, and damage due to tissue lesion, trauma, or natural degeneration. In order to repair the damaged cartilage, many researchers have promoted alginate-based scaffold to use in field of tissue-engineered cartilage due to it is easily to construct the hydrogels which support cell encapsulation and culture. Several studies have shown that alginate-based scaffold can promote mesenchymal stem cells (MSC) differentiation to chondrocyte phenotype, and synthesis of cartilage-specific matrix (Zhao et al., 2013; Van Vlierberghe et al., 2011; Sun and Tan et al., 2013; Xu et al., 2008; Reppel et al., 2005). Meanwhile, sterilized alginate-based composite powder is imposed. So the effective sterilization methods play an important role in the application of biomedical that not only eliminate the risk of infection, but also maintain structure, function and use of materials (Ahmed et al., 2013). However, it is reported that alginate is difficult to sterilize and to handle (Puppi et al., 2010). Even if Draget et al. (1990) produced sterilized alginate by filtration *via* an appropriate submicron filter, it is not very convenient for highly viscous of alginate hydrogel. Generally, moist heat (Hu et al., 2014; Ofori-Kwakye and Martin, 2005), autoclaving (Leo et al., 1990; Vandenbossche et al., 1993; Ofori-Kwakye and Martin, 2005), ethylene oxide (Leo et al., 1990), gamma-irradiation (Lee et al., 2003) and UV (Mao et al., 2012) are used to sterilize the alginate-powder, but for both of them lead to the chain scission and hemolysis of alginate due to the high pressure and temperature which the process of it is called de-polymerization.

* Corresponding author at: UMR 7365 CNRS, Ingénierie Moléculaire et Physiopathologie Articulaire (IMoPA), Biopôle, Université de Lorraine, 54500 Vandoeuvre-lès-Nancy, France.
E-mail address: celine.huselstein@univ-lorraine.fr (C. Huselstein).

http://dx.doi.org/10.1016/j.jmbbm.2017.01.038
Received 26 September 2016; Received in revised form 21 January 2017; Accepted 24 January 2017
Available online 25 January 2017

However, among all these sterilization process, there is no statistic analysis that studies the inter-relationship between the physicochemical characteristics of alginate hydrogel after sterilization and cell behavior.

Alginate (Alg) could be obtained from brown algae and some soil bacteria. This is a linear polysaccharide containing blocks of (1,4)-linked β-D-mannuronic acid (M units) and α-L-guluronic acid (G units) residues which are believed to take part in intermolecular cross-linking with Ca^{2+} to form hydrogels (Lee and Mooney et al., 2012). The structure of alginate hydrogel is similar to the glycosaminoglycan (GAG), which is long unbranched polysaccharides makes up the cartilage (Wang et al., 2009). Several studies reported that alginate-based hydrogel have a good biocompatibility, non-immunogenic and chondrogenic differentiation, when MSC were seeded into hydrogel (Xu et al., 2008; Follin et al., 2015; Guo et al., 2014; Du et al., 2016). Similarly, hyaluronic acid (HA) is a glycosaminoglycan consisting of D-glucuronic acid and D-N-acetylglucosamine units. It is an important component of proteoglycan organization which composed cartilage tissue. Meanwhile, it can contribute to the function of the tissue itself (Collins et al., 2013). It is considered as a chondrogenesis inductor of MSC (Chung and Burdick, 2009). Borzacchiello et al. (2015) made the HA hydrogel through the cross-linking HA molecules with divinyl sulfone (DVS) and have shown it has a good biocompatibility, mechanical and injectability properties suited to biomedical application. So, both alginate and HA natural polymers exhibit properties of biocompatibility, biodegradability, non-immunogenicity and low cost. They can be an attractive hydrogel candidate for cartilage tissue engineering. In our work, we planned to combine the alginate with hyaluronic acid as raw materials to form hydrogel scaffold. Even if the effects of autoclaving on alginate powder properties are known, very few is know about the effect of UV as sterilization treatments on alginate-based composite powder properties and on its capacity to maintain chondrogenic differentiation *in vitro*. Meanwhile, our ultimate goal was to estimate the correlation between physicochemical properties and cell behavior of alginate-based hydrogel during sterilization.

2. Materials and methods

2.1. Sterilization treatments of powder

The powder of 1.5% (m/v) alginate (medium viscosity, Sigma-Aldrich, France) and hyaluronic acid (Acros organics, USA) (ratio 4:1) was sterilized by UV-1 treatment (ultraviolet during 25 min), UV-2 treatment (ultraviolet during 25 min and was turned over during 25 min) (Ultraviolet lamp=2×15 w, wavelength=254 nm, Distance=30 cm, Vilber lourmat, France), autoclaving at 121 °C for 30 min (Advantage-Lab, AL02-07-100, France), non-sterilized (without any treatments for the powder, as to be control). Then, they were homogeneously dissolved in 0.9% sodium chloride (Merck, Germany) to form gel solution by constant stirring in a sterile glass tube.

2.2. Hydrogel scaffold construct, cell culture and chondrogenic differentiation

To prepare gel solution as we described above. A syringe was used to absorb the gel solution before being dropped in a 102 mmol/L $CaCl_2$ (Sigma-Aldrich, France) solution for 10 min, forming spherical beads (Alg/HA) completely. Then the hydrogel beads were washed three times by 0.9% NaCl solution, which was further studied. In addition, we used the spraying method to make the hydrogel scaffold which was previously described with cells (Tritz et al., 2010; Tritz-Schiavi et al., 2010). The spraying system is composed of an airbrush working with a compressor (Mjahed et al., 2008). The spraying bottle containing the gel solution was connected to the airbrush, and then solution was sprayed on a sterile glass plate with the spraying pressure is equal to 0.9 bar, which was quickly and horizontally putted into a bath of 102 mM $CaCl_2$ for 10 min, forming the 3D-Alg/HA hydrogel scaffold. And then scaffolds were washed two times with a 0.9% NaCl solution. These scaffold without cells were kept in 1 mM of $CaCl_2$ at room temperature before Attenuated Total Reflection Fourier Transform Infrared (ATR-FTIR) analysis and mechanical testing.

Wharton's jelly mesenchymal stem cells (WJ-MSC) were isolated by the explant methods from the umbilical cord as previously described (Reppel et al., 2014). Briefly, human umbilical cords were collected after patents' informed consent which was regarded as surgical waste, as well as on the basis of the guidelines for the care and use of an ethic committee of Nancy Hospital. Umbilical cords were washed with 70% ethanol and Hanks' balanced salt solution (HBSS). The umbilical cord vessels were removed and Wharton's jelly aseptically cut into very small pieces which were cultured in a six-well plate with complete medium (Alpha Modified Eagle Medium, α-MEM, Lonza, belgium) with 10% Fetal bovine serum (Sigma-Aldrich, France), 100 IU/mL penicillin (Gibco, France), 100 µg/mL streptomycin (Gibco, France), 2 mM L-glucose (Sigma-Aldrich, France), and 2.5 µg/mL amphotericin B (Gibco, France). They were incubated at 37 °C in 5% CO_2, 5% O_2 incubator. After 7 days, cells have migrated from Wharton's jelly and adhered on plate. Then, Wharton's jelly pieces have been removed and culture medium was changed twice a week until cell subconfluence (80%). After 2 weeks, WJ-MSC were harvested with 0.25% Trypsin-EDTA (Sigma-Aldrich, France) and seeded in a new culture flask with a density 1000 cells/cm². Media were changed three times weekly. This process was repeated until culture up to the third passage. For viability, proliferation and chondrogenic differentiation analysis, WJ-MSC were encapsulated into Alg/HA hydrogel beads, manufactured as previously described (Wang et al., 2008). Scaffolds were cultivated in 6-well plates with induced chondrogenic culture medium which contained DMEM-high glucose (Gibco, Grand Island, NY) supplemented with 10% fetal bovine serum, 2 mM L-glutamine, 100 IU/mL penicillin, 100 µg/mL streptomycin, 2.5 µg/mL amphotericin B, 1 mM $CaCl_2$, 0.1 µM dexamethasone (Sigma-Aldrich, France), 50 µg/mL ascorbate-2-phosphate (Sigma-Aldrich, France), 100 µg/mL sodium pyruvate (Sigma-Aldrich, France), and 40 µg/mL L-proline (Sigma-Aldrich, France). Scaffolds were incubated at 37 °C in a humidified incubator with 5% CO_2, 5% O_2 for 30 days. The differentiation medium was changed three times weekly.

2.3. Chemical properties of hydrogel scaffold

2.3.1. Fourier Transform infrared (FTIR) spectroscopy

Attenuated Total Reflection Fourier Transform Infrared (ATR-FTIR) spectra were recorded on a Fourier transform infrared spectrometer (170SX, Nicolet Co., Madison, WI, USA) to analyse the chemistry of prepared 3D-Alg/HA hydrogel scaffolds during these sterilization methods. Each sample was dried on vacuum desiccator at 60 °C for 24 h, then cut into small pieces and moved onto ATR crystal, which were measured with a FTIR spectrometer. The infrared spectra of the raw materials (dry alginate and hyaluronic acid powders) were also respectively measured with a FTIR spectrometer; the spectra were collected over range of 4000–500 cm^{-1}.

2.3.2. Molecular weights evolution

Size Exclusion Chromatography (SEC) was performed at room temperature to quantify some possible degradation of Alg/HA during treatments. SEC was performed using a Waters HPLC pump equipped with a serial set of SP 806, 805 and 804 OH pack columns (Shodex). Elution was carried out with 0.1 M $NaNO_3$ containing NaN_3 as a bactericide (0.4 g/L) at 0.7 mL/min, and was monitored by Multi Angle Laser Light Scattering detector (MALLS Mini Damn, Wyatt) and differential refractometry (Waters 410) dual detection.

Solution (2 mg/mL) were prepared by dissolution in the same eluent and left under vigorous stirring for 24 h. Filtration of solutions

was carried out right before injection, in order to get rid of possible aggregates. Refractive index increments (dn/dc) equal to 0.154 mL/g and 0.145 mL/g were measured in the same eluent for alginate and hyaluronic acid, respectively. dn/dc used for Alg/HA (ratio 4/1) blend was estimated by the following equation:

$$(dn / dc)_{Alg/HA} = 0.8\ (dn / dc)_{Alg} + 0.2(dn/dc)_{HA} = 0.1522$$

2.4. Physical properties of hydrogel scaffold

2.4.1. Viscosity characterization

The shear viscosity of Alg/HA hydrogel has been measured after treatments of autoclave, UV-1, UV-2 and control (hydrogel obtained from a no sterilized Alg/HA powder). Sample was sheared in between a cone and a plate geometry (diameter=40 mm, angle=2°) mounted on a controlled stress rheometer DHR-3 (TA Instrument). The preparation of Alg/HA gel was manufactured as previously described and all the measurements are done at a temperature of 20 °C. In order to measure the steady-state shear viscosity we performed the following protocol: shear rate $\dot{\varepsilon}$ (s^{-1}) was increased step by step from 0.1 to 100 s^{-1} with a maximum time of 180 s at each shearing point and the shear stress τ (Pa) has been recorded. This protocol ensures that transients have disappeared. The shear viscosity η (Pa. s^{-1}) is defined by the ratio between the shear stress and shear rate: $\eta=\tau/\dot{\varepsilon}$ (De Kee and Chan Man Fong, 1994).

2.4.2. Mechanical testing

The mechanical behavior of 3D-Alg/HA hydrogel scaffolds were characterized for various sterilization treatments using the spherical indentation technique as the following Fig. 1.A-B. The tests were performed on a Zwick/Roll machine, with 5.5 mm diameter steel ball. The indenter was introduced onto the surface of the hydrogel scaffold at different velocities varying from 0.25 to 5 mm/min. Three force-displacement curves were obtained for all velocities and treatments. The effects of the sterilization treatments had been evidenced using the force response corresponding to an indenter displacement of 0.35 mm for all specimens whose thicknesses were between 2 and 3 mm. At the same time, it has been clearly shown that the gel exhibits a well-known viscoelastic mechanical behavior.

2.5. Sterility testing

Hydrogel beads (n≥8) without cells were immersed in Fluid Thioglycollate medium (FTM) (Sigma-Aldrich, France) which was designed to test the growth of bacteria and in Sabouraud 2% Glucose Agar (SGA) (Sigma-Aldrich, France) for fungal cultivation for a period of 7 days at 37 °C. Culture mediums alone served as negative control whereas unsterilized samples served as positive control. Every 2 days, we examined the clouding of the FTM and the appearance of the colonies in the Sabouraud agar indicated contamination and inefficient sterilization.

2.6. Biocompatibility and histological

2.6.1. Cell viability assessment

To assess the viability of encapsulated cells the PI/Annexin-V kit (Life technologies, France) was used. Cells were extracted from Alg/HA hydrogel beads using 55 mM sodium citrate (Sigma-Aldrich, France) and 50 mM EDTA solution (Merck, Darmstadt, Germany) after 3, 5, 10, 20 and 30 days of culture. After centrifugation (320 g, 5 min), cells were suspended in 100 µL of 1X Annexin-liant buffer with 2.5 µL of Annexin V-Alexa 488 and 1 µL of propidium iodide (PI) for 15 min at the room temperature. Cells were detected with fluorescence emission at 530 nm and 575 nm by Gallios flow cytometer (Beckman Coulter, Brea, CA, USA).

2.6.2. Cell proliferation analysis

The proliferation of encapsulated cells in the Alg/HA hydrogel beads was evaluated by using the Alamar Blue™ assay Kit (Thermo scientific, France) for 3, 5, 10, 20 and 30 days. The samples were washed twice with PBS in culture plate, and then Alamar Blue solution was added (10% v/v of DMEM without phenol red) for 4 h at 37 °C in a humidified incubator with 5% CO_2, 5% O_2. The reaction of Alamar Blue was read in a microplate reader at 570 nm and 600 nm. To calculate the percentage reduction of Alamar Blue™ as following equation:

$$\%\ \text{reduction} = \frac{(OD570_{(control)}\times 155677)-(OD600_{(control)}\times 14652)}{(OD570_{(sample)}\times 117216)-(OD600_{(sample)}\times 80586)} \times 100$$

The absorption value of negative control is culture medium and Alamr Blue™. The experiment was performed in quadruplicate.

2.6.3. Histochemical staining

It was performed after 30 days of differentiation of WJ-MSC seeded into each kind of hydrogel bead. Samples were washed with PBS, then kept in the 4% paraformaldehyde (Sigma-Aldrich, France) for 4 h, and lastly washed overnight in 100 mM sodium cacodylate (Sigma) 10 mM $CaCl_2$ and 50 mM $BaCl_2$ (Sigma-Aldrich, France) buffer. The scaffolds were dehydrated, after embedded in paraffin blocks. Samples were cut into serials sections (5 µm) which was stained with Hematoxylin Eosin Saffron (HES), Sirius red and Alcian blue for cell morphology, total collagen and sulfated proteoglycans (GAG), respectively. Microphotographs were taken using a light microscope (LEICA, DMD108, USA). Image analysis was performed using free software Image J 1.50i, and the percentage stain area was estimated using the following relation: sem percentage=(sem/mean)×100 (Goldring et al., 2006). Where sem is the standard error mean for the measured parameter.

2.7. PCA component analysis

The effects of treatment parameters and their correlation with the others characteristics were determined statistically by means of the Principal Component Analysis method (PCA), which through the XLSTAT software (Addinsoft, New York, USA).

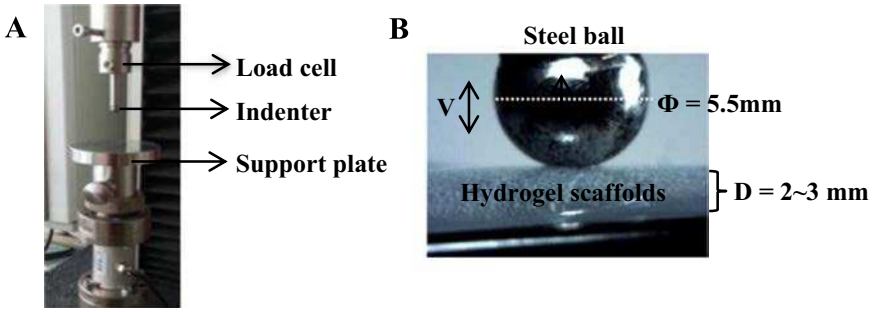

Fig. 1. (A) Apparatus for indentation testing and (B) the illustration of using 5.5mm diameter spherical indenter attached on the surface of 3D-Alg/HA hydrogel scaffolds, which an indenter with a displacement of 0.35 mm at different velocities.

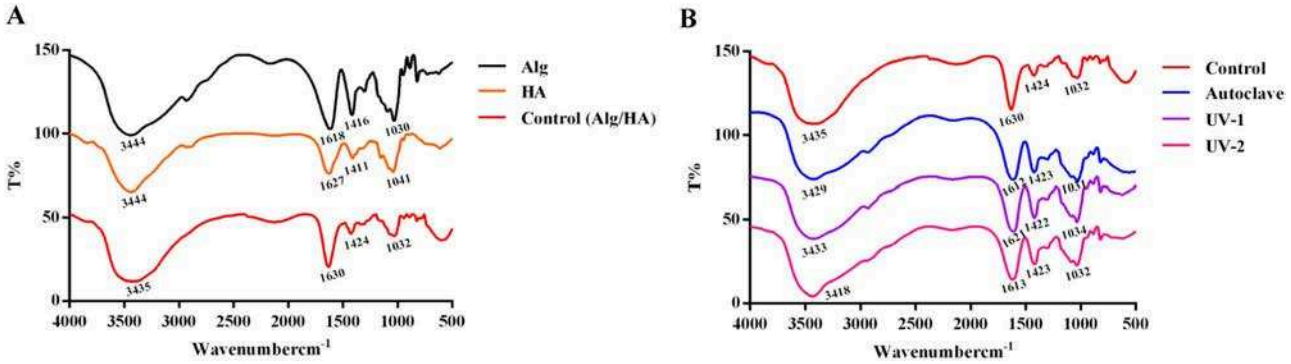

Fig. 2. (A) FTIR spectra of Alg powder, HA powder and Alg/HA hydrogel scaffolds; (B): FTIR spectra of Alg/HA hydrogel scaffolds under exposure to the sterilization methods.

2.8. Statistical analysis

Data are reported and presented as the mean ± standard deviation (SD) (N≥3) and were statistically analyzed by one- or two-way ANOVA (analysis of variance) using GraphPad prism 6 software (GraphPad, San Diego, CA, USA). A value of p less than 0.05 were considered to be significant. If significance existed, a post-hoc analysis was performed using the Bonferonni post-tests to evaluate significance for all experiments.

3. Results and discussion

3.1. FTIR spectra

The FTIR spectra of the Alg powder, HA powder and Alg/HA hydrogel scaffolds are shown in Fig. 2A. For the pure alginate, peaks at 3444, 1030, 1618 and 1416 cm^{-1} were attributed to the stretching of -OH groups, the stretching of C-O-C bonds, the asymmetric and symmetric stretching vibrations of CO_2^-, respectively (Daemi and Barikani, 2012). In case of HA spectrum, peaks at 3444, 1041, 1627 and 1411 cm^{-1} were assigned respectively to the stretching of -OH groups, the stretching of C-O-C bonds, the asymmetric and symmetric stretching vibrations of C=O of amide I functions (Wu, 2012). From the ATR-FTIR spectrum of Alg/HA hydrogel scaffolds, we can observe the asymmetric stretching of C=O bond shifted to 1630 cm^{-1} and symmetric stretching of C=O bond shifted to 1424 cm^{-1}. In addition, the bands of –OH groups shifted from 3444 cm^{-1} to 3435 cm^{-1}. The representative spectra of Alg/HA hydrogel under different sterilization treatments were shown in Fig. 2B. In case of Alg/HA hydrogel, peaks characteristic of carboxylate and amide I groups appeared in the same range. Most important is that no significant shift of characteristic FTIR peaks of Alg/HA hydrogel was observed under different sterilization treatments, which indicated that these sterilization methods have no effect on the chemical functional groups of them. As Mao et al. (2012) demonstrated using UV spectroscopy there was no change in chemical structure of the alginate during de-polymerization process. In addition, we analysis the FTIR peaks of originally pure Alg powders and pure HA powders under treatments of autoclave, UV-1, UV-2 and control, which also further prove without chemical groups changing. These results are shown in supplemental figure (Figs. S1A and 1B).

3.2. Analysis of molar masses

Table 1 shows the result of weight average molecular weight ($\overline{M_w}$) and number average molecular weight ($\overline{M_n}$) of alginate (as Supplemental table. S1) and Alg/HA chains under various sterilization treatments. Here, we found that each sterilization treatment (UV-1, UV-2, and autoclave) led to the degradation of alginate chains even in the Alg/HA blend. In comparison to control, $\overline{M_n}$ and $\overline{M_w}$ for Alg/HA under the treatment of autoclave diminished by about 63% and 52%, respectively, that is much more pronounced that under other treatments (UV-1 and UV-2). Otherwise, the value of $\overline{M_n}$ and $\overline{M_w}$ for Alg/HA under the treatments of UV-1 and UV-2 are very nearly. UV-1 and UV-2 sterilization treatments led to a much less degradation of Alg/HA chains. This phenomenon can be attributed to the absorption of UV energy due to polysaccharide. Since, the formation of free radical through UV light may cleave covalent bonds, which can initiate de-polymerization reaction (Wasikiewicz et al., 2005). While autoclave has more deleterious effect, this is due to the de-polymerization which leads to the breakdown of the main chain backbone of alginate. In conclusion, the autoclave treatment caused an important reduction in $\overline{M_n}$ and $\overline{M_w}$ as compared with control. However, the molecular weight is the most important property of the polymers in the sense that it also governs their mechanical properties, which will be discussed later.

Table 1
Number average molecular weight ($\overline{M_n}$), weight average molecular weight ($\overline{M_w}$) and dispersity ($D=\overline{M_w}/\overline{M_n}$) for Alg/HA under various sterilization methods.

Samples+treatments	$\overline{M_n}$ ×105 (g/mol)	$\overline{M_w}$ ×105 (g/mol)	D
Alg/HA+Control	4,15	4.96	1.19
Alg/HA+Autoclave	1,54	2,39	1.55
Alg/HA+UV-1	2,76	3,78	1.37
Alg/HA+UV-2	2,31	3,44	1.49

3.3. Rheological characterization

The shear viscosity of Alg/HA in gelling state is plotted on Fig. 3 for the three sterilization protocols as for the control sample. Compared to the control samples, the viscosity after UV treatments is roughly decreased, but the fluid keeps its shear thinning behavior, i.e. the

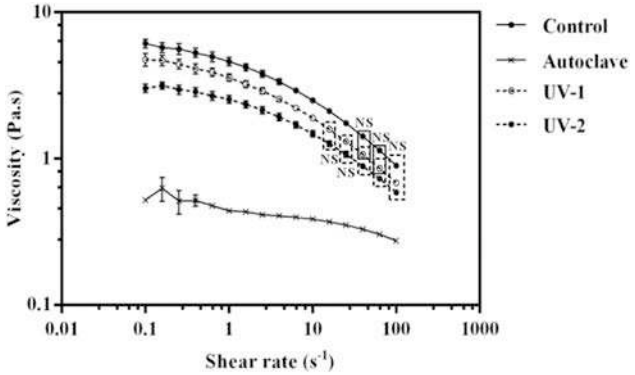

Fig. 3. Shear viscosity of Alg/HA in gelling state under the sterilization treatments (autoclave, UV-1, UV-2 and control) as a function of the shear rate. Control correspond to a hydrogel obtained from a no sterilized Alg/HA powder. The result is expressed as mean ± SD (n=3). No Significant (NS, $p > 0.05$ for UV-1 *vs* UV-2 from 10 s^{-1} to 100 s^{-1}; as $\dot{\varepsilon}$=100 s^{-1}, control *vs* UV-2, control *vs* UV-1 and UV-1 *vs* UV-2).

shear viscosity decreases with the increasing shear rate. The viscosity after autoclave treatment is strongly decreased by one order of magnitude and the shear thinning behaviour is lost. These results are confirmed by the previous study (Lee et al., 2012), which showed that the alginate polymer exhibits a reduction of its viscosity. These methods lead to the alginate chain scission (linked by β (1→4) glycosidic bonds) and hemolysis (de-polymerization).

3.4. Indentation character of hydrogel scaffolds

The hydrogel scaffolds are fairly soft viscoelastic media that require appropriate mechanical characteristics techniques to be investigated. That's why we selected the indentation technique, which is often used for living and synthetic soft materials. This mechanical test can be done at different scales (nano by AFM, micro or macro) and presents the advantage of being fast and non-destructive (Merino et al., 1991; Oyen, 2014; Ahearne et al., 2005), although the strain and stress fields are not uniform. In the present study, we used it to compared the effects of treatment without explicity characterize the mechanical behaviour. Note that the determination of the mechanical behaviour of the hydrogel could only be done by a numerical method such as the finite element method. The main results are given as a function of sterilization treatments in Fig. 4. It illustrates the force-velocity curves of the compression force of 3D-Alg/HA hydrogel scaffolds under these sterilization methods (control, UV-1, UV-2, and autoclave). As mentioned above, we found the mechanical strength (force measured at 0.35 mm indenter displacement). This strain rate sensitivity is significantly lower for autoclave comparing to the other treatments ($p < 0.05$). Moreover, a significant difference in the strength may be observed after UV-2 and autoclave when compared to control. On the other hand, there is not statistically significant difference between UV treatments and control, as well as the value of force for hydrogel under the treatment of UV-2 is almost same to the control at the each velocity.

3.5. Sterilization testing

The efficiency of sterilization approaches on the Alg/HA hydrogel beads without cells were investigated by FTM and SGA from 1 to 7 days to detect the growth of bacteria or funga, respectively. The results are shown in Table 2 and Fig. 5A-B. After 3 days of culture, there is presence of clouding of the thioglycollate broth mediums with hydrogel scaffolds by UV-1 treatment, which indicated that obligate anaerobes grew in the lower areas of the tube. Otherwise, until 7 days, we found that there is no clouding of the thioglycollate broth in the medium for hydrogel scaffolds sterilized by UV-2 and autoclave treatments. Meanwhile, for all of treatment methods, there is no appearance of colonies in the Sabouraud 2% Glucose agar until 7 days of culture while for positive control, we observed colonies at 7 days. In conclusion,

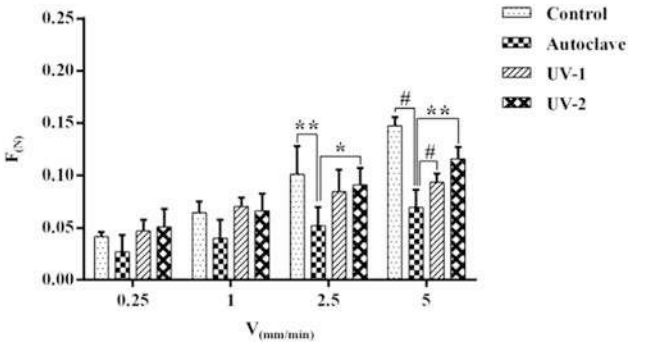

Fig. 4. Typical force-velocity profile of Alg/HA hydrogel scaffolds through the testing of indentation, Date are presented as mean ± SD with n ≥3, analysis of variance (ANOVA). (V=2.5 mm/min, $^{*}p < 0.05$, UV-2 *vs* autoclave; $^{**}p < 0.01$ control *vs* autoclave; and V=5 mm/min, $^{\#}p < 0.001$, control *vs* autoclave, UV-1 *vs* autoclave; $^{**}p < 0.01$, UV-2 *vs* autoclave).

Table 2
Efficiency of sterilization approaches on Alg/HA hydrogels. "+" present contamination of FTM medium or in SGA, "–" present non-pollution when the samples were immersed into the FTM medium or in SGA. (Negative control: culture medium; Positive control: unsterilized sample).

Incubation time (days)								
Treatments	Thioglycollate broth				Sabouraud 2% Glucose Agar			
	1	3	5	7	1	3	5	7
Autoclave	–	–	–	–	–	–	–	–
UV-1	–	+	+	+	–	–	–	–
UV-2	–	–	–	–	–	–	–	–
Positive control	+	+	+	+	+	+	+	+
Negative control	–	–	–	–	–	–	–	–

autoclaving and UV-2 treatment keep hydrogel beads from contamination, which can protect them infection from bacterial and fungal. These results are in agreement with De Moraes MA et al. (2014) study on silk fiber membranes. Moreover, our results showed that UV-radiation for 25 min was not enough to eliminate microorganisms for hydrogel scaffold. It also has an effect on cell behavior of Alg/HA hydrogel scaffolds, which it will be shown later.

3.6. Viability and proliferation of WJ-MSC encapsulated into hydrogel beads

Fig. 6A shows viability of cells encapsulated into hydrogels under three kinds of sterilization treatments (autoclave, UV-1 and UV-2). At the beginning of culture, we found that cell viability in monolayer was significantly higher than other treatments ($^{++++}P < 0.0001$). Meanwhile, it was observed that cell viability increased with the days of culture except for UV-1. After 3 days of culture, the proportion of viable cells after autoclave, UV-1 and UV-2 treatments, were 64.3 ± 1.4%, 50.2 ± 0.2% and 55.3 ± 1.2%, respectively. On D30, cell viability reached 81.3 ± 3.9% for autoclaved samples and 89.3 ± 5.5% for UV-2 treatment. These viability rates were close to those observed during monolayer expansion ($P > 0.05$). In contrast, the cell viability of UV-1 samples always kept lower proportion as compared with others ($^{\#}P < 0.0001$) or monolayer ($^{+++}P < 0.001$). Fig. 6B shows the viable/necrotic/apoptotic of cells seeded in Alg/HA hydrogel scaffolds after 30 days of culture. It exhibited that the proportion of viable cells were 73.4% (autoclave), 47.7% (UV-1), 94.8% (UV-2) and 99.9% (monolayer cells). As well as, the percentages of necrotic and apoptotic cell seeded in hydrogels sterilized by UV-1 treatment are much more than the others maintained in hydrogels sterilized by UV-2 and autoclave treatment. Fig. 6C presents Alamar Blue reduction of encapsulated cells culture in Alg/HA hydrogels. It was found that the Alamar Blue reduction of cells in the hydrogel scaffolds increased for the treatment method of UV-2 and autoclave from 5 days to 30 days, with an increase about 2 fold between UV-2 and autoclave on D 3 *vs*. D 30 of culture. Moreover, the results obtained in UV-2 and autoclave are always higher than UV-1 ($p < 0.001$ from D 5). All these results are correlated with the sterilization efficiency. In fact, Stoppel et al. (2014) showed that UV method during 20 min is not enough to eliminate bacterial persistence of hydrogel, but the long duration of UV treatment (25+25 min) seems to be beneficial for living cells-laden Alg/HA hydrogel scaffolds. The authors agree on the fact that the sterilization time is a prime parameter in clinical medicine (Braghirolli et al., 2014).

3.7. Chondrocytes differentiation of WJ-MSC seeded into hydrogel scaffolds

After 3, 5, 10, 20 and 30 days of culture of WJ-MSC seeded into

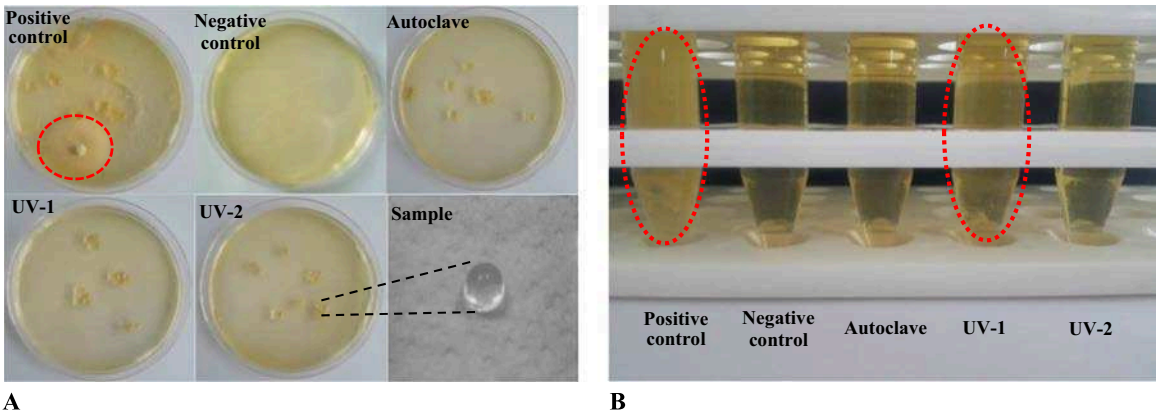

Fig. 5. Efficiency of sterilization treatments on the Alg/HA hydrogel scaffold at 7 days. (A: SGA, there is appearance of white colonies in positive control; B: FTM, there are appearance of phenomena of white haze or flocculent precipitate in positive control and UV-1 treatment).

Alg/HA hydrogel scaffolds, we evaluated the cells organization, cells morphology, GAG and collagen synthesis by histology. Fig. 7A has shown the results obtained from HES coloration. Whatever the sterilization treatments, we found that the repartition of WJ-MSC is uniform into the scaffold and that the cell morphology keeps a round shape. Detected GAG (Fig. 7B) and collagen (Fig. 7C), respectively by

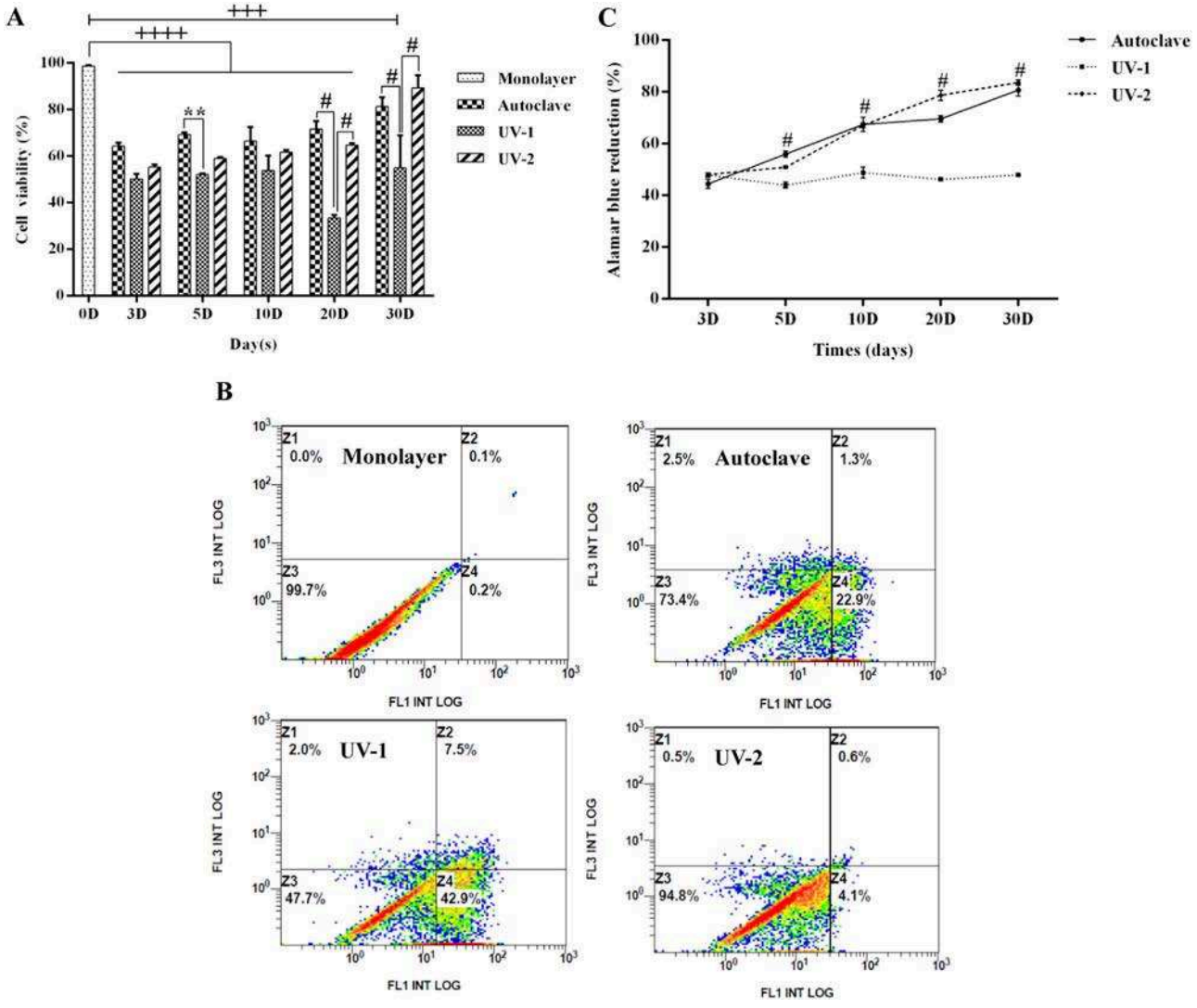

Fig. 6. The viability (A) of encapsulated cells in Alg/HA hydrogel scaffolds was measured by flow cytometry after 3, 5, 10, 20, and 30 days of culture; (B) Flow cytometry analysis of viable/necrotic/apoptotic cells seeded in hydrogel scaffolds at 30 days and (C) the Alamar Blue reduction of encapsulated WJ-MSC culture in Alg/HA hydrogel scaffold by Alamar Blue assay after 3, 5, 10, 20 and 30 days. * or # represent a significant difference in each group (Two-way ANOVA, $^{++++}p < 0.0001$, day x *vs* day 0 (monolayer) for the any treatment; $^{+++}p < 0.001$, day 30 *vs* day 0 for UV-1 treatment; $^{**}p < 0.01$ and $^{\#}p < 0.0001$, autoclave *vs* UV-1, UV-2 *vs* UV-1, autoclave *vs* UV-1 for the same culture time, bars represent the standard deviation, N=3 (viability), N= 4 (Alamar Blue).

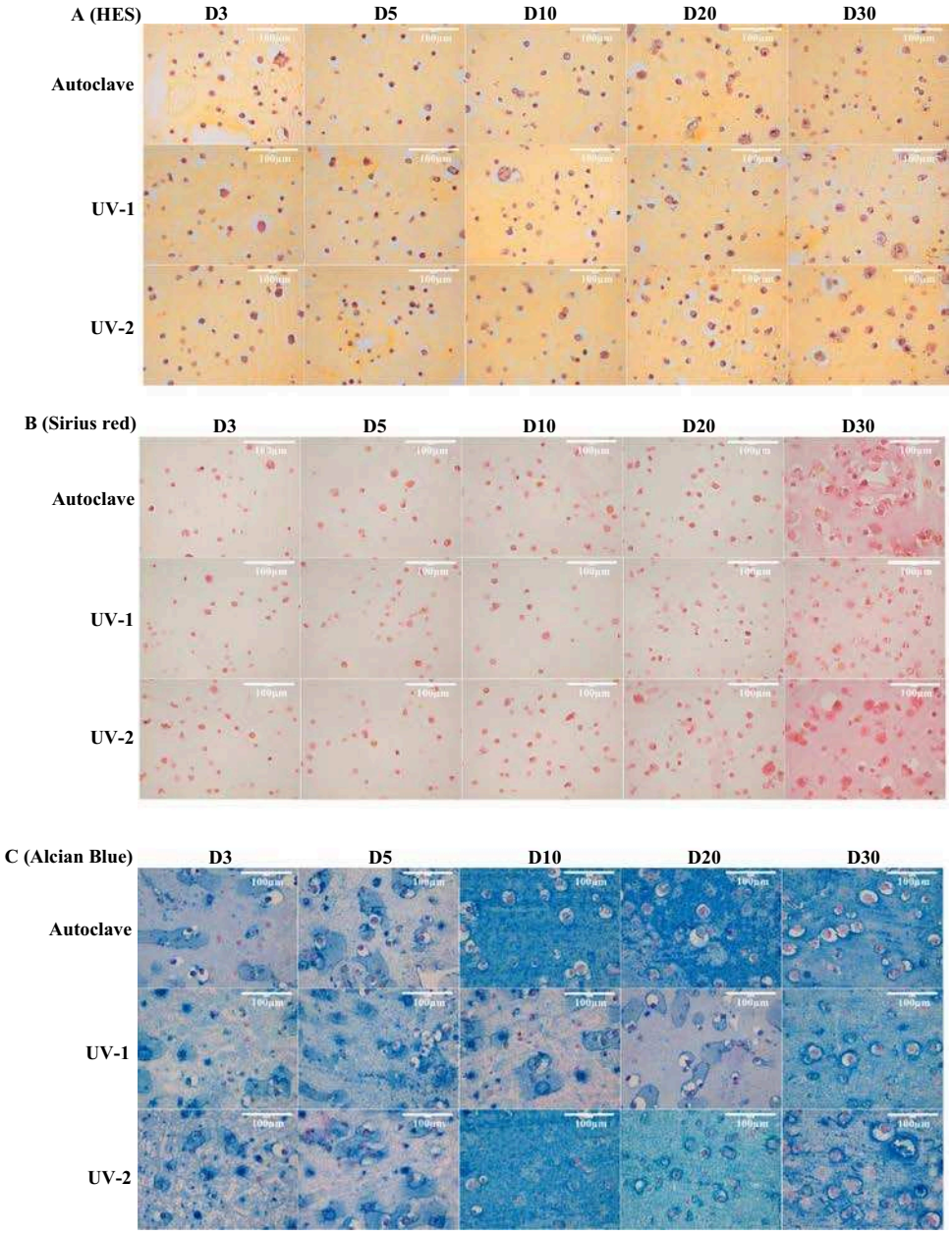

Fig. 7. Histological images of matrix molecules expression by WJ-MSCs encapsulated in Alg/HA hydrogel scaffolds and cultured under the differentiation liquid of chondrocyte after 3, 5, 10, 20 and 30 days. (A) The morphologies of cells in hydrogel scaffold by staining with HES. (B) Collagen synthesis in hydrogel scaffolds by Sirius red staining. (C) Glycosaminoglycan synthesis in hydrogel scaffolds by Alcian Blue staining. Scale bar is 100 μm.

Alcian blue and Sirius red, gradually increased with culture time. Moreover, GAG and collagen synthesis seemed to be greater in hydrogel scaffolds whose powder was sterilized by UV-2 and autoclave compared to hydrogel scaffolds whose powder was sterilized by UV-1. In particular, hydrogel scaffolds whose powder was sterilized by UV-2 stained much more for GAG and collagen than the others treatments after 30 days of culture. Furthermore, after 30 days of chondrogenic differentiation, we measured the percentage of positive stain using ImageJ analysis. The results showed that UV-2 treatment has a significant higher percentage of positive area for collagen (Fig. 8A) as compared with the others treatments ($P < 0.001$). As well as, for the synthesis of GAG (Fig. 8B), highly significant differences were also observed between UV-2 and UV-1 treatment ($^{**}P < 0.01$). From the results above, we can conclude that hydrogel scaffolds with UV-2 treatments may be a good alternative to ensure the cell viability and chondrocyte differentiation of the WJ-MSCs-laden hydrogel.

3.8. PCA component analysis

The effects of treatment parameters and their correlation with the others characteristics were determined statistically by means of the Principal Component Analysis method (PCA), as shown in Fig. 9. In fact, the well-known PCA is used to reveal the internal structure of the present multivariate dataset as a set of coordinates in the corresponding high-dimensional data space. This was done by using an orthogonal transformation to convert the set of observations into a set of uncorrelated variables called principal components (F1 *vs* F2 which represents 84.09% of total variability). In the present case, this procedure was applied to the results of experiments with 16 variables: Control, Autoclave, UV-1, UV-2, M_n, M_W, Viscosity, Viability, Proliferation, Mechanical strength, GAG, Collagen, FTIR $_{(-OH)}$, FTIR $_{(C=O)}$, FTIR $_{(-COO)}$ and FTIR $_{(C-O-C)}$. The PCA bio-plot clearly showed variable parameters are clustered into two groups as A and B (Fig. 9). From view of observation points (1, 2, 3 and 4), physical-chemical

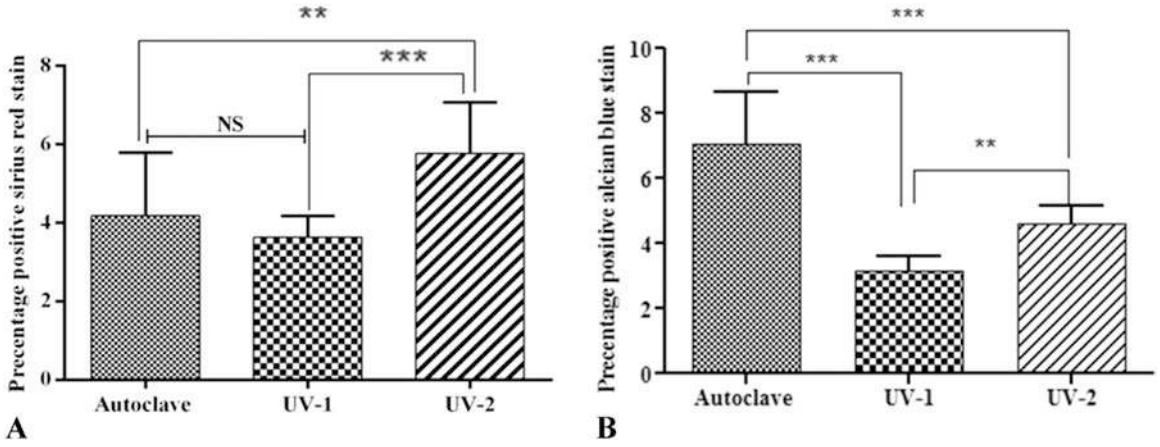

Fig. 8. Sirius red (collagen) positive stain area percentage (A) and Alcian blue (GAG) positive stain area percentage (B) in histological samples. All results are expressed as mean ± SD of the mean (n≥20). ** $p < 0.01$, *** $p < 0.001$ and NS ($p > 0.05$).

parameters (Group A) are negative variables (axis F1). But, the autoclave treatment is relatively further from physical-chemical parameters (Group A), when compared with other treatments. As we described above this is due to de-polymerization of alginate at high temperature. Meanwhile, UV-2 treatment is closed to Group B, which performed the best physical-chemical properties as same as control. For the second principal component (axis F2), biology parameters (Group B) reflected positive variables. It appears that the treatment of UV-2 is located near the viability, proliferation, GAG and collagen parameters as compared with the UV-1 treatment. It seems that UV-2 treatment is beneficial for viable cell as same as autoclave treatment. Moreover, the collagen synthesis seemed to be greater in UV-2 treatment than in the others. It is agreement with results given in Fig. 6 and Fig. 8A, respectively. There is correlation matrix for the studied parameters as shown in Table 3. Without any treatments (control), the Alg/HA hydrogel kept nature properties as $\overline{M_n}$ (0.910), $\overline{M_w}$(0.867), viscosity (0.717) and strength (0.650). For the autoclave treatment, from the view of the biomechanical, it can be seen that autoclave has strong negative affected on molar masses ($\overline{M_n}$: -0.668, $\overline{M_w}$: -0.745), viscosity (-0.884) and strength (−0.915), which is a logical correlation between them. For example, the mechanical properties of alginate hydrogel depending on the viscosity which were determined by weight average molecular weight ($\overline{M_w}$) (Lee and Mooney et al., 2012). More interestingly, this table showed autoclaving produces a concomitant effect on FTIR(C=O) (-0.558), which is also correlated with $\overline{M_n}$ (0.965) and $\overline{M_w}$ (0.942). Actually, when the main chains of Alg/HA or pure alginate are broken during the depolymerization reaction of Alg/HA by autoclaving, each chains will give 2 shorter chains keeping the same chemical composition that the initial ones. It means that shorter chains will have the same chemical groups (FTIR are not changing) with lower M_n. So, decreasing M_n will modify the viscosity or other physical and mechanical properties of Alg/HA hydrogels. From the view of cell behavior, autoclaving has positive effect on the cell viability (0.412) and proliferation (0.451). For UV-1 treatment, one can observe a positive influence on FTIR (C-O-C) (0.927) and negative effect on FTIR (-COO) (-0.816). However, it is not beneficial for cell viability (-0.024) and proliferation (-0.104). For UV-2 treatment, it is can be seen that not only it has positive affected on strength (0,270), but also slightly affected on viscosity (-0.023), $\overline{M_n}$ (-0.243) and $\overline{M_w}$ (-0.157). More importantly, it is beneficial for cell viability (0.544) and prolif-

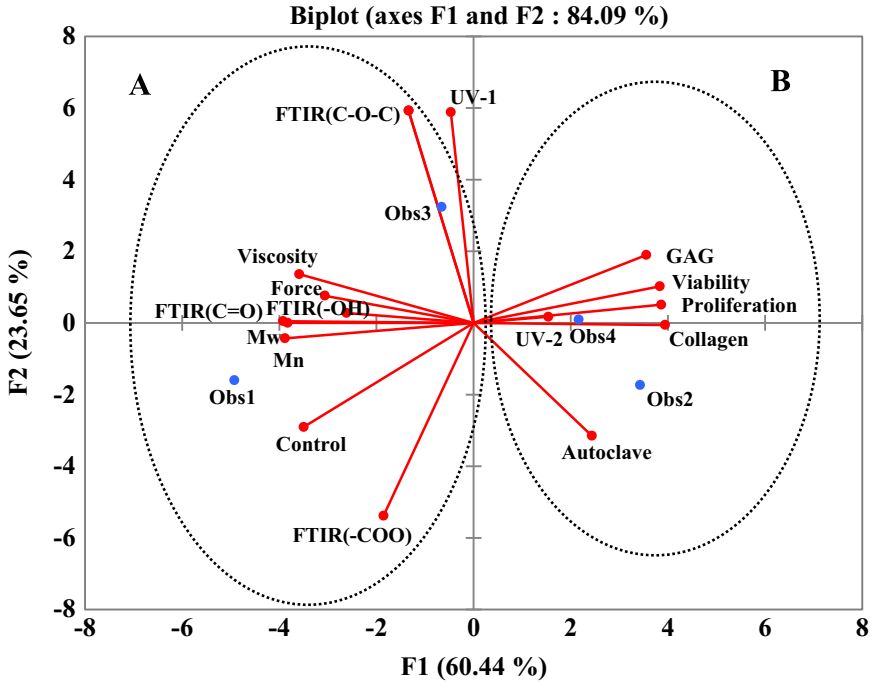

Fig. 9. Illustration of the data set under the new coordinate system defined by the principal components analysis. (axes F1 and F2 representing 84.09%).

Table 3
The correlation matrix for the studied parameters. (Values in bold are different from 0 with a significance level alpha=0.05; Strength: the force of hydrogel scaffolds with a 0.35 mm displacement at 5 mm/min).

Variables	Control	Autoclave	UV-1	UV-2	M_n	M_w	Viscosity	Viability	Proliferation	Strength	GAG	Collagen	FTIR(-OH)	FTIR(C=O)	FTIR(-COO)	FTIR(C-O-C)
Control	1	-0,333	-0,333	-0,333	**0,910**	**0,867**	**0,717**	**-0,931**	**-0,901**	0,650	**-0,929**	**-0,881**	0,549	**0,877**	**0,816**	-0,132
Autoclave	-0,333	1	-0,333	-0,333	**-0,668**	**-0,745**	**-0,884**	0,412	0,451	**-0,915**	0,215	0,594	0,022	-0,558	0,000	-0,662
UV-1	-0,333	-0,333	1	-0,333	0,001	0,035	0,190	-0,024	-0,104	-0,005	0,067	-0,142	0,373	0,159	**-0,816**	**0,927**
UV-2	-0,333	-0,333	-0,333	1	-0,243	-0,157	-0,023	0,544	0,554	0,270	0,647	0,429	**-0,944**	-0,478	0,000	-0,132
M_n	**0,910**	-0,668	0,001	-0,243	1	**0,994**	**0,937**	**-0,941**	**-0,942**	**0,854**	**-0,859**	**-0,977**	0,536	**0,965**	0,556	0,267
M_w	**0,867**	-0,745	0,035	-0,157	**0,994**	1	**0,969**	**-0,901**	**-0,906**	**0,903**	**-0,799**	**-0,959**	0,466	**0,942**	0,510	0,324
Viscosity	0,717	**-0,884**	0,190	-0,023	**0,937**	**0,969**	1	**-0,787**	**-0,808**	**0,952**	-0,644	**-0,896**	0,351	**0,873**	0,323	0,503
Viability	**-0,931**	0,412	-0,024	0,544	**-0,941**	**-0,901**	**-0,787**	1	**0,997**	-0,627	**0,978**	**0,976**	-0,769	**-0,982**	-0,556	-0,183
Proliferation	**-0,901**	0,451	-0,104	0,554	**-0,942**	**-0,906**	**-0,808**	**0,997**	1	-0,636	**0,965**	**0,986**	-0,786	**-0,992**	-0,488	-0,262
Strength	0,650	**-0,915**	-0,005	0,270	**0,854**	**0,903**	**0,952**	-0,627	-0,636	1	-0,470	-0,750	0,060	0,713	0,401	0,360
GAG	**-0,929**	0,215	0,067	0,647	**-0,859**	**-0,799**	-0,644	**0,978**	**0,965**	-0,470	1	**0,911**	**-0,819**	**-0,925**	-0,610	-0,032
Collagen	**-0,881**	0,594	-0,142	0,429	**-0,977**	**-0,959**	**-0,896**	**0,976**	**0,986**	-0,750	**0,911**	1	-0,697	**-0,998**	-0,453	-0,349
FTIR(-OH)	0,549	0,022	0,373	**-0,944**	0,536	0,466	0,351	-0,769	-0,786	0,060	**-0,819**	-0,697	1	0,735	0,108	0,288
FTIR(C=O)	**0,877**	0,159	-0,478	0,965	**0,942**	**0,873**	-0,769	**-0,982**	**-0,992**	0,713	**-0,925**	**-0,998**	0,735	1	0,439	0,348
FTIR(-COO)	**0,816**	0,000	**-0,816**	0,000	0,556	0,510	0,323	-0,556	-0,488	0,401	-0,610	-0,453	0,108	0,439	1	-0,649
FTIR(C-O-C)	-0,132	-0,662	**0,927**	-0,132	0,267	0,324	0,503	-0,183	**-0,992**	0,360	-0,032	-0,349	0,288	0,348	-0,649	1

eration (0.554), but also it has positive affected on the synthesis of GAG (0.647) and collagen (0.429), which depends on a suitable sterilization time (25 min+25 min) and viscosity of hydrogel. Thus, a high viscosity produces a negative effect on cell viability (−0.787) and proliferation (-0.808). In other words, a high of viscosity of gel solution to form hydrogel is not beneficial for cell viability due to the high shear forces required to mix cells with these solutions (Kong et al., 2003; Schneider et al., 2003). Similarly, high molecular masses (M_n and M_w) have negative effect on the cell viability (-0.941, -0.901), proliferation (−0.942, -0.906). In addition, negative correlations between FTIR (-OH), FTIR(C=O) and cell viability (-0.769, -0.982), and proliferation (-0.786, -0.992), and GAG (-0.819, -0.925), and collagen (-0.697, -0.998) may be observed. According to our PCA analysis, it is acquired that a worse viscosity of alginate may be obtained after autoclave treatment. This has consequences on the gel stability and mechanical properties, thereby compromises the use of the gel as a scaffold after this treatment. Furthermore, note that the UV treatment time is an important parameter with regard to the cell behavior (viability, proliferation, GAG and collagen). The duration of 25+25 min (UV2) seems to give better results than simply 25 min (UV1). So, we chose an appropriate shear viscosity of gel solution which is easy to handle and to immobilize cells, but also keep a good mechanical property.

4. Conclusion

The sterilization treatment is crucial process for tissue engineering. We have shown that the mechanical properties of alginate hydrogel depend on the viscosity which was determined by weight average molecular weight ($\overline{M_w}$). Otherwise, the cell behavior in hydrogels depends not only on a suitable sterilization time (25 min+25 min) but also on viscosity of hydrogel. Furthermore, we demonstrated that UV-2 treatment could to be an effective method to sterilize alginate powder, with (i) minimal impact on the mechanical integrity or physical-chemical properties and (ii) ability to maintain alginate cytocompatibility and its ability to induce chondrogenesis from mesenchymal stem cells. In conclusion, the cell behavior of Alg-based hydrogels were not only regulated by physicochemical properties (as molar mass or/and viscosity), but also associated with the controlling of sterilization time.

Acknowledgements

This work was supported by the UMR7365 CNRS-Université de Lorraine, Ingénierie Moléculaire et physiopathologie Articulaire (IMoPA), Biopôle, and “Program Cai Yuanpei 2013–2015” (CSC Nos. 201304490192 and 201304490191) from China Scholarship Council.

Appendix A. Supplementary material

Supplementary data associated with this article can be found in the online version at doi:10.1016/j.jmbbm.2017.01.038.

References

Ahearne, M., Yang, Y., El Haj, A.J., Then, K.Y., Liu, K.K., 2005. Characterizing the viscoelastic properties of thin hydrogel-based constructs for engineering application. J. R. Soc. Interface 2, 455–463.

Ahmed, M., Punshon, G., Darbyshire, A., Seifalian, A.M., 2013. Effects of sterilization treatments on bulk and surface properties of nanocomposite biomaterials. J. Biomed. Mater. Res. B Appl. Biomater. 101, 1182–1190.

Borzacchiello, A., Russo, L., Malle, B.M., Schwach-Abdellaoui, K., Ambrosio, L., 2015. Hyaluronic acid based hydrogels for regenerative medicine applications. Biomed. Res. Int..

Braghirolli, D.I., Steffens, D., Quintiliano, K., Acasigua, G.A., Gamba, D., Fleck, R.A., Petzhold, C.L., Pranke, P., 2014. The Effect of Sterilization Methods on Electronspun Poly(lactide-co-glycolide) and Subsequent Adhesion Efficiency of Mesenchymal Stem Cells, vol. 102, pp. 700–718.

Chung, C., Burdick, J.A., 2009. Influence of three-dimensional hyaluronic acid microenvironments on mesenchymal stem cell chondrogenesis. Tissue. Eng. Part A

15, 243–254.
Collins, M.N., Birkinshaw, C., 2013. Hyaluronic acid based scaffolds for tissue engineering—a review. Carbohydr. Polym. 92, 1262–1279.
Daemi, H., Barikani, M., 2012. Synthesis and characterization of calcium alginate nanoparticles, sodium homopolymannuronate salt and its calcium nanoparticles. Sci. Iran. 19, 2023–2028.
De Kee, D., Chan Man Fong, C.F., 1994. Rheological properties of structured fluids. Polym. Eng. Sci. 34, 438–445.
De Moraes, M.A., Weska, R.F., Beppu, M.M., 2014. Effects of sterilization methods on the physical, chemical, and biological properties of silk fibroin membranes. J. Biomed. Mater. Res B. Appl. Biomater. 102, 869–876.
Draget, K.L., Oestgaard, K., Smidsrod, O., 1990. Homogenous alginate gels: a technical approach. Carbohyd. Polym. 14, 159–178.
Du, W.J., Reppel, L., Leger, L., Schenowitz, C., Huselstein, C., Bensoussan, C., Carosella, E.D., Han, Z.C., Rouas-Freiss, N., 2016. Mesenchymal stem cells derived from human bone marrow and adipose tissue maintain their immunosuppressive properties after chondrogenic differentiation: role of HLA-G. Stem Cells Dev. 25, 1454–1469.
Follin, B., Juhl, M., Cohen, S., Pedersen, A.E., Gad, M., Kastrup, J., Ekblond, A., 2015. Human adipose-derived stromal cells in a clinically applicable injectable alginate hydrogel: phenotypic and immunomodulatory evaluation. Cytotherapy 17, 1104–1118.
Goldring, M.B., Tsuchimochi, K., Ijiri, K., 2006. The control of chondrogenesis. J. Cell. Biochem. **97**, 33–44.
Guo, P., Yuan, Y., Chi, F., 2014. Biomimetic alginate/polyacrylamide porous scaffold supports human mesenchymal stem cell proliferation and chondrogenesis. Mater. Sci. Eng. C Mater. Biol. Appl. 42, 622–628.
Hu, T., Yang, Y., Tan, L., Yin, T., Wang, Y., Wang, G., 2014. Effects of gamma irradiation and moist heat for sterilization on sodium alginate. Biomed. Mater. Eng. 24, 1837–1849.
Kong, H.J., Smith, M.K., Mooney, D.J., 2003. Designing alginate hydrogels to maintain viability of immobilized cells. Biomaterials 24, 4023–4039.
Lee, D.W., Choi, W.S., Byun, M.W., Park, H.J., Yu, Y.M., Lee, C.M., 2003. Effect of gamma-irradiation on degradation of alginate. J. Agric. Food Chem. 51, 4819–4823.
Lee, K.Y., Mooney, D.J., 2012. Alginate: properties and biomedical applications. Prog. Polym. Sci. 37, 106–126.
Leo, W.J., McLoughlin, A.J., Malone, D.M., 1990. Effects of sterilization treatment on some properties of alginate solutions and gels. Biotechnol. Prog. 6, 51–53.
Mao, S., Zhang, T., Sun, W., Ren, X.H., 2012. The depolymerization of sodium alginate by oxidative degradation. Pharm. Dev. Technol. 17, 763–769.
Merino, J.C., Martin, B., Pastor, J.M., 1991. Mechanical indentation tester designed to control and measure in real time the microhardness process. Meas. Sci. Technol. 2, 740–753.
Mjahed, H., Porcel, C., Senger, B., Chassepot, A., Netter, P., Gillet, P., Decher, G., J.C. Voegel, J.C., Schaaf, P., Benkirane-jessel, N., boulmedais, F., 2008. Micro-stratified architectures based on successive stacking of alginate gel layers and poly(L-lysine)–hyaluronic acid multilayer films aimed at tissue engineering. Soft Matter 4, 1422–1429.
Ofori-Kwakye, K., Martin, G.P., 2005. Viscolelastic characterisation of calcium alginate gels intended for wound healing. J. Sci. Technol. 25, 46–52.
Oyen, M.L., 2014. Mechanical characterization of hydrogel materials. Int. Mater. Rev. 59, 44–59.
Puppi, D., Chiellini, F., Piras, A.M., Chiellini, E., 2010. Polymeric materials for bone and cartilage repair. Prog. Polym. Sci. 35, 403–440.
Reppel, L., Schiavi, J., Charif, N., Leger, L., Yu, H., Pinzano, A., Henrionnet, C., Stoltz, J.F., D. Bensoussan, D., Huselstein, C., 2005. Chondrogenic induction of mesenchymal stromal/stem cells from Wharton's jelly embedded in alginate hydrogel and without added growth factor: an alternative stem cell source for cartilage tissue engineering. Stem Cell. Res. Ther. 6, 260–273.
Reppel, L., Margossian, T., Yaghi, L., Moreau, P., Mercier, N., Leger, L., Hupont, S., Stoltz, J.F., Bensoussan, D., Huselstein, C., 2014. Hypoxic culture conditions for mesenchymal stromal/stem cells from wharton's jelly: a critical parameter to consider in a therapeutic context. Curr. Stem Cell. Res. Ther. 9, 306–318.
Schneider, S., Feilen, P.J., Kraus, O., Haase, T., Sagban, T.A., Lehr, H.A., Beyer, J.R., Pommersheim, R., Weber, M.M., 2003. Biocompatibility of alginates for grafting: impact of alginate molecular weight. Artif. Cells. Blood Substit. Immobil. Biotechnol. 31, 383–394.
Stoppel, W.L., White, J.C., Horava, S.D., Henry, A.C., Roberts, S.C., Bhatia, S.R., 2014. Terminal sterilization of alginate hydrogels: efficacy and impact on mechanical properties. J. Biomed. Mater. Res B Appl. Biomater. 102, 877–884.
Sun, J., Tan, H., 2013. Alginate-based biomaterials for regenerative medicine application. Materials. 6, 1285–1309.
Tritz, J., Rahouadj, R., De Isla, N., Charif, N., Pinzano, A., Mainard, D., Bensoussan, D., Netter, P., Stoltz, J.F., Benkirane-Jessel, N., Huselstein, C., 2010. Designing a three-dimensional alginate hydrogel by spraying method for cartilage tissue engineering. Soft Matter 6, 5165–5174.
Tritz-Schiavi, J., Charif, N., Henrionnet, C., de Isla, N., Bensoussan, D., Magdalou, J., Stoltz, J.F., Benkirane-jessel, N., Huselstein, C., 2010. Original approach for cartilage tissue engineering with mesenchymal stem cells. Biomed. Mater. Eng. 20, 167–174.
Van Vlierberghe, S., Dubruel, P., Schacht, E., 2011. Biopolymer-based hydrogels as scaffolds for tissue engineering application: a review. Biomacromolecules 12, 1387–1408.
Vandenbossche, G.M., Remon, J.P., 1993. Influence of the sterilization process on alginate dispersions. J. Pharm. Pharmacol. 45, 484–486.
Wang, X., Wenk, E., Zhang, X., Meinel, L., Vunjak-Novakovic, G., Kaplan, D.L., 2009. Growth factor gradients via microsphere delivery in biopolymer scaffolds for osteochondral tissue engineering. J. Control. Release. 134, 81–90.
Wang, Y., de Isla, N., Huselstein, C., Wang, B., Netter, P., Stoltz, J.F., Muller, S., 2008. Effect of alginate culture and mechanical stimulation on cartilaginous matrix synthesis of rat dedifferentiated chondrocytes. Biomed. Mater. Eng. 18, S47–S54.
Wasikiewicz, J.M., Yoshii, F., Nagasawa, N., Wach, R.A., Mitomo, H., 2005. Degradation of chitosan and sodium alginate by gamma radiation, sonochemical and ultraviolet methods. Radiat. Phys. Chem. 73, 287–295.
Wu, Y., 2012. Preparation of low-molecular-weight hyaluronic acid by ozone treatment carbohydrate polymer. Carbohydr. Polym. 89, 709–712.
Xu, J., Wang, W., Ludeman, M., Cheng, K., Hayami, T., Lotz, J.C., Kapila, S., 2008. Chondrogenic differentiation of human mesenchymal stem cells in three-dimensional alginate gels. Tissue Eng. Part A 14, 667–680.
Zhao, W., Jin, X., Cong, Y., Liu, Y.Y., Fu, J., 2013. Degradable natural polymer hydrogels for articular cartilage tissue engineering. J. Chem. Technol. Biotechnol. 88, 327–339.

Supplemental results-1:

(1) FTIR spectra

We analysis the FTIR peaks of originally pure Alg powders and pure HA powders under treatments of autoclave, UV-1, UV-2 and control (Error! Reference source not ound.). There is no significant shift of characteristic FTIR peaks of pure Alg or pure HA power was observed under different sterilization treatments, which also further prove without chemical groups changing.

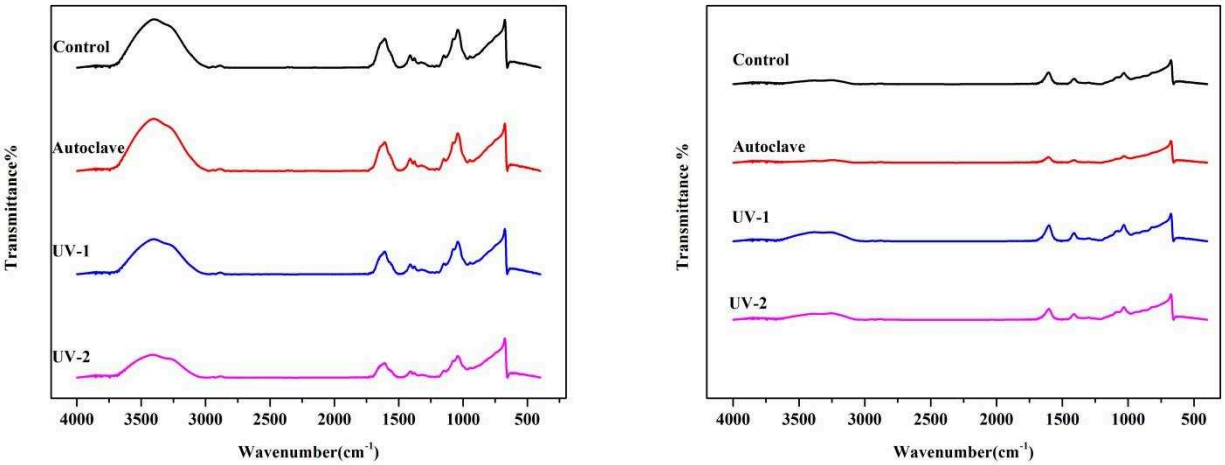

Figure 28: FTIR spectra of pure Alg powders (left) and pure HA powders (right) under exposure to the sterilization methods

(2) Determination of water content in Alg/HA hydrogel

Water content in hydrogel is not only to provide a moist environment, but also adjusting the permeation of nutrients, drug, gases, protein into the cells or targeted absorption site (*Kamoun EA et al, 2015*). **Figure 29** shows that swelling ratio of Alg/HA hydrogels under the sterilization treatments (autoclave, UV-1 and UV-2). There is no significant difference between UV-1 and UV-2 treatment, which was much closed to control. However, it can be seen that the value of swelling ratio for Alg/HA hydrogel by autoclaving was significantly lower than others. The reason is autoclaving resulted in depolymerization of alginate chains, and the water is very difficult blocked by the segments of depolymerized alginate, which make the ratio of polymer-to-water in hydrogel increased.

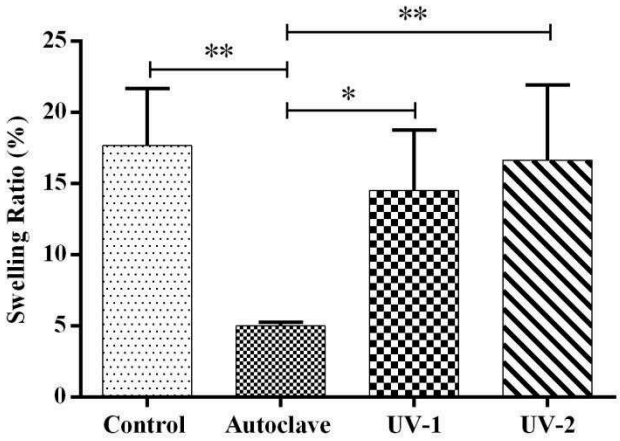

Figure 29: Swelling behavior of Alg/HA hydrogel under these sterilization treatments (autoclave, UV-1 and UV-2) ($^{*}p < 0.05$, autoclave vs UV-1; $^{**}p < 0.01$, control vs autoclave, autoclave vs UV-2).

(3) Comparing the viscosity of experimental groups and commercial groups

Here, we purchased the NOVAMATRIX® sodium alginate (sterile sodium alginate) from commercial vendors. It operates according to GMP guidelines; ISO 9001:2008 and ISO 13485:2003. Four kinds of gelling were prepared from Alg/HA powder sterilization from different processes as shown in **Table 4**. We found the viscosity of Alg/HA under UV-2 treatment was significantly higher than the Alg/HA from Alg NOVAMATRIX. So, we suggested that UV-2 could be as an effective sterilization method. The effectiveness of UV-2 sterilization is as same as commercial sterilization.

Table 4: Preparation of the Alg/HA gelling under the different treatments (HA: Accros, France)

Materials + treatment	Proportion of Alg and HA	Reference information
Alg/HA + Control	4:1	medium viscosity, A2033, Sigma
Alg/HA + Autoclave	4:1	medium viscosity, A2033, Sigma
Alg/HA + UV-2	4:1	medium viscosity, A2033, Sigma
NOVAMATRIX (Alg)/HA	4:1	PRONOVA SLM100

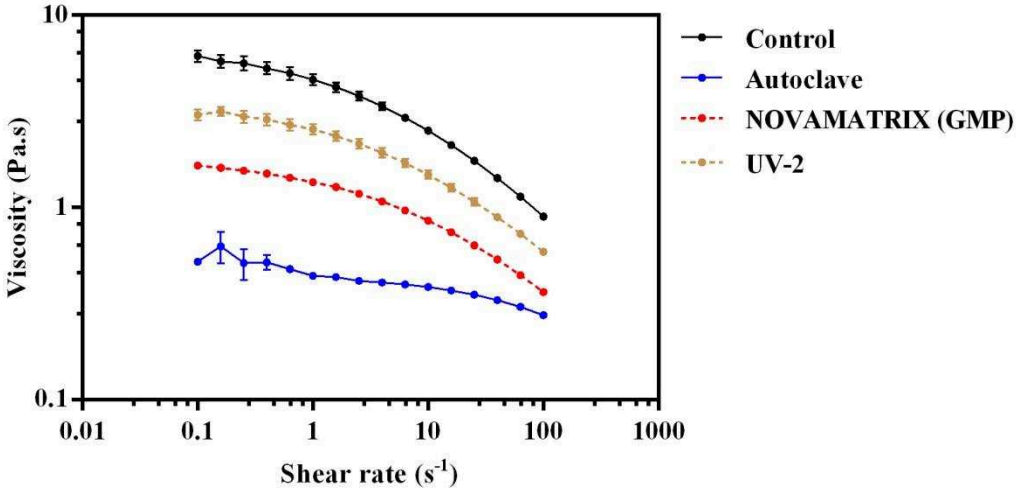

Figure 30: Comparison of Alg/HA viscosity between experimental and GMP Alginate products.

Supplemental results-2:

Evaluation of physicochemical and biological properties of alginate-hydroxyapatite hydrogel after the different sterilization treatments

Physicochemical: The performance of the shear viscosity of Alg/Hap gelling under the different sterilization treatments are shown in **Figure 31 (A)**. In comparison with control, the viscosity after UV treatment is slightly decreased, that keep the shear thinning behavior of the fluid. However, the viscosity after autoclave treatment is strongly decreased, which resulted in the loosing of shear thinning behavior. In other words, the UV treatments modify the amplitude of the viscosity but not the fluid behavior compared to autoclave treatment which strongly modifies the amplitude and the rheological behavior of the fluid. This performing of viscosity is in response to the results of molar masses, there is positive relationship between them. **Figure 31 (B)** illustrates the force-velocity curves of the compression force of Alg/Hap hydrogel scaffolds under these sterilization methods (control, UV-1, UV-2, and autoclave). As the velocity equal to 2.5 or 5 mm/min, we found the mechanical strength is significantly lower ($^{**}p < 0.01$) for autoclaving comparing to the others (control and UV). Moreover, No significantly difference between UV-1 and UV-2 treatment, but also the value force for hydrogel under the UV (-1,-2) treatment is

almost same to the control at the each velocity. The results have shown that no significant shift of characteristic FTIR peaks of Alg/Hap hydrogel was observed under different sterilization treatments as shown in **Figure 31 (C)**. This means that the different sterilization treatments have no changed the chemical groups of Alg/Hap hydrogels.

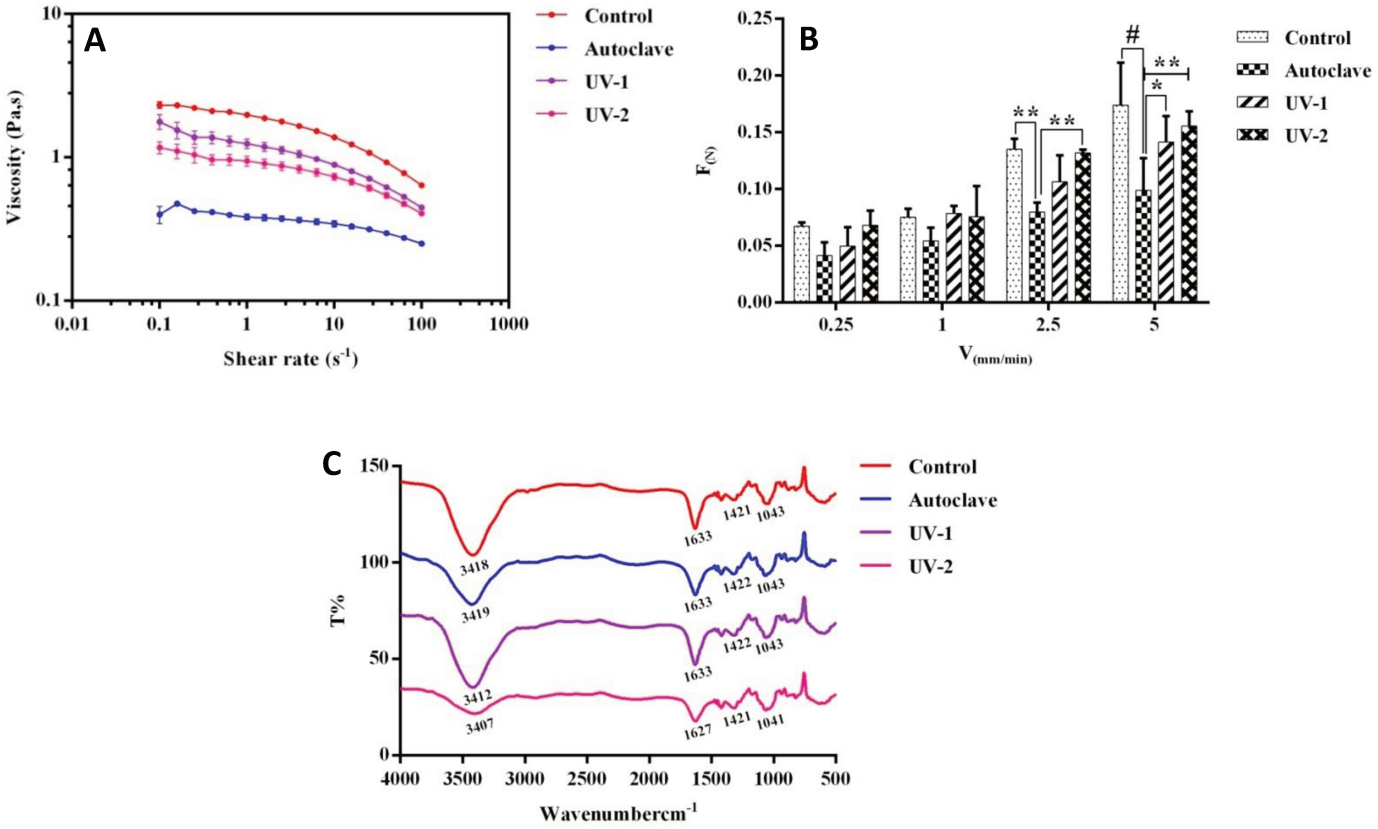

Figure 31: (A): Shear viscosity of Alg/Hap in gelling state under the sterilization treatments (autoclave, UV-1, UV-2 and control) as a function of the shear rate. (B): Typical force-velocity profile of Alg/Hap hydrogel scaffolds through the testing of indentation (the force measured at 0.35 mm indenter displacement), Date are presented as mean ± SD with n ≥3, analysis of variance (ANOVA). (V=2.5 mm/min, $^{**}p < 0.01$, control *vs* autoclave, UV-2 *vs* autoclave; and V=5 mm/min, $^{\#}p < 0.0001$, control *vs* autoclave, $^{**}p < 0.01$, UV-2 *vs* autoclave, $^{*}p < 0.05$, UV-1 *vs* autoclave). (C): FTIR spectra of Alg/Hap hydrogel scaffold under the different sterilization methods.

Biological: **Figure 32** shown the viable/necrotic/apoptotic of seeded cells into Alg/Hap hydrogels after 30 days of culture. It exhibited that the proportion of viable cells were 96.4% (autoclave), 85.9% (UV-1), 98.1% (UV-2) and 99.8% (monolayer cells). As well as, the percentage of cell necrotic and apoptotic by UVs and autoclave kept a lower expression as compared with monolayer.

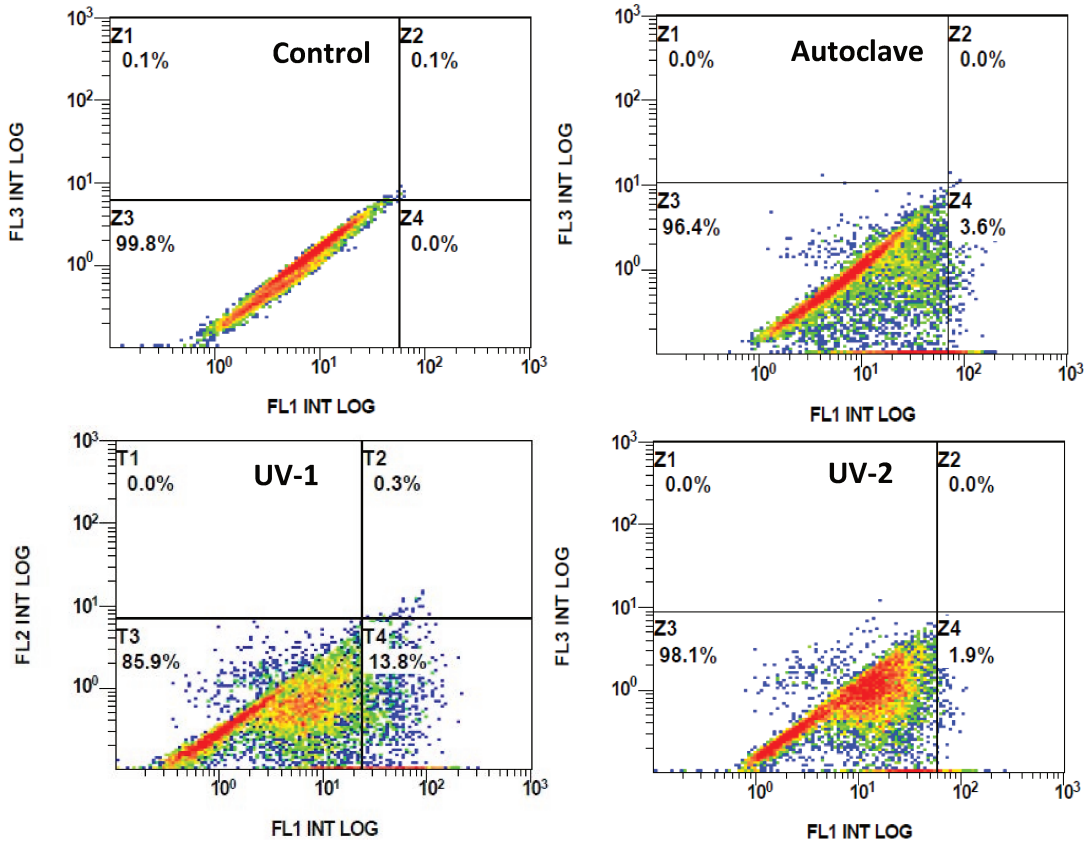

Figure 32: Flow cytometry analysis of viable/necrotic/apoptotic cells seeded in hydrogel scaffolds at 30 days.

In addition, we also evaluated the characters of Alg/Hap hydrogels through molar mass (as powder state), sterility testing and proliferation, and chondrogenic differentiation. Finally, we found UV treatment seems to be better sterilization methods for Alg/Hap hydrogel, which can also keep a good biocompatibility, differentiation characteristic and minimal effects on mechanical properties, viscosity, molar mass for hydrogels without changing chemical functional groups, as well as eliminates the infection of bacterial and fungus. These results which as same as Alg/HA hydrogel performance.

IV. Effect of microenvironment induced by 3D scaffolds on cell behavior: from differentiation to immune properties.

ARTICLE 3:

Effect of microenvironment induced by 3D scaffolds on cell behavior: from differentiation to immune properties. Relationship among of mechanical and biological properties.

Hao Yu, Ghislaine Cauchois, Franck Demeurie, Pascal Thomann, Jean-François Schmitt, Nicolas Louvet, Dominique Dumas, Yun Chen, Rachid Rahouadj, Céline Huselstein

Biomacromolecules, 2017, submitted

Effect of microenvironment induced by 3D scaffolds on cell behavior: from differentiation to immune properties. Relationship among of mechanical and biological properties.

Hao Yu [a,b], Ghislaine Cauchois [a,b], Franck Demeurie[c], Pascal Thomann[c], Jean-François Schmitt [c], Nicolas Louvet [c], Dominique Dumas [d], Yun Chen [e], Rachid Rahouadj [c], Céline Huselstein [a,b,*]

[a] UMR 7365 CNRS, Ingénierie Moléculaire et Physiopathologie Articulaire (IMoPA), Biopôle, Université de Lorraine, 54500, Vandoeuvre-lès-Nancy, France

[b]Fédération de Recherche 3209, Bioingénierie Moléculaire Cellulaire et Thérapeutique, 54500 Vandoeuvre-lès-Nancy, France

[c] UMR 7563 CNRS, Group of Biomechanics and Bioengineering, Université de Lorraine, 54500 Vandoeuvre-lès-Nancy, France

[d] UMR 7365 CNRS - Plateforme d'Imagerie Cellulaire et Tissulaire. Université de Lorraine, 54500 Vandoeuvre-lès-Nancy, France

[e] Department of Biomedical Engineering, School of Basic Medical Science, Wuhan University, Wuhan 430071, China

Abstract

As we known, many researchers had used the hydrogel scaffolds-laden mesenchymal stem cells to repair articular cartilage or subchondral bone defects due to hydrogel could be used as matrix models to mimic 3D cellular microenvironments and MSCs with the potentials of multi-differentiation and ability of immunoregulation. In this study, we had encapsulated Wharton's jelly mesenchymal stem cells (WJMSCs) into two 3D hydrogel scaffolds under cultuing liquid of chondrocyte differentiation, one is alginate (Alg)/hyaluronic acid (HA) hydrogels which will mimic cartilage and another is alginate (Alg)/hydroxyapatite (Hap) hydrogels which will mimic subchondral bone. On the basis of all of original results and principal component analysis, we found that there were inter-relationship among in the mechanical, biological and immunological properties. For example, there is a positive correction between strength and PEG_2; the changing of cell phenotype is connected with the microenvironment (physical

property) of hydrogel; loss of surface markers is associated with immunoregulatory factors secreted by MSCs.

Keywords: alginate; hyaluronic acid; hydroxyapatite; immune properties; chondrogenic differentiation;

1. Introduction

Articular cartilage may undergo degeneration and functional losses from inflammatory causes, trauma, aging, and other less common diseases. Moreover, the damaged of articular cartilage has the limited regenerative capacity due to a lack of cells and vessels.[1, 2] Researchers have been using different repair and regenerative treatments, such as microfracture, autologous chondrocytes transplantation (ACI) and mosaicplasty/osteochondral grafting.[3] However, there are some disadvantages for these treatments as lack of regenerative hyaline cartilage tissue, donor site morbidity, and limited available tissues.[4] Limitation of these treatments for cartilage defects has prompted the field of tissue-engineered cartilage. In particular, 3D hydrogel-based scaffold causes the extensive concern more and more due to their remarkable properties, such as high water content, high biocompatibility, injectability, ease of modification and similarity to native extracellular matrix (ECM).[5,6,11] In the meantime, Wharton's jelly mesenchymal stem cells (WJ-MSCs) are a promising adult stem cell source with potential of immunomodulatory properties and chondrogenic differentiation, which can be widely used to embed into hydrogels to repair the damaged of articular cartilage.[7-9] It is generally known that the relationship between hydrogels and mesenchymal stem cells is complicated, even though many researchers reported that the structure and composition (physical properties) of hydrogels have significant influence on cellular behavior, including cell proliferation, migration, alignment, differentiation, shape and phenotype.[10-13] For example, the mechanical property of supramolecular HA hydrogels was modulated by changing the cross-linking density for the controlled chondrogenesis of human mesenchymal stem cells (hMSCs).[14] However, only a little is known about how does the mechanical properties of hydrogel scaffolds-laden WJMSCs change during the

process of differentiation, which further influence on the performance of cell behavior, but also, the expression of immunogenic markers after chondrogenic differentiation of WJMSC seeded into hydrogel has been poorly investigated. Thus, to find what are inter-relationship between the characteristics (mechanical, biological, immunologic properties) turns to be necessary.

Alginate is one of the most important natural biomaterials because it forms a stable hydrogels by cooperative binding with divalent cations such as Ca^{2+} or Ba^{2+}, which have been widely used in cartilage tissue engineering due to its biocompatibility, degradability and low immunological stimulation.[15] Alginate hydrogels are generally deigned and used as matrix to support MSC encapsulation and culture, and synthesis of cartilage-specific macromolecules in chondrogenic differentiation.[16,17] Hyaluronic acid (HA) is a natural component of native cartilage, which can regulate the synthesis of proteoglycans in cartilage tissues. So, HA hydrogels have been extensively used for the encapsulation of MSC in cartilage tissue engineering.[18-20] In our lab, we demonstrated chondrogenic differentiation of WJMSC embedded in alginate/hyaluronic acid hydrogel without adding growth factors.[8] Hydroxyapatite (Hap) resembles the inorganic component of bone matrix, and is widely considered suitable for bone tissue engineering due to its excellent biocompatibility, affinity to biopolymers and osteoconductive properties, which can improve bone regeneration and mechanical properties as it is introduced into hydrogels as cell scaffolds.[21-23]

The main purpose of the present work is to study the influence of 3D hydrogel (Alg/HA and Alg/Hap) substrate mechanical conditions on WJ-MSC behavior during the chondrogenic differentiation, as proliferation, phenotype, cytoskeleton, differentiation and immunoregulation; then to further analysis of the inter-correlation in among of characterizes as: mechanical properties, biological properties and immunological properties, which can provide a useful principle for optimizing 3D-hydrogel scaffold design to create “Clinical supporter” repair the damage of cartilage. According to our previous studying, we shown that UV as an

effective method of sterilization, not only it can keep the physical-chemical properties of alginate/Hyaluronic acid hydrogel and cytocompatibility, but also induce chondrogenesis from mesenchymal stem cells.[24] So we will continue to use the UV as a sterilization method.

2. Materials and Methods

2.1 Preparation of gel solution

The powders of 1.5% (m/v) alginate (medium viscosity, Sigma-Aldrich, France)/hyaluronic acid (Acros organics, USA) (ratio 4:1) and alginate/hydroxyapatite (Diameter is 25 µm, Science Applications Industries, Lyon, France) (ratio 19:1) were sterilized by UV treatment for 50 min (Ultraviolet lamp = 2×15 w, wavelength = 254 nm, Distance = 30 cm, Vilber lourmat, France), respectively.[24] Then, they were separately homogeneously dissolved in 0.9% sodium chloride (Merck, Germany) to form gel solution by constant stirring in a sterile glass tube.

2.2 Construction of Alg/HA, Alg/Hap hydrogel scaffolds

To prepare gel solution as we described above. We used the spraying method to make the hydrogel scaffold, which was previously used.[17, 25] In brief, the spraying system consisted of an airbrush working with a compressor.[26] The spraying bottle containing the alginate-based gel solution was connected to the airbrush, and then solution was sprayed on a sterile glass plate with the spraying pressure being equal to 0.9 bar, which was quickly and horizontally putted into a bath of 102 mM $CaCl_2$ for 10 minutes, forming the 3D-hydrogel scaffolds (Alg/HA and Alg/Hap). Then, the scaffolds were washed twice with a 0.9% NaCl solution before being cut with a biopsy punch (Cylinders, 5mm diameter, Stiefel).

2.3 Swelling behavior of the hydrogel

Swelling behavior of hydrogel scaffolds were immersed in phosphate buffered saline (PBS) (pH7.2) at room temperature. The samples were taken out from PBS after 12 h, wiped with filter paper to remove surface droplets and weighed (W_t). Then, hydrogels were frozen at -20 °C and lyophilized at -80°C for 12 h, and weighted (W_0)

again. The swelling ratio Q_m was calculated using the following equation: [27] $Q_M = (W_t - W_0)/W_0 \times 100$ %.

Where W_t and W_0 represent the weight of swollen and dried hydrogels, respectively.

2.4 Isolation and cultivation of Wharton's jelly mesenchymal stem cells

This study was approved by the ethical committee of Nancy Hospital, and no authorization of this committee was necessary for their collection. Fresh human umbilical cords were collected after full-term births with patients' informed consent. WJ-MSC were isolated and cultivated as previously described.[12] Briefly, Umbilical cord samples were rinsed with 70 % ethanol and Hanks' balanced salt solution (HBSS). Next, the umbilical cord vessels were removed manually from cord segments and Wharton's jelly aseptically cut into very small pieces (2 to 3 mm^3) before placing them in a six well plate. The pieces were cultured in α-MEM (Lonza, Walkersville, MD, USA) with 10% fetal bovine serum (Sigma-Aldrich, France), 100 IU/mL penicillin (Gibco, France), 100 µg/mL streptomycin (Gibco, France), 2 mM L-glucose (Sigma-Aldrich, France), and 2.5 µg/mL amphotericin B (Gibco, France). They were incubated at 37°C in 5% CO_2, 5% O_2 incubator. After 7 days, cells migrated from Wharton's jelly and adhered on plate, taken out of the pieces, changed the medium and continued culture until cell subconfluence (80%). After 2 weeks, WJ-MSC were harvested with 0.25% Trypsin-EDTA (Sigma-Aldrich, France), media were changed three times weekly and grown up to P3.

2.5 Cell seeding into hydrogel scaffolds and chondrogenic differentiation

At the third passage, WJ-MSC were harvested with Trypsin-EDTA and seeded at 3×10^6 cells/mL in Alg/HA, Alg/Hap gel solution, respectively. Scaffolds-loaded cells were also fabricated by the spraying method, as above mentioned. Alg-based hydrogel scaffolds (Cylinders) were culture during 30 days in 6-well plates with induced chondrogenic culture medium which contained DMEM-high glucose (Gibco, Grand Island, NY) supplemented with 10% fetal bovine serum, 2 mM L-glutamine, 100 U/mL penicillin, 100 µg/mL streptomycin, 2.5 µg/mL amphotericin B, 1 mM $CaCl_2$, 0.1 µM dexamethasone (Sigma-Aldrich, France), 50 µg/mL ascorbate-2-phosphate

(Sigma-Aldrich, France), 100 µg/mL sodium pyruvate (Sigma-Aldrich, France), and 40 µg/mL L-proline (Sigma-Aldrich, France). Scaffolds were incubated at 37℃ under a humidified atmosphere with 5% CO_2, 5% O_2, and differentiation medium was changed twice a week. Cylinders with cells were obtained for biological and mechanical experiments. During chondrogenic differentiation, after 10, 20 and 30 days of culture, Cells were extracted from hydrogel scaffolds using 55 mM sodium citrate (Sigma-Aldrich, France) and 50 mM EDTA solution (Merck, Darmstadt, Germany) for 5 min. After centrifugation (320 g, 5 min), viability, phenotype, immunophenotypic, mRNA and collagen expression were analyzed.

2.6 Mechanical properties of hydrogel scaffolds seeded cells during the days of culture

After 10, 20 and 30 days of culture, the mechanical properties of Alg/HA and Alg/Hap hydrogel scaffolds (with and without cells) were characterized by using the spherical indentation technique. Hydrogel scaffolds were immersed in less DMEM in a Petri dish and load applied using a smooth steel indenter tip with R = 0.5mm. The indenter was pressed into the surface of the hydrogel scaffold at a rate of 0.15 mm/min, using the force response corresponding to an indenter displacement of 1 mm for all specimens whose thicknesses were between 2 and 3 mm. The force-displacement curves ($n \geq 6$) were obtained for all velocities and samples.

2.7 Viability and proliferation of seeded cells into the hydrogels

Viability of cells encapsulation in hydrogel scaffolds was measured by PI/Annexin-V kit (Life technologies, France). Cells were suspended in 100 µL of 1X Annexin-liant buffer with 2.5 µL of Annexin V-Alexa 488 and 1 µL of propidium iodide (PI) for 15 min at the room temperature. After incubation, 200 µL of 1X Annexin-liant buffer were added to each sample. Then, cells were detected with fluorescence emission at 530 nm and 575 nm by Gallios flow cytometer (Beckman Coulter, Brea, CA, USA).

Cell proliferation of cell cultured in hydrogel scaffolds was evaluated by using the Alamar Blue™ assay Kit (Thermo scientific, France). Media were removed at specific time points (10, 20 and 30 days), washed with PBS in culture plate and immersed in

10% Alamar Blue solution (prepared in DMEM medium without phenol red) for 4 hours at 37 ℃ in a humidified incubator with 5% CO_2, 5% O_2. The reaction of Alamar Blue was read in a microplate reader at 570 nm and 600 nm. To calculate the percentage reduction of Alamar Blue™ as following equation:

$$\% \text{ reduction} = \frac{(OD570_{(control)} \times 155677) - (OD600_{(control)} \times 14652)}{(OD570_{(sample)} \times 117216) - (OD600_{(sample)} \times 80586)} \times 100$$

The absorption value of negative control is culture medium and Alamr Blue™. The experiment was performed in quadruplicate.

2.8 Phenotypic analysis of cells in the hydrogels during chondrogenic differentiation

Cell surface antigen expression by WJ-MSCs in hydrogel scaffolds was detected using flow cytometry, and the monolayer expansion as to be control. Briefly, the extraction of cells from hydrogel scaffolds as described before. To perform phenotypic analysis MSC were incubated with fluorescein isothiocyanate (FITC)- or phycoerythrin (PE)-conjugated mouse anti-human antibodies CD90-FITC, CD34-PE, CD44-FITC, CD105-PE, CD45-FITC, CD166-PE and CD73-PE (Beckman Coulter, Brea, CA, USA) for 30 minutes at room temperature. Negative and isotype (FITC and PE) controls were performed. After immunofluorescence staining, for each sample 10,000 events were counted by Gallios flow cytometer (Beckman Coulter, Brea, CA, USA).

2.9 Morphology of cells cultured in the hydrogels and cytoskeletal assessment

After 30 days of culture, the micromorphology of the cells cultured in the hydrogels was observed by SEM with an accelerating voltage of 5 kV. Briefly, samples were washed with PBS, fixed in 4 wt% paraformaldehyde for 2 h and post-fixed for 2 h in 1 wt% OsO_4. Then, they were progressively dehydrated in a series of alcohols after rewashing with PBS, vacuum-dried, and coated with gold for SEM (JEOL JSM-6300F, USA) observation. Cytoskeleton organization of cell-laden hydrogels was observed by fluorescent labeling of F-actin fibers. Samples were washed with PBS then fixed with 4% (w/v) paraformaldehyde solution for 10 min (Sigma, France), after samples permeabilization with 0.1% Triton X-100 solution (Sigma, France) for 15 min at the

room temperature, and stained with Alexa Fluor 488 Phalloïdin (Invitrogen, France) for 30 min. Finally, samples were washed twice with DMEM without phenol red and their flurescence images were captured using a laser scanning confocal microscope (Leica TCS SP2, Microsystem Inc).

2.10 Differentiation potential of WJ-MSCs into the alginate-based hydrogel scaffolds

2.10.1 Transcript analysis

MSC were rinsed with PBS three times to remove residual alginate. Briefly, RNA was extracted from cells using trizol (Invitrogen, France). Total RNA was purified by RNeasy Plus mini kit (Qiagen, Hilden, Germany) according to the manufacturer's instructions. RNA concentration was evaluated by spectrophotometry and RNA quality was analyzed by electrophoresis through a 1% agarose gel. RNA was then reverse-transcripted to cDNA templates using iScript™ cDNA Synthesis Kit (Bio-rad, Hercules, CA, USA) according to the manufacture's protocol. Quantitative polymerase chain reaction (PCR) was performed using iTaq™ Universal SYBR® Green Supermix (Bio-rad) and the Applied Biosystems StepOne Plus (Life Technologies Corporation, USA) during 40 cycles to quantitatively analyze gene expression. Primer sequences are given in Table 1. The method $2^{-\Delta\Delta Ct}$ (Nolan et al., 2006) is used to determine the relative expression levels of the mRNAs under the various experimental conditions after normalization with respect to the reference gene RP29.

Table 1 Target cDNA primers sequences used for RT-PCR

Gene	Forward sequence (5'- 3')	Reverse sequence (5'- 3')	TM (°)
RP29	GGGTCACCAGCAGCTGTACT	CAGACACGACAAGAGCGAGA	60
Sox9	GAGGCAGAGGAGGCCACGGA	CCGGAGGAGGAGTGTGGCGA	55
Col2a1	ATGACAATCTGGCTCCCAAC	GAACCTGCTATTGCCCTCTG	60
Aggrecan	TCTGTAACCCAGGCTCCAAC	CTGGCAAAATCCCCACTAAA	62
Runx2	GCTGTTATGAAAAACCAAGT	GGGAGGATTTGTGAAGAC	56

OPN	CCACGGACCTGCCAGCAACC	GGCAACGGGGATGGCCTTGT	54
OCN	CCTTTGTGTCCAAGCAGGAG	CGGATTGAGCTCACACACCT	53

2.10.2 Collagen assay

Expression of collagen in the cells cultured in the hydrogels was determined by flow cytometry. The extraction of cells from hydrogel scaffolds as described before. Cells were incubated for 45 min with rabbit anti-human type I, II, and X collagen antibodies (1:20) (Merck, Darmstadt, Germany). Afterwards, specimens were washed with PBS-PSA and centrifuged, cells were incubated for 30 min with secondary antibody: a goat anti-rabbit IgG Alexa Fluor 488 (1:20) (Invitrogen, Carlsbad, CA, USA). Immunofluorescence labeling was detected using Gallios flow cytometer (Beckman Coulter, Brea, CA, USA).

2.10.3 Histological

The cell-laden hydrogel scaffolds were washed with PBS and fixed with 4% paraformaldehyde (Sigma Aldrich, France) for 4 hours. After that, the samples were embedded in paraffin and sectioned in 5 µm thickness. The sections were stained with Sirius red and Alcian blue for total collagen and sulfated proteoglycans (GAG), respectively. Microphotographs were taken using a light microscope (LEICA, DMD108, USA).

2.11 Immunological properties

2.11.1 Flow cytometer assay

Immune antigen expression in cells were examined using monoclonal antibodies specific for CD80, CD86, CD40 and HLA-DR (MACS, Miltenui Biotec, France) conjugated with FITC and PE, respectively. Acquisitions and data analysis were performed using the Gallios flow cytometer. Results are expressed as percentage of positive cells or as mean relative fluorescence intensity, obtained as a ratio between the mean fluorescence intensity of cells stained with specific mAb and the mean fluorescence intensity obtained with isotype control.

2.11.2 ELISA array

During the chondrocyte differentiation, the culture supernatants were harvested after centrifuging to collect all the secretory proteins. Vascular endothelial growth factor (VEGF), hepatocyte growth factor (HGF), Prostaglandin E2 (PEG_2), and Transforming growth factor beta 1 (TGF-β_1) were chosen as the immunoregulatory factors. All of these factors were determined by enzyme-linked immunosorbent assay (ELISA) using a commercially available ELISA kit (R&D Systems, BD Biosciences, San Diego, CA). ELISA was performed according to the manufacturer's instructions. All samples and standards were measured in duplicate.

2.12 Principal component analysis

To explore relationships between the physical properties and biological characters for the hydrogel scaffolds, we carried out a principal components analysis (PCA), which through the XLSTAT software (Addinsoft, New York, USA).

2.13 Data analysis and statistics

All quantitative data were averaged and expressed as mean ± standard deviation (SD) ($N \geq 3$). Statistical analyses were conducted using GraphPad Prism 6 software (GraphPad San Diego, CA, USA). Data were evaluated using one- or two-way ANOVA analysis of variance. Differences were considered statistically significant at $p < 0.05$.

3. Results and Discussion

3.1 Swelling Ratio Measurement

Swelling ratio of hydrogels is an important factor for substance exchange in tissue engineering.[28] As shown in Figure 1, the swelling ratio of pure-alginate hydrogels was slightly higher than that of hydrogels contained HA ($p > 0.05$). However, the swelling ratio significantly decreased with incorporation of Hap particles into alginate hydrogel ($p < 0.05$). This is mainly due to the Hap showed hydrophobic properties and had poor ability of absorbing water compared with highly hydrophilic alginate. Or, hap particles take the amount of space inside the hydrogels network available to accommodate water. In other words, addition of Hap particles into alginate hydrogels not only decreased the swelling behavior of hydrogels, but also changed

the mechanical properties compared with Alg/HA hydrogels, which will be discussed later.

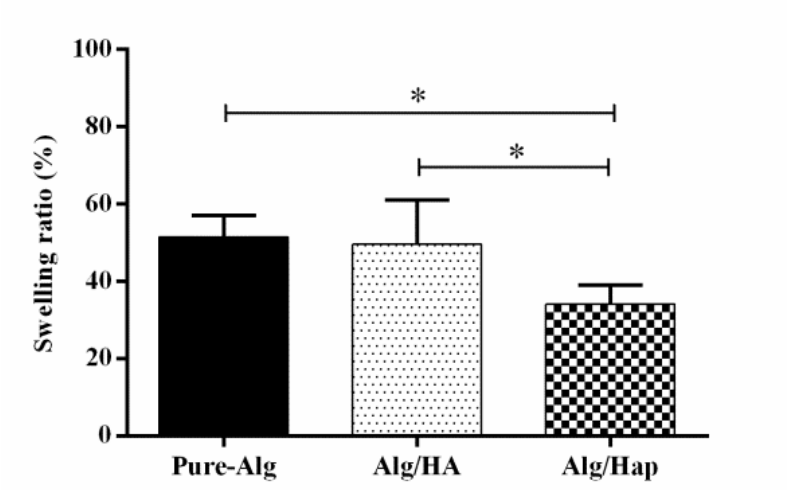

Figure 1: Swelling ratio of pure-Alg, Alg/HA and Alg/Hap hydrogels after swelling in PBS at room temperature. $^{*}p < 0.05$, Pure Alg *vs* Alg/HA, Alg/HA *vs* Alg/Hap; Error bars represent means ± standard deviation for n = 5.

3.2 Mechanical properties

In this study, during chondrogenic differentiation process, the mechanical strength of hydrogel scaffolds was determined in vitro by applying a compressive load to the hydrogel (with or without cells) at each time points. Results of indentation testing on hydrogel scaffolds is shown in Figure 2, at 10 days, it was normally observed that the mechanical strength of Alg/Hap hydrogels (with or without cells) significantly increased in comparison with Alg/HA hydrogels (with or without cells) ($^{***}p < 0.001$), which due to the incorporation of Hap particles into alginate to reinforce microstructure and mechanical properties of hydrogels. Additionally, there was no significant difference in strength between the Alg/HA (with or without cells) and Alg/hap hydrogels (with or without cells) ($p > 0.05$). However, we found that the mechanical strength of all of hydrogel scaffolds decreased during the time of culture. This phenomenon was due to sodium ions in the media replacing calcium in the alginate that resulted in a reversal of the crosslinking caused by the $CaCl_2$.[29] On the other hand, Ca^{2+} plays an important role in regulating of the mechanical properties of hydrogels through electrostatic force, which was formed between Ca^{2+} and

proteoglycans.[30] Interestingly, the mechanical strength of Alg/Hap with cells was significantly higher than Alg/HA without cells after 20 days. This could be caused by the rapid growth of cell seeded into Alg/Hap hydrogels, which further lead to the reorganization of fibers, production of ECM and the application of intrinsic strains; it also was in agreement with results of cell proliferation and cytoskeleton. This will be discussed later. From these results, the mechanical strength of hydrogel was increased by the incorporation of Hap particles, as well as the releasing of Ca^{2+} is expected to change mechanical properties of alginate hydrogel scaffolds.

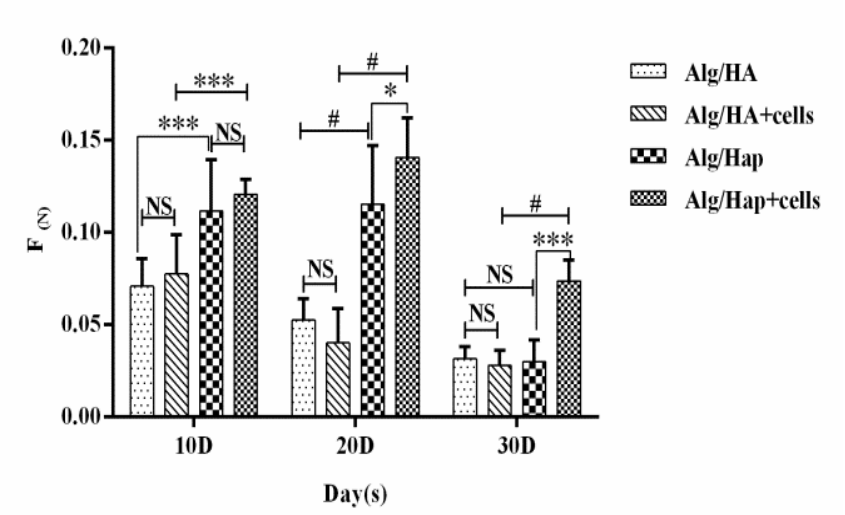

Figure 2: Typical force-velocity profile of the hydrogels (with and without cells) in different days, * or # represent a significant difference in each group (Two-way ANOVA, ***p < 0.001, Alg/HA *vs* Alg/Hap, Alg/HA + cells *vs* Alg/Hap + cells for 10 days; *p < 0.05 or #p < 0.0001, Alg/Hap *vs* Alg/Hap + cells, Alg/HA *vs* Alg/Hap, Alg/HA + cells *vs* Alg/Hap + cells for 20 days; ***p < 0.001, Alg/Hap *vs* Alg/Hap + cells for 30 days; p > 0.05 (NS) means no significant difference in each group). Result is mean ± SD of six measurements.

3.3 Analysis of cell proliferation and viability in the hydrogels

Alamar blue (AB) assay was performed to quantify the proliferation of encapsulated cells into two kinds of hydrogels during the process of chondrocyte differentiation. As shown in Figure 3A, it was found that the AB reduction of cells in hydrogels increased with increasing days. At the beginning of culture, the Alg/HA hydrogels showed higher fluorescence intensity (**p < 0.01), which indicated that AB reduction of cell in Alg/HA hydrogels was significantly higher than that of Alg/Hap hydrogels. However, the cells in Alg/Hap hydrogels proliferated faster than in the Alg/Hap

hydrogels at 30 days ($^{***}p < 0.001$). It was probably due to Hap increased the matrix stiffness, which further leaded to increase proliferation. This observation is well consistent with the previous reports that the stiff substrates contribute a better circumstance for cell proliferation than the soft ones.[31, 32] In other word, the stiffer substrate has beneficial for cell to aggregate through cell traction force, which is regulated by cell adhesion molecules of the adjacent cells, and it has further effected on the architecture of cytoskeletal, which will be discussed later. The viability of cells encapsulated into hydrogels was analyzed 10, 20 and 30 days (figure 3B). It was observed that cell viability slightly increased with the days of culture, but also these viability rates were close to those observed during monolayer expansion ($p > 0.05$). Meanwhile, No significant difference was observed between Alg/HA and Alg/Hap hydrogels at each time points. Figure 3C shows the viable/ necrotic/apoptotic of cells seeded in hydrogels after 30 days of culture. It exhibited that the proportion of viable cells were 96.0% (Alg/HA) and 98.3% (Alg/Hap). As well as, the percentages of necrotic and apoptotic cell seeded in two hydrogels are less than 4 %.

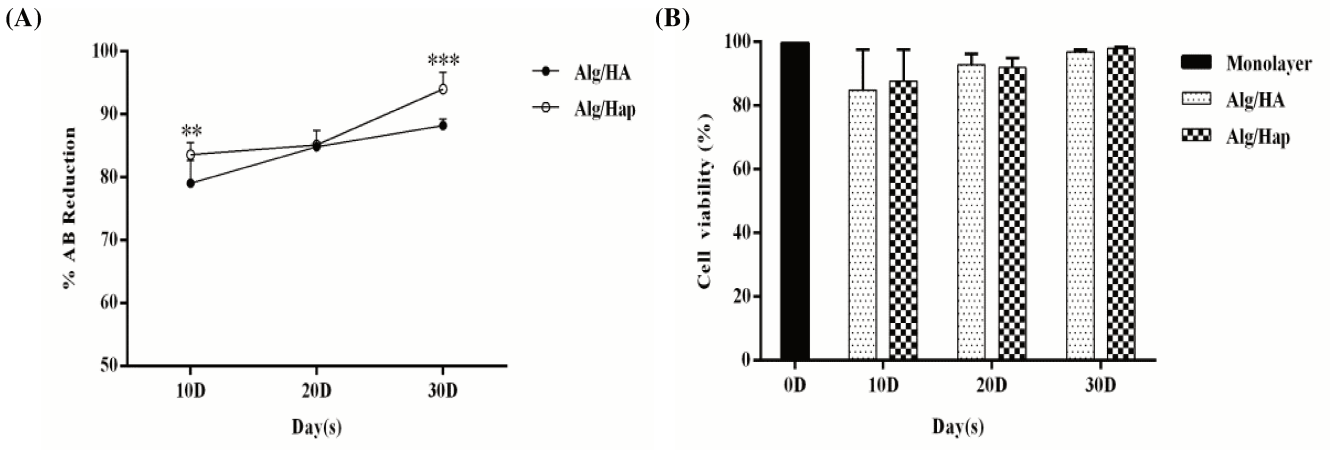

(C)

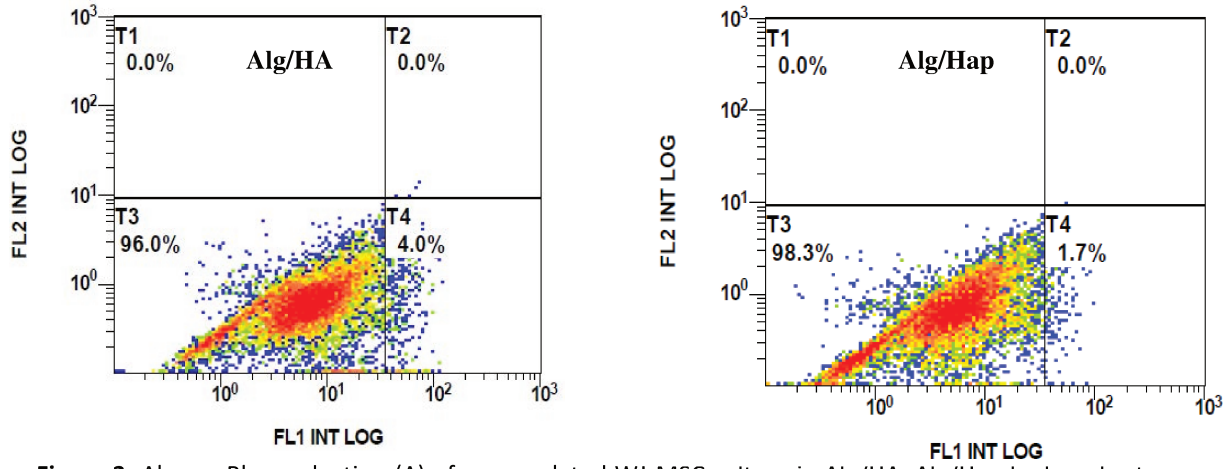

Figure 3: Alamar Blue reduction (A) of encapsulated WJ-MSC culture in Alg/HA, Alg/Hap hydrogels at 10, 20 and 30 days; (B) The viability of encapsulated cells in hydrogels was measured by flow cytometry after 3, 5, 10, 20, and 30 days of culture and (C) Flow cytometry analysis of viable/necrotic/apoptotic cells seeded in hydrogels at 30 days. * represent a significant difference in each group (Two-way ANOVA, $^{**}p < 0.01$ or $^{***}p < 0.001$ Alg/HA *vs* Alg/Hap, at day 10 and 30), bars represent the standard deviation, N= 4 (Alamar Blue), N=3 (viability).

3.4 Phenotypic analysis

Flow cytometric analysis of cells derived from both monolayer and 3D culture groups (Figure 4). During monolayer expansion, WJ-MSCs were positive for mesenchymal markers CD90, CD73, CD105, CD44 and CD166, and negative for the hematopoietic markers CD34, CD45 and HLA-DR, which as reported in previous studies and were clearly in favor of a chondrogenic potential.[8, 33] In the 3D environment and during chondrogenic differentiation, it was found that the proportions of positive WJMSC for mesenchymal markers decreased (except CD44 in Alg/HA hydrogel) significantly from 10 and up to 30 days, as compared with monolayer expansion. We noted about HA can directly bind to CD 44 receptors, which play an important role in the process of chondrogenesis, therefore the expression of CD44 remained high and stable for Alg/HA hydrogels. For other negative markers, with no significant differences between monolayer and 3D culture groups at 30 days. These results was consistent with our previous study showing a similar result for mesenchymal markers expression of human MSCs cultured in hydrogels, [34] as well as Lee HJ et al. reported that the expression of CD90, CD44, CD166 and CD73 were decreased by the 3D

alginate hydrogel (without hyaluronic acid) culture during the chondrogenic differentiation process.[35] Ullah M et al and others also presented that chondrogenically differentiated hMSCs reduced their expression for these surface antigens (CD44, CD73, CD90, CD105, and CD166).[36-38] These surface markers were recommended to be identify the chondrogenically differentiated cells,[39-42] as they have active differentiation signaling pathways, chondrogenic character, and biological paradigms of the differentiated state.[34,36] This phenomenon as the changing of mesenchymal markers was concerned with the culture conditions. In other words, their expression was shown to change depending on the microenvironment but not specific negative markers in chondrocytes.[35, 43, 44] As Hagmann S et al. reported the expansion medium can have a significant influence on surface marker expression of mesenchymal stromal cells.[45] However, another explanation is that down-regulation of these markers in a 3D hydrogel with a limited number of adhesion sites, as compared with two dimensional cultured controls.[46, 47] Moreover, in 3D culture groups, the proportions of cell-surface markers were no significantly difference ($p > 0.05$) in Alg/HA compared to Alg/Hap hydrogels after 30 days. Interestingly, some surface markers have been associated with immunosuppressive capacity of MSCs, which also provided a reference for immunophenotypic analysis of cells seeded into hydrogels. It will be discussed next.

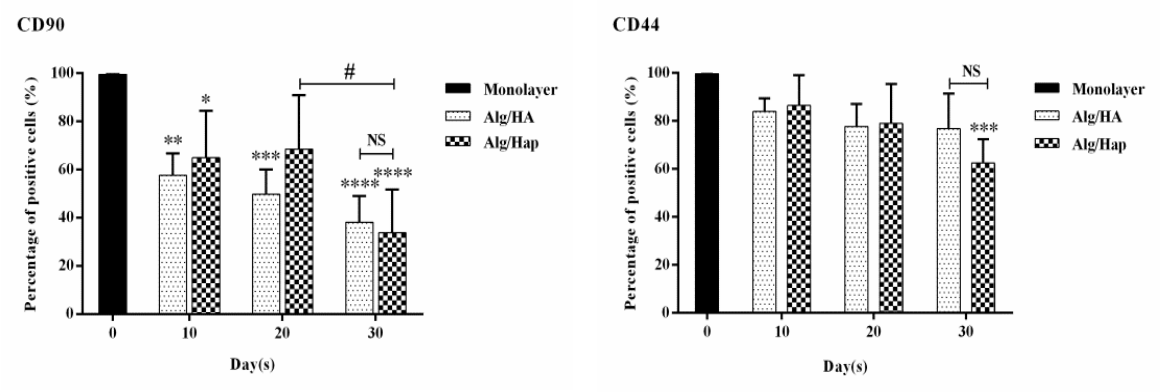

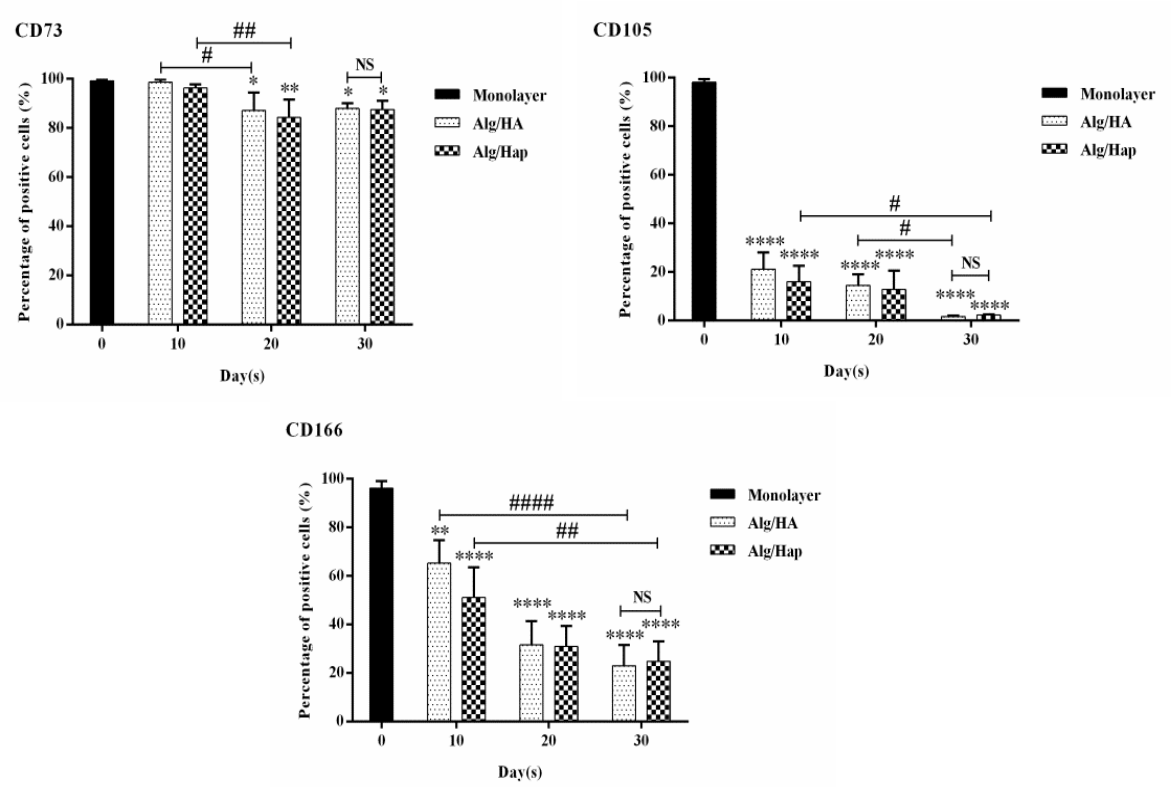

Figure 4: Flow cytometric analysis of the expression of surface markers by WJ-MSCs during monolayer expansion (prior to encapsulation in the hydrogel) and throughout scaffold culture. The results are shown as percentages of positive cells. All results are expressed as mean ± standard error of the mean (n ≥ 3). $^{*}p < 0.05$, $^{**}p < 0.01$, $^{***}p < 0.001$ and $^{****}p < 0.0001$, day x *vs* day 0 (monolayer) for the same culture time; $^{\#}p < 0.05$, $^{\#\#}p < 0.01$ and $^{\#\#\#\#}p < 0.0001$, day 10 *vs* day 20, day 10 *vs* day 30 or day 20 *vs* day 30 for the same hydrogel scaffold; WJ-MSCs were positive for CD90, CD44, CD166, CD73 and CD105 expression. NS, no significant difference between Alg/HA and Alg/Hap at 30 days.

3.5 Immunofluorescence staining and microscopy

The cytoskeleton of cells within the two hydrogels after 30 days were examined by phalloidin staining of F-actin, with the results presented in Figure 5(A). It is seen that cells aggregation with extensive stress fibers was observed in the Alg/Hap hydrogel. In contrast, the morphology of cells into the Alg/HA hydrogels were spherical and non-clustered, which is due to the increasing of substrate stiffness by incorporated Hap particles into alginate hydrogel. In other words, increasing in cellular traction stress with substrate stiffness increased.[48] Cell morphology of the encapsulated cells in the hydrogels was further analyzed by SEM as Figure 5(B). More peripherally

located stress fibers are seen in the cells in Alg/Hap hydrogel. Whereas, which lack actin stress fibers and more cell remained nearly spherical morphology in the Alg/HA hydrogels. This phenomenon was also caused by a homogenously dispersion of Hap particles within the entire substance and it almost completely covers the hydrogel surface. Especially, the distance between particles and cells are much closed. Interestingly, for the Alg/Hap hydrogels, more wrinkles were apparent at the cells periphery as compared with Alg/HA hydrogels, it can be attributed the mechanical forces of cells applying on the substrate.[49] Therefore, the incorporation of Hap particles modified the substance stiffness and enhanced cell traction force, which resulted in the extension of stress fibers.

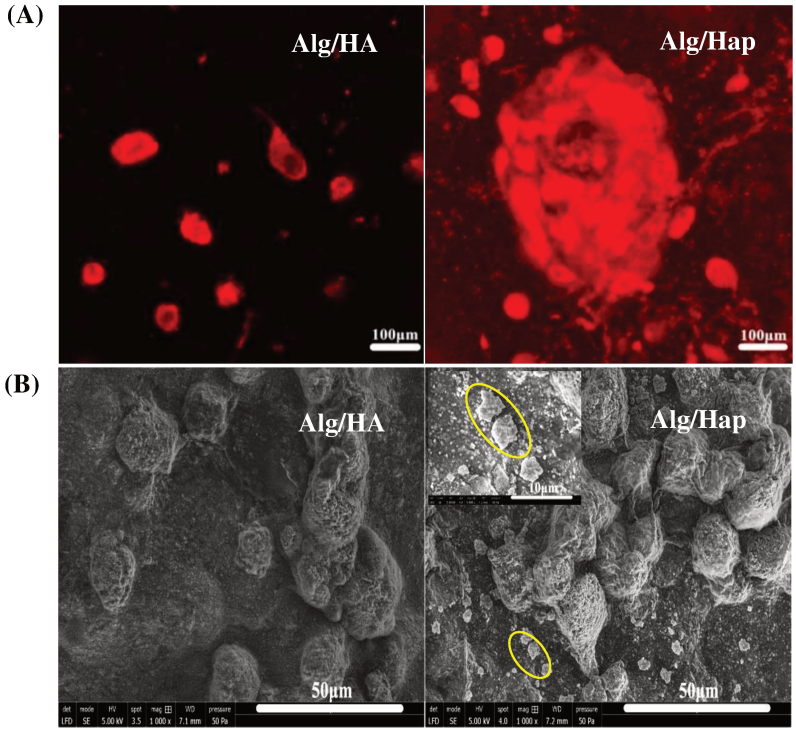

Figure 5: Influence of particles on the cytoskeleton and morphology of WJ-MSCs after 30 days. ((A): F-actin content (Phalloïdin staining; red) of seeded cells into hydrogels (scale bars, 100µm); (B): SEM images of cell seeded into the hydrogels (scale bars, 50) and high magnifications of Hap crystals (5000X, yellow circle)).

3.6 Chondrogenic differentiation

3.6.1 Transcript analysis

The expression of genes was qualitatively detected using real-time PCR during chondrogenic differentiation. Figure 6(A) shows the expression levels of major chondrogenic markers including Sox9, aggrecan (ACAN) and collagen type II (Col2a1). It was found that the expression of these chondrogenic markers in WJMSCs seeded into the hydrogels increased with increasing days. More importantly, these markers expressed by cells in Alg/HA hydrogels was significantly higher than that of Alg/Hap hydrogels in each time points. After 30 days, with a strong upregulation of cartilage-specific transcript expression for Alg/HA hydrogel, which is not only depended on the chondrogenic differentiation medium, but also associated with HA as a native component of cartilage, and cells may interact with HA via cell surface receptors, the hydrogels could influence stem cell differentiation.[50]

Relative expression of other markers such as Runx2, osteopontin (OPN) or osteocalcin (OCN) was also analyzed during chondrogenic differentiation as Figure 6(B). For both of hydrogels, it was observed that Runx2 (Hypertrophic cartilage markers) expression slightly increased with the days of culture, as well as Runx2 expression was significantly higher in Alg/Hap compared to Alg/HA hydrogels. This mainly reason is Hap as the inorganic phase of bone with osteoconductive properties, which modulate the performance of the hydrogels with potential applications for bone tissue engineering.[51] Furthermore, OPN and OCN were less expressed by cells in all the hydrogels, which was also contributed to hap incorporated into hydrogels even though it was cultured in chondrogenic differentiation medium.

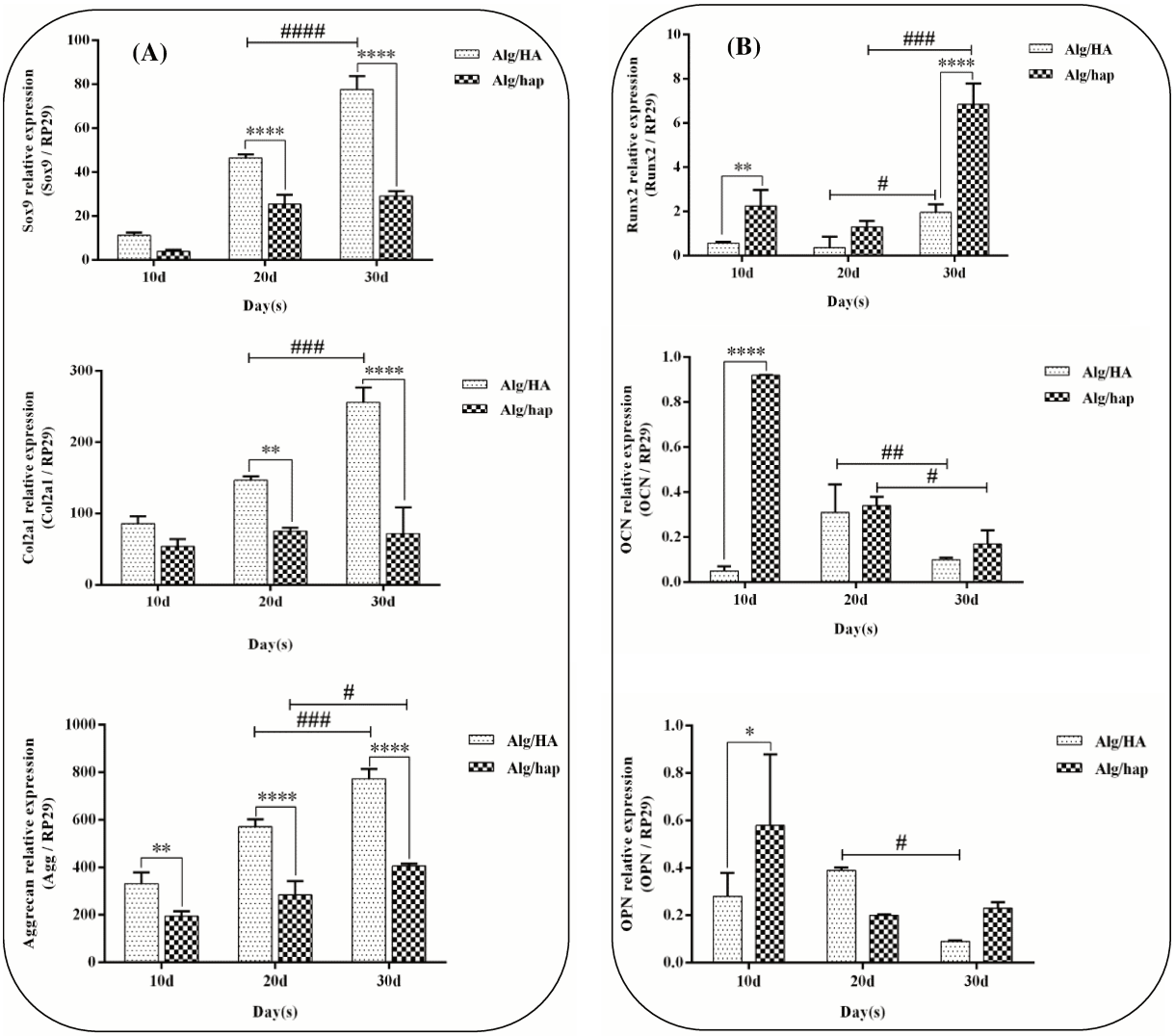

Figure 6: Mean relative expression of specific genes evaluated by quantitative RT-PCR during 30 days of chondrogenic induction. (A) The cartilage-related genes: Sox9, Col2a1 and Aggrecan. (B) The bone-related genes: Runx2, OPN and OCN. Date is presented as mean ± SD with n ≥ 3. $^{*}p < 0.05$, $^{**}p < 0.01$ and $^{****}p < 0.0001$, Alg/HA *vs* Alg/Hap for a same culture time; $^{\#}p < 0.05$, $^{\#\#}p < 0.01$, $^{\#\#\#}p < 0.001$ and $^{\#\#\#\#}p < 0.0001$, day 20 *vs* day 30 for the same hydrogel scaffold.

3.6.2 Quantification of collagen expression

Synthesis of collagen produced by the cells encapsulated in the hydrogels as shown in Figure 7. In the case of Alg/HA hydrogel, the relative expression of Col II increased over time ($p < 0.05$), When cultured for 30 days, the expression of Col II in Alg/HA was much higher than that of Alg/Hap hydrogels ($p < 0.05$). In contrast, the synthesis of Col I and Col X by cells seeded into Alg/HA hydrogels decreased with increasing days. In other words, Alg/Hap hydrogels seemed to produce more Col I and Col X.

These results obtained for matrix synthesis analysis were consistent with those obtained for transcript analysis. This finding assured that the Alg/HA hydrogels, compared with Alg/Hap hydrogels, did better in improving the chondrogenic differentiation of WJMSCs. For Alg/hap hydrogels, it has led to the osteogenic differentiation of parts of cells during chondrogenic differentiation.

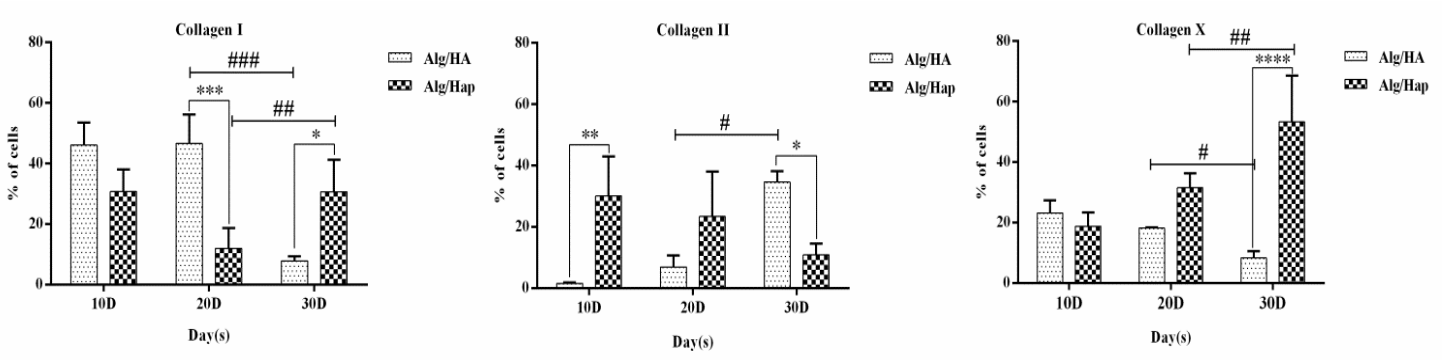

Figure 7: Flow cytometric analysis of the expression of collagen (I, II and X) by seeded WJ-MSCs into the hydrogels (Alg/HA and/or Alg/Hap) during chondrogenic differentiation. The result is expressed as mean ± SD (n ≥ 3). $^{*}p < 0.05$, $^{**}p < 0.01$, $^{***}p < 0.001$ and $^{****}p < 0.0001$, Alg/HA *vs* Alg/Hap for a same culture time; $^{\#}p < 0.05$, $^{\#\#}p < 0.01$ and $^{\#\#\#}p < 0.001$, day 20 *vs* day 30 for the same hydrogel scaffold.

3.6.3 Histological staining

During chondrogenic differentiation, cartilaginous matrices production of the WJ-MSCs after 30 days of culture in the hydrogels were further investigated by histological staining. Proteoglycans and total collagen were stained by Alcian blue and Sirius red, respectively. As shown in Figure 8, it was observed that cell cultured in Alg/HA hydrogels showed positive staining of proteoglycans, which it was seemed to be greater than that in Alg/Hap hydrogels. Meanwhile, Sirius red staining indicated that both of hydrogels showed total collagen synthesis, and no obviously difference between Alg/HA and Alg/Hap hydrogels. However, according to the results of collagen expression, collagen II were observed in this pericellular space for Alg/HA hydrogels, but also types I and X collagen was exclusively pericellular for Alg/Hap hydrogels.

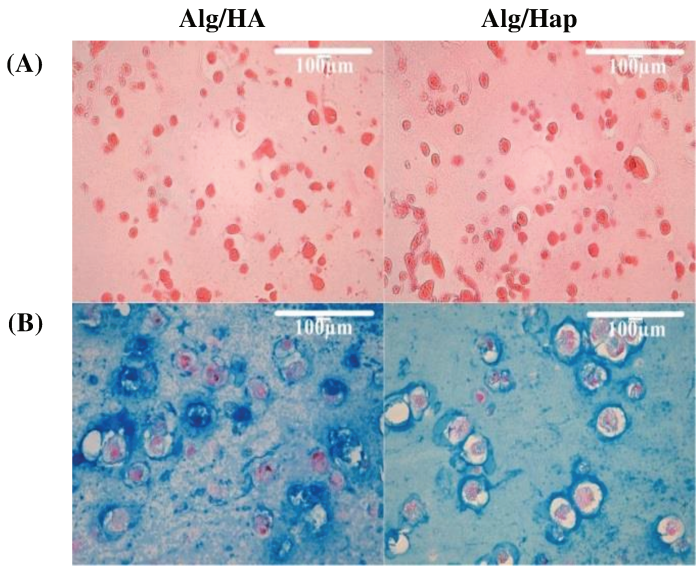

Figure 8: Histological analysis of seeded WJ-MSCs into hydrogel scaffolds and cultured under the differentiation liquid of chondrocyte after 30 days. (A) Collagen synthesis in hydrogel scaffolds by Sirius red staining. (B) Glycosaminoglycan synthesis in hydrogel scaffolds by Alcian Blue staining. Scale bar is 100 µm.

3.7 Immunological properties

It is known to all that B7 superfamily (CD40, CD80 and CD86) and HLA-DR are of critical importance for their role as costimulatory in immune processes.[52] Here, we examined the expression of costimulatory molecules on WJMSCs seeded into hydrogel during chondrogenic differentiation by FACS analysis (Figure 9). Both of hydrogel-laden cells showed negative expression with the days of culture, which are almost same as monolayer. These findings indicate that co-stimulatory molecule can maintain co-inhibitory roles after chondro-differentiated WJMSC as well as undifferentiated WJMSC did. This result which in agreement with La Rocca G et al and Lee HJ et al reporting.[53, 54] It means that the composition of hydrogels has no effects on the performance of costimulatory molecules on cells seeded into hydrogels.

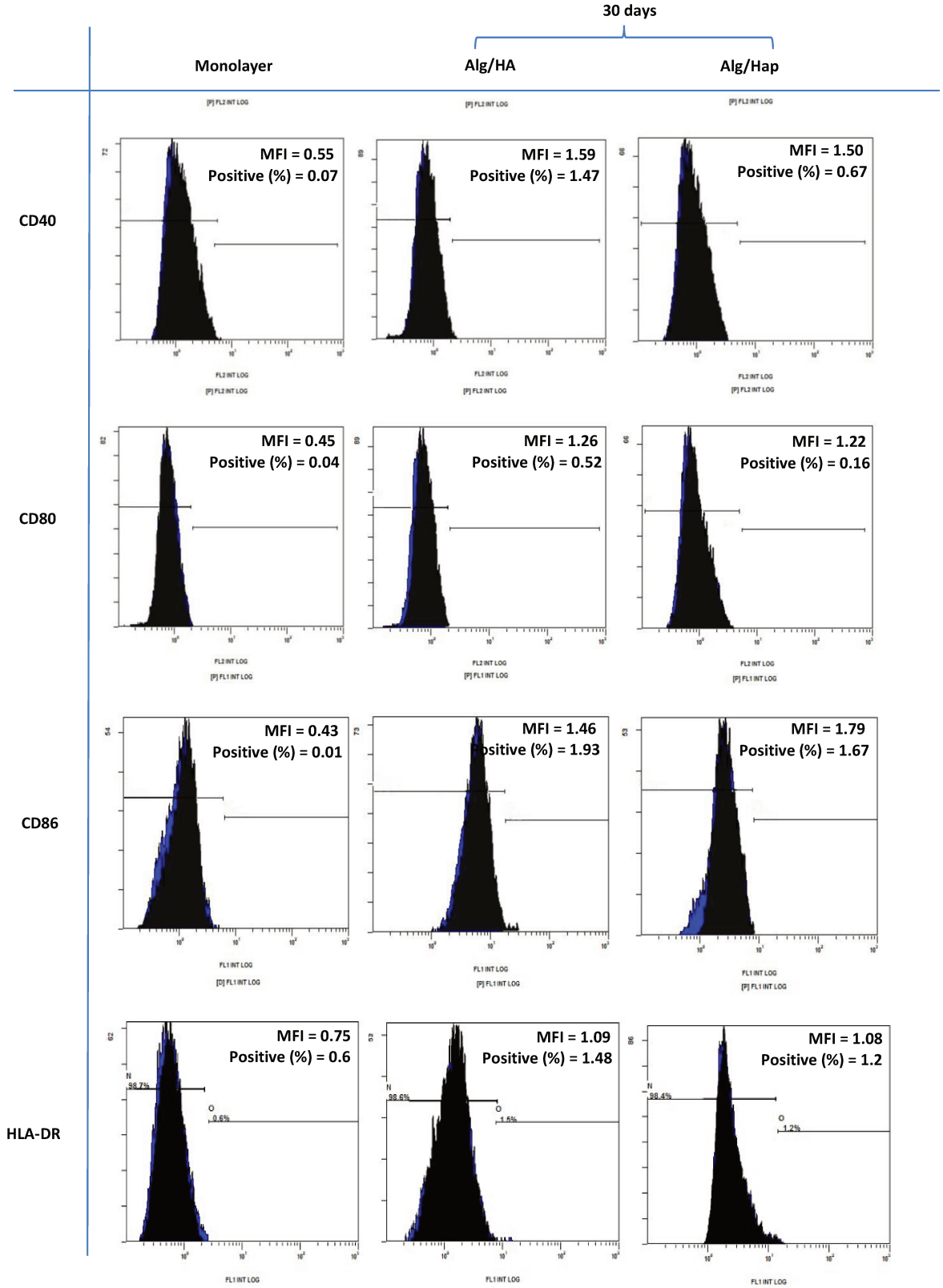

Figure 9: Detection of costimulatory molecules on WJ-MSCs by flow cytometry. Expression of costimulatory molecules (CD40, CD80, CD86 and HLA-DR) on encapsulated WJ-MSCs into hydrogels cultured in chondrogenic differentiation medium at 30 days.

The secretion of immune-related soluble factors by WJMSCs seeded in the hydrogels, including PGE2, HGF, VEGF and TGF-β1 normalized by total protein contents. As shown in Figure 10, all of these factors exhibited the different trends. In briefly, the production of PGE_2 and TGF-β_1 increased gradually in 3D hydrogel constructs during the whole culturing time. This result was consistent with the results that MSCs in hydrogel could secrete various immunoregulatory factors.[55] In other words, scaffolds structures may regulate the immunological properties of MSCs through modulating their secretion of immunoregulatory factors.[55-57] As well as, it was found that the expressing of these factors (PGE_2 and TGF-β_1) secretion by cells seeded into Alg/Hap hydrogels were significantly higher than that of Alg/HA hydrogels. This phenomenon is due to the secretion of immunoregulatory factors for cells were consistent with the tendency of scaffold contraction.[55] The incorporation of Hap particles into hydrogel resulted in higher cell density and more cell-cell interactions as observed through (Figure 3A), which further improved the contraction activities of hydrogel. However, in contrast, we observed that the expression of HGF and VEGF decreased in 3D hydrogels with over time. It may be issued in the positive surface markers of cells decreased during differentiation process. For examples, Campioni D et al reported the a loss of immunosuppressive activity by MSCs was connected with the reducing of positive mesenchymal marker CD90,[58] and $CD34^+/CD90^+$ cells of human adipose tissue differentiate in endothelial cells was associated with the production of VEGF.[59] By the way, for VEGF, Chen XY et al reported that it could inhibit the expression of aggrecan and type II collagen at the gene and protein levels,[60] thus the decreasing of VEGF expression may be associated with up-regulation of aggrecan and Col II as shown in figure 6 and 7. From these results, we speculated that the secretion of immune-related soluble factors of WJMSCs seeded into hydrogels not only determined by native hydrogel structures, but also associated with a loss of mesenchymal markers on cells during chondrogenic differentiation process. So to provide a suitable microenvironment for the MSCs is becoming necessary. Finally, it indicated that the mechanical properties of hydrogel scaffolds could play a vital role

in meditating the secretion of immunoregulatory factors by WJMSCs during chondrocyte differentiation.

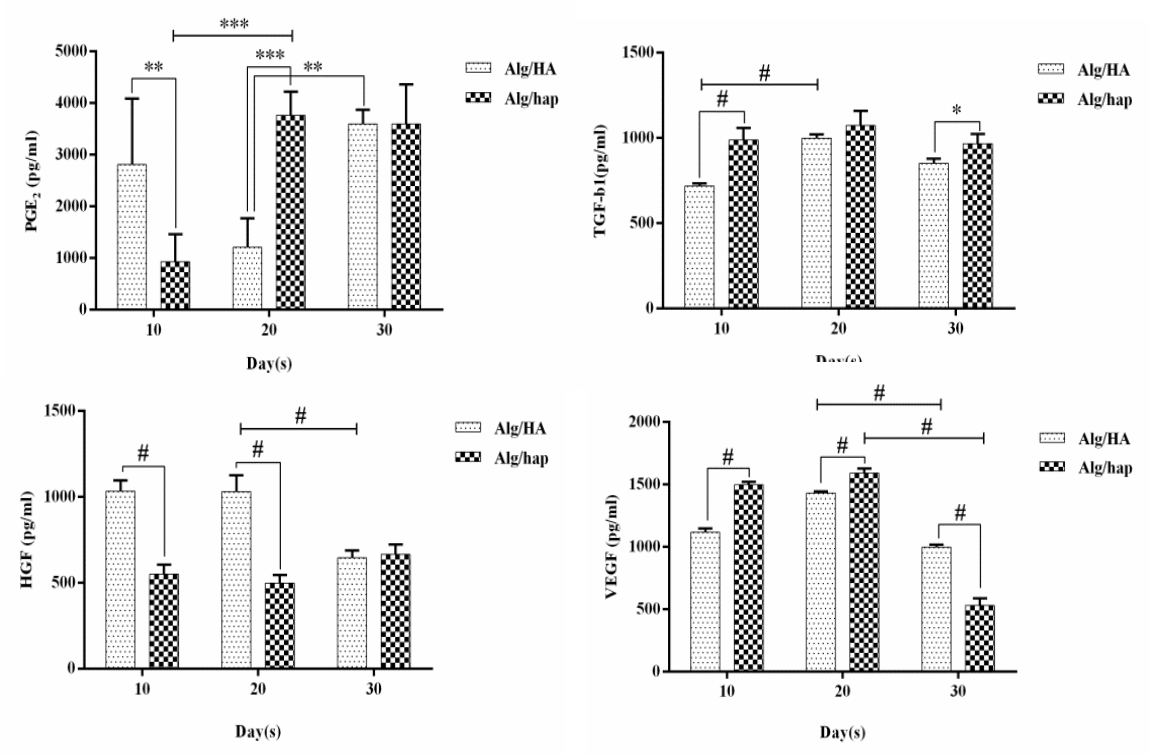

Figure 10: ELISA analysis of cytokines (PGE_2, HGF, VEGF and TGF-β1) of encapsulated WJ-MSCs into the hydrogel scaffolds during chondrogenic differentiation from 10 to 30 days. Data expressed as mean ± SD (n = 4), Two-Way ANOVA, $^{*}p < 0.05$, $^{**}p < 0.01$, $^{***}p < 0.001$ and $^{\#}p < 0.0001$, Alg/HA *vs* Alg/Hap for a same culture time.

3.8 PCA component analysis

Principal component analysis (PCA) method is useful in helping to determine underlying relationships between 29 biological-physical properties variables and 2 alginate-based hydrogels (Alg/HA and Alg/Hap) scaffolds. While to our knowledge this method has not been previously used to elucidate how mechanical properties of hydrogel scaffolds can affect biological properties including biochemical and immunology properties. The results of the PCA analysis are shown in **Figure 11(a, b)**. As seen in **Figure 11a** (biological variables), we find that the first principal component (F1) explains 77.70% of the observed variance while the second principal component F2) explains 22.30% (F1 vs F2 which represents 100% of total variability). A projection of the variable parameters onto Fs 1 and 2 clearly separates them into

two distinct clusters as A and B groups, corresponding to the different hydrogel that were used. From view of observation points Obs1, a positive correlation (Group B) is observed between Alg/HA hydrogel scaffolds and some of variables (Co-stimulators, cartilage-related genes and VEGF) that corresponded to F1. As well as there is a high correlation coefficient (Group A) between Alg/Hap hydrogel scaffolds and other variables (bone-related genes, proliferation, HGF and TGF-β1) from the view of observation points Obs2 (corresponding to F1). For the physical variables, this representation (score plot) is shown in **figure 11 b**. Here, the PCA score plot also utilizes the first principal component representing 60.97% of variance, and it already shows clear two clusters of the data (Group A and B). In term of view point 1, Alg/HA is positively associated with swelling behavior and strength (-), which is in accordance with the results of **Figure 1 and 2**. However, Alg/Hap (Group B) is opposed with the Alg/HA and contributes to the second principal component, which is associated with strength (+). This identified the two groups of the variable parameters as we saw in our initial analysis.

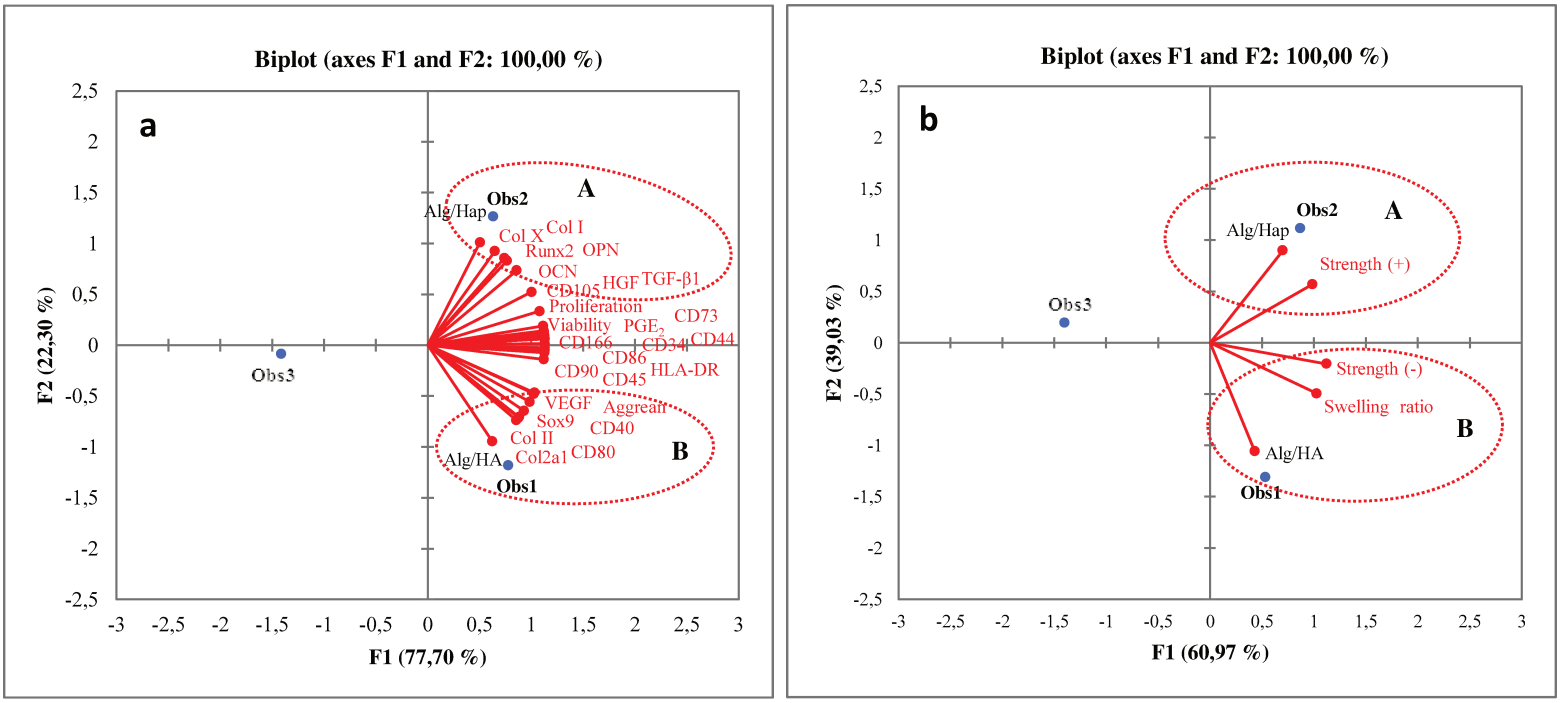

Figure 11: Illustration of the data set under the new coordinate system defined by the principal components analysis. (Axes F1 and F2 representing 100%), (a) biological properties; (b) physical properties.

In order to further analysis, the inter-relationship among of the 29 biological-physical properties variables, there is correlation matrix for the studied parameters as shown in Table 2, 3 and 4. For correlations, significant correlations are displayed in bold. As observed for the Alg/HA and Alg/Hap hydrogels, no significant correlations in all of the variable parameters, that is corresponding to our original analysis results. For the biological parameters (table 2, 3), the viability and proliferation characters were positively associated with surface markers (CD73 and CD166) and some of immunoregulatory factors (PEG_2 and HGF) secreted by MSCs. For the surface markers of cells, there was also positively relation in among of markers as CD73 *vs* CD166. Meanwhile, our data indicates that no expression of co-stimulatory molecules for seeded WJMSCs into the hydrogels during the process of chondrocyte differentiation, which is also corrected with the expression of cartilage-related genes as CD80 (Sox 9 (0.997) and Col2a1: 1.000) or surface markers as CD86 (CD90 (1.000) and HLA-DR (0.998)). In addition, we observed that the surface markers of WJMSCs have an inseparable relationship with the cytokines secreted by MSCs, for example, the surface markers (CD166) have significantly positive affected on PEG_2, TGF-β1and HGF, as well as the CD44 and CD73 have positive impacted on PEG_2 (0.999, 1.000) and HGF (0.997, 0.999), respectively. As table 4 shown the inter-relationship of physical properties, we found that no significant correction between parameters. On the basis of principal component analysis and above results, we found that there was the inter-correction of mechanical, biology and immunoregulatory for seeded WJMSCs into different hydrogels (Alg/HA and Alg/Hap) during chondrogenic lineage differentiation.

Table 2, 3 The correlation matrix for the studied biological parameters. (Values in bold are different from 0 with a significance level alpha=0.05, all of the value of parameters were taken at 30 days)

Variables	Alg/HA	Alg/Hap	Viability	Proliferation	CD90	CD44	CD73	CD105	CD166	HLA-DR	Sox9	Col2a1
Alg/HA	**1**	-0,500	0,492	0,451	0,587	0,539	0,504	0,279	0,442	0,649	0,928	0,962
Alg/Hap	-0,500	**1**	0,508	0,547	0,407	0,460	0,496	0,692	0,556	0,334	-0,142	-0,244
Viability	0,492	0,508	**1**	**0,999**	0,994	**0,999**	**1,000**	0,973	**0,998**	0,982	0,780	0,711
Proliferation	0,451	0,547	**0,999**	**1**	0,987	0,995	**0,998**	0,983	**1,000**	0,972	0,751	0,678
CD90	0,587	0,407	0,994	0,987	**1**	**0,998**	0,995	0,941	0,986	0,997	0,846	0,786
CD44	0,539	0,460	**0,999**	0,995	**0,998**	**1**	**0,999**	0,959	0,994	0,991	0,813	0,748
CD73	0,504	0,496	**1,000**	**0,998**	0,995	**0,999**	**1**	0,970	**0,998**	0,984	0,789	0,720
CD105	0,279	0,692	0,973	0,983	0,941	0,959	0,970	**1**	0,985	0,911	0,616	0,531
CD166	0,442	0,556	**0,998**	**1,000**	0,986	0,994	**0,998**	0,985	**1**	0,969	0,743	0,670
HLA-DR	0,649	0,334	0,982	0,972	0,997	0,991	0,984	0,911	0,969	**1**	0,885	0,832
Sox9	0,928	-0,142	0,780	0,751	0,846	0,813	0,789	0,616	0,743	0,885	**1**	0,995
Col2a1	0,962	-0,244	0,711	0,678	0,786	0,748	0,720	0,531	0,670	0,832	0,995	**1**
Aggrecan	0,851	0,028	0,876	0,852	0,924	0,900	0,882	0,741	0,847	0,952	0,985	0,962
Runx2	-0,240	0,961	0,727	0,758	0,645	0,689	0,718	0,865	0,765	0,583	0,138	0,035
OPN	-0,125	0,922	0,803	0,829	0,730	0,769	0,795	0,918	0,835	0,674	0,253	0,151
OCN	0,101	0,811	0,916	0,933	0,865	0,893	0,911	0,984	0,937	0,822	0,464	0,369
Col I	-0,271	0,969	0,705	0,737	0,620	0,665	0,695	0,849	0,744	0,556	0,106	0,003
Col II	0,952	-0,209	0,736	0,704	0,808	0,772	0,745	0,561	0,696	0,852	**0,998**	**0,999**
Col X	-0,368	0,989	0,628	0,664	0,537	0,585	0,618	0,790	0,672	0,468	0,004	-0,100
CD40	0,890	-0,051	0,834	0,808	0,891	0,863	0,842	0,685	0,802	0,924	0,996	0,981
CD80	0,954	-0,217	0,731	0,699	0,803	0,767	0,740	0,554	0,691	0,848	**0,997**	**1,000**
CD86	0,604	0,389	0,991	0,984	**1,000**	0,997	0,993	0,934	0,982	**0,998**	0,857	0,798
PGE_2	0,500	0,500	**1,000**	**0,998**	0,995	**0,999**	**1,000**	0,971	**0,998**	0,983	0,786	0,718
HGF	0,476	0,524	**1,000**	**1,000**	0,991	**0,997**	**0,999**	0,977	**0,999**	0,978	0,769	0,698
VEGF	0,846	0,039	0,880	0,858	0,928	0,905	0,887	0,748	0,852	0,955	0,984	0,960
TGF-β1	0,403	0,591	0,995	**0,999**	0,977	0,988	0,994	0,991	**0,999**	0,958	0,714	0,637

Variables	Aggrecan	Runx2	OPN	OCN	Col I	Col II	Col X	CD40	CD80	CD86	PGE_2	HGF	VEGF	TGF-β1
Alg/HA	0,851	-0,240	-0,125	0,101	-0,271	0,952	-0,368	0,890	0,954	0,604	0,500	0,476	0,846	0,403
Alg/Hap	0,028	0,961	0,922	0,811	0,969	-0,209	0,989	-0,051	-0,217	0,389	0,500	0,524	0,039	0,591
viability	0,876	0,727	0,803	0,916	0,705	0,736	0,628	0,834	0,731	0,991	**1,000**	**1,000**	0,880	0,995
proliferation	0,852	0,758	0,829	0,933	0,737	0,704	0,664	0,808	0,699	0,984	**0,998**	**1,000**	0,858	**0,999**
CD90	0,924	0,645	0,730	0,865	0,620	0,808	0,537	0,891	0,803	**1,000**	0,995	0,991	0,928	0,977
CD44	0,900	0,689	0,769	0,893	0,665	0,772	0,585	0,863	0,767	0,997	**0,999**	**0,997**	0,905	0,988
CD73	0,882	0,718	0,795	0,911	0,695	0,745	0,618	0,842	0,740	0,993	**1,000**	**0,999**	0,887	0,994
CD105	0,741	0,865	0,918	0,984	0,849	0,561	0,790	0,685	0,554	0,934	0,971	0,977	0,748	0,991
CD166	0,847	0,765	0,835	0,937	0,744	0,696	0,672	0,802	0,691	0,982	**0,998**	**0,999**	0,852	**0,999**
HLA-DR	0,952	0,583	0,674	0,822	0,556	0,852	0,468	0,924	0,848	**0,998**	0,983	0,978	0,955	0,958
Sox9	0,985	0,138	0,253	0,464	0,106	**0,998**	0,004	0,996	**0,997**	0,857	0,786	0,769	0,984	0,714
Col2a1	0,962	0,035	0,151	0,369	0,003	**0,999**	-0,100	0,981	**1,000**	0,798	0,718	0,698	0,960	0,637
Aggrecan	**1**	0,305	0,414	0,608	0,274	0,971	0,174	0,997	0,970	0,932	0,880	0,866	**1,000**	0,823
Runx2	0,305	**1**	0,993	0,942	**0,999**	0,071	0,991	0,228	0,063	0,629	0,721	0,740	0,315	0,792
OPN	0,414	0,993	**1**	0,974	0,989	0,187	0,968	0,341	0,179	0,716	0,797	0,813	0,424	0,858
OCN	0,608	0,942	0,974	**1**	0,930	0,402	0,888	0,543	0,396	0,854	0,912	0,923	0,616	0,951
Col I	0,274	**0,999**	0,989	0,930	**1**	0,039	0,995	0,197	0,031	0,604	0,698	0,718	0,284	0,772
Col II	0,971	0,071	0,187	0,402	0,039	**1**	-0,064	0,987	**1,000**	0,820	0,743	0,723	0,969	0,665
Col X	0,174	0,991	0,968	0,888	0,995	-0,064	**1**	0,096	-0,072	0,519	0,621	0,643	0,184	0,703
CD40	0,997	0,228	0,341	0,543	0,197	0,987	0,096	**1**	0,986	0,900	0,840	0,824	0,996	0,775
CD80	0,970	0,063	0,179	0,396	0,031	**1,000**	-0,072	0,986	**1**	0,815	0,737	0,718	0,967	0,659
CD86	0,932	0,629	0,716	0,854	0,604	0,820	0,519	0,900	0,815	**1**	0,992	0,988	0,936	0,973
PGE_2	0,880	0,721	0,797	0,912	0,698	0,743	0,621	0,840	0,737	0,992	**1**	**1,000**	0,885	0,994
HGF	0,866	0,740	0,813	0,923	0,718	0,723	0,643	0,824	0,718	0,988	**1,000**	**1**	0,871	0,997
VEGF	**1,000**	0,315	0,424	0,616	0,284	0,969	0,184	0,996	0,967	0,936	0,885	0,871	**1**	0,829
TGF-β1	0,823	0,792	0,858	0,951	0,772	0,665	0,703	0,775	0,659	0,973	0,994	0,997	0,829	**1**

Table 4 The correlation matrix for the studied physical parameters. (Values in bold are different from 0 with a significance level alpha=0.05, Strength (-): the force of hydrogel scaffolds without cells; Strength (+): the force of hydrogel scaffolds with cells; all of the value of parameters were taken at 30 days)

Variables	Alg/HA	Alg/Hap	Swelling ratio	Strength (-)	Strength (+)
Alg/HA	**1**	-0,500	0,741	0,538	-0,136
Alg/Hap	-0,500	**1**	0,211	0,461	0,926
Swelling ratio	0,741	0,211	**1**	0,965	0,564
Strength (-)	0,538	0,461	0,965	**1**	0,762
Strength (+)	-0,136	0,926	0,564	0,762	**1**

4. Conclusions

Through analysis of the mechanical, biological and immunological properties of two 3D hydrogel scaffolds, the results indicated that Hap successfully improved mechanical properties of hydrogel, which decreased swelling ratio and changed cell behavior as cytoskeleton, proliferation of cell, which also improved the production of PGE_2 and TGF-β_1 as compared with Alg/HA hydrogels. The expression of the mesenchymal markers as (CD44, CD73, CD90, CD105, and CD166) was decreased by 3D hydrogel (Alg/HA and Alg/Hap) culture during the time of culture. Besides, during chondrogenic differentiation, Alg/HA hydrogel scaffolds showed strong upregulation of cartilage-specific transcript expression, meanwhile, Alg/Hap hydrogel scaffolds presented slightly upregulation of bone-specific transcript expression from 10 to 30 days. In addition, both of hydrogel--laden MSCs did not express the costimulatory surface antigens CD40, CD80, and CD86. However, the expression of HGF and VEGF decreased in 3D hydrogel scaffolds. Then, we have developed the inter-relationship among of the 29 biological-physical properties. It was found that mechanical, biological and immunological properties are also affected by each other. The findings would provide guidance in 3D-hydrogel scaffold designs for cartilage/subchondral bone tissue engineering to control the cell behavior and immunological properties through the regulation of mechanical properties.

Acknowledgements

This work was supported by the UMR7365 CNRS-Université de lorraine, Ingénierie Moléculaire et physiopathologie Articulaire (IMoPA), Biopôle, and “Program Cai Yuanpei 2013-2015” (CSC No. 201304490192 and 201304490191) from China Scholarship Council. Thanks for the China Scholarship Council (award to Hao YU for 4 years’ PhD study abroad at the Université de Lorraine).

References

1) Foldager, C.B.; Bünger, C.; Nielsen, A.B.; Ulrich-Vinther, M.; Munir, S.; Everland, H.; Lind, M. Dermatan sulphate in methoxy polyethylene glycol-polylactide-co-glycolic acid scaffolds upregulates fibronectin gene expression but has no effect on in vivo osteochondral repair. *Int Orthop* **2012**, *36* (7), 1507-13.
2) Melton, J.T.; Wilson, A.J.; Chapman-Sheath, P.; Cossey, A.J. TruFit CB ® bone plug: chondral repair, scaffold design, surgical technique and early experiences. *Expert Rev Med Devices* **2010**, *7* (3), 333-41.
3) Makris, E.A.; Gomoll, A.H.; Malizos, K.N.; Hu, J.C.; Athanasiou, K.A. Repair and tissue engineering techniques for articular cartilage. *Nat Rev Rheumatol* **2015**, *11* (1), 21-34.
4) Siclari, A.; Mascaro, G.; Gentili, C.; Cancedda, R.; Boux, E. A cell-free scaffold-based cartilage repair provides improved function hyaline-like repair at one year. *Clin Orthop Relat Res* **2012**, *470* (3), 910-919.
5) Yang, J.; Shrike Zhang, Y. ; Yue, K.; Khademhosseini, A. Cell-laden hydrogels for osteochondral and cartilage tissue engineering. *Acta Biomater* **2017**, *S1742-7061* (17), 30036-3.
6) Chuah, Y.J.; Peck, Y. ; Lau, J.E.; Hee, H.T.; Wang, D.A. Hydrogel based cartilaginous tissue regeneration: recent insights and technologies. *Biomater Sci* 2017, DOI: 10.1039/c6bm00863a.
7) He, H.; Nagamura-Inoue, T.; Takahashi, A.; Mori, Y.; Yamamoto, Y.; Shimazu, T.; Tsunoda, H.; Tojo, A. Immunosuppressive properties of Wharton's jelly-derived mesenchymal stromal cells in vitro. *Int J Hematol* **2015**, *102* (3), 368-78.
8) Reppel, L.; Schiavi, J.; Charif, N.; Leger, L.; Yu, H.; Pinzano, A.; Henrionnet, C.; Stoltz, J.F.; Bensoussan, D.; Huselstein, C. Chondrogenic induction of mesenchymal stromal/stem cells from Wharton's jelly embedded in alginate hydrogel and without added growth factor: an alternative stem cell source for cartilage tissue engineering. *Stem Cell Res Ther* **2015**, *6*, 260–273.
9) Chen, X.; Zhang, F.; He, X.; Xu, Y.; Yang, Z.; Chen, L.; Zhou, S.; Yang, Y.; Zhou, Z.; Sheng, W.; Zeng, Y. Chondrogenic differentiation of umbilical cord-derived mesenchymal stem cells in type I collagen-hydrogel for cartilage engineering. *Injury* **2013**, *44* (4), 540-9.

10) Yeung, T.; Georges, P.C.; Flanagan, L.A.; Marg, B.; Ortiz, M.; Funaki, M.; Zahir, N.; Ming, W.;Weaver, V.; Janmey, P.A. Effects of substrate stiffness on cell morphology, cytoskeletal structure, and adhesion. *Cell Motil Cytoskeleton* **2005**, *60* (1), 24-34.

11) Engler, A.J.; Sen, S.; Sweeney, H.L.; Discher, D.E. Matrix elasticity directs stem cell lineage specification. *Cell* **2006**, *126* (4), 677–689.

12) Li, Y.Y.; Choy, T.H.; Ho, F.C.; Chan, P.B. Scaffold composition affects cytoskeleton organization, cell-matrix interaction and the cellular fate of human mesenchymal stem cells upon chondrogenic differentiation. *Biomaterials* **2015**, *52*, 208-20.

13) Tsou, Y.H.; Khoneisser, J.; Huang, P.C.; Xu,X. Hydrogel as a bioactive material to regulate stem cell fate. *Bioactive Materials*, **2016**, 1 (1), 39-55.

14) Jung, H.; Park, J.S.; Yeom, J.; Selvapalam, N.; Park, K.M.; Oh, K.; Yang, J.A.; Park, K.H.; Hahn, S.K.; Kim, K. 3D tissue engineered supramolecular hydrogels for controlled chondrogenesis of human mesenchymal stem cells. *Biomacromolecules* **2014**, *15* (3), 707-14.

15) Andersen, T.; Auk-Emblem, P.; Dornish, M. 3D Cell Culture in Alginate Hydrogels. *Microarrays (Basel)* **2015**, *4* (2), 133-61.

16) Ma, H.L.; Hung, S.C.; Lin, S.Y.; Chen, Y.L.; Lo, W.H. Chondrogenesis of human mesenchymal stem cells encapsulated in alginate beads. *J Biomed Mater Res A* **2003**, *64*, 273–81.

17) Tritz-Schiavi, J.; Charif, N.; Henrionnet, C.; de Isla, N.; Bensoussan, D.; Magdalou, J.; Benkirane-Jessel, N.; Stoltz, J.F.; Huselstein, C. Original approach for cartilage tissue engineering with mesenchymal stem cells. *Biomed Mater Eng* **2010**, *20* (3), 167–74.

18) Chung, C.; Burdick, J.A. Influence of three-dimensional hyaluronic acid microenvironments on mesenchymal stem cell chondrogenesis. *Tissue Eng Part A* **2009**, *15* (2), 243–54.

19) Chung, J.Y.; Song, M.; Ha, C.W.; Kim, J.A.; Lee, C.H.; Park, Y.B. Comparison of articular cartilage repair with different hydrogel-human umbilical cord blood-derived mesenchymal stem cell composites in a rat model. *Stem Cell Res Ther* **2014**, *5* (2), 39.

20) Bian, L.; Guvendiren, M.; Mauck, R.L.; Burdick, J.A. Hydrogels that mimic developmentally relevant matrix and N-cadherin interactions enhance MSC chondrogenesis. *Proc Natl Acad Sci USA* **2013**, *110* (25), 10117-22.

21) Zhao, L.; Weir, M.D.; Xu, H.H. An injectable calcium phosphate-alginate hydrogel umbilical cord mesenchymal stem cell paste for bone tissue engineering. *Biomaterials* **2010**, *31*(25), 6502-6510.

22) Thorpe, A.A.; Creasey, S.; Sammon, C.; Le Maitre, C.L. Hydroxyapatite nanoparticle injectable hydrogel scaffold to support osteogenic differentiation of human mesenchymal stem cells. *Eur Cell Mater* **2016**, *32*, 1-23.

23) Bendtsen, S.T.; Quinnell, S.P.; Wei, M. Development of a novel alginate-polyvinyl alcohol-hydroxyapatite hydrogel for 3D bioprinting bone tissue engineered scaffolds. *J Biomed Mater Res A* **2017**, DOI: 10.1002/jbm.a.36036.

24) Yu, H.; Cauchois, G.; Schmitt, J.F.; Louvet, N.; Six, J.L.; Chen, Y.; Rahouadj, R.; Huselstein, C. Is there a cause-and-effect relationship between physicochemical properties and cell behavior of alginate-based hydrogel obtained after sterilization? *J Mech Behav Biomed Mater* **2017**, *68*, 134-143.

25) Tritz, J., Rahouadj, R., De Isla, N., Charif, N., Pinzano, A., Mainard, D., Bensoussan, D.,Netter, P., Stoltz, J.F., Benkirane-Jessel, N., Huselstein, C. Designing a three dimensional alginate hydrogel by spraying method for cartilage tissue engineering. *Soft Matter* **2010**, *6*, 5165–5174.

26) Mjahed, H., Porcel, C., Senger, B., Chassepot, A., Netter, P., Gillet, P., Decher, G., J.C. Voegel, J.C., Schaaf, P., Benkirane-jessel, N., boulmedais, F. Micro-stratified architectures based on successive stacking of alginate gel layers and poly(L-lysine)–hyaluronic acid multilayer films aimed at tissue engineering. *Soft Matter* **2008**, 4,1422–1429.

27) Li, X.M.; Chen, S.W.; Li, J.C.; Wang, X.L.; Zhang, J.; Kawazoe, N.; Chen, G.P. 3D culture of chondrocytes in gelatin hydrogels with different stiffness. *Polymers* **2016**, *8* (8), 269.

28) Tan, H.; Rubin, J.P.; Marra, K.G. Direct synthesis of biodegradable polysaccharide derivative hydrogels through aqueous diels alder chemistry, *Macromol Rapid Commun* **2011**, *32* (12), 905-11.

29) LeRoux, M.A.; Guilak, F.; Setton, L. A. Compressive and shear properties of alginate gel: Effects of sodium ions and alginate concentration. *J Biomed Mater Res* **1999**, *47*, 46-53.

30) Wan, L.Q.; Jiang, J.; Arnold, D.E.; Guo, X.E.; Lu, H.H.; Mow, V.C. Calcium Concentration Effects on the Mechanical and Biochemical Properties of Chondrocyte-Alginate Constructs. *Cell Mol Bioeng* **2008**, *1*(1), 93-102.

31) Discher, D.E.; Janmey, P.; Wang, Y.L. Tissue cells feel and respond to the stiffness of their substrate. *Science* **2005**, *310* (5751), 1139-43.

32) Oh, S.H.; An, D.B.; Kim, T.H.; Lee, J.H. Wide-range stiffness gradient PVA/HA hydrogel to investigate stem cell differentiation behavior. *Acta Biomater* **2016**, 35, 23-31.

33) Lo Iacono, M.; Anzalone, R.; Corrao, S.; Giuffrè, M.; Di Stefano, A.; Giannuzzi, P.; Cappello, F.; Farina, F.; La Rocca, G. Perinatal and wharton's jelly-derived mesenchymal stem cells in cartilage regenerative medicine and tissue engineering strategies. *Open Tissue Eng Regen Med J* **2011**, *4*, 72–81.

34) Reppel, L.; Margossian, T.; Yaghi, L.; Moreau, P.; Mercier, N.; Leger, L.; Hupont, S.; Stoltz, J.F.; Bensoussan, D.; Huselstein, C. Hypoxic culture conditions for mesenchymal stromal/stem cells from Wharton's jelly: a critical parameter to consider in a therapeutic context. *Curr Stem Cell Res Ther* **2014**, *9* (4), 306–18.

35) Lee, H. J.; Choi, B.H.; Min, B.H.; Park, S.R. Changes in surface markers of human mesenchymal stem cells during the chondrogenic differentiation and dedifferentiation processes in vitro. *Arthritis Rheum* **2009**, *60* (8), 2325-32.

36) Ullah, M.; Eucker, J.; Sittinger, M.; Ringe, J. Mesenchymal stem cells and their chondrogenic differentiated and dedifferentiated progeny express chemokine receptor CCR9 and chemotactically migrate toward CCL25 or serum. *Stem Cell Res Ther* **2013**, *4* (4) 99.

37) Jin, H.J.; Park, S.K.; Oh, W.; Yang, Y.S.; Kim, S.W. Down-regulation of CD105 is associated with multi-lineage differentiation in human umbilical cord blood-derived mesenchymal stem cells. *Biochem Biophys Res Comm* **2009**, *381* (4), 676–81.

38) Baer, P.C.; Griesche, N.; Luttmann, W.; Schubert, R.; Luttmann, A.; Geiger, H. Human adipose-derived mesenchymal stem cells in vitro: evaluation of an optimal expansion medium preserving stemness. *Cytotherapy* **2010**, *12* (1), 96-106.

39) Jiang, T.; Liu, W.; Lv, X.; Sun, H.; Zhang, L.; Liu, Y.; Zhang, W.J.; Cao, Y.; Zhou, G. Potent in vitro chondrogenesis of CD105 enriched human adipose-derived stem cells. *Biomaterials* **2010**, *31* (13), 3564–71.

40) Ode, A.; Schoon, J.; Kurtz, A.; Gaetjen, M.; Ode, J.E.; Geissler, S.; Duda, G.N. CD73/5'-ectonucleotidase acts as a regulatory factor in osteo-/chondrogenic differentiation of mechanically stimulated mesenchymal stromal cells. *Eur Cell Mater* **2013**, *25*, 37–47.

41) Bian, L.; Guvendiren, M.; Mauck, R.L.; Burdick, J.A. Hydrogels that mimic developmentally relevant matrix and N-cadherin interactions enhance MSC chondrogenesis. *Proc Natl Acad Sci USA* **2013**, *110* (25), 10117–22.

42) Nagase, T.; Muneta, T.; Ju, Y.J.; Hara, K.; Morito, T.; Koga, H.; Nimura, A.; Mochizuki, T.; Sekiya, I.. Analysis of the chondrogenic potential of human synovial stem cells according to harvest site and culture parameters in knees with medial compartment osteoarthritis. *Arthritis Rheum* **2008**, *58* (5), 1389–98.

43) Yang, J.W.; de Isla, N.; Huselstein, C.; Sarda-Kolopp, M.N.; Li, N.; Li, Y.P.; Jing-Ping, O.Y.; Stoltz, J.F.; Eljaafari, A. Evaluation of human MSCs cell cycle, viability and differentiation in micromass culture. *Biorheology* **2006**, *43* (3-4), 489-96.

44) Grogan, S.P.; Barbera, A.; Diaz-Romero, J.; Cleton-Jansen, A.M.; Soeder, S.; Whiteside, R.; Hogendoorn, P.C.; Farhadi, J.; Aigner, T.; Martin, I.; Mainil-Varlet, P. Identification of markers to characterize and sort human articular chondrocytes with enhanced in vitro chondrogenic capacity. *Arthritis Rheum* **2007**, *56* (2), 586-95.

45) Hagmann, S.; Moradi, B.; Frank, S.; Dreher, T.; Kämmerer, P.W.; Richter, W.; Gotterbarm, T. Different culture media affect growth characteristics, surface marker distribution and chondrogenic differentiation of human bone marrow-derived mesenchymal stromal cells. *BMC Musculoskelet Disord* 2013, 14, 223.

46) Karlsen, T.A.; Mirtaheri, P.; Shahdadfar, A; Fløisand, Y.; Brinchmann, J.E. Effect of three-dimensional culture and incubator gas concentration on phenotype and differentiation capability of human mesenchymal stem cells. *J Cell Biochem* **2011**, *112* (2), 684-93.

47) Follin, B.; Juhl, M.; Cohen, S.; Pedersen, A.E.; Gad, M.; Kastrup, J.; Ekblond, A. Human adipose-derived stromal cells in a clinically applicable injectable alginate hydrogel: Phenotypic and immunomodulatory evaluation. Cytotherapy **2015**, *17* (8), 1104-18.

48) Chaudhuri, O., Gu, L., Darnell, M., Klumpers, D., Bencherif, S.A., Weaver, J.C., Huebsch, N., Mooney, D.J. Substrate stress relaxation regulates cell spreading. *Nat Commun* **2015**, *6*:6364.

49) Wozniak, M.A.; Chen, C.S. Mechanotransduction in development: a growing role for contractility. *Nat Rev Mol Cell Biol* **2009**, *10*, 34–43.

50) Chung, C.; Burdick, J.A. Influence of three-dimensional hyaluronic acid microenvironments on mesenchymal stem cell chondrogenesis. *Tissue Eng Part A* **2009**, *15* (2), 243-54.

51) Zhou, H.; Lee, J. Nanoscale hydroxyapatite particles for bone tissue engineering. *Acta Biomater* **2011**, *7* (7), 2769-81.

52) Klyushnenkova, E.; Mosca, J.D.; Zernetkina, V.; Majumdar, M.K.; Beggs, K.J.; Simonetti, D.W.; Deans, R.J.; McIntosh, K.R. T cell responses to allogeneic human mesenchymal stem cells: immunogenicity, tolerance, and suppression. *J Biomed Sci* **2005**, *12*, 47–57.

53) La Rocca, G.; Lo Iacono, M.; Corsello, T.; Corrao, S.; Farina, F.; Anzalone, R. Human Wharton's jelly mesenchymal stem cells maintain the expression of key immunomodulatory molecules when subjected to osteogenic, adipogenic and chondrogenic differentiation in vitro: new perspectives for cellular therapy. *Curr Stem Cell Res Ther* **2013**, *8* (1), 100-13.

54) Lee, H.J.; Kang, K.S.; Kang, S.Y.; Kim, H.S.; Park, S.J.; Lee, S.Y.; Kim, K.D.; Lee, H.C.; Park, J.K.; Paik, W.Y.; Lee, L.; Yeon, S.C. Immunologic properties of differentiated and undifferentiated mesenchymal stem cells derived from umbilical cord blood. *J Vet Sci* **2016**, *17* (3), 289 -97.

55) Yang. J.; Chen, X.; Yuan, T.; Yang, X.; Fan, Y.; Zhang, X. Regulation of the secretion of immunoregulatory factors of mesenchymal stem cells (MSCs) by collagen-based scaffolds during chondrogenesis. *Mater Sci Eng C Mater Biol Appl* **2017**, *70* (Pt2), 983-991.

56) Yuan, T.; Li, K.; Guo, L.; Fan, H.; Zhang, X. Modulation of immunological properties of allogeneic mesenchymal stem cells by collagen scaffolds in cartilage tissue engineering. *J Biomed Mater Res A* **2011**, *98* (3), 332-41.

57) Yuan, T.; Zhang, L.; Li, K.; Fan, H.; Fan, Y.; Liang, J.; Zhang, X. Collagen hydrogel as an immunomodulatory scaffold in cartilage tissue engineering. *J Biomed Mater Res B Appl Biomater* **2014**, *102* (2), 337-44.

58) Campioni, D.; Rizzo, R.; Stignani, M.; Melchiorri, L.; Ferrari, L.; Moretti, S.; Russo, A.; Bagnara, G.P.; Bonsi, L.; Alviano, F.; Lanzoni, G.; Cuneo, A.; Baricordi, O.R.; Lanza, F. A. Decreased positivity for CD90 on human mesenchymal stromal cells (MSCs) is associated with a loss of immunosuppressive activity by MSCs. *Cytometry B Clin Cytom* **2009**, *76* (3), 225-30.

59) De Francesco, F.; Tirino, V. ; Desiderio, V.; Ferraro, G.; D'Andrea, F.; Giuliano, M.; Libondi, G.; Pirozzi, G.; De Rosa, A.; Papaccio, G. Human CD34+/CD90+ ASCs Are Capable of Growing as Sphere Clusters, Producing High Levels of VEGF and Forming Capillaries. *PloS One* **2009**, *4* (8), e6537.

60) Chen, X.Y.; Hao, Y.R.; Wang, Z.; Zhou, J.L.; Jia, Q.X.; Qiu, B. The effect of vascular endothelial growth factor on aggrecan and type II collagen expression in rat articular chondrocytes. *Rheumatol Int* **2012**, *32* (11), 3359-64.

Discussion

Recently, Wharton's jelly represents an attractive and alternative source of MSC for the development of new approaches in cellular and tissue engineering. It seems to offer advantages over adult MSC, which make it possible to consider their use in cell therapy in long term. WJ-MSC exhibited a relative stability in terms of *in vitro* proliferation, viability, senescence and multipotency differentiation capacities, etc under *in vitro* condition. In the first part of our work, we identified the characters of extracted WJ-MSC from umbilical cord. Thus, WJ-MSC fit the criteria of the International Society for Cellular Therapy (*Dominici M et al, 2006*). They express mesenchymal markers such as CD73, CD90, and CD105 and are negative for hematopoietic ones (CD45, CD34) (*Wang HS et al, 2004; Conconi MT et al, 2011; Anzalone R et al, 2010*). Furthermore, WJ-MSC have higher colony forming unit-fibroblast (CFU-F) (*Baksh D et al, 2007*) and have a high ex vivo proliferation index and low population doubling times. *Nekanti U* et al showed that WJ-MSC can undergo a 300-fold expansion within six to seven passages without any abnormal karyotypes (*Nekanti U et al, 2010; Troyer D L et al, 2008*). So, we suggested that WJ-MSC could be used as stem cell resource in regenerative cartilage.

As we known that the lesions of cartilage from the partial- to full-thickness are affecting people of all ages. In order to mimic the organization of cartilage tissue, many people promoted the multilayer scaffolds with a good capacity for repairing the damaged tissue. The ideal hydrogel graft for the treatment of articular cartilage defects needs to match the mechanical and functional properties of the native tissue. So, it is necessary to assay the physical properties and cell behavior of hydrogel what will be fabricated by initiate HA and Hap. In this part, we mainly focused on the characterization of Alg/HA and Alg/Hap hydrogel, comparison of them from mechanical properties and viscosity behavior, as well as evaluation of the cell proliferation, viability and differentiation of WJ-MSC encapsulated into Alg/HA and/or Alg/Hap during the process of chondrogenic differentiation. For the

rheological characterization of Alg/HA and Alg/Hap in gelling state, it found that the viscosity of hydrogel after autoclaving is further lower than the control's one. It was caused by the reaction of depolymerization of alginate chains under a higher temperature (*Leo WJ et al, 1990; Holme HK et al, 2008*). Put simply, alginate is a block copolymer, and their physical properties rely heavily on the sequence of these blocks. However, the autoclaving treatment caused the β-elimination reaction of 1-4 glycosidic linkage for the depolymerization of alginate (*Holme HK et al, 2003*). That is also why the strength of Alg/HA and Alg/Hap hydrogel scaffolds decreased by autoclaving. At the same time, Alg/Hap hydrogels have good mechanical properties as compared with Alg/HA hydrogels, which due to hap particles reinforce the strength of hydrogels (*Román J et al, 2011*). For cell behavior of WJ-MSC seeded into the Alg/HA and Alg/Hap hydrogels, we found the cell viability and cell proliferation of Alg/Hap is significantly better than Alg/HA hydrogel from 10 to 30 days. This could depend on the shear viscosity and tensile strength of hydrogel, as we described in the article 1. Through these experiments, we found the autoclave treatment has negatively affected on the shear viscosity and mechanical properties of Alg/HA and Alg/Hap hydrogels. Thus, to find an effective sterilization method is turning to be necessary, which can keep the native characters of alginate-based hydrogel as well as maintain the cell behavior of hydrogel-laden cells.

For the third part, sterilization is defined as the process where all the viable organisms are killed. It can be achieved by physical, chemical and physiochemical methods. Many of sterilization treatments (autoclave, Gamma irradiation, ethanol, ethylene oxide, moist heat) are commonly used to directly sterilize hydrogel, polymeric or biologic scaffolds (*Dearth CL et al, 2016; Rnjak-Kovacina J et al, 2015*). But, it is well known that these common sterilization treatments lead to the alginate chain scission (linked by β (1→4) glycosidic bonds) and hemolysis (de-polymerization) (*Hu T et al, 2014; Leo WJ et al, 1990*). Cardoso DA *et al* (*Cardoso D A et al, 2014*) reported that γ-irradiation, autoclave and partial periodate oxidation affect the molecular weight of alginate. If autoclave changed the mechanical properties of

hydrogels, Stoppel WL *et* al (*Stoppel WL et al, 2014*) showed that UV method during 20 min is not enough to eliminate bacterial persistence of hydrogel. To select an effective sterilization treatment of alginate-based materials, one must ensure it does not damage its functional properties. In our study, we investigated the effect of sterilization by autoclave, or UV (during 25 and 50 minutes) on alginate/hyaluronic acid hydrogel scaffolds. This set has been yet described as promoting mesenchymal stem cell differentiation into chondrocytes (*Reppel L et al, 2015*). We tried to make inter-relationship between all these parameters and sterilization process and for the first time the effect of sterilization has been determined on biological, mechanical and physicochemical properties of hydrogel scaffolds. Through the ATR-FTIR analysis we found that there is no significant shift of characteristic FTIR peaks of Alg/HA hydrogel, pure alginate powders and pure hyaluronic acid powders under autoclave, UV-1, UV-2 or control treatments, which indicated that these sterilization methods have no effect on the chemical functional groups of them. Mao S *et al* (*Mao S et al, 2012*) demonstrated using UV spectroscopy there was no change in chemical structure of the alginate during de-polymerization process. The molecular weight is the most important property of the polymers in the sense that it also governs their mechanical properties. That is why we analyzed the average molecular weight of composite of Alg/HA in powder after autoclave, UV-1, UV-2 and control. So we found that the autoclave treatment caused an important reduction in $\overline{M_n}$ and $\overline{M_w}$ but also in viscosity as compared with control. These results are confirmed by the previous study (*Lee KY et al, 2012*), which showed that the alginate polymer exhibits a reduction of its molecular weight and its viscosity, due to the de-polymerization which leads to the breakdown of the main chain backbone of alginate. In addition, UV treatment produces a slight decrease in molecular mass and viscosity for Alg/HA, and showes no significant difference between UV-1 and UV-2. This phenomenon can be attributed to the absorption of UV energy due to polysaccharide. Since, the formation of free radical through UV light may cleave covalent bonds, which can initiate de-polymerization reaction (*Wasikiewicz JM et al, 2005*). Therefore, as UV

treatment has no deleterious effect on the properties of alginate, it can be used to maintain the stability and structural homogeneous of hydrogel scaffolds. Moreover, the hydrogel scaffolds are fairly soft viscoelastic media that require appropriate techniques of mechanical characterisation to be investigated. That's why we selected the indentation technique, which is often used for living and synthetic soft materials. This mechanical test can be done at different scales (nano by AFM, micro or macro) and presents the advantage of being fast and non-destructive (*Merino JC et al, 1991; Oyen ML et al, 2014; Ahearne M et al, 2005*), although the strain and stress fields are not uniform. In the present study, we used it to compared the effects of treatment without explicity characterize the mechanical behaviour. Note that the determination of the mechanical behaviour of the hydrogel could only be done by a numerical method such as the finite element method. The main results are given as a function of sterilization treatments in figure 4 of article 2. However, the authors agree on the fact that the sterilization time is a prime parameter in clinical medicine (*Braghirolli DI et al, 2014*). Effects of UV treatment time (UV-1: 25 min, UV-2: 25+25 min) and autoclaving on the sterility and biocompatibility of hydrogel beads were studied by FTM with SGA, PI/Annexin-V kit and Alamar Blue™ assay Kit. As shown in table 2 and figure.5 of article 2, there is clouding of the thioglycollate broth in the medium for hydrogel beads by UV-1 treatment. In contrast, autoclaving and UV-2 treatment keep hydrogel beads from contamination, which can protect them infection from bacterial and fungal. This result is in agreement with De Moraes MA et al (*De Moraes MA et al, 2014*) study on silk fiber membranes. Our results showed that UV-radiation for 25 min was not enough to eliminate microorganisms for hydrogel scaffold. Nevertheless, the long duration of UV treatment (25+25 min) seems to be an effective sterilization condition, but also is beneficial for living cells-laden Alg/HA hydrogel scaffolds. In fact, the viability results obtained with UV-2 showed that the average living percentage of cells arrived at 82 ± 10% at 30 days, as after autoclaving. Microscopic evaluation of the encapsulated WJ-MSC showed that, whatever the sterilization process, at the beginning of the

culture, the encapsulated undifferentiated stem cells remained as a single-cell suspension. However, during cartilage differentiation (30 days), extracellular matrix was synthetized. Histochemical staining with Alcian Blue and Sirius Red which are specific for GAG and collagen synthesis, respectively, confirmed the amount of extracellular matrix synthesis from 10 days for GAG and 30 days for collagen. More important is the synthesis of GAG and collagen in UV-2-hydrogel beads are more than others after 30 days of culture. From the results above, we can conclude that hydrogel scaffolds with UV-2 treatments may be a good alternative to ensure the cell viability and chondrocyte differentiation of the WJ-MSCs-laden hydrogel. Through the PCA component analysis, we had furtherly interpreted the inter-correlations between the different treatments and variables as seen in article 2. Finally, this work shown that the cell behavior in alginate-based hydrogels was not only regulated by physicochemical properties (as molar mass or/and viscosity), but also associated with the controlling of sterilization time.

For osteochondral defeat, to use stratified scaffold to mimic zonal organization of cartilage will be necessary. We will use the Alg/Ha hydrogels and Alg/Hap hydrogels to mimic cartilage and subchondral bone, respectively. According to previously results, UV can be as an effective sterilization treatment to sterilize Alg/HA and Alg/Hap hydrogel. In this part, we have mainly studied the physical properties, biological characters and immunomodulatory properties of alginate-based hydrogel-laden WJ-MSC during chondrogenesis. To explore how scaffold composition modulate the mechanical, biological (chondrocyte differentiation, cell behavior) and secretion of immunoregulatory factors in MSCs encapsulated into Alg/HA and Alg/Hap hydrogels, respectively. For the physical properties of hydrogels, the results of physical properties (swelling ratio, mechanical properties) shown hap particles have decreased the swelling ratio of alginate-based hydrogel and have improved the mechanical strength of alginate-based hydrogel, which due to the Hap with hydrophobic properties and have a normal mechanical strength as bone tissue. More interestingly, we found the mechanical strength of alginate-based hydrogels

(with/without cells) decreased during the time of culture. This is likely due to the calcium metabolism and the changes in calcium concentration under culturing condition (*Wan LQ et al, 2008*). Whereupon, how to dynamic adjust the mechanical strength of alginate-based hydrogel-laden cells is becoming very important. This is our problem to be solved in the future. In the biological part, their proliferation, phenotypic and differentiation were evaluated. The results shown that the proliferation of cell in Alg/HA hydrogels was significantly higher than that of Alg/Hap hydrogels after 30 days. It depended on the Hap particles have increased the stiffness of matrix, which lead to increase cell's proliferation (*Discher DE et al, 2005*). During the chondrogenic differentiation from 10 to 30 days, as the results of RT-PCR and flow cytometry shown, Alg/HA hydrogels were beneficial for the expression of chondrogenesis-related markers (So9, Col2a1 and ACAN). Bu also Alg/Hap hydrogels have expressed osteogenic-related genes (Runx2, OPN, OCN, Col I and Col X) as compared with Alg/HA hydrogel. Both Alg/HA and Alg/Hap hydrogels with a potential to mimic the zonal organization of cartilage defect. Histological staining was furtherly verified the differentiation character of WJ-MSC seeded into hydrogel. MSC are endowed with outstanding immunoregulatory features, some studies have exhibited the scaffold could mediate the expression of MHC molecules on the surface of MSCs (*Yuan T et al, 2011; Park JS et al, 2015*). However, there is in lack of if the scaffold properties could regulate immunoregulatory activity of seeded MSCs. Thus, we focused on wheatear the alginate-based hydrogel composition could modulate the secretion of soluble factors by seeded WJ-MSCs during the chondrogenic differentiation. Here, flow-cytometry and ELISA results showed changing of the soluble factors by secreted WJ-MSCs seeded into hydrogel with different composition. The results shown that immunoregulatory factors (HGF and VEGF) expression decreased from 10 to 30 days, this phenomena was caused by a loss of mesenchymal markers, as shown in figure 4 of article 3. Meanwhile, expression of soluble factors (TGF-β1) of Alg/Hap-laden WJ-MSCs were higher than Alg/HA-laden WJ-MSCs, as a result of Hap particles have improved the contraction

activities of hydrogel, that is the particles lead to more cell-cell interactions as seen in figure 5 of article 3. For the VEGF expression, Alg/HA-laden WJ-MSCs expressed much more than Alg/Hap-laden WJ-MSCs, which were associated with the up-regulation of collagen II and aggrecan during differentiation. Taken together, the native hydrogel structures could play a vital role in meditating the secretion of immunoregulatory factors by MSCs seeded into alginate-based hydrogels during chondrogenic differentiation. Finally, through the PCA analysis, we developed a correlation-ship in among of parameters including hydrogel, physical properties, cell behavior and immunomodulation properties.

Conclusions and perspectives

WJ-MSC with maintenance of their proliferating, differentiation potential and immune properties promise to be an interesting source of MSC for cartilage tissue engineering or cell therapy. To repair osteochondral defeats, multiphasic scaffolds are required to mimic the physiological properties and structure of two different tissues as cartilage and subchondral bone. In this part, before we will plan to use the Alg/HA and Alg/Hap to mimic cartilage and subchondral bone, respectively. It is necessary to compare the Alg/HA and Alg/Hap hydrogels in mechanical property and cytocompatibility. The results shown that Alg/Hap hydrogel presented a good mechanical properties and cytocompatibility as compared with Alg/HA hydrogel. As well as the autoclaving treatment has negatively influenced native characters (viscosity and mechanical property) of hydrogels. As everyone knows, almost all of the biologic scaffold materials was fabricated by the originally polymer as a powder state.

To find an effective sterilization method is becoming important for the polymer prior to clinical use. However, there is no system statistics analysis to evaluate the interrelationship of the characteristics of alginate-based polymer after sterilization. In our work, we used autoclaving and UVs (UV-1: 25min; UV-2: 50min) to sterilize the alginate (Alg) / hyaluronic acid (HA) composite powder, which formed hydrogel. Then, we evaluate the correlation between physicochemical properties and cell behavior for the properties of the originally polymer during sterilization, through the principal component analysis (PCA). Mainly results are as follows: (1): The cell behavior of alginate-based hydrogels was not only regulated by physicochemical properties (as molar mass or/and viscosity), but also associated with the controlling of sterilization time. (2): UV-2 treatment could to be an effective method as compared with others, which minimal impact on the mechanical integrity or physical-chemical properties and maintain its cytocompatibility and its ability to induce chondrogenesis from mesenchymal stem cells. From these results, it will

provide a basis for choosing an effective method of sterilization, but also importantly exhibit the relationship between physicochemical properties and cell behavior of alginate-based hydrogel after sterilization. UV-2 sterilization also provides better mechanical properties on Alg hydrogel than GMP Alg. According to above results shown, both of Alg/HA and Alg/Hap hydrogels were sterilized by UV-2 treatment, then to analyse mechanical, biological and immunological properties. Mainly results are as follows: (1): Hap has improved mechanical properties of hydrogel, which decreased swelling ratio and changed cell behavior as cytoskeleton, proliferation of cell. (2): Hap also has improved the production of PGE_2 and TGF-β1 as compared with Alg/HA hydrogels. (3): The expression of the mesenchymal markers as (CD44, CD73, CD90, CD105, and CD166) was decreased by 3D hydrogel (Alg/HA and Alg/Hap) culture during the time of culture. (4): Alg/HA hydrogel scaffolds showed strong upregulation of cartilage-specific transcript expression, meanwhile, Alg/Hap hydrogel scaffolds presented slightly upregulation of bone-specific transcript expression from 10 to 30 days. (5): Both of hydrogel--laden MSCs did not express the costimulatory surface antigens CD40, CD80, and CD86. However, the expression of HGF and VEGF decreased in 3D hydrogel scaffolds. (6): The mechanical, biological and immunological properties are also affected by each other after PCA analysis. These results could provide a basically reference in designing of alginate-based hydrogel to repair cartilage or osteochondral defects. In addition, for alginate-based hydrogel, UV sterilization treatment would be an effective method as same as alginate NOVAMATRIX, which might be used in pre-clinical sterilization.

References

Ahmed EM. Hydrogel: Preparation, characterization, and applications: A review. J Adv Res, 2015; 6(2):105-21.

Aheame M, Jones E, Rapp A, Mathieu J. High touch through high tech: The impact of salesperson technology usage on sales performance via mediating mechanisms. Management science, 2008; 54(4): 671–685.

Ahearne M, Yang Y, El Haj AJ, Then KY, Liu KK. Characterizing the viscoelastic properties of thin hydrogel-based constructs for tissue engineering applications. J R Soc Interface, 2005; 2(5):455-63.

Almeida HV, Eswaramoorthy R, Cunniffe GM, Buckley CT, O'Brien FJ, Kelly DJ. Fibrin hydrogels functionalized with cartilage extracellular matrix and incorporating freshly isolated stromal cells as an injectable for cartilage regeneration. Acta Biomater, 2016; 36:55-62.

Anzalone R, Lo Iacono M, Corrao S, Magno F, Loria T, Cappello F, Zummo G, Farina F, La Rocca G. New emerging potentials for human Wharton's jelly mesenchymal stem cells: immunological features and hepatocyte-like differentiated capacity. Stem Cells Dev, 2010; 19(4):423-38.

Ashton RS, Banerjee A, Punyani S, Schaffer DV, Kane RS. Scaffolds based on degradable alginate hydrogels and poly (lactide-co-glycolide) microspheres for stem cell culture. Biomaterials, 2007; 28(36):5518-25.

Aspberg A. The different roles of aggrecan interaction domains. J Histochem Cytochem, 2012; 60(12):987-96.

Athanasiou KA, Darling EM, Hu JC. Articular Cartilage Tissue Engineering. Synthesis Lectures on Tissue Engineering, 2009, 182 papers.

Atala A, Kim W, Paige KT, Vacanti CA, Retik AB. Endoscopic treatment of vesicoureteral reflux with a chondrocyte-alginate suspension. The Journal of Urology, 1994, 152(2 Pt 2):641-3.

Awad HA, Wickham MQ, Leddy HA, Gimble JM, Guilak F. Chondrogenic differentiation of adipose-derived adult stem cells in agarose, alginate, and gelatin scaffolds. Biomaterials, 2004; (25):3211-3222.

References

Aydelotte MB, Greenhill RR, Kuettner KE. Differences between sub-populations of cultured bovine articular chondrocytes II Proteoglycan metabolism. Connect Tissue Res, 1988; 18(3):223-34.

Baksh D, Yao R, Tuan RS. Comparison of proliferative and multilineage differentiation potential of human mesenchymal stem cells derived from umbilical cord and bone marrow. Stem Cells, 2007; 25(6):1384-92.

Barry F, Boynton RE, Liu B, Murphy JM. Chondrogenic differentiation of mesenchymal stem cells from bone marrow: differentiation-dependent gene expression of matrix components. Exp Cell Res, 2001; 268(2):189-200.

Beyzadeoglu T, Onal A, Ivkovic A. Matrix-induced autologous chondrocyte implantation for a large chondral defect in a professional football player: a case report. J Med Case Rep, 2012; 6:173.

Beyzadeoglu T, Akgun U, Tasdelen N, Karahan M. Prediction of semitendinosus and gracilis autograft sizes for ACL reconstruction. Knee Surg Sports Traumatol Arthrosc, 2012; 20(7):1293-7.

Bernardo ME, Zaffaroni N, Novara F, Cometa AM, Avanzini MA, Moretta A, Montagna D, Maccario R, Villa R, Daidone MG, Zuffardi O, Locatelli F. Human bone marrow derived mesenchymal stem cells do not undergo transformation after long-term in vitro culture and do not exhibit telomere maintenance mechanisms. Cancer Res, 2007; 67(19):9142-9.

Benvenuto F, Ferrari S, Gerdoni E, Gualandi F, Frassoni F, Pistoia V, Mancardi G, Uccelli A. Human mesenchymal stem cells promote survival of T cells in a quiescent state. Stem Cells, 2007; 25(7):1753-60.

Bertin P, Rannou F, Grange L, Dachicourt JN, Bruel P, Emery C, Grandfils N and Taieb C. Annual Cost of Patient with Osteoarthrotis of the Hip and Knee in France. Journal of Musculoskeletal Pain, 2014; 4:356-364.

Bigdeli N, Karlsson C, Strehl R, Concaro S, Hyllner J, Lindahl A. Coculture of human embryonic stem cells and human articular chondrocytes results in significantly altered phenotype and improved chondrogenic differentiation. Stem Cells, 2009; 27(8):1812-21.

Bryant SJ, Anseth KS. Controlling the spatial distribution of ECM components in degradable PEG hydrogels for tissue engineering cartilage. J Biomed Mater Res A, 2003; 64(1):70-9.

Brandl F, Sommer F, Goepferich A. Rational design of hydrogels for tissue engineering: impact of physical factors on cell behavior. Biomaterials, 2007; 28(2):134-46.

References

Brittberg M. Autologous chondrocyte transplantation. Clin Orthop Relat Res, 1999; (367Suppl): S147-55.

Braghirolli DI, Steffens D, Quintiliano K, Acasigua GA, Gamba D, Fleck RA, Petzhold CL, Pranke P. The effect of sterilization methods on electronspun poly (lactide-co-glycolide) and subsequent adhesion efficiency of mesenchymal stem cells. J Biomed Mater Res B Appl Biomater, 2014; 102(4):700-8.

Brennen WN, Denmeade SR, Isaacs JT. Mesenchymal stem cells as a vector for the inflammatory prostate microenvironment. Endocr Relat Cancer, 2013; 20(5):R269-90.

Burdick JA, Prestwich GD. Hyaluronic acid hydrogels for biomedical applications. Adv Mater, 2011; 23(12):H41-56.

Bugbee W, Cavallo M, Giannini S. Osteochondral allograft transplantation in the knee. Journal of Knee Surgery, 2012.

Bhattacharjee A, Bansal M. Collagen structure: the Madras triple helix and the current scenario. IUBMB Life, 2005; 57(3):161-72.

Can A, Karahuseyinoglu S. Concise review: human umbilical cord stroma with regard to the source of fetus-derived stem cells. Stem Cells, 2007; 25(11):2886-95.

Carlin R, Davis D, Weiss M, Schultz B, Troyer D. Expression of early transcription factors Oct-4, Sox-2 and Nanog by porcine umbilical cord (PUC) matrix cells. Reprod Biol Endocrinol, 2006; 4:8.

Caliari SR, Burdick JA. A practical guide to hydrogels for cell culture. Nat Methods, 2016; 13(5):405-14.

Cardoso DA, Ulset AS, Bender J, Jansen JA, Christensen BE, Leeuwenburgh SC. Effects of physical and chemical treatments on the molecular weight and degradation of alginate-hydroxyapatite composites. Macromol Biosci, 2014; 14(6):872-80.

Cao HJ, Wang MD, Li SG, Zhu L, Zheng JH. Paracrine effect of bone marrow mesenchymal stem cells on proliferation, apoptosis, and alpha-actin-2 expression in hepatic stellate cells. Genet Mol Res, 2017; 16(1).

Ceonzo K, Gaynor A, Shaffer L, Kojima K, Vacanti CA, Stahl GL. Polyglycolic acid-induced inflammation: role of hydrolysis and resulting complement activation. Tissue Eng, 2006; 12(2):301-8.

Conconi MT, Burra P, Di Liddo R, Calore C, Turetta M, Bellini S, Bo P, Nussdorfer GG, Parnigotto PP. CD105 (+) cells from Wharton's jelly show in vitro and in vivo myogenic differentiative potential. Int J Mol Med, 2006; 18(6):1089-96.

Conconi MT, Tommasini M, Liddo RD, Calore C, Parnigotto PP. Phenotype and differentiation potential of stromal populations obtained from various zones of human umbilical cord: an overview. The Open Tissue Engineering and Regenerative Medicine Journal, 2011, 4, 6-20.

Cook D, Genever P. Regulation of mesenchymal stem cell differentiation. Transcriptional and Translational Regulation of Stem Cells, 2013, Book.

Collins MN, Birkinshaw C. Hyaluronic acid based scaffolds for tissue engineering--a review. Carbohydr Polym, 2013; 92(2):1262-79.

Collins MN, Birkinshaw C. Investigation of the swelling behavior of crosslinked hyaluronic acid films and hydrogels produced using homogeneous reactions. J applied polymer science, 2008; 109(2):923-931.

Chang CH, Lin FH, Kuo ZF, Liu HC. Cartilage tissue engineering. Biomedical Engineering: Applications, Basis and Communications, 2005; 17(2):61-72.

Chan EP, Hu Y, Johnson PM, Suo Z, Stafford CM. Spherical indentation testing of poroelastic relaxations in thin hydrogel layers. Soft Matter, 2012; 8:1492–1498.

Chang J, Nakajima H, Poole CA. Structural colocalisation of type VI collagen and fibronectin in agarose cultured chondrocytes and isolated chondrons extracted from adult canine tibial cartilage. J Anat, 1997; 190 (Pt 4):523-32.

Chen J, Chen H, Li P, Diao H, Zhu S, Dong L, Wang R, Guo T, Zhao J, Zhang J. Simultaneous regeneration of articular cartilage and subchondral bone in vivo using MSCs induced by a spatially controlled gene delivery system in bilayered. Biomaterials, 2011; 32(21):4793-805.

Choudhery MS, Badowski M, Muise A, Pierce J, Harris DT. Donor age negatively impacts adipose tissue-derived mesenchymal stem cell expansion and differentiation. J Transl Med, 2014; 12:8.

Clegg T.E., Caborn D, Mauffrey C. Viscosupplementation with hyaluronic acid in the treatment for cartilage lesions: a review of current evidence and future directions. Eur J Orthop Surg Traumatol, 2013; 23(2):119-24.

Corcione A, Benvenuto F, Ferretti E, Giunti D, Cappiello V, Cazzanti F, Risso M, Gualandi F, Mancardi GL, Pistoia V, Uccelli A. Human mesenchymal stem cells modulate B-cell functions. Blood, 2006; 107(1):367-72.

Cui L, Wu Y, Cen L, Zhou H, Yin S, Liu G, Liu W, Cao Y. Repair of articular cartilage defect in non-weight bearing areas using adipose derived stem cells loaded polyglycolic acid mesh. Biomaterials, 2009; 30(14):2683-93.

Doulabi AH, Mequanint K, Mohammadi H. Blends and Nanocomposite Biomaterials for Articular Cartilage Tissue Engineering. Materials, 2014; 7, 5327-5355.

Dai J, Rabie AB. VEGF: an essential mediator of both angiogenesis and endochondral ossification. J Dent Res, 2007; 86(10):937-50.

Das RK, Gocheva V, Hammink R, Zouani OF, Rowan AE. Stress-stiffening-mediated stem-cell commitment switch in soft responsive hydrogels. Nat Mater, 2016; 15(3):318-25.

Das RH, van Osch GJ, Kreukniet M, Oostra J, Weinans H, Jahr H. Effects of individual control of pH and hypoxia in chondrocyte culture. J Orthop Res, 2010; 28(4):537-45.

Dai L, Zhang X, Hu X, Zhou C, Ao Y. Silencing of microRNA-101 prevents IL-1β-induced extracellular matrix degradation in chondrocytes. Arthritis Res Ther, 2012; 14(6):R268.

Dearth CL, Keane TJ, Carruthers CA, Reing JE, Huleihel L, Ranallo CA, Kollar EW, Badylak SF. The effect of terminal sterilization on the material properties and in vivo remodeling of a porcine dermal biologic scaffold. Acta Biomater, 2016; 33:78-87.

De Kee D, CF Chan Man Fong. Rheological properties of structured fluids. Polymer engineering and science, 1994; 34(5): 438-445.

De Moraes MA, Weska RF, Beppu MM. Effects of sterilization methods on the physical, chemical, and biological properties of silk fibroin membranes. J Biomed Mater Res B Appl Biomater, 2014; 102(4):869-76.

Deng W, Han Q, Liao L, You S, Deng H, Zhao RC. Effects of allogeneic bone marrow-derived mesenchymal stem cells on T and B lymphocytes from BXSB mice. DNA Cell Biol, 2005; 24(7):458-63.

Discher DE, Janmey P, Wang YL. Tissue cells feel and respond to the stiffness of their substrate. Science, 2005; 310(5751):1139-43.

Dominici M, Le Blanc K, Mueller I, Slaper-Cortenbach I, Marini F, Krause D, Deans R, Keating A, Prockop Dj, Horwitz E. Minimal criteria for defining multipotent mesenchymal stromal cells. The International Society for Cellular Therapy position statement. Cytotherapy, 2006; 8(4):315-7.

Dounchis JS, Bae WC, Chen AC, Sah RL, Coutts RD, Amiel D. Cartilage repair with autogenic perichondrium cell and polylactic acid grafts. Clin Orthop Relat Res, 2000; (377):248-64.

Djouad F, Plence P, Bony C, Tropel P, Apparailly F, Sany J, Noël D, Jorgensen C Immunosuppressive effect of mesenchymal stem cells favors tumor growth in allogeneic animals. Blood, 2003; 102(10):3837-44.

References

Engler AJ, Sen S, Sweeney HL, Discher DE. Matrix elasticity directs stem cell lineage specification. Cell, 2006; 126(4):677-89.

El Omar R, Beroud J, Stoltz JF, Menu P, Velot E, Decot V. Umbilical cord mesenchymal stem cells: the new gold standard for mesenchymal stem cell-based therapies? Tissue Eng Part B Rev, 2014; 20(5):523-44.

Fabian C, Naaldijk Y, Leovsky C, Johnson AA, Rudolph L, Jaeger C, Arnold K, Stolzing A. Distribution pattern following systemic mesenchymal stem cell injection depends on the age of the recipient and neuronal health. Stem Cell Res Ther, 2017; 8(1):85.

Feng Y, Kopplin G, Sato K, Draget KI, Vårum KM. Alginate gels with a combination of calcium and chitosan oligomer mixtures as crosslinkers. Carbohydr Polym, 2017; 156:490-497.

Feng Q, Lin S, Zhang K, Dong C, Wu T, Huang H, Yan X, Zhang L, Li G, Bian L. Sulfated hyaluronic acid hydrogels with retarded degradation and enhanced growth factor retention promote hMSC chondrogenesis and articular cartilage integrity with reduced hypertrophy. Acta Biomater, 2017; S1742-7061(17):30118-6.

Fong CY, Chak LL, Biswas A, Tan JH, Gauthaman K, Chan WK, Bongso A. Human Wharton's jelly stem cells have unique transcriptome profiles compared to human embryonic stem cells and other mesenchymal stem cells. Stem Cell Rev, 2011; 7(1):1-16.

Friedlaender GE, Strong DM, Tomford WW, Mankin HJ. Long-term follow-up of patients with osteochondral allografts. A correlation between immunologic responses and clinical outcome. Orthop Clin North Am, 1999; 30(4):583-8.

Friedenstein AJ, Chailakhyan RK, Latsinik NV, Panasyuk AF, Keiliss-Borok IV. Stromal cells responsible for transferring the microenvironment of the hemopoietic tissues. Cloning in vitro and retransplantation in vivo. Transplantation, 1974; 17(4):331-40.

Freed LE, Marquis JC, Nohria A, Emmanual J, Mikos AG, Langer R. Neocartilage formation in vitro and in vivo using cells cultured on synthetic biodegradable polymers. J Biomed Mater Res, 1993; 27(1):11-23.

Freda MC, Kearney M. The role of peer review for scholarly journals in the information age. J Nurs Scholarsh, 2005; 37(1):87-94.

Ganji F, Vasheghani-Farahani S, Vasheghani-Farahani E. Theoretical description of hydrogel swelling: a review. Iranian Polymer Journal, 2010; 19 (5):375-398.

Gao P, Han P, Jiang D, Yang S, Cui Q, Li Z. Effects of the donor age on proliferation, senescence and osteogenic capacity of human urine-derived stem cells. Cytotechnology, 2017 Apr 13.

Ge W, Jiang J, Arp J, Liu W, Garcia B, Wang H. Regulatory T-cell generation and kidney allograft tolerance induced by mesenchymal stem cells associated with indoleamine 2, 3-dioxygenase expression. Transplantation, 2010; 90(12):1312-20.

Getgood AM, Kew SJ, Brooks R, Aberman H, Simon T, Lynn AK, Rushton N. Evaluation of early-stage osteochondral defect repair using a biphasic scaffold based on a collagen-glycosaminoglycan biopolymer in a caprine model. Knee, 2012; 19(4):422-30.

Glennie S, Soeiro I, Dyson PJ, Lam EW, Dazzi F. Bone marrow mesenchymal stem cells induce division arrest anergy of activated T cells. Blood, 2005; 105(7):2821-7.

Gibas I, Janik H, Stràńkowski M, Panzarini E, Dini L. Poly (alkymide) and poly (vinil alcohol) medical hydrogels—testing with U937. Cell Linechem Chem Technol, 2009.

Gómez-Leduc T, Hervieu M, Legendre F, Bouyoucef M, Gruchy N, Poulain L, de Vienne C, Herlicoviez M, Demoor M, Galéra P. Chondrogenic commitment of human umbilical cord blood-derived mesenchymal stem cells in collagen matrices for cartilage engineering. Sci Rep, 2016; 6:32786.

Gong JP, Katsuyama Y, Kurokawa T, Osada Y. Double-Network Hydrogels with Extremely High Mechanical Strength. Adv mater, 2003; 15(14): 1155-1158.

González-Díaz EC, Varghese S. Hydrogels as Extracellular Matrix Analogs. Gels, 2016; 2(3): 20.

Gomoll AH, Madry H, Knutsen G, van Dijk N, Seil R, Brittberg M, Kon E. The subchondral bone in articular cartilage repair: current problems in the surgical management. Knee Surg Sports Traumatol Arthrosc, 2010; 18(4):434-47.

Goyal D, Keyhani S, Lee EH, Hui JH. Evidence-based status of microfracture technique: a systematic review of level I and II studies. Arthroscopy, 2013; 29:1579-1588.

Grassel S, Ahmed N. Influence of cellular microenvironment and paracrine signals on chondrogenic differentiation. Front Biosci, 2007; 12:4946-56.

Grodzinsky AJ, Levenston ME, Jin M, Frank EH. Cartilage tissue remodeling in resopnse to mechanical forces. Ann Rev Biomed Eng, 2000; 2:691-713.

Gigant-Huselstein C, Hubert P, Dumas D, Dellacherie E, Netter P, Payan E, Stoltz JF. Expression of adhesion molecules and collagen on rat chondrocyte seeded into alginate and hyaluronate based 3D biosystems. Influence of mechanical stresses. Biorheology, 2004; 41(3-4):423-31.

Haraguchi K, Takehisa T. Nanocomposite hydrogels: a unique organic-inorganic network structure with extraordinary mechanical, optical, and swelling/de-swelling properties. Adv mater, 2002; 14(16):1120-1123.

Hambach L, Neureiter D, Zeiler G, Kirchner T, Aigner T. Severe disturbance of the distribution and expression of type VI collagen chains in osteoarthritic articular cartilage. Arthritis Rheum, 1998; 41(6):986-96.

Heng BC, Cao T, Lee EH. Directing stem cell differentiation into the chondrogenic lineage in vitro. Stem Cells, 2004; 22(7):1152-67.

Heymer A, Bradica G, Eulert J, Nöth U. Multiphasic collagen fibre–PLA composites seeded with human mesenchymal stem cells for osteochondral defect repair: an in vitro study. J Tissue Eng Regen Med, 2009; 3(5):389-97.

Highley CB, Prestwich GD, Burdick JA. Recent advances in hyaluronic acid hydrogels for biomedical applications. Curr Opin Biotechnol, 2016; 40:35-40.

Hiemenz PC, Lodge TP. Polymer chemistry, Book. 2007.

Holme HK, Davidsen L, Kristiansen A, Smidsrød O. Kinetics and mechanisms of depolymerization of alginate and chitosan in aqueous solution. Carbohydr Polym, 2008; 73(4):656-64.

Holme HK, Lindmo K, Kristiansen A, Smidsrød O. Thermal depolymerization of alginate in the solid state. Carbohydr Polym, 2003; 54(4):431-438.

Hutmacher DW. Scaffolds in tissue engineering bone and cartilage. Biomaterials, 2000; 21(24):2529-2543.

Huebsch N, Gilbert M, Healy KE. Analysis of sterilization protocols for peptide-modified hydrogels. J Biomed Mater Res B Appl Biomater, 2005; 74(1):440-7.

Hu T, Yang Y, Tan L, Yin T, Wang Y, Wang G. Effects of gamma irradiation and moist heat for sterilization on sodium alginate. Biomed Mater Eng, 2014; 24(5):1837-49.

Ingber DE. Cellular mechanotransduction: putting all the pieces together again. The FASEB journal, 2006; 20(7):811-827.

Isakson M, de Blacam C, Whelan D, McArdle A, Clover AJ. Mesenchymal Stem Cells and Cutaneous Wound Healing: Current Evidence and Future Potential. Stem Cells Int, 2015;831095.

Jakobsen RB, Shahdadfar A, Reinholt FP, Brinchmann JE. Chondrogenesis in a hyaluronic acid scaffold: comparison between chondrocytes and MSC from bone marrow and adipose tissue. Knee Surg Sports Traumatol Arthrosc. 2010; 18(10):1407-16.

Jarvinen L, Badri L, Wettlaufer S, Ohtsuka T, Standiford TJ, Toews GB, Pinsky DJ, Peters-Golden M, Lama VN. Lung resident mesenchymal stem cells isolated from human lung allografts inhibit T cell proliferation via a soluble mediator. J Immunol, 2008; 181(6):4389-96.

Jadalannagari S, Aljitawi OS. Ectodermal Differentiation of Wharton's Jelly Mesenchymal Stem Cells for Tissue Engineering and Regenerative Medicine Applications. Tissue Eng Part B Rev, 2015; 21(3):314-22.

Jessica Tritz, Rachid Rahouadj, Natalia de Isla, Naceur Charif, Astrid Pinzano, Didier Mainard, Danielle Bensoussan, Patrick Netter, Jean-François Stoltz, Nadia Benkirane-Jessel and Céline Huselstein. Designing a three-dimensional alginate hydrogel by spraying method for cartilage tissue engineering. Soft matter, 2010; 6:5165-5174.

Jiang Y, Tuan RS. Origin and function of cartilage stem/progenitor cells in osteoarthritis. Nat Rev Rheumatol, 2015; 11(4):206-12.

Jyothi Prasanna S, Sowmya Jahnavi V. Wharton's Jelly Mesenchymal Stem Cells as Off-The-Shelf Cellular Therapeutics: A Closer Look into their Regenerative and Immunomodulatory Properties. The Open Tissue Engineering and Regenerative Medicine Journal, 2011; 4:28-38.

Kamoun EA, Chen X, Mohy Eldin MS, Kenawy ES, Crosslinked poly (vinyl alcohol) hydrogels for wound dressing applications: A review of remarkably blended polymers. Arabian Journal of Chemistry, 2015; 8(1):1-14.

Kamoun EA, Kenawy ES, Tamer TM, EL-Meligy MA, Mohy Eldin MS. Poly (vinyl alcohol)-alginate physically crosslinked hydrogel membranes for wound dressing applications: characterization and bio-evaluation. Arabian Journal of Chemistry, 2015; 8(1):38-47.

Karajanagi SS, Yoganathan R, Mammucari R, Park H, Cox J, Zeitels SM, Langer R, Foster NR. Application of a dense gas technique for sterilizing soft biomaterials. Biotechnol Bioeng, 2011; 108(7):1716-25.

Kalaszczynska I, Ferdyn K. Wharton's jelly derived mesenchymal stem cells: future of regenerative medicine? Recent findings and clinical significance. Biomed Res Int, 2015:430847.

Kanjickal D, Lopina S, Evancho-Chapman MM, Schmidt S, Donovan D. Effects of sterilization on poly (ethylene glycol) hydrogels. J Biomed Mater Res A, 2008; 87(3):608-17.

Katsara O, Mahaira LG, Iliopoulou EG, Moustaki A, Antsaklis A, Loutradis D, Stefanidis K, Baxevanis CN, Papamichail M, Perez SA. Effects of donor age, gender, and in vitro cellular aging on the phenotypic, functional, and molecular characteristics of mouse bone marrow-derived mesenchymal stem cells. Stem Cells Dev, 2011; 20(9):1549-61.

Khetan S, Guvendiren M, Legant W.R., Cohen DM, Chen CS, Burdick JA. Degradation-mediated cellular traction directs stem cell fate in covalently crosslinked three-dimensional hydrogels. Nat Mater, 2013; 12(5):458-65.

Kircher J, Patzer T, Magosch P, Lichtenberg S, Habermeyer P. Osteochondral autologous transplantation for the treatment of full-thickness cartilage defects of the shoulder. J Bone Joint Surg Br, 2009; 91(4):499-503.

Kim YS, Park EH, Kim YC, Koh YG, Lee JW. Factors associated with the clinical outcomes of the osteochondral autograft transfer system in osteochondral lesions of the talus second-look arthroscopic evaluation. Am J Sports Med, 2012; 40(12):2709-19.

Kim YS, Park EH, Lee HJ, Koh YG, Lee JW. Clinical comparison of the osteochondral autograft transfer system and subchondral drilling in osteochondral defects of the first metatarsal head. Am J Sports Med, 2012; 40(8):1824-33.

Kim IL, Mauck RL, Burdick JA. Hydrogel design for cartilage tissue engineering: a case study with hyaluronic acid. Biomaterials, 2011; 32(34):8771-82.

Kirchhof S, Goepferich AM, Brandl FP. Hydrogels in ophthalmic applications. European Journal of Pharmaceutics and Biopharmaceutics, 2015; 25:227-238.

Kircher J, Patzer T, Magosch P, Lichtenberg S, Habermeyer P. Osteochondral autologous transplantation for the treatment of full-thickness cartilage defects of the shoulder. J Bone Joint Surg Br, 2009; 91(4):499-503.

Kim TK, Sharma B, Williams CG, Ruffner MA, Malik A, McFarland EG, Elisseeff JH. Experimental model for cartilage tissue engineering to regenerate the zonal organization of articular cartilage. Osteoarthritis Cartilage, 2003; 11(9):653-64.

Klein TJ, Rizzi SC, Reichert JC, Georgi N, Malda J, Schuurman W, Crawford RW, Hutmacher DW. Strategies for zonal cartilage repair using hydrogels. Macromol Biosci, 2009; 9(11):1049-58.

Klein TJ, Malda J, Sah RL, Hutmacher DW. Tissue engineering of articular cartilage with biomimetic zones. Tissue Eng Part B Rev, 2009; 15(2):143-57.

Klein TJ, Schumacher BL, Schmidt TA, Li KW, Voegtline MS, Masuda K, Thonar EJ, Sah RL. Tissue engineering of stratified articular cartilage from chondrocyte subpopulations. Osteoarthritis Cartilage, 2003; 11(8):595-602.

Kloxin AM, Benton JA, Anseth KS. In situ elasticity modulation with dynamic substrates to direct cell phenotype. Biomaterials, 2010; 31(1):1-8.

Kloxin AM, Kloxin CJ, Bowman CN, Anseth KS. Mechanical properties of cellularly responsive hydrogels and their experimental determination. Adv Mater, 2010; 22(31):3484-94.

Kloxin AM, Tibbitt MW, Kasko AM, Fairbairn JA, Anseth KS. Tunable hydrogels for external manipulation of cellular microenvironments through controlled photodegradation. Adv Mater, 2010; 22(1):61-6.

Kloxin AM, Kasko AM, Salinas CN, Anseth KS. Photodegradable hydrogels for dynamic tuning of physical and chemical properties. Science, 2009; 324(5923):59-63.

Klanl C, Chen LW, Wu YJ, Albert JY, Burton BY. Structure and function of aggrecan. Cell Research, 2002; 12, 19-32.

Knudson C.B., Knudson W. Hyaluronan and CD44: modulators of chondrocyte metabolism. Clin Orthop Relat Res, 2004; (427 Suppl):S152-62.

Knight MM, Ross JM, Sherwin AF, Lee DA, Bader DL, Poole CA. Chondrocyte deformation within mechanically and enzymatically extracted chondrons compressed in agarose. Biochim Biophys Acta, 2001; 1526(2):141-6.

La Rocca G, Anzalone R, Corrao S, Magno F, Loria T, Lo Iacono M, Di Stefano A, Giannuzzi P, Marasà L, Cappello F, Zummo G, Farina F. Isolation and characterization of Oct-4+/HLA-G+ mesenchymal stem cells from human umbilical cord matrix: differentiation potential and detection of new markers. Histochem Cell Biol, 2009; 131(2):267-82.

La Rocca G, Lo Iacono M, Corsello T, Corrao S, Farina F, Anzalone R. Human Wharton's Jelly Mesenchymal Stem Cells Maintain the Expression of Key Immunomodulatory Molecules When Subjected to Osteogenic, Adipogenic and Chondrogenic Differentiation In Vitro: New Perspectives for Cellular Therapy. Curr Stem Cell Res Ther, 2013; 8(1):100-13.

Lee KY, Shim J, Lee HG. Mechanical properties of gellan and gelatin composite films. Carbohydrate Polymers, 2004; 56(2):251-254.

Lee KY, Mooney DJ. Alginate: properties and biomedical applications. Progress in Polymer Science, 2012; 37(1):106-126.

Leo WJ, McLoughlin AJ, Malone DM. Effects of sterilization treatments on some properties of alginate solutions and gels. Biotechnol Prog, 1990; 6(1):51-3.

Lee DW, Choi WS, Byun MW, Park HJ, Yu YM, Lee CM. Effect of gamma-irradiation on degradation of alginate. J Agric Food Chem, 2003; 51(16), 4819–4823.

Lefebvre V, Smits P. Transcriptional control of chondrocyte fate and differentiation. Birth Defects Res C Embryo Today, 2005; 75(3):200-12.

Li Y, Qu YH, Wu YF, Liu L, Lin XH, Huang K, Wei J. Bone marrow mesenchymal stem cells suppressing activation of allogeneic cytokine-induced killer/natural killer cells either by direct or indirect interaction. Cell Biol Int, 2015; 39(4):435-45.

Liu S, Hou KD, Yuan M, Peng J, Zhang L, Sui X, Zhao B, Xu W, Wang A, Lu S, Guo Q. Characteristics of mesenchymal stem cells derived from Wharton's jelly of human umbilical cord and for fabrication of non-scaffold tissue-engineered cartilage. J Biosci Bioeng, 2014; 117(2):229-35.

Liu Y, Chen F, Liu W, Cui L, Shang Q, Xia W, Wang J, Cui Y, Yang G, Liu D, Wu J, Xu R, Buonocore SD, Cao Y. Repairing large porcine full-thickness defects of articular cartilage using autologous chondrocyte-engineered cartilage. Tissue Eng, 2002; 8(4):709-21.

Liu M, Yu X, Huang F, Cen S, Zhong G, Xiang Z. Tissue engineering stratified scaffolds for articular cartilage and subchondral bone defects repair. Orthopedics, 2013; 36(11):868-73.

Liu S, Yuan M, Hou K, Zhang L, Zheng X, Zhao B, Sui X, Xu W, Lu S, Guo Q. Immune characterization of mesenchymal stem cells in human umbilical cord Wharton's jelly and derived cartilage cells. Cell Immunol, 2012; 278(1-2):35-44.

Lin S, Sangaj N, Razafiarison T, Zhang C, Varghese S. Influence of physical properties of biomaterials on cellular behavior. Pharm Res, 2011; 28(6):1422-30.

Lin Z, Craig W, Xu JK, Zheng MH. The chondrocyte: biology and clinical application. Tissue Eng, 2006; 12(7): 1971-1984.

Lu L, Zhu X, Valenzuela RG, Currier BL, Yaszemski MJ. Biodegradable polymer scaffolds for cartilage tissue engineering. Clin Orthop Relat Res, 2001; (391 Suppl):S251-70.

Lopa S, Madry H. Bioinspired scaffolds for osteochondral regeneration. Tissue Engineering Part A, 2014; 20(15-16): 2052-2076.

Lories RJ, Luyten FP. The bone-cartilage unit in osteoarthritis. Nat Rev Rheumatol, 2011; 7(1):43-9.

Lo CM, Wang HB, Dembo M, Wang YL. Cell movement is guided by the rigidity of the substrate. Biophys J, 2000; 79(1):144-52.

Lories RJ, Luyten FP. The bone-cartilage unit in osteoarthritis. Nat Rev Rheumatol, 2011; 7(1):43-9.

Lyons TJ, McClure SF, Stoddart RW, McClure J. The normal human chondro-osseous junctional region: evidence for contact of uncalcified cartilage with subchondral bone and marrow spaces. BMC Musculoskelet Disord, 2006; 7:52.

Ma S, Xie N, Li W, Yuan B, Shi Y, Wang Y. Immunobiology of mesenchymal stem cells. Cell Death and Differentiation, 2014; 21, 216–225.

Madry H, Grün UW, Knutsen G. Cartilage repair and joint preservation medical and surgical treatment options. Dtsch Arztebl Int, 2011; 108(40):669-77.

Madry H, van Dijk CN, Mueller-Gerbl M. The basic science of the subchondral bone. Knee Surg Sports Traumatol Arthrosc, 2010; 18(4):419-33.

Maroudas A, Bayliss MT, Uchitel-Kaushansky N, Schneiderman R, Gilav E. Aggrecan turnover in human articular cartilage: use of aspartic acid racemization as a marker of molecular age. Arch Biochem Biophys, 1998; 350(1):61-71.

Mao S, Zhang T, Sun W, Ren X. The depolymerization of sodium alginate by oxidative degradation. Pharm Dev Technol, 2012; 17(6):763-9.

Marklein RA, Burdick JA. Spatially controlled hydrogel mechanics to modulate stem cell interactions. Soft Matter, 2010; 6:136-143.

Marmorat C, Arinstein A, Koifman N, Talmon Y, Zussman E, Rafailovich M. Cryo-imaging of hydrogels supermolecular structure. Sci Rep, 2016; 6:25495.

Ma HL, Hung SC, Lin SY, Chen YL, Lo WH. Chondrogenesis of human mesenchymal stem cells encapsulated in alginate beads. J Biomed Mater Res A, 2003; 64(2):273-81.

Marc Farine. Instrumented Indentation of Soft Materials and Biological Tissues. ETH Zurich, PhD Thesis, 2013.

McBeath R, Pirone DM, Nelson CM, Bhadriraju K, Chen CS. Cell shape, cytoskeletal tension, and RhoA regulate stem cell lineage commitment. Dev Cell, 2004; 6(4):483-95.

McAlinden A, Zhu Y, Sandell LJ. Expression of type II procollagens during development of the human intervertebral disc. Biochem Soc Trans, 2002; 30(Pt 6):831-8.

McGuirk JP, Weiss ML. Promising cellular therapeutics for prevention or management of graft-versus-host disease (a review). Placenta, 2011; 32 Suppl 4:S304-10.

Merino JC, Martin B, Pastor JM. Mechanical indentation tester designed to control and measure in real time the microhardness process. Meas Sci Technol, 1991; 2:740.

Michigami T. Current understanding on the molecular basis of chondrogenesis. Clin Pediatr Endocrinol, 2014; 23(1):1-8.

Mouw JK, Case ND, Guldberg RE, Plaas AH, Levenston ME. Variations in matrix composition and GAG fine structure among scaffolds for cartilage tissue engineering. Osteoarthritis Cartilage, 2005; 13(9):828-36.

Muzzarelli RA, Greco F, Busilacchi A, Sollazzo V, Gigante A. Chitosan, hyaluronan and chondroitin sulfate in tissue engineering for cartilage regeneration: a review. Carbohydr Polym, 2012; 89(3):723-39.

Nauta AJ, Fibbe WE. Immunomodulatory properties of mesenchymal stromal cells. Blood, 2007; 110:3499–506.

Naji A, Rouas-Freiss N, Durrbach A, Carosella ED, Sensébé L, Deschaseaux F. Concise review: combining human leukocyte antigen G and mesenchymal stem cells for immunosuppressant biotherapy. Stem Cells, 2013; 31(11):2296-303.

Najib El Haddad. Mesenchymal stem cells: immunology and therapeutic benefits. Stem Cells in Clinic and Research, 2011; P60-81.

Nehrer S, Dorotka R, Domayer S, Stelzeneder D, Kotz R. Treatment of full-thickness chondral defects with hyalograft C in the knee: a prospective clinical case series with 2 to 7 years' follow-up. Am J Sports Med, 2009; 37 Suppl 1:81S-87S.

Nekanti U, Rao VB, Bahirvani AG, Jan M, Totey S, Ta M. Long-term expansion and pluripotent marker array analysis of Wharton's jelly-derived mesenchymal stem cells. Stem Cells Dev, 2010; 19(1):117-30.

Nejadnik H, Diecke S, Lenkov OD, Chapelin F, Donig J, Tong X, Derugin N, Chan R.C., Gaur A, Yang F, Wu JC, Daldrup-Link HE. Improved approach for chondrogenic differentiation of human induced pluripotent stem cells. Stem Cell Rev, 2015; 11(2):242-53.

Nooeaid P, Salih V, Beier JP, Boccaccini AR. Osteochondral tissue engineering: scaffolds, stem cells and applications. J Cell Mol Med, 2012; 16(10):2247-70.

Oliveira JM, Rodrigues MT, Silva SS, Malafaya PB, Gomes ME, Viegas CA, Dias IR, Azevedo JT, Mano JF, Reis RL. Novel hydroxyapatite/chitosan bilayered scaffold for osteochondral tissue-engineering applications: Scaffold design and its performance when seeded with goat bone marrow stromal cells. Biomaterials, 2006; 27(36):6123-37.

Olderøy MØ, Lilledahl MB, Beckwith MS, Melvik JE, Reinholt F, Sikorski P, Brinchmann JE. Biochemical and structural characterization of neocartilage formed by mesenchymal stem cells in alginate hydrogels. PLoS One, 2014; 9(3):e91662.

Omidian H, Park K. Hydrogel. Fundamentals and application of controlled release drug delivery. Part of the series advances in deliver science and technology, pp75-105.

Orth P, Rey-Rico A, Venkatesan JK, Madry H, Cucchiarini M. Current perspectives in stem cell research for knee cartilage repair. Stem Cells Cloning, 2014; 7:1-17.

Oyen ML. Mechanical characterisation of hydrogel materials. J international materials reviews, 2013; 59(1):44-59.

Pawar SN, Edgar KJ. Alginate derivatization: A review of chemistry, properties and applications. Biomaterials, 2012; 33(11):3279-305.

Park JS, Suryaprakash S, Lao YH, Leong KW. Engineering mesenchymal stem cells for regenerative medicine and drug delivery. Methods, 2015; 84:3-16.

Park H, Kim D, Lee KY. Interaction-tailored cell aggregates in alginate hydrogels for enhanced chondrogenic differentiation. J Biomed Mater Res A, 2017; 105(1):42-50.

Panseri S, Russo A, Cunha C, Bondi A, Di Martino A, Patella S, Kon E. Osteochondral tissue engineering approaches for articular cartilage and subchondral bone regeneration. Knee Surg Sports Traumatol Arthrosc, 2012; 20(6):1182-91.

Perka C, Spitzer RS, Lindenhayn K, Sittinger M, Schultz O. Matrix-mixed culture: new methodology for chondrocyte culture and preparation of cartilage transplants. J Biomed Mater Res, 2000; 49(3):305-11.

Pelham RJ Jr, Wang Y. Cell locomotion and focal adhesions are regulated by substrate flexibility. Proc Natl Acad Sci USA, 1997; 94(25):13661-5.

Peyton SR, Putnam AJ. Extracellular matrix rigidity governs smooth muscle cell motility in a biphasic fashion. J Cell Physiol, 2005; 204(1):198-209.

Poinern GE, Brundavanam RK, Mondinos N, Jiang ZT. Synthesis and characterisation of nanohydroxyapatite using an ultrasound assisted method. Ultrason Sonochem, 2009; 16(4):469-74.

Pomin VH, Mourão PA. Specific sulfation and glycosylation-a structural combination for the anticoagulation of marine carbohydrates. Front Cell Infect Microbiol, 2014; 4:33.

Poole CA, Ayad S, Gilbert RT. Chondrons from articular cartilage V Immunohistochemical evaluation of type VI collagen organisation in isolated chondrons by light, confocal and electron microscopy. J Cell Sci. 1992; 103 (Pt 4):1101-10.

Plumas J, Chaperot L, Richard MJ, Molens JP, Bensa JC, Favrot MC. Mesenchymal stem cells induce apoptosis of activated T cells. Leukemia, 2005; 19(9):1597-604.

Puppi D, Chiellini F, Piras AM, Chiellini E. Polymeric materials for bone and cartilage repair. 2010; 35(4)403-440.

Ramasamy R, Fazekasova H, Lam EW, Soeiro I, Lombardi G, Dazzi F. Mesenchymal stem cells inhibit dendritic cell differentiation and function by preventing entry into the cell cycle. Transplantation, 2007; 83(1):71-6.

Raghunath J, Rollo J, Sales KM, Butler PE, Seifalian AM. Biomaterials and scaffold design: key to tissue-engineering cartilage. Biotechnol Appl Biochem, 2007; 46(Pt 2):73-84.

Rajaram A, Chen XB, Schreyer DJ. Strategic design and recent fabrication techniques for bioengineered tissue scaffolds to improve peripheral nerve regeneration. Tissue Eng Part B Rev, 2012; 18(6):454-67.

Reis CP, Neufeld RJ, Vilela S, Ribeiro AJ, Veiga F. Review and current status of emulsion/dispersion technology using an internal gelation process for the design of alginate particles. J Microencapsul, 2006; 23(3):245-57.

Rennerfeldt DA, Renth AN, Talata Z, Gehrke SH, Detamore MS. Tuning mechanical performance of poly (ethylene glycol) and agarose interpenetrating network hydrogels for cartilage tissue engineering. Biomaterials, 2013; 34(33):8241-57.

Reppel L, Schiavi J, Charif N, Leger L, Yu H, Pinzano A, Henrionnet C, Stoltz JF, Bensoussan D, Huselstein C. Chondrogenic induction of mesenchymal stromal/stem cells from Wharton's jelly embedded in alginate hydrogel and without added growth factor: an alternative stem cell source for cartilage tissue engineering. Stem Cell Res Ther, 2015; 6:260.

Román J, Cabañas M.V., Peña J, Vallet-Regí M. Control of the pore architecture in three-dimensional hydroxyapatite-reinforced hydrogel scaffolds. Sci Technol Adv Mater, 2011; 12(4):045003.

Risbud M, Ringe J, Bhonde R, Sittinger M. In vitro expression of cartilage-specific markers by chondrocytes on a biocompatible hydrogel: implications for engineering cartilage tissue. Cell Transplant, 2001; 10(8):755-63.

Rnjak-Kovacina J, DesRochers TM, Burke KA, Kaplan DL. The effect of sterilization on silk fibroin biomaterial properties. Macromol Biosci, 2015; 15(6):861-74.

Ryan MC, Sieraski M, Sandell LJ. The human type II procollagen gene: identification of an additional protein-coding domain and location of potential regulatory sequences in the promoter and first. Genomics, 1990; 8(1):41-8.

Sandell LJ, Sugai JV, Trippel SB. Expression of collagens I, II, X, and XI and aggrecan mRNAs by bovine growth plate chondrocytes in situ. J Orthop Res, 1994; 12(1):1-14.

Sakaguchi Y, Sekiya I, Yagishita K, Muneta T. Comparison of human stem cells derived from various mesenchymal tissues: superiority of synovium as a cell source. Arthritis Rheum, 2005; 52(8):2521-9.

Sechriest VF, Miao YJ, Niyibizi C, Westerhausen-Larson A, Matthew HW, Evans CH, Fu FH, Suh JK. GAG-augmented polysaccharide hydrogel: a novel biocompatible and biodegradable material to support chondrogenesis. J Biomed Mater Res, 2000; 49(4):534-41.

Sengers BG, Heywood HK, Lee DA, Oomens CW, Bader DL. Nutrient utilization by bovine articular chondrocytes: a combined experimental and theoretical approach. J Biomech Eng, 2005; 127(5):758-66.

Seibel MJ, Robins SP, Bilezikian JP. Dynamics of bone and cartilage metabolism: principles and clinical applications. Book, 2006.

Selmani Z, Naji A, Zidi I, Favier B, Gaiffe E, Obert L, Borg C, Saas P, Tiberghien P, Rouas-Freiss N, Carosella ED, Deschaseaux F. Human leukocyte antigen-G5 secretion by human mesenchymal stem cells is required to suppress T lymphocyte and natural killer function and to induce CD4+CD25highFOXP3+ regulatory T cells. Stem Cells, 2008; 26(1):212-22.

Selmani Z, Naji A, Gaiffe E, Obert L, Tiberghien P, Rouas-Freiss N, Carosella ED, Deschaseaux F. HLA-G is a crucial immunosuppressive molecule secreted by adult human mesenchymal stem cells. Transplantation, 2009; 87(9 Suppl):S62-6.

Schulz RM, Bader A. Cartilage tissue engineering and bioreactor systems for the cultivation and stimulation of chondrocytes. Eur Biophys J, 2007; 36(4-5):539-68.

Schiavi J, Reppel L, Charif N, de Isla N, Mainard D, Benkirane-Jessel N, Stoltz JF, Rahouadj R, Huselstein C. Mechanical stimulations on human Bone Marrow Mesenchymal Stem Cells enhance cells differentiation in a 3D layered scaffold. J Tissue Eng Regen Med, 2017 May 9.

Siclari A, Mascaro G, Gentili C, Cancedda R, Boux E. A cell-free scaffold-based cartilage repair provides improved function hyaline-like repair at one year. Clin Orthop Relat Res, 2012; 470(3):910-9.

Sivan SS, Wachtel E, Roughley P. Structure, function, aging and turnover of aggrecan in the intervertebral disc. Biochim Biophys Acta, 2014; 1840(10):3181-9.

Stoppel WL, White JC, Horava SD, Henry AC, Roberts SC, Bhatia SR. Terminal sterilization of alginate hydrogels: efficacy and impact on mechanical properties. J Biomed Mater Res B Appl Biomater, 2014; 102(4):877-84.

Sun J, Tan H. Alginate-based biomaterials for regenerative medicine applications. Materials, 2013; 6(4), 1285-1309.

Sun JY, Zhao X, Illeperuma WR, Chaudhuri O, Oh KH, Mooney DJ, Vlassak JJ, Suo Z. Highly stretchable and tough hydrogels. Nature, 2012; 489(7414):133-6.

Solomn DJ, Warren RE. Marrow stimulation and microfracture for the repair of articular cartilage lesions. Cartilage Repair Strategies, 2007 pp 69-84.

Shohara R, Yamamoto A, Takikawa S, Iwase A, Hibi H, Kikkawa F, Ueda M. Mesenchymal stromal cells of human umbilical cord Wharton's jelly accelerate wound healing by paracrine mechanisms. Cytotherapy, 2012; 14(10):1171-81.

Takahashi K, Tanabe K, Ohnuki M, Narita M, Ichisaka T, Tomoda K, Yamanaka S. Induction of pluripotent stem cells from adult human fibroblasts by defined factors. Cell, 2007; 131(5):861-72.

Tautzenberger A, Kovtun A, Ignatius A. Nanoparticles and their potential for application in bone. Int J Nanomedicine, 2012; 7:4545-4557.

Tamamura Y, Otani T, Kanatani N, Koyama E, Kitagaki J, Komori T, Yamada Y, Costantini F, Wakisaka S, Pacifici M, Iwamoto M, Enomoto-Iwamoto M. Developmental regulation of Wnt/β-catenin signals is required for growth plate assembly, cartilage integrity, and endochondral ossification. J Biol Chem, 2005; 280(19):19185-95.

Tan H, Marra KG. Injectable, biodegradable hydrogels for tissue engineering applications. Materials, 2010; 3(3): 1746-1767.

Thomson JA, Itskovitz-Eldor J, Shapiro SS, Waknitz MA, Swiergiel JJ, Marshall VS, Jones JM. Embryonic stem cell lines derived from human blastocysts. Science, 1998; 282(5395):1827.

Thorpe AA, Creasey S, Sammon C, Le Maitre CL. Hydroxyapatite nanoparticle injectable hydrogel scaffold to support osteogenic differentiation of human mesenchymal stem cells. Eur Cell Mater, 2016; 32:1-23.

Toh WS, Lee EH, Guo XM, Chan JK, Yeow CH, Choo AB, Cao T. Cartilage repair using hyaluronan hydrogel-encapsulated human embryonic stem cell-derived chondrogenic cells. Biomaterials, 2010; 31(27):6968-80.

Toh WS, Yang Z, Liu H, Heng BC, Lee EH, Cao T. Effects of culture conditions and bone morphogenetic protein 2 on extent of chondrogenesis from human embryonic stem cells. Stem Cells, 2007; 25(4):950-60.

Toh WS, Lee EH, Cao T. Potential of human embryonic stem cells in cartilage tissue engineering and regenerative medicine. Stem Cell Rev, 2011; 7(3):544-59.

Tohfafarosh M, Baykal D, Kiel JW, Mansmann K, Kurtz SM. Effects of gamma and e-beam sterilization on the chemical, mechanical and tribological properties of a novel hydrogel. J Mech Behav Biomed Mater, 2016; 53:250-6.

Tritz-Schiavi J, Charif N, Henrionnet C, de Isla N, Bensoussan D, Magdalou J, Benkirane-Jessel N, Stoltz J.F., Huselstein C. Original approach for cartilage tissue engineering with mesenchymal stem cells. Biomed Mater Eng, 2010; 20(3):167-74.

Troyer DL, Weiss ML. Wharton's jelly-derived cells are a primitive stromal cell population. Stem Cells, 2008; 26(3):591-9.

Tisato V, Naresh K, Girdlestone J, Navarrete C, Dazzi F. Mesenchymal stem cells of cord blood origin are effective at preventing but not treating graft-versus-host disease. Leukemia. 2007; 21(9):1992-9.

Uccelli A, Moretta L, Pistoia V. Immunoregulatory function of mesenchymal stem cells. Eur J Immunol, 2006; 36:2566–2573.

Uematsu K, Hattori K, Ishimoto Y, Yamauchi J, Habata T, Takakura Y, Ohgushi H, Fukuchi T, Sato M. Cartilage regeneration using mesenchymal stem cells and a three-dimensional poly-lactic-glycolic acid (PLGA) scaffold. Biomaterials, 2005; 26(20):4273-9.

Urist MR, Nogami H, Mikulski A. A bone morphogenetic polypeptide. Calcif Tissue Res, 1976; 21 Suppl: 81-7.

Vats A, Bielby RC, Tolley N, Dickinson SC, Boccaccini AR, Hollander AP, Bishop AE, Polak JM. Chondrogenic differentiation of human embryonic stem cells: the effect of the micro-environment. Tissue Eng, 2006; 12(6):1687-97.

Valiyaveettil M, Achur RN, Muthusamy A, Gowda DC. Characterization of chondroitin sulfate and dermatan sulfate proteoglycans of extracellular matrices of human umbilical cord blood vessels and Wharton's jelly. Glycoconj J, 2004; 21(6):361-75.

Van Vlierberghe S, Dubruel P, Schacht E. Biopolymer-based hydrogels as scaffolds for tissue engineering applications: a review. Biomacromolecules, 2011; 12(5):1387-408.

Vellasamy S, Tong CK, Azhar NA, Kodiappan R, Chan SC, Veerakumarasivam A, Ramasamy R. Human mesenchymal stromal cells modulate T-cell immune response via transcriptomic regulation. Cytotherapy, 2016; 18(10):1270-83.

Vinatier C, Mrugala D, Jorgensen C, Guicheux J, Noël D. Cartilage engineering: a crucial combination of cells, biomaterials and biofactors. Trends Biotechnol, 2009; 27(5):307-14.

Volpi N, Schiller J, Stern R, Soltés L. Role, metabolism, chemical modifications and applications of hyaluronan. Curr Med Chem, 2009; 16(14):1718-45.

Wan LQ, Jiang J, Arnold DE, Guo XE, Lu HH, Mow VC. Calcium Concentration Effects on the Mechanical and Biochemical Properties of Chondrocyte-Alginate Constructs. Cell Mol Bioeng, 2008; 1(1):93-102.

Wang F, Ying Z, Duan X, Tan H, Yang B, Guo L, Chen G, Dai G, Ma Z, Yang L. Histomorphometric analysis of adult articular calcified cartilage zone. J Struct Biol, 2009; 168(3):359-65.

Wang Y, Zhang Z, Chi Y, Zhang Q, Xu F, Yang Z, Meng L, Yang S, Yan S, Mao A, Zhang J, Yang Y, Wang S, Cui J, Liang L, Ji Y, Han ZB, Fang X, Han ZC. Long-term cultured mesenchymal stem cells frequently develop genomic mutations but do not undergo malignant transformation. Cell Death Dis, 2013; 4:e950.

Wang Y, Meng H, Yuan X, Peng J, Guo Q, Lu S, Wang A. Fabrication and in vitro evaluation of an articular cartilage extracellular matrix-hydroxyapatite bilayered scaffold with low permeability for interface tissue. Biomed Eng Online, 2014; 13:80.

Wang X, Wenk E, Zhang X, Meinel L, Vunjak-Novakovic G, Kaplan DL. Growth factor gradients via microsphere delivery in biopolymer scaffolds for osteochondral tissue engineering. J Control Release, 2009; 134(2):81-90.

Wang M, Yang Y, Yang D, Luo F, Liang W, Guo S, Xu J. The immunomodulatory activity of human umbilical cord blood-derived mesenchymal stem cells in vitro. Immunology, 2009; 126(2):220-32.

Wang CC, Yang KC, Lin KH, Liu HC, Lin FH. A highly organized three-dimensional alginate scaffold for cartilage tissue engineering prepared by microfluidic technology. Biomaterials, 2011; 32(29):7118-26.

Wasikiewicz JM, Yoshii F, Nagasawa N, Wach RA, Mitomo H. Degradation of chitosan and sodium alginate by gamma radiation, sonochemical and ultraviolet methods. Radiation Physics and Chemistry, 2005; 73(5):287-295.

Waterman RS, Tomchuck SL, Henkle SL, Betancourt AM. A new mesenchymal stem cell (MSC) paradigm: polarization into a pro-inflammatory MSC1 or an Immunosuppressive MSC2 phenotype. PLoS One, 2010; 5(4):e10088.

Weiss ML, Medicetty S, Bledsoe AR, Rachakatla RS, Choi M, Merchav S, Luo Y, Rao MS, Velagaleti G, Troyer D. Human umbilical cord matrix stem cells: preliminary characterization and effect of transplantation in a rodent model of Parkinson's disease. Stem Cells, 2006; 24(3):781-92.

Weiss ML, Anderson C, Medicetty S, Seshareddy KB, Weiss RJ, VanderWerff I, Troyer D, McIntosh KR. Immune properties of human umbilical cord Wharton's jelly-derived cells. Stem Cells, 2008; 26(11):2865-74.

Wozniak MA, Chen CS. Mechanotransduction in development: a growing role for contractility. Nat Rev Mol Cell Biol, 2009; 10(1):34-43.

Wu C, Tian B, Qu X, Liu F, Tang T, Qin A, Zhu Z, Dai K. MicroRNAs play a role in chondrogenesis and osteoarthritis (review). Int J Mol Med, 2014; 34(1):13-23.

Xue D, Zheng Q, Zong C, Li Q, Li H, Qian S, Zhang B, Yu L, Pan Z. Osteochondral repair using porous poly (lactide-co-glycolide)/nano-hydroxyapatite hybrid scaffolds with undifferentiated mesenchymal stem cells in a rat model. J Biomed Mater Res A, 2010; 94(1):259-70.

Xing L, Jiang Y, Gui J, Lu Y, Gao F, Xu Y, Xu Y. Microfracture combined with osteochondral paste implantation was more effective than microfracture alone for full-thickness cartilage repair. Knee Surg Sports Traumatol Arthrosc, 2013; 21(8):1770-6.

Yang SM, Huang S, Feng CJ, Fu XB. Umbilical cord-derived mesenchymal stem cells: strategies, challenges, and potential for cutaneous regeneration. Frontiers of Medicine, 2012; 6 (1): 41-47.

Yang B, Guo H, Zhang Y, Chen L, Ying D, Dong S. MicroRNA-145 regulates chondrogenic differentiation of mesenchymal stem cells by targeting Sox9. PLoS One, 2011; 6(7):e21679.

Yoshida CA, Komori T. Role of Runx proteins in chondrogenesis. Critical Reviews™ in Eukaryotic Gene Expression, 2005; 15(3) 243-254.

Yoo HS, Lee EA, Yoon JJ, Park TG. Hyaluronic acid modified biodegradable scaffolds for cartilage tissue engineering. Biomaterials, 2005; 26(14):1925-33.

Youn I, Choi JB, Cao L, Setton LA, Guilak F. Zonal variations in the three-dimensional morphology of the chondron measured in situ using confocal microscopy. Osteoarthritis Cartilage, 2006; 14(9):889-97.

Yuan T, Li K, Guo L, Fan H, Zhang X. Modulation of immunological properties of allogeneic mesenchymal stem cells by collagen scaffolds in cartilage tissue engineering. J Biomed Mater Res A, 2011; 98(3):332-41.

Zheng L, Fan HS, Sun J, Chen XN, Wang G, Zhang L, Fan YJ, Zhang XD. Chondrogenic differentiation of mesenchymal stem cells induced by collagen-based hydrogel: an in vivo study. J Biomed Mater Res A. 2010; 93(2):783-92.

Zhou C, Yang B, Tian Y, Jiao H, Zheng W, Wang J, Guan F. Immunomodulatory effect of human umbilical cord Wharton's jelly-derived mesenchymal stem cells on lymphocytes. Cell Immunol, 2011; 272(1):33-8.

Zhou G, Liu W, Cui L, Wang X, Liu T, Cao Y. Repair of porcine articular osteochondral defects in non-weightbearing areas with autologous bone marrow stromal cells. Tissue Eng, 2006; 12(11):3209-21.

Zhu J, Marchant RE. Design properties of hydrogel tissue-engineering scaffolds. Expert Rev Med Devices, 2011; 8(5):607-26.

Zhu Y, Wan Y, Zhang J, Yin D, Cheng W. Manufacture of layered collagen/chitosan-polycaprolactone scaffolds with biomimetic microarchitecture. Colloids Surf B Biointerfaces, 2014; 113:352-60.

Zhou H, Lee J. Nanoscale hydroxyapatite particles for bone tissue engineering. Acta Biomater, 2011; 7(7):2769-81.

Appendix

Other pubilications:

(1) Chen Li, Meng He, Zan Tong, Yinping Li, Wen Sheng, Lan Luo, Yu Tong, Hao Yu, Céline Huselstein and Yun Chen. Construction of biocompatible regenerated cellulose/SPI composite beads using high-voltage electrostatic technique. RSC Adv. 2016, 6, 52528-52538.

(2) Yu H, Li W, Liu X, Li C, Ni H, Wang X, Huselstein C, Chen Y. Improvement of functionality after chitosan-modified zein biocomposites. J Biomater Sci Polym Ed. 2017 Feb; 28(3):227-239.

Résumé

Dans le domaine de l'ingénierie du cartilage, les hydrogels à base d'alginate (Alg) et de cellules souches mésenchymateuses (CSM) sont utilisés comme biomatériaux pouvant être utilisés pour combler des lésions cartilagineuses plus ou moins profondes. Cependant, pour reproduire l'organisation zonale du cartilage, des biomatériaux multiphasiques sont nécessaires. Afin de guider la différenciation des CSM dans les différentes strates du biomatériau, sans apports de facteurs de croissance, des composants naturels du cartilage (acide hyaluronique, HA) ou de la matrice osseuse (hydroxyapatite, Hap) peuvent être ajoutés à l'alginate. L'objectif de ce travail de thèse consiste à analyser l'impact de la composition de biomatériaux à base d'alginate enrichi soit en HA soit en Hap sur le comportement des CSM. La première partie de notre travail à consister à évaluer le comportement des CSM issues de la gelée de Wharton dans ces hydrogels. Nos résultats mettent en évidence que les hydrogels d'Alg/Hap possèdent non seulement de meilleures propriétés mécaniques que les hydrogels Alg/HA et favorisent la viabilité des CSM ainsi que leur différenciation par rapport aux CSM ensemencées dans un hydrogel d'Alg/HA. La méthode de stérilisation du biomatériau représente une étape incontournable, dont on doit impérativement évaluer les multiples effets, en particulier pour ce qui touche au comportement des cellules, mais aussi au maintien de l'intégrité des propriétés physicochimiques de l'hydrogel. Ainsi, dans une seconde partie du travail, nous avons montré que le traitement de stérilisation par autoclave induisait un effet négatif sur les caractéristiques initiales de l'hydrogel à base d'alginate. Il ressort également de cette investigation sur les modes de stérilisation, que la stérilisation des hydrogels avec des UV est plus efficace et permet de préserver au mieux les propriétés spécifiques de l'hydrogel, notamment de l'Alg/HA. Enfin, dans une troisième partie de notre travail, nous avons évalué l'évolution des propriétés mécaniques au cours de la différenciation et l'impact de celles-ci sur la différenciation des CSM ainsi que sur leurs propriétés immunomodulatrices. A partir de ces résultats, nous avons montré que les caractéristiques physico-chimiques des hydrogels d'Alg/ha et Alg/hap influençaient non seulement le potentiel de différenciation des CSM-GW mais également la sécrétion des facteurs solubles impliqués dans l'immunomodulation. Ces propriétés physico-chimiques étant influencées dès le procédé de stérilisation, il est alors conseillé de les prendre en compte dans toutes les étapes de l'ingénierie tissulaire.

Mots clés: Cellules souches mésenchymateuses de la gelée de Wharton, Stérilisation, hydrogel d'alginate, Différenciation chondrocytaire, Ingénierie Tissulaire du Cartilage.

Abstract

In the field of cartilage engineering, alginate (Alg)-based hydrogels and mesenchymal stem cells (MSC) are widely used as raw biomaterials and stem cells which can be used to fill cartilage lesions of varying depth. However, to reproduce the zonal organization of articular cartilage, a graft multilayer is necessary. In order to guide the differentiation of MSCs in different strata of the biomaterials, without input of growth factors, natural cartilage components (hyaluronic acid, HA) or bone matrix (hydroxyapatite, Hap) can be added into the alginate. The aim of this work is to analyze the impact of the composition of alginate enriched either in HA or in Hap on the behavior of MSCs. The first part of our work is to evaluate the behavior of WJ-MSCs into these hydrogels. Our results have shown that Alg/ Hap hydrogels not only possess better mechanical properties than Alg/HA hydrogels, but also promote the viability of MSCs and their differentiation from MSC seeded into the Alg/HA hydrogel. The sterilization method of biomaterial is an essential step, the multiple effects of which must be evaluated, in particular as regards the behavior of the cells, but also to maintain the integrity of the physicochemical properties of hydrogel. Thus, in a second part of this work, we showed that the autoclave sterilization treatment induced a negative effect on the initial characteristics of alginate hydrogel. It is also apparent from this investigation of the sterilization modes that the sterilization of hydrogels with UV is more efficient and makes it possible to preserve the specific properties of the hydrogel as best as possible, in particular Alg/HA. Finally, in a third part of our work, we also evaluated the evolution of the mechanical properties during the differentiation and the impact of these on the differentiation of MSCs and their immunomodulatory properties. From these results, we have shown that the physico-chemical characteristics of Alg / ha and Alg/hap hydrogels influence not only the differentiation potential of WJ-MSC but also the secretion of soluble factors involved in immunomodulation. Since these physicochemical properties are influenced by the sterilization process, it is advisable to take them into account in all stages of tissue engineering.

Keywords: Wharton's jelly mesenchymal stem cells, Sterilization, Alg/HA, Alg/Hap, Chondrogenic differentiation, Cartilage tissue engineering